MECHANISMS OF ANTIBIOTIC RESISTANCE AND PATHOGENESIS IN *Acinetobacter baumannii*

By

Marguerite Indriati Hood

Dissertation

Submitted to the Faculty of the

Graduate School of Vanderbilt University

in partial fulfillment of the requirements

for the degree of

DOCTOR OF PHILOSOPHY

in

Microbiology and Immunology

August, 2012

Nashville, Tennessee

Approved:	Date:
_Timothy Cover, Chair_____	__5/16/2012_____
_Timothy Blackwell_____	__5/16/2012_____
_Terence Dermody_____	__5/16/2012_____
_Dean Ballard_____	__5/16/2012_____
_Eric Skaar_____	__5/16/2012_____

ACKNOWLEDGEMENTS

Throughout my graduate career I have been extremely fortunate to work alongside outstanding colleagues in the laboratory, in the Department of Pathology, Microbiology and Immunology, in the Medical Scientist Training Program and in the Vanderbilt community as a whole.

I must begin by thanking my mentor, Eric Skaar, for his overwhelming support and guidance throughout my graduate career. Eric, you have been at various times a cheerleader, a mentor, an advocate and a friend. Thank you for giving me the opportunity to pursue a project that was at many times uncertain, but always challenging and exciting. Thank you also for providing a positive and stimulating work environment and for always challenging me to reach my full potential. Finally, thank you for being a positive example and showing me how much fun a career in science can be.

Thanks to all of the members of the Skaar lab with whom I have had the pleasure of interacting over the last five years. Thanks to Amanda McCoy, Keith Adams and Jeff Mason who each contributed directly to my thesis work. Thank you, Victor Torres for helping me get oriented to the lab in the first few months of my rotation and for all of the helpful and entertaining discussions we enjoyed when we shared "The Island". Thanks to former members Michelle Reniere, Devin Stauff and Ahmed Attia and current members, Gleb Pishchany, Cathy Wakeman, Allison Farrand, Thomas Kehl-Fie, Kate Haley, Laura Anzaldi, Neal Hammer, Jim Cassat, Kyle Becker, Lorenzo Olive and Brittany Mortenson for your friendship, discussions and feedback. Thank you all for making the Skaar lab such fun and stimulating place to work. Thank you, Thomas Kehl-Fie, for all of your help

with infections and in getting started working with calprotectin. Thanks to Ahmed Attia for helpful discussions. Thanks to Kyle Becker, Brittany Mortenson and Mike Nodo for your willingness to carry on the Acinetobacter work after I leave.

I am thankful to my numerous collaborators both at Vanderbilt and at other institutions. Thank you to Paul Dunman and his graduate student, Anna Jacobs and post doctoral fellow, Christelle Roux, for their assistance with transcriptional analyses of *A. baumannii*. I also thank Anna for helpful discussions regarding the generation of deletion mutants in *A. baumannii*. Thank you to Lisa Zimmerman of the Ayers Institute for her assistance with proteomic data analyses. Thanks also to Rosemary Verrall of the Vanderbilt Clinical Microbiology Laboratory for providing assistance with interpretation of MIC values for *A. baumannii*. I would like to thank Drs. Anthony Campagnari (State Univerisity of New York at Buffalo), Robert Bonomo (Case Western Reserve University) and Herbert Schweizer (Colorado State University) for providing *A. baumannii* clinical strains and plasmids for generating knockouts. I also thank Luis Actis (Miami University) for providing plasmids for complementation and GFP expression as well as for helpful discussions. Thank you Carl Johnson for helpful advice and for allowing us to borrow your dark box for the circadian rhythm project. Thanks to Sebastian Joyce an Charles Spencer for providing the MyD88$^{-/-}$ mice.

I am also grateful for the support and guidance I have received from the members of my thesis committee, Timothy Cover (chair), Timothy Blackwell, Terry Dermody and Dean Ballard. Thanks in particular to Timothy Blackwell for helpful discussions and for providing mice and reagents for numerous inflammation-related projects. Thanks to Tim Cover for helpful advice and discussion regarding whole genome sequencing. Thanks to

Terry also for all of the opportunities and support you have provided through the MSTP. Thank you to the staff of the Department of Pathology, Microbiology and Immunology and the former Department of Microbiology and Immunology for your administrative support.

Thank you to my family for always supporting me. I could not have made it this far without you. Thank you to all of my friends in Nashville, at Houghton and back home in Nova Scotia. You have each helped me in getting to where I am today.

This work was supported in part by the National Institutes of Health [NIAID AI091771 to E.P.S.]; a Howard Hughes Medical Institute International Student Research Fellowship to M.I.H.; a Burroughs Wellcome Fund grant to E.P.S.; and the National Institute of General Medical Studies [T32 GM07347 to Vanderbilt University Medical Scientist Training Program].

TABLE OF CONTENTS

PAGE

LIST OF TABLES

LIST OF FIGURES

LIST OF ABBREVIATIONS

Casp1	caspase 1
Ccl	CC chemokine ligand
Ccr	CC chemokine receptor
CD40lg	CD40 ligand
CFU	colony forming units
Crp	C reactive protein
CT	circadian time
Cxcl	CXC chemokine ligand
Cxcr	CXC chemokine receptor
hpi	hours post infection
ICU	intensive care unit
Ifn-γ	Interferon-γ
IL	Interleukin
Itgam	Integrin alpha M
LBA	Luria Bertani Agar
LBM	Luria Bertani medium
LD	light dark
LOD	limit of detection
LPS	lipopolysaccharide
MHA	Mueller Hinton Agar
MHB	Mueller Hinton Broth

MyD88	Myeloid Differention 88
NFκB	Nuclear factor kappa B
RPMI	Roswell Park Memorial Institute (cell culture medium)
RR	constant dim red light
TLR	Toll-like receptor
TNF	Tumor necrosis factor
Tnfrsf	TNF receptor sub-family
TSB	tryptic soy broth
Xcr	Chemokine (C motif) receptor
ZT	zeitgeber time

I. INTRODUCTION

As intensive care medicine has evolved as a specialty, significant advances have been made in the treatment of patients in this setting. Despite these promising advances, infections remain a significant challenge in the care of the critically ill. Epitomizing this challenge, *A. baumannii* has gained increasing recognition as a cause of nosocomial infections. *A. baumannii* has established itself within the hospital niche where it is responsible for between 3 and 20 percent of total ICU infections worldwide (291). In addition, *A. baumannii* is among the most frequent causes of infection following natural disasters and in American and Canadian battlefield casualties in the Middle East (134, 139, 140, 199, 227, 242, 245, 277, 280). The burden of *A. baumannii* disease is particularly pronounced in the developing world where this organism is among the top three causes of nosocomial pneumonia and blood stream infections (8). In these infections, mortality rates can reach up to 100 percent in certain clinical settings (94, 273). Compounding these problems is the growing burden of *A. baumannii* disease caused by multidrug resistant strains, which leave few therapeutic options (71, 167, 193, 225). Surveillance data from numerous countries in North America, Europe and Asia place multidrug resistance rates in *A. baumannii* at between 48 and 85 percent of isolates, with the highest rates in Asia and Eastern Europe (82, 93, 94, 128). Although currently rare, pan-drug resistance has been reported for *A. baumannii* (16, 45, 85, 86, 272). The emergence of bacteria resistant to all clinically available antibiotics is a sentinel event signaling the dawn of a post-antibiotic era.

As rates of multidrug and pan-drug resistance increase, development of new antibacterials to treat these infections languishes. Since the introduction of tigecycline in 2005, there have been no new drugs developed to treat infections caused by MDR Gram-negative bacilli such as *A. baumannii* (31). Notably, resistance to tigecycline emerged rapidly in *A. baumannii* and the first mechanisms were reported as early as 2007 (224, 255). As a result, *A. baumannii* is currently listed as an organism for which acquired resistance may be a problem. Based on these facts, it is clear that novel approaches for the development of drugs to treat Gram-negative bacteria are desperately needed. Toward this end, the work described in the following chapters addresses this need by elucidating mechanisms of *A. baumannii* antibiotic resistance and pathogenesis and the critical host factors that defend against this organism.

Antibiotic resistance mechanisms utilized by *A. baumannii*

A. baumannii is a relatively new problem in the hospital setting. As a result, basic aspects of *A. baumannii* physiology, antibiotic resistance and pathogenesis are only beginning to be elucidated. Armed with its arsenal of antibiotic resistance determinants and its ability to persist for long periods on dry surfaces, *A. baumannii* is poised for survival in the hospital niche (28, 127, 225). Antibiotic resistance has been investigated extensively at the genetic level revealing specific resistance mechanisms against a number of antibiotics. These resistance mechanisms include antibiotic efflux (e.g. AdeABC, AbeM), enzymatic inactivation (e.g. AmpC, OXA-like beta-lactamases), and decreased permeability of the outer membrane (e.g. loss of CarO, 33-36kDa Omp) (28, 58, 108, 167, 181, 201, 225, 232, 235, 269, 283, 290). In addition, whole-genome

sequencing approaches comparing MDR *A. baumannii* with susceptible strains have highlighted additional genetic features that potentially contribute to antibiotic resistance. One feature common to MDR *A. baumannii* is the presence of one or more large resistance islands containing up to 90 genes associated with antibiotic resistance (6, 118, 286). The size of these islands makes them prominent features in the genomes sequenced to date. However, the size and composition of resistance islands varies considerably among MDR *A. baumannii* and many antibiotic resistance genes present in MDR strains do not reside within a discrete resistance island (6, 60, 70, 118, 270, 286). These studies highlight the diversity of antibiotic resistance mechanisms encoded at the genetic level in *A. baumannii* and the complexity of antibiotic resistance in this nosocomial pathogen.

Although considerable progress has been made towards identifying genes associated with resistance, few studies have investigated the mechanisms regulating resistance in *A. baumannii* (7, 58, 87, 181, 232). In particular, little is known about whether resistance phenotypes are constitutive and therefore static, or whether resistance is modulated in response to external signals. Genomic comparisons between pathogenic *A. baumannii* and the non-pathogenic *A. baylyi* strain ADP1 have highlighted a subset of 475 genes referred to as the pan-*A. baumannii* accessory genes that are conserved among pathogenic strains but absent from ADP1 (6). As noted by Adams, *et al.*, approximately 12% of the pan-*A. baumannii* genes encode predicted transcription factors, suggesting that *A. baumannii* has acquired extensive regulatory capacity as a consequence of growth in association with the human host. Further underscoring its regulatory needs, *A. baumannii* can survive under a wide variety of environmental conditions, which is highlighted by an ability to survive desiccation for long periods of time, resist

antimicrobials and utilize a broad range of nutrient sources (127, 255, 283). Taken together, *A. baumannii* is a metabolically versatile organism whose clinical burden is compounded by the acquisition of large antibiotic resistance islands and the capacity to adapt readily to new antimicrobial insults. The work described in *Chapters II* and *III* elucidate the ability of *A. baumannii* to respond to signals from the environment in order to augment its intrinsic antibiotic resistance profile.

A. baumannii pathogenesis and host response

A. baumannii is an opportunistic pathogen that rarely causes disease in healthy individuals. *A. baumannii* pneumonia, which is the most frequent manifestation of *A. baumannii* infection, presents with an acute course, and is associated with high mortality (39, 214, 248). Despite this demonstrated clinical pathology, *A. baumannii* elaborates few known virulence factors. Few *A. baumannii* virulence factors have been identified and characterized *in vivo*. These include Outer Membrane Protein A (OmpA) Penicillin Binding Protein 7/8 (PBP 7/8) and Phospholipase D (Pld), among others (52, 123, 254). Other putative virulence factors of *A. baumannii* include iron acquisition systems and genes involved in biofilm formation, but only a subset of these have demonstrated roles *in vivo* (34, 74, 91, 157, 239, 249). This work represents progress toward understanding *A. baumannii* pathogenesis, but it is clear that there remains much to be discovered. In *Chapters III* and *V* the contributions of LpsB and ZnuB to pathogenesis are defined. This work establishes LPS biosynthesis and Zn acquisition as important processes during colonization of the host.

In addition to identifying virulence factors, investigating the interaction of bacterial factors with the host is fundamental to our understanding of the pathogenic mechanisms employed by *A. baumannii*. LPS is an important pathogen-associated molecular pattern of Gram-negative bacteria. LPS initiates the inflammatory response, which is critical in the host's defense against invading pathogens. However, LPS-induced inflammation can result in significant pathology making this molecule an important virulence factor of Gram-negative bacteria. In addition to its direct role in virulence, LPS is also critical for maintaining the integrity of the outer membrane. LPS biosynthesis therefore stands out as a viable target for development of novel drug targets. The typical LPS structure consists of lipid A (endotoxin), inner and outer core oligosaccharides and O-linked polysaccharides, or O-antigen (**Figure 1**). Lipid A represents the most conserved structure and nearly all Gram-negative bacteria possess orthologues of the canonical lipid A synthesis genes found in *E. coli* (129, 240). While the oligosaccharide core is often well conserved within a given genus, the structures can vary considerably between unrelated bacteria. The core is assembled by a series of glycosyltransferases, which each demonstrate high substrate specificity (202). The high degree of specificity observed in glycosyltransferases and the sequential addition of carbohydrates within the core means that disruption of a single enzyme can lead to loss of

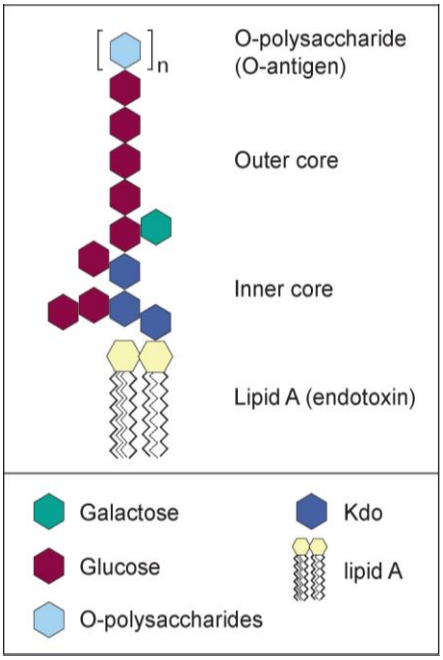

Figure 1: Schematic diagram of LPS from *A. baumannii* strain 19606 (292).

a branching chain or a truncated LPS molecule with loss of the O-antigen. The structures of LPS derived from several *A. baumannii* strains have been determined (177, 292, 293). However, despite the predicted role for *A. baumannii* LPS in the pathogenesis of infections caused by this organism, the genes involved in LPS biosynthesis were not characterized prior to this work. The experimental results discussed in *Chapter III* demonstrate the identification of a glycosyltransferase involved in the first step of LPS biosynthesis and define the role for this protein in antibiotic resistance and pathogenesis.

As introduced above, LPS is recognized by the host and serves as a potent inflammatory signal. Lipid A is the primary determinant of the potency of a given LPS molecule. This property is based on the affinity of lipid A for the TLR4/MD-2 complex on host cells (36, 266). Binding of lipid A to the receptor complex leads to activation of NFκB and expression of proinflammatory cytokines such as tumor necrosis factor (TNF) α, interleukin (IL)-1β and IL-6 (36). Other components of LPS are also important in mediating pathogen-host interactions. Core oligosaccharides, in particular, are bound by host proteins such as surfactant protein D, and promote internalization of bacteria through interaction with cell surface receptors (19, 260, 294, 317). The latter event also leads to rapid activation of NFκB (260). It is not known whether this mechanism of binding and internalization occurs with *A. baumannii* LPS. It is known, however, that *A. baumannii* LPS induces a robust proinflammatory response. The contribution of LPS to pathogenesis and inflammation are discussed in *Chapters III* and *IV*.

Defining the host response to *A. baumannii* is critical to understanding *A. baumannii* pathogenesis. Although much attention has focused on how the innate immune response contributes to clearance of *A. baumannii*, evidence exists in the

literature that the inflammatory response may also contribute to pathogenesis. Clinical data from patients with Acute Respiratory Distress Syndrome (ARDS) suggest that high levels of proinflammatory cytokine concentrations in bronchoalveolar lavage fluid (BALF) correlate with increased susceptibility to infections (28, 29). Consistently, pro-inflammatory cytokines such as TNFα, IL-1β and IL-6 stimulate growth of *Acinetobacter spp. in vitro* (19, 27). In addition, animal models of *A. baumannii* infection have highlighted the possibility for differential roles for some components of innate immunity in response to *A. baumannii* (22, 35). For example, neutrophils are required for bacterial clearance in experimental *A. baumannii* pneumonia (35, 46). However, infections in NADPH phagocyte oxidase deficient mice suggest that increased inflammation in the absence of normal effector (i.e. killing) function may actually promote infection (35). Taken together these data suggest that there exists a balance between beneficial inflammation that leads to bacterial clearance and pathologic inflammation that paradoxically promotes *A. baumannii* infection. However, characteristics of the inflammatory response elicited by *A. baumannii* that may be beneficial or pathologic to the host have not been defined. Furthermore, neither the contribution of specific bacterial factors to the inflammatory response *in vivo*, nor the contribution of inflammation to *A. baumannii* pathogenesis has been elucidated. *Chapter IV* presents data demonstrating that transposon mutants of *A. baumannii* induce a host response that effectively clears a WT *A. baumannii* infection. This work demonstrates the intricacy of the pathogen-host interaction in that aberrant expression of a PAMP in the transposon mutants completely abrogates the pathogenesis of the mutant and exerts a dominant negative effect on WT bacteria.

A version of the following section (*Chapter I, Nutritional Immunity: Expoiting essentiality and toxicity at the pathogen-host interface*) was previously published in Nature Reviews Microbiology 10, 525-537 (August 2012) | doi:10.1038/nrmicro2836

© 2012 Macmillan Publishers Limited. All rights reserved

Nutritional immunity: Exploiting essentiality and toxicity at the pathogen-host interface

Transition metals occupy an essential niche within biological systems. Their electrostatic properties stabilize substrates or reaction intermediates in the active sites of enzymes, while their heightened reactivity is harnessed for catalysis. However, the latter property renders transition metals toxic at high concentrations. Bacteria, like all living organisms, must regulate the levels of these elements in order to satisfy physiological needs while avoiding harm. It is therefore not surprising that the host capitalizes on both the essentiality and toxicity of transition metals to defend against bacterial invaders. Fe acquisition by *A. baumannii* has been studied extensively, but nothing is currently known about the role for other metals in *A. baumannii* pathogenesis (4, 34, 72, 74, 77, 124, 208, 316). *Chapter V* presents data identifying a Zn acquisition system in *A. baumannii* and demonstrates its role in pathogenesis. This work establishes a role for Zn at the *A. baumannii*-host interface. However, emerging evidence in the literature demonstrates that the role for transition metals in bacterial infections is more complex than simply the withholding of essential metals by the host. The sections below discuss established and emerging paradigms in nutrient metal homeostasis at the pathogen-host interface.

Transition metals at the pathogen-host interface

Transition metals function in a number of crucial biological processes and are therefore necessary for the survival of all living organisms. These metals are frequently incorporated into metalloproteins including metalloenzymes, storage proteins and transcription factors. The functional roles of transition metals in biological systems can

be broken down broadly into non-catalytic functions, redox and non-redox catalysis. Of the redox active metals, Fe is most commonly used, followed by Cu and Mo (12). In both eukaryotes and prokaryotes, approximately 50 percent of nonheme Fe and Cu proteins are oxidoreductases or other electron transfer proteins (12). In addition, heme Fe is an important cofactor for respiration, as well as various biosynthetic and metabolic processes. Although Mg is the most prevalent non-redox metal found in enzymes, Zn is the most common transition metal (12). Zn can serve structural as well as catalytic roles in proteins. Interestingly, the distribution of Zn-binding proteins differs significantly between bacteria, archaea and eukaryotes with enzymes constituting approximately 80 percent of the zinc proteomes of archaea and bacteria but less than 50 percent in eukaryotes (13). Zn-dependent transcription factors make up 44 percent of the eukaryotic zinc proteome demonstrating that Zn plays an important role in gene regulation in higher organisms (13). Consequently, Zn-binding proteins make up a larger proportion of the total proteome in eukaryotes as compared to bacteria and archaea (11).

All living organisms require transition metals in order to survive; yet the catalytic activity imparted by these metals also potentiates their toxicity. It is therefore necessary that the levels of transition metals be carefully controlled. Moreover, the mechanisms used to limit the availability of free metals also serves as a countermeasure against invading bacteria. The human body is a rich reservoir of essential nutrients for those bacteria that have evolved the mechanisms to exploit this resource. In order to prevent infection with pathogenic organisms, humans, like other mammals, restrict access to essential metals in a process termed “nutritional immunity”. Originally coined to refer to restriction of iron availability by the host, the term “nutritional immunity” can also be

applied to mechanisms for withholding other essential transition metals or directing the toxicity of these metals against microbial invaders. This review will focus on four of these metals, namely Fe, Mn, Zn and Cu and discuss the roles for these metals at the pathogen-host interface. In addition, emerging paradigms in nutritional immunity will be reviewed, including host strategies for metal intoxication, the interplay between host genetics and the outcome of bacterial infections, and the extension of nutritional immunity to include non-metals.

Fe limitation: a universal strategy in innate defense

Fe is the fourth most abundant element in the Earth's crust and the most abundant transition metal in the human body. In bacteria, Fe is a co-factor of many enzymes and as such plays a crucial role in diverse physiological processes such as DNA replication, transcription and central metabolism (12). Furthermore, the Fe-containing protoporphyrin heme is incorporated into cytochromes, thus participating in energy generation through respiration. Fe is required by virtually all bacterial pathogens. Therefore, vertebrates limit Fe access to exploit this requirement as a potent defense against infection (299, 301). As a result, bacteria must elaborate systems for acquiring Fe in order to successfully colonize host tissues. Recent reviews have focused on bacterial systems for acquiring Fe and the mechanisms utilized by vertebrate hosts to withhold Fe from invading bacteria (35, 42, 102, 205, 215). These mechanisms are discussed below to allow comparison with other systems.

Mechanisms for withholding iron from invading bacteria

To prevent access to Fe, vertebrates use a number of proteins that render this valuable nutrient largely inaccessible to bacteria that lack sophisticated Fe-capturing systems (**Figure 2a**). The vast majority of Fe within vertebrates is complexed to heme, a tetrapyrrole ring encircling a singular Fe atom and the cofactor of the oxygen transport protein hemoglobin. Hemoglobin is further contained within circulating erythrocytes, representing an additional barrier to access by pathogens. If free hemoglobin or heme is released from erythrocytes, these molecules are rapidly bound by haptoglobin and hemopexin, respectively. Therefore, for bacterial pathogens to access this rich Fe pool, they must lyse erythrocytes, remove heme from hemoglobin or hemopexin, then liberate Fe from the macrocyclic conjunction of heme.

In addition to heme, Fe is stored intracellularly in the Fe storage protein ferritin and is therefore only accessible to intracellular pathogens or to extracellular pathogens following host cell lysis. At physiological pH, extracellular Fe^{2+} is oxidized to the insoluble Fe^{3+} and mobilized by the serum protein transferrin, which binds Fe^{3+} with exceptionally high affinity. Free Fe is also bound by lactoferrin, a globular glycoprotein of the transferrin family that is present in secretions such as breast milk, tears, and saliva. Notably, lactoferrin is present within the granules of polymorphonuclear leukocytes and is therefore a crucial component of the innate response to infection.

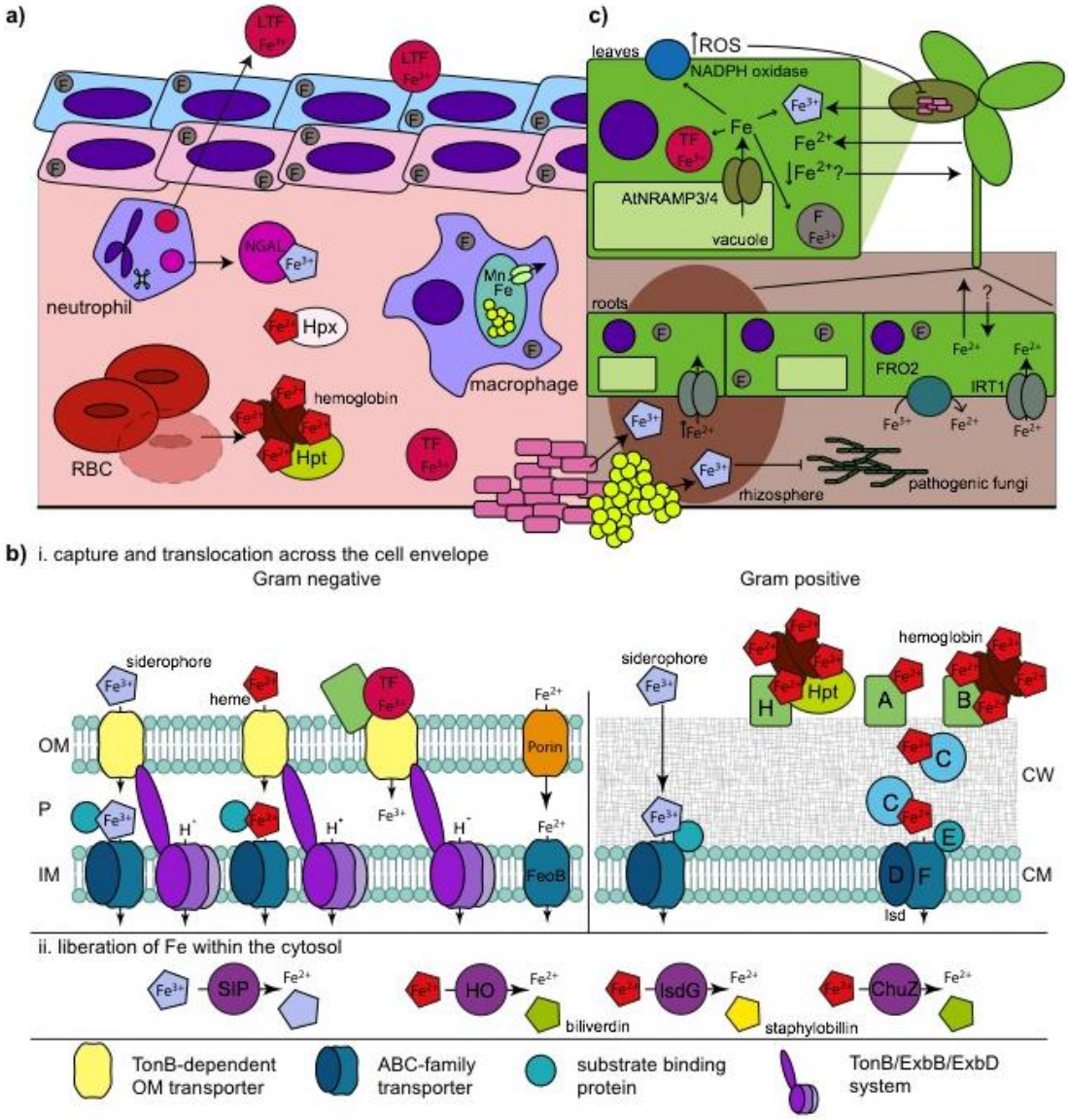

Figure 2. Fe limitation and Fe acquisition during bacterial infections.
a. Overview of Fe limitation strategies in the vertebrate host. Fe^{3+} is stored intracellularly in complex with ferritin (F), bound by serum transferrin (TF) or bound by lactoferrin (LTF) at mucosal surfaces. In the blood, Fe^{2+} is complexed with heme, which is bound by hemoglobin within red blood cells (RBCs). Upon red cell lysis, hemoglobin is bound by haptoglobin (Hpt) and free heme is scavenged by hemopexin (Hpx). **b.** Representative Fe acquisition systems expressed by Gram negative and Gram positive pathogens. Both Gram negative and Gram positive pathogens possess systems to acquire Fe^{3+}-siderophores, Fe^{2+}-heme, Fe^{3+} from transferrin and/or free Fe^{2+}. Not all systems are expressed by the same organism. TF, transferrin; SIP, siderophore interacting protein; Hpt, haptoglobin; OM, outer membrane; P, periplasm; IM, inner membrane; CW, cell wall; CM, cytoplasmic membrane. **c.** Overview of the interactions between pathogenic and symbiotic bacteria with their plant hosts. Bacterial infection induces the expression of AtNRAMP3/4 in plant cell vacuoles and subsequent translocation of Fe into the cytosol, which contributes to generation of reactive oxygen species (ROS). Bacterial siderophores induce an iron deficiency response, which is transmitted to roots via an unknown molecular signal. In roots, up-regulation of FRO2 leads to reduction of Fe^{3+} in the soil to Fe^{2+} and import by the Fe transporter IRT1. Symbiotic bacteria associated with the rhizosphere secrete siderophores which inhibit growth of pathogenic fungi and facilitate iron acquisition in roots. F, ferritin; TF, transferrin; ROS, reactive oxygen species.

Bacterial iron acquisition

All bacterial pathogens must have mechanisms to circumvent nutritional immunity. In the case of Fe, these strategies are numerous and vary considerably across organisms. Perhaps the most elegant strategy to circumvent host-mediated Fe sequestration is that of *Borrelia burgdorferi*, the causative agent of Lyme disease. By substituting Mn in place of Fe within its Fe-requiring enzymes, this organism does not require Fe to infect its host (234). However, as discussed in subsequent sections, the host encodes additional mechanisms to restrict Mn availability.

Organisms that must acquire Fe do so using different strategies that can be generally divided into siderophore acquisition systems and heme acquisition systems (Figure 1b). Siderophores are low molecular weight Fe chelators that are secreted by bacterial cells and bind Fe with an affinity that surpasses that of transferrin and lactoferrin (10^{23} M^{-1}) (259). Utilization of siderophore-bound Fe first requires recognition by cognate receptors at the bacterial cell surface. As these molecules are too large to diffuse through non-selective porins in the outer membranes of Gram-negative bacteria, energy-dependent transport of siderophores is mediated through TonB-dependent receptors. The periplasm of Gram-negative bacteria lacks ATP or ionic gradients that can drive transport across the outer membrane. Therefore, energy from the proton motive force generated at the inner membrane is harnessed by the TonB-ExbB-ExbD system to mediate outer membrane transport. In the periplasm, substrate binding protein (SBP) components of ATP-binding cassette (ABC) family transporters recognize the siderophore-Fe complex and ultimately shuttle this complex to the cognate transporter. Gram-positive bacteria also express SBPs, however these proteins are tethered to the

cytoplasmic membrane. In both Gram-positive and Gram-negative bacteria, once siderophores are internalized into the cytoplasm, the Fe is released through reduction to Fe^{2+} or through enzymatic degradation of the siderophore. The end result is the release of Fe for use as a nutrient source. To combat siderophore-mediated Fe acquisition, vertebrates produce neutrophil gelatinase-associated lipocalin (NGAL), also known as lipocalin 2 or siderocalin, which binds and sequesters siderophores away from bacteria (89). However, some bacteria produce 'stealth' siderophores that evade siderocalin by chemical modification (2).

Heme acquisition systems typically involve a cell surface receptor for either heme or hemoproteins, which pass heme through a membrane transport system into the cytoplasm. Several well-characterized systems have been described in Gram-negative bacteria (35, 57). In Gram-positive bacteria, the major systems described to date include the Fe-regulated surface determinant (Isd) system found in many *Firmicutes* as well as Shr, Shp and HtsABC found in the *Streptococci* (111, 130, 185, 203, 209). The first step in heme transport involves binding of heme, hemoglobin, or hemoglobin-haptoglobin complexes by cell wall-anchored receptors (Gram-positive) or TonB-dependent receptors (Gram-negative) (76, 217, 230, 231, 282, 315). Heme is then extracted from hemoglobin and relayed to a substrate binding protein associated with a heme-specific ABC family transporter that mediates translocation into the cytoplasm (165, 176, 182, 200, 209, 315).

In addition to surface bound receptors for heme and hemoproteins, some Gram-negative and Gram-positive bacteria produce secreted proteins that complex heme, which are known as hemophores and are functionally analogous to siderophores (43, 84, 97).

Once bound to heme, hemophores are recognized by hemophore receptors and the heme is internalized.

Upon translocation into the bacterial cytoplasm heme is degraded by heme catabolizing enzymes (**Figure 2b**). These heme oxygenases can be classified into three different enzyme families. The HO-1 family of heme oxygenases is evolutionarily related to the eukaryotic heme degrading enzymes (304). HO-1 family members are present in both Gram-negative and Gram-positive bacteria and degrade heme to free Fe and biliverdin (304). The IsdG-family heme oxygenases are found in both Gram-negative and Gram-positive bacteria, and these enzymes degrade heme to Fe and the chromophore, staphylobilin (49, 101, 237, 244). More recently, a third family of heme oxygenases represented by the *Campylobacteri jejuni* ChuZ enzyme has been described (312, 313). The product of ChuZ-mediated heme degradation is not yet known.

Although Fe is predominantly transported in the chelated form, a number of bacteria transport free Fe^{2+} using the FeoB family of transporters (17, 40, 183, 220, 221, 288). FeoB is a large membrane protein containing a GTP-binding domain that is similar to eukaryotic G proteins(40). GTPase activity is necessary for Fe^{2+} transport and coupling of the G protein and membrane transporter as domains within the same protein make FeoB unique compared to eukaryotic G-protein coupled receptors(183). FeoB is typically co-expressed with FeoA, a small SH3-domain protein likely found within the cytoplasm and FeoC, which is thought to act as a Fe-S dependent repressor(40). Overall, FeoB represents a unique family of bacterial transition metal transporters whose members are important for virulence in numerous pathogens (17, 220, 221, 288).

Table 1. Selected bacterial iron uptake systems referenced in the text.

Substrate	Cell surface	Cell wall/ periplasm	Cytoplasmic membrane	Pathogens (disease)
Heme, Hemoglobin, Hpt/hemoglobin	IsdA (heme)(231)	IsdC (165, 176)	IsdDEF(176)	*S. aureus* (multiple) (185)
	IsdB (hemoglobin) (230, 282)			
	IsdH (Hpt/hemoglobin) (76)			
	IsdXI/X2(84) (secreted hemophores)			*B. anthracis* (anthrax) (182)
	Shp (heme) (209)		HtsABC (209, 315)	*Streptococcus pyogenes* (pharyngitis, necrotizing fasciitis)
	Shr (methemoglobin) (217, 315)			
		SvpA (203)	HupDGC (130)	*Listeria monocytogenes* (listeriosis) (130, 203)
	HmuR	HmuT	HmuSUV	*Yersinia pestis* (plague)
	PhuR	PhuT	PhuSUV	*Pseudomonas aeruginosa* (multiple, immune compromised host)
Transferrin (Fe^{3+})	TbpA (R/OMT), TbpB			*Neisseria spp*. (meningitis, gonorrhea) (206, 261)
Siderophore			SirABC (Staphyloferrin B)(47)	*S. aureus, S. pyogenes*
			HtsABC, Fhu (Staphyloferrin A) (23)	*S. aureus*
	FepA (enterobactin)	FepB	FepCD (ABC-family)	
	FpvA (pyoverdine)		*pyoverdine dissociates in periplasm	*Pseudomonas aeruginosa*
Fe^{2+}			FeoB (G protein)	*Escherichia coli* (gastrointestinal and urinary tract infections) (183)
				Helicobacter pylori (peptic ulcer disease) (288)
				Xanthamonas oryzae pv. Oryzae (bacterial blight in rice) (221)
				Campylobacter jejuni (220)
				Streptococcus suis (17)

Nutritional immunity is not a defensive strategy that is exclusive to vertebrates. A number of mechanisms for Fe restriction exist in plants and invertebrates including the

expression of ferritins and transferrins (83, 95, 159). In the entomopathogen, *Photorhabdus luminescens*, Fe availability may serve as an important signal for the switch between symbiotic colonization and pathogenic infection. In these bacteria, certain iron acquisition systems are crucial for virulence but dispensable for symbiosis (297). Similarly, iron acquisition via siderophores serves as a virulence strategy for phytopathogens, while siderophores produced by symbiotic bacteria in the rhizosphere can be beneficial to plants (**Figure 2c**). Clearly, iron acquisition is important for both bacterial pathogenesis and symbiosis.

Roles for Fe in plant-microbe interactions.

As introduced above, plants express a number of mechanisms for Fe restriction including ferritins and transferrins. In addition, plants express at least four different members of the natural resistance-associated macrophage protein (NRAMP) family of Mn and Fe transporters. The role for NRAMP transporters in immunity was first appreciated in vertebrates, where phagosomal NRAMP1 pumps both Mn and Fe out of the phagosome, thus reducing Fe and Mn availability to pathogens within this compartment (122). In *Arabidopsis thaliana*, AtNRAMP3 and AtNRAMP4 are up-regulated in the plant vacuole in response to *Erwinia chrysamthemii* infection and are important for Fe transport and host defense (263). It is not clear, however, whether Fe withholding from the bacterium is the primary mechanism of AtNRAMP3/4-mediated plant defenses. AtNRAMP3/4 contribute to H_2O_2 accumulation in infected leaves suggesting that extrusion of Fe from the vacuole to the cytoplasm may be important for generating the oxidative burst (263). The role for nutritional immunity in plant defenses

is also evidenced by the fact that Fe acquisition systems are required for virulence in a number of phytopathogens (83, 221). Siderophore biosynthesis and uptake systems are the most common mechanism employed by phytopathogens to acquire nutrient Fe from their hosts (159). Beyond facilitating Fe uptake by pathogenic bacteria, siderophores have been shown to exert effects on Fe distribution and overall physiology within the plant host (**Figure 2c**) (63, 263). These effects include induction of the salicylic acid signaling pathway in leaves and an Fe deficiency response in roots (63, 263). Interestingly, symbiotic bacteria within the rhizosphere also produce siderophores (251). These bacteria promote plant growth and their siderophores are thought to benefit the plants by defending against pathogenic fungal species as well as by enhancing Fe acquisition in roots (64, 158, 159, 251). In addition to siderophores, *Xanthomonas oryzae* pv. oryzae, which causes bacterial blight in rice, expresses FeoB and this Fe acquisition system is necessary for pathogenesis (221). Clearly, Fe availability is a crucial component of both pathogenic and symbiotic relationships between plants and bacteria. Moreover, withholding of iron is a conserved innate immune strategy across multiple kingdoms of life.

Host mechanisms for chelating Mn and Zn at mucosal and epithelial surfaces

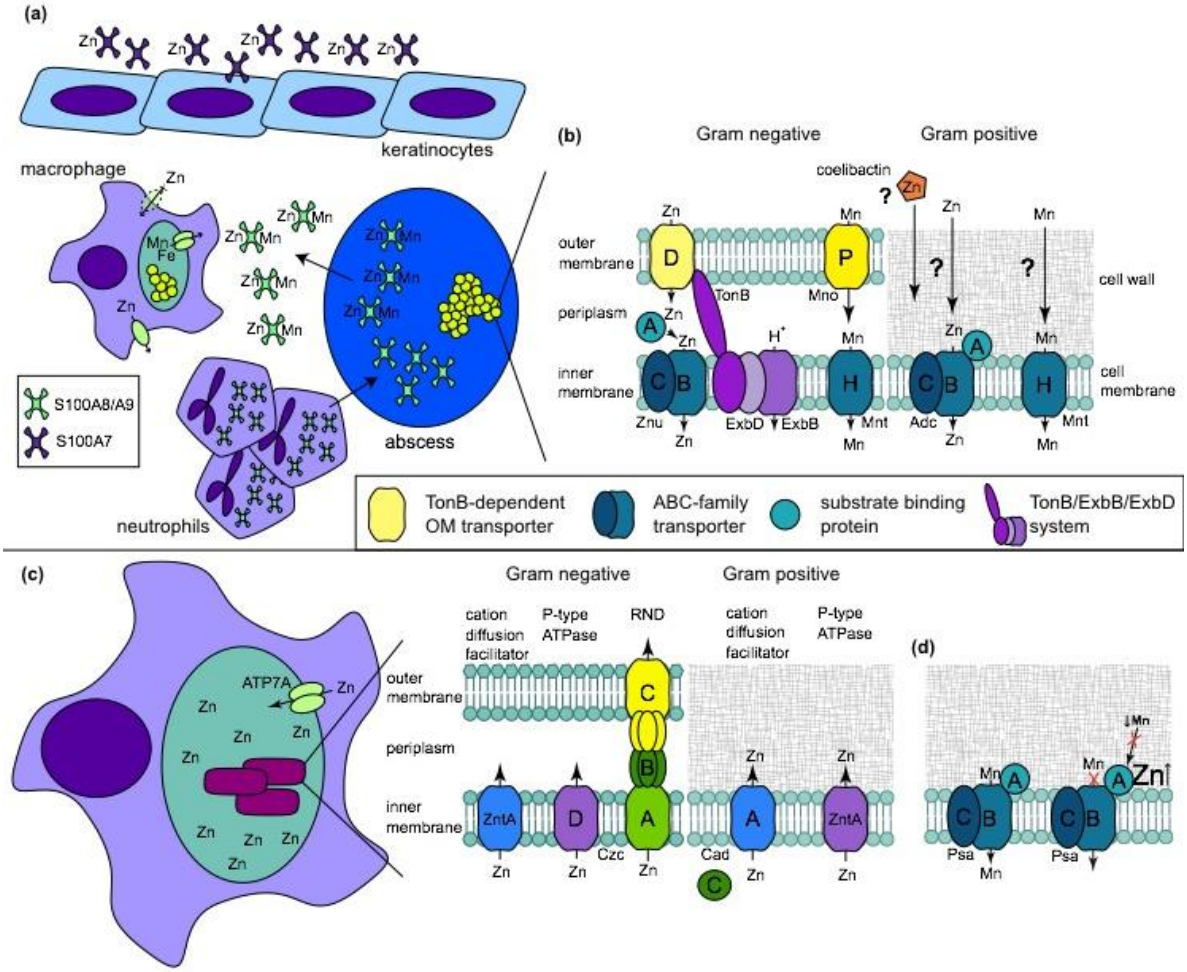

Figure 3. Mn and Zn homeostasis at the pathogen-host interface.
a. Zn and Mn sequestration by S100 family proteins at epithelial surfaces and within tissue abscesses. S100A7 is released at epithelial surfaces where it inhibits bacterial invasion through chelation of Zn. In deep tissues, infection leads to recruitment of neutrophils which deliver calprotectin (S100A8/A9) to the infection site. Calprotectin inhibits bacterial growth through chelation of Mn and Zn and is thought to be transported away from the abscess by an as yet unknown mechanism. Engulfment of bacteria by macrophages leads to decreased Zn uptake and increased Zn efflux from the cytoplasm and efflux of Mn and Fe from the phagosome by NRAMP1. **b**. Representative Mn and Zn uptake systems expressed by pathogenic bacteria. **c.** Proposed mechanisms of Zn intoxication employed by the host and Zn detoxification systems expressed by pathogens. Upon infection, Zn accumulates in the phagolysosome where it is toxic to bacteria. Gram negative and Gram positive bacteria primarily alleviate Zn toxicity through efflux of excess Zn from the cytoplasm. **d.** Proposed mechanism for Zn toxicity in bacteria. When the extracellular Zn:Mn ratio is high, Zn binds the SBP of Mn-specific transporters, preventing Mn binding and uptake.

Mn and Zn in pathogen-host interactions

Nutritional immunity is not limited to strategies for withholding Fe (137). Mn and Zn also play vital roles within bacteria. Mn serves a catalytic role in many proteins and is important in oxidative stress resistance (15, 184, 271, 284). In some bacteria, Mn can replace the more reactive Fe in Fe-containing proteins, reducing oxidative damage to these proteins (271). Furthermore, Mn-dependent superoxide dismutases are encoded by many pathogens, indicating that these organisms require Mn to defend against superoxide (136). Zn is the second most abundant transition metal in most living systems and can serve both catalytic and structural roles within proteins (104). In fact, it is estimated that Zn-binding proteins represent approximately 4-8 percent of all proteins encoded in the genomes of prokaryotes (11). Given these crucial roles for Mn and Zn in bacterial physiology, it is not surprising that sequestration of these nutrient metals is an important innate defense strategy.

Chelating Mn and Zn at mucosal and epithelial surfaces

The S100 family of proteins is a large family of calcium binding proteins found within vertebrates. A number of S100 proteins have been implicated in defense against infection, and S100A7, S100A8/A9 and S100A12 are key factors in nutritional immunity (Figure 3a). S100A7, also known as psoriasin, is secreted by keratinocytes and inhibits microbial growth through the chelation of nutrient Zn (98). S100A12, also known as calgranulin C, binds both Zn and Cu *in vitro* and Cu-S100A12 participates in the generation of superoxide species (194, 195). It is not yet known whether the antimicrobial properties of this protein result from generation of superoxide or through

nutrient metal sequestration. S100A8 and S100A9 function as a heterodimer known as calprotectin (also referred to as MRP 8/14 and calgranulin A/B). Calprotectin makes up approximately 40 percent of the protein composition of the neutrophil cytoplasm and this protein is highly antimicrobial against a variety of bacterial and fungal pathogens (56, 186, 285). The antibacterial activity of calprotectin results from chelation of nutrient Mn and Zn (56). Chelation of Mn and Zn by calprotectin is mediated through two high-affinity binding sites both of which are capable of binding Zn with nanomolar affinity while only one binds Mn with such affinity (136). Since the initial report defining the role for calprotectin in protection against *Staphylococcus aureus* infection, this protein has been implicated in defense against infection by *Salmonella* Typhimurium and the fungal pathogens *Aspergillus spp*. and *Candida spp.* (26, 164, 186, 285). However, as discussed below, some pathogens have evolved elegant mechanisms to counteract or exploit the antimicrobial properties of calprotectin.

In addition to their metal chelating properties, psoriacin, calprotectin, and S100A12 (also known as calgranulin C) have proinflammatory properties and serve as markers for many inflammation-mediated pathologies (116). Given the multiple roles for these S100 proteins in nutrient metal chelation and inflammation, it remains to be determined whether the inflammatory properties of these proteins are impacted by metal binding.

Bacterial Mn and Zn acquisition systems

The importance of Mn and Zn acquisition to pathogenesis has been demonstrated in a number of organisms including *S.* Typhimurium, *Campylobacter jejuni*, *Yersinia*

spp., *Brucella abortus*, and *Streptococcus* spp. (9, 14, 38, 44, 204, 226). The mechanisms of Mn and Zn transport across the outer membrane of Gram-negative bacteria are not completely defined. Although previously believed to diffuse through non-selective porins, designated transporters have recently been described suggesting that in some bacteria the outer membrane provides a selective barrier to these essential nutrients (Figure 3b). One such example is MnoP of *Bradyrhizobium japonicum,* which is a Mn-selective channel that facilitates transport of free Mn across the outer membrane (110).

Although transport of Mn through MnoP is thought to be passive, transport of Zn across the outer membrane may be an energy-dependent process powered by the TonB-ExbB-ExbD system. A Zn-regulated TonB-dependent receptor designated ZnuD, has been described in *Neisseria meningitidis* and orthologues of this receptor are encoded in the genomes of several pathogens(274). ZnuD shares sequence similarity with the heme transporter HumA of *Morexalla catarrhalis* and facilitates heme acquisition when expressed in *E. coli* (151). These findings, together with the dual regulation of ZnuD by Zur (Zn uptake regulator) and Fur (Fe uptake regulator), suggest that ZnuD may participate in both Zn and heme acquisition(151). Alternatively, cross-regulation of ZnuD may stem from an increased need for exogenous heme under Zn-limiting conditions, since some endogenous heme biosynthetic enzymes require Zn (160).

Zn-chelating compounds analogous to siderophores have not been identified in pathogenic bacteria. However, a putative tsinkosphore (“tsinkos” is greek for Zn) biosynthetic operon, the coelibactin gene cluster, has been identified in the antibiotic producing bacterium *Streptomyces coelicolor*. In *S. coelicolor* this gene cluster is regulated by Zur in a Zn-dependent manner, supporting a role for this cluster and its

putative product in the transport of Zn (133). Moreover, pyochelin from *Pseudomonas aeruginosa* binds Zn and Cu with high affinity *in vitro,* although transport of Zn-pyochelin has not been demonstrated *in vivo* (33). Nonetheless, the possibility remains that pathogenic bacteria secrete small molecule Zn chelators as a strategy to acquire this nutrient during infection.

The import of Mn and Zn across the cytoplasmic membrane of both Gram-positive and Gram-negative bacteria is primarily facilitated by either ATP-binding cassette (ABC)-family transporters or NRAMP family transporters (137, 145). These include high affinity uptake systems such as ZnuABC, AdcBCA and MntABC as well as the NRAMP-family Mn transporter MntH (9, 14, 38, 44, 204, 226, 284). Some FeoB orthologues may also transport Mn (61). Translocation of Mn and Zn by ABC family transporters is analogous to that described above for siderophores and heme. Several examples of Mn and Zn acquisition systems are depicted in **Figure 3b** and listed in **Table 2**.

A number of Mn and Zn transporters have demonstrated roles in pathogenesis, but a direct role in evading nutrient chelation by calprotectin or other host proteins has generally not been demonstrated. One exception is the recent evidence that *S.* Typhimurium expressing the ZnuABC zinc uptake system are resistant to calprotectin mediated Zn chelation (164). This system allows *S.* Typhimurium to resist the high levels of calprotectin that accumulate in the intestine following infection. Moreover, *S.* Typhimurium exploits calprotectin-mediated Zn-chelation in order to outcompete the host's microbiota, which are less well adapted to the resulting nutrient deplete environment (164).

Table 2. Selected bacterial transporters of Mn and Zn.

Mn^{2+} uptake	
MnoP (Outer membrane)	*Bradyrhizobium japonicum* (110)
MntABC (ABC-family)	*Neisseria gonorrhoeae* (284)
PsaBCA (ABC-family)	*Streptococcus pneumoniae* (210)
MntH (NRAMP-family)	*Brucella abortus* (10)
	Yersinia spp. (44, 226)
Zn^{2+} uptake	
ZnuABC (ABC-family)	*Campylobacter jejuni* (62)
	Salmonella spp. (9, 38)
ZnuD (outer membrane)	*Neisseria meningitides* (274)
AdcBCA, AII (ABC-family)	*S. pneumonia (22)*

Exploiting Mn and Zn toxicity to kill invading bacteria

In addition to mechanisms for withholding nutrient metals from invading bacteria, increasing evidence is emerging to suggest that mammalian nutritional immunity harnesses the toxic properties of transition metals to kill bacteria. It was recently determined that following engulfment of either *Mycobacterium tuberculosis (Mtb)* or *E. coli*, macrophages release Zn from intracellular stores which then accumulates in the phagolysosome (30). Survival within the phagolysosome depends on the expression of a Zn efflux system in *Mtb*, supporting the idea that bacteria encounter Zn toxicity *in vivo* and that the ability to resist Zn toxicity is important for pathogenesis (30).

Bacterial Mn and Zn detoxification is primarily mediated by P-type ATPases (**Figure 3c**). These ATP-driven pumps have narrow substrate specificity, which is dictated by a membrane-embedded metal recognition site (115). Zn can also be exported via RND-family transporters that span the inner membrane, periplasm and outer membrane of Gram-negative bacteria. In this case, energy from the proton motive force drives efflux from the cytoplasm or periplasm to the cell exterior. The requirement for Mn and Zn efflux systems in the pathogenesis of several bacteria suggests that bacteria

encounter Mn and Zn toxicity *in vivo* (30, 252, 289). However, the mechanisms by which Mn and Zn cause toxicity are not fully known. Emerging data suggest that maintaining a defined ratio of transition metals is important for bacterial physiology (126, 187). For example, PsaA of *S. pneumoniae* binds both Mn and Zn, while only Mn is transported by the cognate ATP-dependent permease (68, 155). In this case, increasing the Zn:Mn extracellular ratio leads to high-affinity binding of Zn to PsaA, blocking Mn uptake and thus potentiating the effects of Mn depletion (187). Additionally, the Zn efflux transporter *czcD* is up-regulated under Mn-limiting conditions, suggesting that Zn toxicity may be enhanced under Mn-deplete conditions (210).

Cu: new insights into an ancient antibacterial agent

Humans have recognized the antibacterial effects of Cu for millennia and have exploited this property for industrial and medical purposes (257). Despite the long history of Cu use as an antimicrobial, we have only recently begun to appreciate that Cu has a role in innate defense. The accumulation of Cu at sites of infection was first demonstrated in *Mtb* pulmonary infections where it was found that Cu resistance is necessary for *Mtb* virulence (307). In the mammalian host, bacteria encounter Cu within the phagolysosomes of macrophages. Interferon gamma induces expression of the Cu transporter Ctr1, which actively takes up Cu from the extracellular environment (302). Atox1 then shuttles Cu to ATP7A, a Cu transporter on the phagolysosomal membrane, facilitating Cu accumulation within this compartment (141, 143, 302) (**Figure 4a**).

The mechanisms of Cu toxicity are not completely understood; however, accumulating evidence suggests that toxicity may be multifactorial involving both

oxidative damage and disruption of Fe-S clusters. Like Fe, Cu(I) can undergo Fenton chemistry, reacting with H_2O_2 to produce hydroxyl radicals which in turn damage lipids, proteins and DNA (**Figure 4a**). Cu enhances the bactericidal capacity of macrophages *in vitro*, an effect which is further magnified by the addition of H_2O_2 and reversed by the addition of the antioxidant ebselen (302). In addition to oxidative damage, recent characterization of a *copA* mutant of *N. gonorrhoeae* revealed a role for Cu in potentiating nitrosative stress (69). CopA is a Cu exporter with homologues found in a number of bacteria. Loss of this protein in *N. gonorrhoeae* leads to increased sensitivity to copper and nitrosative stress. Cervical epithelial cells produce NO in response to gonococcal infection (78); however, it is not yet known whether gonococci are exposed to extracellular Cu at this site of infection or whether Cu intoxication occurs following engulfment by immune cells. Finally, Cu also targets Fe-S clusters in dehydratases involved in processes such as branched-chain amino acid synthesis. The resulting disruption of crucial metabolic processes can be reversed by addition of pathway end products in some bacteria (3, 178). Since addition of pathway end products does not reverse Cu toxicity in all bacteria, it is likely that multiple mechanisms of toxicity exist (3). The precise mechanism of toxicity likely depends on the bacterium and the physiological conditions in which Cu is encountered.

Cu acquisition and detoxification in bacteria

The mechanisms of Cu acquisition in bacteria are largely unknown. Methane oxidizing bacteria (methanotrophs) utilize Cu in their methane monooxygenases (MMOs) and Cu accumulation regulates the switch from soluble, Cu-independent sMMO to the membrane-bound, Cu-dependent pMMO (99, 138, 146) (**Figure 4b**). Methanotrophs

produce Cu-chelating compounds known as chalkophores ("chalko" is Greek for copper) or methanobactins (mbs) (21, 138, 142). Mbs produced by *Methylosinus trichosporium* OB3b bind Cu(I) with affinities in the range of 10^{19} – 10^{20} M^{-1} depending on pH (80, 100). Internalization of methanobactin is dependent on the TonB/ExbB/ExbD system and is thus proposed to be analogous to siderophore uptake utilizing TonB-dependent receptors and ABC-family transporters (20). It remains to be determined whether pathogenic bacteria express compounds similar to methanobactin to acquire Cu. In addition to methanobactin-mediated transport, unchelated Cu can also be taken up by the cell, presumably by diffusion through outer membrane porins (20).

In contrast to the dearth of information regarding mechanisms of Cu uptake, the mechanisms of Cu detoxification have been characterized in multiple pathogenic bacteria and these systems are often necessary for pathogenesis (3, 264, 265, 296, 307). Bacteria possess several lines of defense against Cu toxicity, beginning with their relatively low physiological need for Cu and the physical localization of Cu-dependent proteins outside the cytoplasm. In addition, bacteria possess multiple mechanisms to detoxify the cytoplasm and periplasm in the presence of excess Cu. In general, this involves expression of cytoplasmic Cu chaperones, Cu exporters and periplasmic multicopper oxidases (257). Mycobacterial Cu resistance involves expression of the cytoplasmic Cu chaperone, MymT, the Cu(I) transporter, CtpV, and a mycomembrane transporter, MctB (88, 166, 296, 307) (**Figure 4c**). Both CtpV and MctB are necessary for full virulence of *Mtb* (296, 307). In Gram-negative bacteria, Cu resistance is likewise mediated by the expression of Cu exporters. The gastrointestinal pathogen, *Salmonella enterica* sv. Typhimurium expresses two independently regulated P-type ATPases, CopA and GolT.

Expression of *copA* is induced by CueR/SctR in the presence of Cu together with genes encoding a putative periplasmic Cu chaperone, CueP, and the multicopper oxidase CuiD/CueO (3, 144, 216). The latter functions to oxidize Cu(I) to Cu(II) in the periplasm and homologues of this protein are necessary for Cu resistance in several bacteria (3, 144, 218). In addition to CopA, *E. coli* also expresses an RND-family Cu exporter known as CusABC. CopA and CusABC are independently regulated, and expression of these two systems provides a graded response to different levels of Cu toxicity (218). Cu detoxification strategies in Gram-positive bacteria are mostly analogous to those of Gram-negative bacteria. In some cases, a second P-type ATPase, CopB, as well as a putative cytoplasmic Cu chaperone, CopZ, are coexpressed with CopA (171). The multitude of Cu detoxification systems expressed by pathogenic bacteria highlights the importance of Cu intoxication as a host defense strategy and the applicability of Cu as an antimicrobial agent.

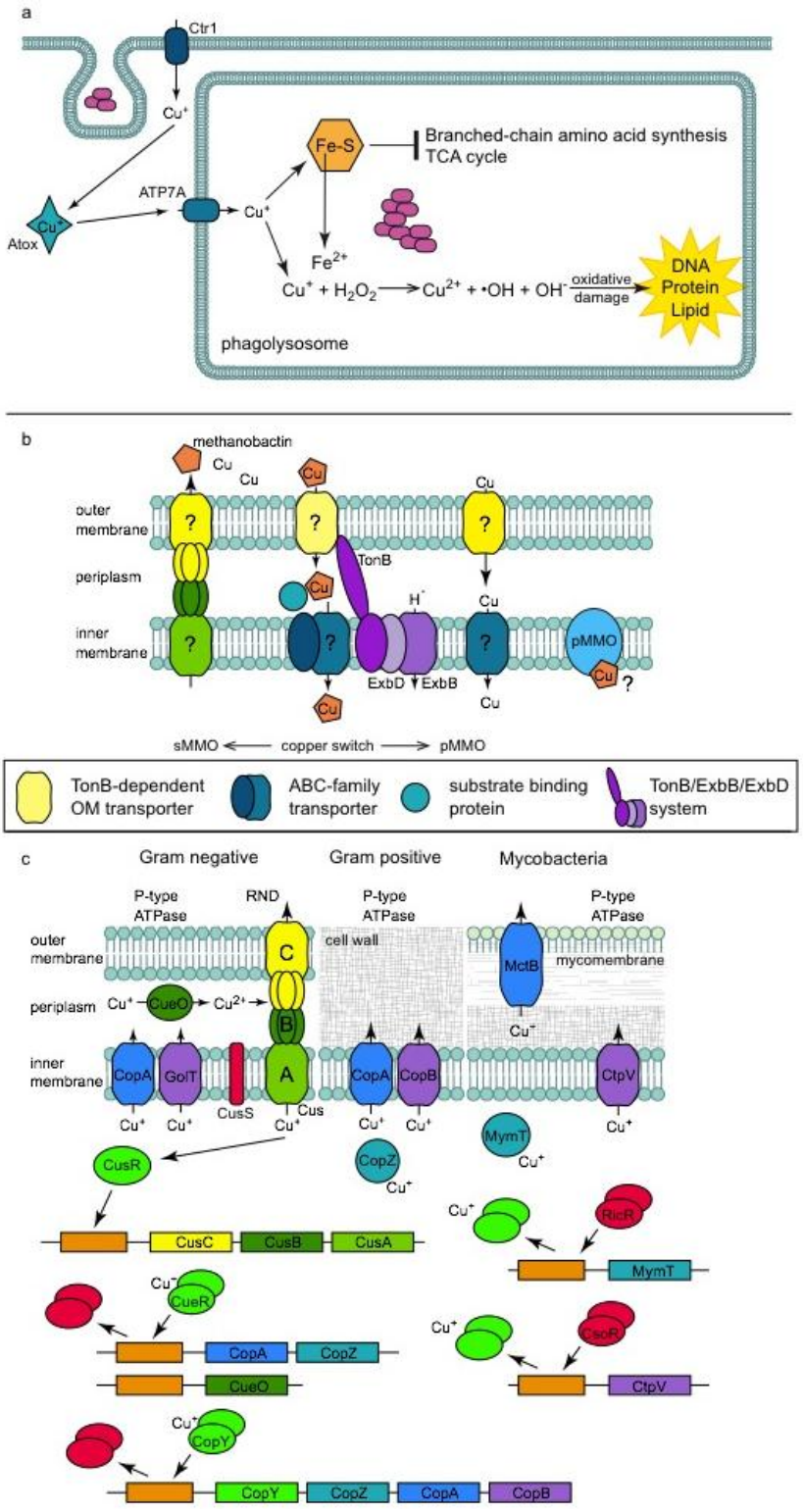

Figure 4. New insights into the roles for Cu in innate immunity. **a.** Mechanisms of Cu intoxication within macrophages. Following phagocytosis of bacteria, interferon gamma induces expression of the Cu importer Ctr1. Cu is bound by Atox1 and shuttled to the phagosomal Cu transporter, ATP7A. Accumulation of copper within the phagolysosome contributes to bacterial killing through multiple mechanisms including disruption of Fe-S cluster-containing bacterial proteins and generation of reactive oxygen species. This leads to inhibition of bacterial metabolic processes and damage to DNA, proteins and lipids. **b.** Cu acquisition systems in methanotrophs. Methanotrophs produce a copper chelating compound, methanobactin, which is secreted via an unknown mechanism. Cu acquisition occurs through import of Cu-methanobactin or free Cu and accumulation of intracellular Cu induces the switch from sMMO to pMMO utilization. **c.** Cu detoxification systems expressed by pathogenic bacteria. Bacteria encode multiple mechanisms to detoxify the cytoplasm or periplasm from excess Cu including expression of Cu efflux systems, periplasmic multicopper oxidases and cytoplasmic Cu chaperones. As indicated by the numerous transcriptional activators and repressors depicted, many bacteria express several independently regulated Cu detoxification systems, which provide a graded response to Cu toxicity.

Evolutionary perspectives on nutrient metal acquisition and pathogenesis

The direct impact of nutritional immunity on human infectious diseases becomes clear when considering patients with inherited defects in transition metal homeostasis. To date this is primarily restricted to defects in Fe homeostasis, although inherited disorders in Cu (Wilson's disease) and Zn (hyperzincemia/hypercalprotectinemia) homeostasis have been described. Hypercalprotectinemia, thought to be an inherited condition, is associated with autoimmunity but it remains to be determined whether these patients experience alterations in their ability to fight infections (121, 256). In contrast, it is well established that patients with Fe overload conditions are often susceptible to numerous infectious diseases. For example, frequent transfusions in patients with thalassemias and other chronic anemias lead to excess Fe that predisposes these patients to infections (156, 295). Patients with inherited or acquired forms of the Fe storage disorder, hemochromatosis, are particularly susceptible to infections with enteric Gram-negative pathogens such as *Vibrio vulnificus* and *Yersinia enterocolitica* (96, 174). Interestingly, macrophages from patients with the inherited form of hemochromatosis resulting from the C282Y mutation in the gene *HFE* are very low in Fe. This observation led to the hypothesis that these patients are resistant to infection by intracellular pathogens such as *S. typhi*, the causative agent of typhoid fever, and *Mtb*, the replication of which depends on intracellular Fe pools. If this is the case, resistance to some pathogens may provide evolutionary pressure to maintain this allele within the population (300).

The existence of bacterial receptors that specifically recognize Fe or heme-binding proteins of their preferred or obligate hosts exemplifies the central role for nutritional immunity in the host-pathogen relationship. For example, *Staphylococcus*

aureus IsdB preferentially binds human hemoglobin over hemoglobin from other species, demonstrating that *S. aureus* has evolved to recognize hemoglobin from its primary host with greater affinity (230, 282). This interaction plays an important role in pathogenesis as *S. aureus* preferentially utilizes human hemoglobin as an Fe source and transgenic mice expressing human hemoglobin are more susceptible to *S. aureus* infection in an IsdB-dependent manner (230). The structural basis for IsdB binding to human hemoglobin has not been determined. However, the co-crystal structure of IsdH NEAT domain 1 with human hemoglobin demonstrates interactions with several residues that differ between human and mouse hemoglobin and thus may mediate preferential recognition of the human protein (150). Host Fe source preference is not unique to *S. aureus* as other bacterial pathogens that preferentially colonize humans also grow better on human hemoglobin compared to hemoglobin from other species (230). In addition, the obligate human pathogens *N. meningitidis* and *N. gonorrhoeae* express the transferrin binding receptors TbpA and TbpB, which preferentially recognize human transferrin (261, 311). Species specificity appears to be dictated by interactions between TbpA with residues on transferrin that are unique to the human protein (206). Both the examples of IsdB from *S. aureus* and TbpA from *Neisseria spp.* introduce the intriguing possibility that polymorphisms in human hemoglobin or human transferrin may impact susceptibility or resistance to infection.

Conclusions and areas for ongoing or future study in nutritional immunity

Advances in our understanding of nutritional immunity and the requirements of pathogens for transition metal homeostasis have led to numerous clinical and industrial

applications. Cu has been used to prevent bacterial overgrowth on industrial surfaces and introduced into numerous medical devices to reduce the risk of bacterial infections (29, 41, 190). In addition, siderophores have been used therapeutically in patients with Fe overload disorders, and chalkophores show promise in treating Wilson's disease, an inherited copper storage disorder (276, 314).

It is clear that nutrient limitation by the host and nutrient acquisition by bacteria are crucial processes in the pathogenesis of infectious diseases. Likewise, transition metal intoxication has emerged as an important component of host defense while bacterial detoxification systems are necessary for pathogenesis. To date, much of the work in nutritional immunity has focused on transition metals. However, bacterial pathogens also rely on their hosts for additional nutrients such as carbon, nitrogen and sulfur. Emerging evidence suggests that successful adaptation to the host environment depends on the ability to take advantage of the available or predominant carbon sources (109, 233, 250, 279, 305). This is particularly true of intracellular pathogens whose nutrient pool is the host cell cytoplasm (79, 236). Unlike nutrient metal restriction by the host, it remains to be determined whether specific mechanisms to limit non-metal nutrients are components of nutritional immunity.

As the field of nutritional immunity progresses many important questions remain open. Bacterial transition metal acquisition systems have been extensively characterized for their roles in virulence. Despite this fact, the precise mechanisms through which nutrient metal starvation impact bacterial processes has not been clearly defined. This represents an area for active ongoing investigation. One recent example is the demonstration that Mn chelation by calprotectin inhibits bacterial superoxide defenses (136). *S. aureus*

encodes two Mn-dependent superoxide dismutases (SODs). Treatment with calprotectin sensitizes *S. aureus* to superoxide generating compounds by limiting Mn availability and thus reducing SOD activity. Furthermore, *S. aureus* is more sensitive to neutrophil killing following exposure to calprotectin. These findings lead to a model in which neutrophils deliver a double hit to *S. aureus* by delivering calprotectin to the site of infection (i) where calprotectin chelates available Mn and Zn (ii). Mn chelation by calprotectin reduces SOD activity (iii), thereby sensitizing *S. aureus* to ROS generated by the neutrophil (iv) (**Figure 5**). Given the important role for Mn in resistance to oxidative stress in other bacteria, as well as the possibility that Zn chelation by CP could inhibit Cu/Zn-SODs, this model may be generally applicable to numerous pathogens (210).

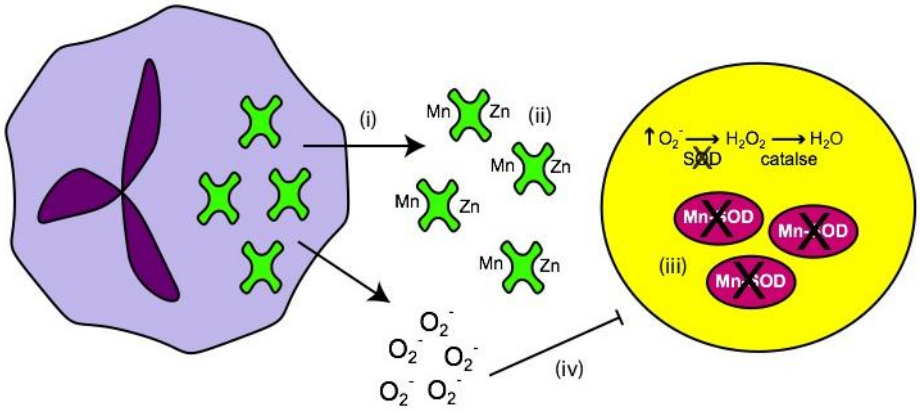

Figure 5. Overview of the impact of CP on *S. aureus* superoxide defenses.

Bacterial genomes encode a multitude of predicted metal-dependent enzymes, however many of their functions and metal co-factor requirements have not been experimentally validated. Moreover, whether additional host proteins contribute to nutrient limitation and the contribution of metalloproteins to processes such as immune cell recruitment, trafficking and activation remain to be determined. Metals have a tremendous impact on the outcome of all host-microbe interactions. Therefore, defining

the mechanisms and molecular machinery at play during the struggle for nutrient metal has the potential to uncover new therapeutic targets for the treatment of both plant and animal infections.

A version of the following chapter (*Chapter II: Acinetobacter baumannii increases tolerance to antibiotics in response to extracellular NaCl*) was previously published in *Antimicrobial Agents And Chemotherapy*, 2010, 54: 3, 1029–1041| doi: 10.1128/AAC.00963-09.

Copyright © 2010, American Society for Microbiology. All Rights Reserved.

II. *Acinetobacter baumannii* increases tolerance to antibiotics in response to extracellular NaCl

Introduction

Acinetobacter baumannii is well adapted to the hospital environment where infections caused by this organism are associated with significant morbidity and mortality. Genetic determinants of antimicrobial resistance have been described extensively, yet the mechanisms through which *A. baumannii* regulates antibiotic resistance have not been defined. An extensive regulatory capacity is encoded within the genome of *A. baumannii,* which likely contributes to this organism's ability to adapt to a broad range of environmental conditions. Based on these facts, we hypothesize that *A. baumannii* must possess mechanisms to sense and respond to the external environment, and that the associated regulatory systems may contribute to antibiotic resistance in this organism. In an attempt to identify the regulatory mechanisms governing resistance in *A. baumannii* we first sought to identify environmental signals encountered within the hospital environment or the human host that contribute to antibiotic resistance. We examined sodium chloride (NaCl) specifically as NaCl is ubiquitous within the hospital environment and within the human host, and is found at varying concentrations in drug formulations, wound dressings, intravenous fluids, body fluids and on the surface of the skin, among other sites. Through proteomic and transcriptional analyses our work establishes that NaCl, and more broadly monovalent cations, are important environmental signals sensed by *A. baumannii*. Specifically, NaCl exposure induces a regulatory

cascade that ultimately results in decreased susceptibility to antibiotics of distinct classes. Our data further demonstrate that this response to NaCl is conserved among MDR clinical isolates and that NaCl-induced antibiotic tolerance is likely multi-factorial, being mediated through both transcriptional and post-translational regulation of cell envelope composition. Taken together, these data demonstrate that *A. baumannii* regulates its intrinsic antibiotic resistance profile in response to a commonly encountered environmental signal, underscoring the adaptability of this organism to growth within the hospital environment and within its host.

Materials and Methods

Bacterial strains, media and antibiotics

The reference strain ATCC 17978 and the sequenced clinical strain AYE were obtained from the American Type Culture Collection (Manassas, Virginia). Clinical isolates were obtained from the University of Nebraska Medical Center (Omaha, NE). *A. baumannii* strain AB0057 was a gift from Dr. Robert Bonomo (Case Western Reserve University, Cleveland, OH) and *A. baumannii* strains AB900 and AB307-0294 were gifts from Dr. Anthony Campagnari (State University at Buffalo, Buffalo, NY). All experiments were performed using the reference strain ATCC 17978 unless otherwise specified. Bacteria were routinely maintained on Mueller Hinton Agar (MHA) or broth (MHB). All antibiotics and the efflux pump inhibitor Phenyl-Arginine β-naphthylamide (PAβN) were obtained from Sigma-Aldrich (St. Louis, MO). Stock solutions of antibiotics were made in water, stored at -80 °C and thawed on ice prior to use.

SDS-PAGE analysis of supernatant proteins

Overnight cultures of *A. baumannii* ATCC 17978 were diluted 1:100 in Luria Broth (LB) +/- 200 mM NaCl or MHB (without NaCl) and MHB supplemented with NaCl or KCl to final concentrations of 50, 90, 150 or 300 mM and incubated at 37 °C with shaking at 180 rpm. Bacteria were harvested by centrifugation and supernatants were collected and filtered through 0.22 μm syringe filters (Millipore Corporation, Billerica, MA) to remove residual cells. Proteins were precipitated from the supernatants by addition of cold trichloroacetic acid (TCA) to a final concentration of 20 % (v/v) and the samples were incubated at 4 °C overnight. Precipitated proteins were pelleted by centrifugation (20 minutes, 10,500 x *g*), washed once with cold ethanol (100 %) and resuspended in Laemmli sample buffer (62.5 mM Tris, 10 % v/v glycerol, 2 % wt/v sodium dodecylsulfate, 5 % v/v 2-mercaptoethanol, 0.001 % wt/v bromophenol blue) (24). Proteins were resolved by SDS-PAGE in 15 % polyacrylamide gels and visualized by staining with Coomassie Brilliant Blue (Pierce, Rockford, IL).

Protein sample preparation for proteomic analysis

For proteomic analyses, *A. baumannii* was cultured as above in LB +/- 200 mM NaCl. Proteins were precipitated from filtered supernatants by addition of ammonium sulfate to 80 % saturation and incubating with constant mixing at 4 °C for 4 hours. Precipitated proteins were pelleted by centrifugation (10,500 x *g*, 20 minutes) and resuspended in 600 μl Tris-buffered saline (150 mM NaCl, 10 mM Tris, pH 7.6). The samples were dialyzed into Tris buffer (20 mM Tris pH 7.5, 100 mM NaCl, 1 mM EDTA, 0.02 % sodium azide) overnight, mixed with Laemmli sample buffer and electrophoresed

approximately 2 cm into a 15 % polyacrylamide gel. Gels were stained with Colloidal Blue, destained with water, and the entire protein-containing region was excised and subjected to in-gel trypsin digestion using a standard protocol [Ham 2005]. Briefly, the gel regions were washed with 100 mM ammonium bicarbonate for 15 minutes and the proteins were reduced with 5 mM DTT in fresh ammonium bicarbonate for 20 minutes at 55° C. After cooling to room temperature, iodoacetamide was added to 10 mM final concentration and placed in the dark for 20 minutes at room temperature. The solution was discarded and the gel pieces washed with 50 % acetonitrile/50 mM ammonium bicarbonate for 20 minutes, followed by dehydration with 100 % acetonitrile. The liquid was removed and the gel pieces were completely dried, re-swelled with 0.8 □g of modified trypsin (Promega, Madison, WI) in 100 mM NH_4HCO_3 and digested overnight at 37 °C. Peptides were extracted by three changes of 60 % acetonitrile/0.1 % trifluoroacetic acid, and all extracts were combined and dried *in vacuo*. Samples were reconstituted in 30 □L 0.1 % formic acid for LC-MS-MS analysis.

LC-MS-MS Analysis and Protein Identification

Resulting peptides were analyzed using a Thermo Finnigan LTQ ion trap instrument equipped with a Thermo MicroAS autosampler and Thermo Surveyor HPLC pump, Nanospray source, and Xcalibur 2.0 SR2 instrument control. Peptides were separated on a packed capillary tip (Polymicro Technologies, 100 □m X 11 cm) with Jupiter C18 resin (5 □m, 300 Å, Phenomenex) using an in-line solid-phase extraction column (100 □m X 6 cm) packed with the same C18 resin [using a frit generated with liquid silicate Kasil 1 (Cortes 1987)] similar to that previously described (25). The flow

from the HPLC pump was split prior to the injection valve to achieve flow-rates of 700 nL-1000 □L/min at the column tip. Mobile phase A consisted of 0.1 % formic acid and Mobile phase B consisted of 0.1 % formic acid in acetonitrile. A 95 min gradient was performed with a 15 min washing period (100 % A for the first 10 min followed by a gradient to 98 % A at 15 minutes) to allow for solid-phase extraction and removal of any residual salts. Following the washing period, the gradient was increased to 25 % B by 50 min, followed by an increase to 90 % B by 65 min and held for 9 min before returning to the initial conditions. Tandem spectra were acquired using a data-dependent scanning mode in which one full MS scan (*m/z* 400-2000) was followed by 9 MS-MS scans. Tandem spectra were searched against the *Acinetobacter* subset of the UniRef100 database using the SEQUEST algorithm. The database was concatenated with the reverse sequences of all proteins in the database to allow for the determination of false positive rates. Protein matches were preliminarily filtered using the following criteria: cross-correlation (X_{corr}) value of ≥ 1.0 for singly charged ions, ≥ 1.8 for doubly charged ions, and ≥ 2.5 for triply charged ions. A ranking of primary score (RSp) of ≤ 5 and a preliminary score (Sp) of ≥ 350 were also required for positive peptide identifications. Once filtered based on these scores, all proteins identified by less than two peptides were eliminated, resulting in false positive rates of < 1 %. SEQUEST output was then filtered using IDPicker using a false positive ID threshold (default is 0.05 or 5 % false positives) based on reverse sequence hits in the database. Protein reassembly from identified peptide sequences is done with the aid of a parsimony method recently described by Zhang *et al*., which identifies indiscernible proteins (protein groups) that can account for the identified peptides (310). Only proteins present in each of three independent samples

were considered in subsequent analyses. The relative abundance of each protein was estimated by counting total spectra corresponding to each protein ID and normalizing first to the size of the predicted protein and subsequently to spectral counts for EF-Tu. EF-Tu was selected for sample normalization as this protein is a highly abundant cytoplasmic protein that is constitutively expressed under a wide range of tested conditions and its abundance in culture supernatants was not expected to change in response to NaCl (unpublished data). Data from three independent samples were averaged for each condition (low and high NaCl) and statistically significant differences were determined by Student's *t* test ($p \leq 0.05$).

Growth conditions for bacterial RNA isolation

Overnight cultures of *A. baumannii* strain ATCC 17978 were diluted 1:100 in fresh medium (LB for microarray only and TSB or MHB for quantitative RT-PCR) or medium supplemented with 150 or 200 mM NaCl. Cultures were grown at 37 °C to early exponential and stationary phases then mixed with an equal volume of ice-cold ethanol:acetone (1:1) or with two volumes RNA protect bacterial reagent, and stored at -80 °C. For RNA isolation, mixtures were thawed on ice and cells were collected by centrifugation. Cells were disrupted either mechanically or by enzymatic lysis. For mechanical disruption, cell pellets were washed once and suspended in TE buffer (10 mM Tris-HCl, 1 mM EDTA, pH 7.6). Cell suspensions were transferred to lysing matrix B tubes (MP Biomedicals, Solon, OH) and were lysed by two cycles of mechanical disruption in a FP120 shaker (Thermo Scientific, Waltham, MA) at settings 5.0 and 4.5 for 20 s. Cell debris was removed by centrifugation at 16,000 x *g* at 4 °C for 10 min. For

enzymatic lysis, bacterial pellets were suspended in TE buffer containing 15 mg/ml lysozyme and 20 mg/ml proteinase K (QIAGEN, Valencia, CA) and incubated at 37 °C for 1 hour. Following mechanical or enzymatic lysis total RNA was isolated from cell lysates using Qiagen RNeasy® Mini columns following the manufacturer's recommendation for prokaryotic RNA purification (QIAGEN, Valencia, CA). RNA concentrations were determined spectrophotometrically (OD_{260} 1 = 40 μg/ml).

GeneChip® Analyses

Ten micrograms of each RNA sample was reverse transcribed, fragmented, 3' biotinylated, and hybridized to an *A. baumannii* GeneChip®, following the manufacturer's recommendations for antisense prokaryotic arrays (Affymetrix, Santa Clara, CA). The GeneChips® used in this study, PMDACBA1, are custom-made microarrays that were developed based on the genomic sequence of *A. baumannii* strain ATCC 17978 and all additional unique *A. baumannii* GenBank entries that were available at the time of design (270). In total, 3731 predicted *A. baumannii* open reading frames and 3892 ATCC17978 intergenic regions greater than 50 base pairs in length are represented on PMDACBA1. GeneChip® data for biological replicates were normalized, averaged, and analyzed using GeneSpring GX 7.3.1 Analysis Platform software (Agilent Technologies; Redwood City, CA). Genes that were considered differentially expressed in response to NaCl exhibited ≥ 2-fold increase or decrease in transcript titer in comparison to mock treated cells, were determined to be "present" by Affymetrix algorithms during the induced condition, and demonstrated a significant change in expression ($p \leq 0.05$) as determined by Student's *t* test. Transcripts demonstrating

significant changes were divided based on whether they were up-regulated or down-regulated and organized according to the Cluster of Orthologous Groups (COG) functional classifications (***Appendix I,* Tables 12 and 13**).

Quantitative RT-PCR confirmation of microarray results

To validate the results of the microarray analyses, five predicted transporters and two transcriptional regulators for which transcripts were increased in response to NaCl were selected for confirmation by quantitative real-time reverse transcriptase PCR. To confirm that NaCl exerted similar changes in gene expression in MHB, we examined expression of representative transporters that were up-regulated in high NaCl in the array, as well as *carO*, which was down-regulated in NaCl. Reverse transcription was carried out on 2 μg total RNA using 200 units M-MLV reverse transcriptase and 1 μg random hexamers according to the manufacturer's protocol (Promega, Madison, WI). Real-time PCR was performed using Platinum® SYBR green qPCR SuperMix-UDG (Invitrogen, Carlsbad, CA). Each 20 μl reaction contained 10 μl SuperMix, 200 nM primers, and 10 ng cDNA template (0.01 ng template for 16S rRNA). Primers for real-time PCR are listed in *Appendix I,* **Table 11**. The efficiency of each primer pair was determined by carrying out RT-PCR on serial dilutions of cDNA and the specificity was verified by melting curve analyses (95°C for 1 minute followed by melting at 1°C decrements for 10 seconds from 95°C to 35°C). Following verification of primer efficiency and specificity, RT-PCR analyses were routinely carried out according to the following amplification protocol: 50 °C for 2 minutes (UDG incubation), 95 °C for 2 minutes and 40 cycles of 95 °C for 15 seconds, 58 °C for 30 seconds and 72 °C for 30 seconds in an iQ5 Real-Time PCR

Detection System (Bio-Rad). Data were analyzed using iQ5 Optical System Software, version 2.0 (Bio-Rad) and relative quantification was determined by the $\Delta\Delta C_t$ method normalizing to 16S rRNA.

Growth curve and MIC analyses of antimicrobial resistance

Overnight cultures of *A. baumannii* were diluted 1:100 in MHB without NaCl and grown to an OD_{600} of 0.4. The cultures were then diluted to a final cell density of 10^5 CFU/ml in 100 μl MHB or MHB supplemented with NaCl (150 mM) or KCl (150 mM) with or without the following antibiotics: amikacin, 4.5 mg/L; gentamicin, 1.125 mg/L; colistin, 0.75 or 1.5 mg/L, imipenem, 0.0625 mg/L; or levofloxacin, 0.09 mg/L. These antibiotic concentrations were selected because they were at or just below the inhibitory concentration for *A. baumannii* strain 17978 grown without NaCl. For efflux inhibition assays, *A. baumannii* was incubated with the efflux pump inhibitor PAβN (60 mg/L) for 30 minutes at room temperature prior to addition of antibiotics. The growth curves were performed in triplicate in 96-well, round-bottom plates (Corning Inc., Corning, NY), incubating the cultures for 12 hours at 37°C with shaking at 180 rpm. Bacterial growth was monitored by measuring the optical density of the culture at 600 nm at 2-hour intervals. Minimum inhibitory concentrations were determined by broth microdilution according to NCCLS standards except that medium (MHB) was supplemented with 150 mM NaCl where indicated.

Results

A. baumannii secretes antibiotic resistance determinants and virulence factors in response to NaCl.

To investigate the response of *A. baumannii* to external signals that may be encountered within the hospital environment or upon infection of the human host, we first examined proteins released into culture supernatants upon exposure of *A. baumannii* to a variety of conditions. Tested conditions included several types of rich growth media (tryptic soy broth [TSB], Luria broth [LB], brain-infusion broth, brain-heart infusion broth), iron limitation in rich or minimal media, pH ranging from 5.5-8.5, and high concentrations of NaCl (**Figure 6** and data not shown). Of these conditions, we noted the most striking difference in supernatant protein profiles when *A. baumannii* was cultured in high NaCl. Specifically, supplementation with 200 mM NaCl produces an overall increase in proteins released into culture medium (**Figure 6**).

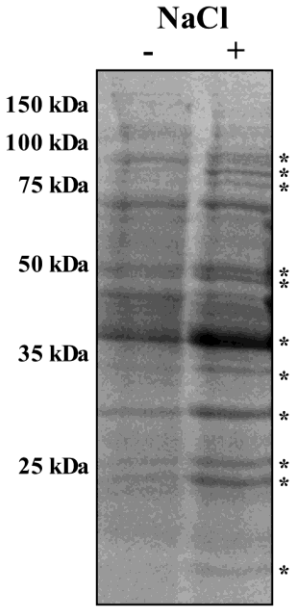

Figure 6. NaCl induces increased release of proteins into culture supernatants.

Total protein was precipitated with trichloroacetic acid from filtered supernatants of *A. baumannii* grown to stationary phase in LB (-) or LB supplemented with 200 mM NaCl (+) and resolved by SDS-PAGE in 15 % polyacrylamide gels. * = bands that increase in high NaCl.

To rule out the possibility that the increased abundance of protein in culture media was the result of increased cell lysis or disruption of the bacterial membrane, we assessed membrane damage upon NaCl exposure. Propidium iodide-staining of cells taken at several time points upon culture in low or high NaCl

followed by flow cytometric analyses showed no significant difference in the proportion of stained cells (membrane-compromised), to unstained cells (live, membrane intact) (data not shown). These results suggest that the increased release of proteins into the extracellular environment upon culture in NaCl is independent of cell lysis or membrane damage. To determine if this response involved a subset of proteins or represented a global increase in protein secretion, we identified secreted proteins from *A. baumannii* grown in LB +/- 200 mM NaCl by liquid chromatography/tandem mass spectrometry (LC/MS/MS). Searching resultant tandem spectra against *Acinetobacter* sequences led to positive identification of approximately 60 proteins in *A. baumannii* supernatants (**Table 3**; for complete experimental details and data analysis, see *Chapter II,* Materials and Methods). These proteins were comprised predominantly of membrane and periplasmic proteins with few predicted cytoplasmic proteins, further confirming that the increased abundance of proteins upon NaCl exposure is not due to increased cell lysis. Notably, a large number of the identified proteins were differentially secreted in response to NaCl (**Table 3**). Outer membrane proteins were overrepresented among proteins that increased significantly in high NaCl, while intracellular proteins involved in metabolism and protein folding generally showed little changes between the two conditions. We predict that the lack of change in intracellular proteins between the two conditions reflects the fact that these proteins are not likely secreted. Rather, identification of these proteins in supernatants likely results from a limited amount of cell lysis that occurs during normal bacterial growth in both conditions. Interestingly, proteins associated with antibiotic resistance also increased significantly in high NaCl. These were CarO and the 33-36 kDa outer membrane protein (omp), which are two porins with predicted roles in antibiotic

transport through the outer membrane. CarO has been shown to form non-selective pores and loss or inactivation of this porin has been associated with increased resistance to carbapenems (163, 181, 247). The 33-36kDa omp has not been characterized as extensively as CarO, however loss of this predicted porin has also been associated with resistance to carbapenems in *A. baumannii* (54). In addition to these two porins we observed a significant increase in the abundance of two chromosomally encoded beta-lactamases (AmpC and OXA-95) and outer membrane protein A (OmpA). OmpA has been implicated in virulence, both in cell culture and animal models of *A. baumannii* pathogenesis, and is modeled to contribute to biofilm formation (50-52, 91). These changes in protein abundance in culture supernatants suggest that *A. baumannii* regulates expression and/or secretion of specific proteins in response to NaCl. Furthermore, the large number of outer membrane proteins and proteins associated with antibiotic resistance suggests that the response to NaCl in *A. baumannii* may have an impact on antibiotic resistance.

Table 3: Proteins identified by LC/MS/MS analysis of supernatants from *A. baumannii* cultured in LB or LB + 200 mM NaCl.

Accession #	Description	Average Spectral Count[a]		*p*-value[b]	Predicted MW (kDa)
		High NaCl	Low NaCl		
Outer Membrane					
YP_001085848	**Outer membrane protein A**	1.605	0.355	0.033	38.4
YP_001085848	**Outer membrane protein A**	6.282	1.091	0.022	38.4
YP_001085848	**Outer membrane protein A**	14.415	2.104	0.018	38.4
YP_001085848	**Outer membrane protein A**	2.380	0.465	0.008	38.4
YP_001086308	**putative outer membrane protein**	6.629	1.083	0.044	25.6
YP_001085614	**peptidoglycan-associated lipoprotein**	1.564	0.209	0.032	20.8
YP_001083918	**putative outer membrane protein**	3.332	0.863	0.018	22.5
YP_001085744	**outer-membrane lipoproteins carrier protein**	1.581	0.393	0.042	25.1
YP_001084998	putative outer membrane protein	0.161	0.036	0.100	91.9
YP_001084997	**putative outer membrane protein**	1.866	0.908	0.005	8.2
YP_001085452	lipoprotein	0.274	0.110	0.191	29.9
Antibiotic Resistance					
YP_001083108	putative RND type efflux pump involved in aminoglycoside resistance	2.764	0.881	0.101	36.7

YP_001086288	**33-36 kDa outer membrane protein - associated with carbapenem resistance**	1.753	0.338	0.033	34.0
YP_001085388	beta-lactamase (AmpC)				
YP_001083548	carboxy-terminal protease for penicillin-binding protein	0.453	0.273	0.304	80.4
YP_001085752	RND family drug transporter (AdeK)	0.160	0.082	0.115	52.9
YP_001085752	**RND family drug transporter (AdeK)**	0.445	0.082	0.022	52.9
YP_001084546	**beta-lactamase OXA-95**	0.739	0.166	0.021	31.4
YP_001085557	**29 kDa outer membrane protein (CarO)**	1.132	0.263	0.036	29.0
YP_001085388	**beta-lactamase (AmpC)**	0.271	0.071	0.041	46.4
Hypothetical Proteins					
YP_001085392	**hypothetical protein**	1.399	0.308	0.019	44.6
YP_001084326	hypothetical protein	2.091	1.128	0.169	18.8
YP_001084552	**putative signal peptide**	1.078	0.358	0.008	20.8
YP_001085962	putative signal peptide, metallo-beta-lactamase superfamily	0.385	0.309	0.410	31.9
YP_001084993	**putative signal peptide**	0.398	0.197	0.037	30.9
YP_001084084	**putative Signal Peptide (Contains OsmY region)**	0.665	0.133	0.048	24.7
YP_001083928	outer membrane lipoprotein	1.100	0.269	0.152	12.2
YP_001083365	hypothetical protein	0.666	0.223	0.053	14.7
Protein Synthesis/Chaperone Proteins					
YP_001083352	protein chain elongation factor EF-Tu	1.000	1.000	---	44.5
YP_001083902	elongation factor G	0.212	0.195	0.781	78.8
YP_001085682	60 kDa chaperonin	0.340	0.336	0.912	57.2
YP_001084601	30S ribosomal protein S1	0.179	0.205	0.761	61.1
YP_001085965	chaperone protein dnaK	0.138	0.152	0.871	69.5
YP_001084218	ATP-dependent protease, Hsp 100	0.057	0.081	0.575	95.3
YP_001083134	thiol:disulfide interchange protein	0.460	0.142	0.155	23.2
YP_001086079	50S ribosomal protein L3	0.317	0.193	0.213	22.5
Bacterial Programmed Cell Death					
YP_001085817	bacteriolytic lipoprotein entericidin B	3.731	0.661	0.176	5.0
YP_001085544	putative serine protease	0.416	0.127	0.200	50.2
Cell Wall Biosynthesis					
YP_001086026	putative lytic murein transglycosylase, soluble	1.048	0.832	0.234	76.5
YP_001085967	putative membrane-bound lytic murein transglycosylase	0.526	0.430	0.706	47.9
YP_001085340	**membrane-bound lytic murein transglycosylase B**	0.481	0.183	0.036	36.9
Glucose Metabolism					
YP_001083999	aldose 1-epimerase precursor	4.167	2.989	0.236	41.5
YP_001084980	**glucose dehydrogenase**	2.795	1.313	0.031	14.8
YP_001084980	**quinoprotein glucose dehydrogenase-B precursor**	0.979	0.487	0.023	52.8
YP_001084927	**enolase**	0.118	0.183	0.025	46.4
TCA cycle					
YP_001085734	succinyl-CoA ligase [ADP-forming] subunit alpha	0.179	0.403	0.067	30.7
YP_001085733	succinyl-CoA synthetase beta chain	0.192	0.329	0.383	41.4
YP_001085497	isocitrate dehydrogenase	0.116	0.077	0.551	82.5
YP_001083613	aconitate hydratase 1	0.055	0.060	0.896	100.3
Electron Transport Chain					
YP_001084520	**glutamate/aspartate transport protein**	4.596	0.855	0.025	32.1
YP_001083240	**ATP synthase subunit beta**	0.109	0.190	0.023	50.3
Q6FAL6	**glutaminase-asparaginase**	0.613	0.122	0.050	37.9

YP_001086024	malate dehydrogenase	0.239	0.294	0.442	35.4
YP_001083238	ATP synthase subunit alpha	0.098	0.121	0.453	56.0
Antioxidant					
YP_001084237	**alkyl hydroperoxide reductase, C22 subunit**	0.264	0.410	0.025	20.7
Other					
YP_001085613	Protein TolB precursor	1.085	0.648	0.705	46.4
YP_001085247	CsuA/B	0.922	0.860	0.774	18.7
YP_001084991	protein RecA	0.145	0.232	0.301	37.8
Q6F9W2	host factor I for bacteriophage Q beta replication	0.321	0.317	0.956	17.1

[a]Spectral counts were averaged from three independent replicates after first normalizing to the size of the expected protein and subsequently to an internal constitutively expressed protein (EF-Tu).
[b]*P*-values were determined by Student's *t* test. Boldface type indicates proteins that exhibit a statistically significant difference in abundance between the low and high NaCl samples.

NaCl induces up-regulation of putative efflux transporters.

The results of our proteomic analyses of supernatant proteins suggest that *A. baumannii* orchestrates the release of proteins into culture media upon exposure to high concentrations of NaCl. To determine if these changes are transcriptionally mediated we sought to determine the global transcriptional response to NaCl by microarray analyses. *A. baumannii* was cultured as above in LB +/- 200 mM NaCl. RNA was isolated from stationary phase bacteria and analyzed by hybridization to Affymetrix GeneChip® arrays. Over 150 genes were found to be significantly up-regulated in response to NaCl (*Appendix I*, **Table 12**). Genes involved in inorganic ion transport and metabolism, secondary metabolite biosynthesis, transport and catabolism, and transcriptional regulation were among those most highly represented in the up-regulated transcripts. We also observed up-regulation of several genes associated with pilus formation and a cluster of genes involved in biosynthesis and transport of the siderophore acinetobactin, which is involved in resistance to iron starvation (74). Interestingly, we observed down-regulation of *carO* and the 33-36kDa Omp (6.4-fold and 2.7-fold, respectively; *Appendix I*, **Table 13**) and constitutive expression of OmpA, AmpC and OXA-95, all of which were

increased in abundance in the proteomic analyses of culture supernatants. These results suggest that the increased presence of these proteins in culture media is not likely controlled at the transcriptional level. Given that many of the proteins that increased in abundance in culture supernatants showed decreased transcript levels, it is possible that release of these proteins represents a post-translational mechanism for down-regulating their membrane abundance.

One class of genes in which many members were up-regulated is that of putative efflux transporters. Approximately 20% of the up-regulated transcripts belong to genes encoding putative transport proteins (**Table 4 and Figure 7A**). The overrepresentation of transporter genes in the up-regulated transcripts is striking and to our knowledge has not been observed in other bacteria in which global transcriptional responses to NaCl or osmotic stress have been investigated (18, 290). Of the 33 transcripts encoding components of 25 distinct transporters that increased in high NaCl, 18 (14 distinct transporters) belong to families in which members have been associated with transport of antibiotics or other toxic compounds (179, 181, 275). These include the Resistance-Nodulation-Division family (RND), the Drug/Metabolite Transporter family (DMT), the ATP-binding Cassette (ABC) family and the Major Facilitator Superfamily (MFS). In addition, two genes (A1S_2141 and A1S_1814) are predicted to encode transporters for K^+ or Na^+, respectively (**Figure 7a**). To validate the microarray results we selected a subset of genes for confirmation by quantitative RT-PCR. Specifically, we selected five transporters with predicted roles in antibiotic resistance, as well as two TetR-family transcriptional regulators that were significantly up-regulated in the high NaCl condition (*Appendix I,* **Table 12**). Representative qPCR results are given in **Figure 7b**, which

confirmed that the tested transcripts were increased in high NaCl as compared to the low NaCl condition. Notably, five transcripts displayed a dose-response to NaCl with a further increase in expression at 260 mM NaCl as compared to 200mM NaCl. Taken together, these results demonstrate that NaCl induces significant changes in gene expression in *A. baumannii*. Furthermore, these results demonstrate extensive regulation of efflux transporters upon NaCl exposure, which may contribute to antibiotic resistance.

Table 4: Predicted transporters that were found to be significantly upregulated in response to NaCl by microarray analysis

Locus tag	Description	Fold-induction[a]
A1S_1769	**putative RND family drug transporter**	2.9
A1S_2304	**putative RND family drug transporter**	2.9
A1S_2932	**heavy metal efflux pump (CzcA)**	2.6
A1S_2934	**heavy metal RND efflux outer membrane protein (CzcC)**	16.0
A1S_3445	**putative RND family cation/multidrug efflux pump**	3.2
A1S_0565	**DMT family permease**	2.1
A1S_1323	**DMT family permease**	3.4
A1S_1992	**DMT family permease**	2.6
A1S_1284	ABC-type nitrate/sulfonate/bicarbonate transport systems	2.3
A1S_1286	ABC-type nitrate/sulfonate/bicarbonate transport systems	10.1
A1S_1287	ABC nitrate/sulfonate/bicarbonate family transporter	2.0
A1S_1361	ABC-type spermidine/putrescine transport system	2.2
A1S_1362	ABC-type Fe^{3+} transport system	9.4
A1S_1722	putative ATP-binding component of ABC transporter	2.0
A1S_2378	putative ABC transporter	14.3
A1S_2388	putative ferric acinetobactin transport system	4.0
A1S_2389	putative ferric acinetobactin transport system	23.2
A1S_1751	**$AdeA_2$ membrane fusion protein**	25.9
A1S_1752	**$AdeA_1$ membrane fusion protein**	8.7
A1S_2376	**putative ABC-type antimicrobial peptide transport system**	11.8
A1S_2377	**putative ABC-type multidrug transport system**	3.6
A1S_3420	**MATE family drug transporter**	12.1
A1S_0596	**putative transporter**	2.2
A1S_0915	**putative MFS transporter**	3.2
A1S_1331	major facilitator superfamily	2.7
A1S_1739	major facilitator superfamily	4.1
A1S_2198	**putative mutlidrug resistance protein**	2.4
A1S_3146	**multidrug efflux transport protein**	17.6
A1S_1209	putative benzoate transport porin (BenP)	16.2
A1S_1814	predicted Na^+-dependent transporter	2.5
A1S_1956	putative amino acid permease	2.0
A1S_2141	potassium-transporting ATPase A chain	2.4
A1S_3251	transporter, LysE family	3.9

[a]Fold-induction in transcript level in LB + 200 mM NaCl relative to LB without NaCl supplementation. Boldface type indicates transporters with predicted roles in extrusion of antibiotics or other toxic compounds from the cell.

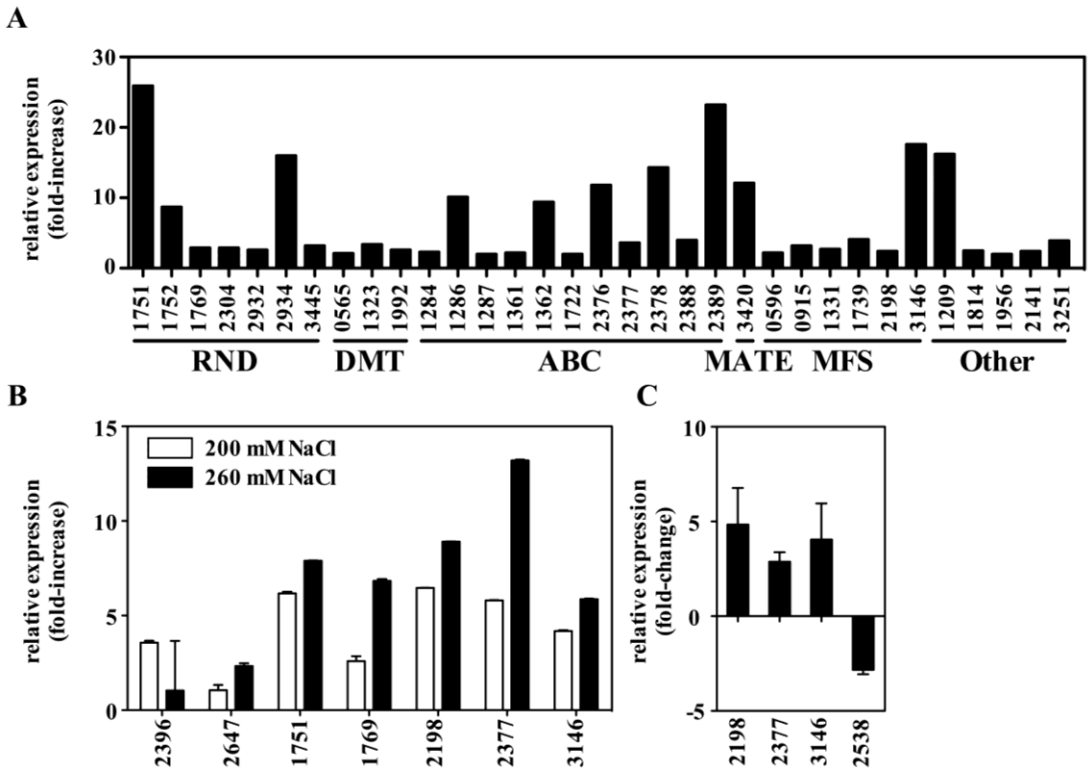

Figure 7: *A. baumannii* up-regulates putative efflux transporters upon culture in high NaCl media

A) RNA was extracted from *A. baumannii* grown to stationary phase in LB or LB supplemented with 200 mM NaCl. The fold-change in transcript levels determined by microarray analyses are shown for putative transporters that increased significantly in *A. baumannii* upon culture in LB supplemented with 200 mM NaCl relative to *A. baumannii* cultured without NaCl supplementation. RND = Resistance-Nodulation-Division; DMT = Drug/Metabolite Transporter; MFS = Major Facilitator Superfamily; MATE = Multidrug and Toxic Compound Extrusion family; ABC = ATP-Binding Cassette superfamily; **B)** Fold-change in transcript levels of selected transporters and transcriptional regulatory genes in 200 mM and 260 mM NaCl as compared to media alone as determined by real-time PCR. The fold-change in expression was determined using the $\Delta\Delta C_t$ method. Error bars represent one standard deviation (SD) from the mean and in some cases are too small to be seen. The data are representative of at least three independent biological replicates. **C)** Fold-change in transcript levels of selected genes in MHB + 150 mM NaCl relative to MHB without NaCl as determined by real-time PCR. Error bars represent the mean ± SD. Each bar represents the average of three independent biological replicates. Expression changes comparing MHB + NaCl to MHB alone were statistically significant ($p < 0.05$ by Student's *t* test) for each gene tested.

NaCl induces tolerance to distinct classes of antibiotics.

The changes observed in gene expression and secreted protein profile suggest that the response to NaCl in *A. baumannii* may lead to increased resistance to antibiotics. MHB is the recommended medium for antibiotic susceptibility testing, therefore we first sought to confirm that NaCl induces similar changes in gene expression and protein

secretion in MHB as observed in LB. Furthermore, since MHB is formulated without NaCl, this medium permits improved titration of NaCl concentrations and therefore better resolution of the dose-response to NaCl. Quantitative RT-PCR results demonstrated that NaCl induces increased expression of representative transporter genes as well as down-regulation of the transcript for CarO, further supporting the microarray analyses (**Figure 7c**). *A. baumannii* was cultured in MHB or MHB supplemented with NaCl at concentrations between 50 and 300 mM and the resulting supernatant proteins were examined by SDS-PAGE. Consistent with the results obtained in LB, there was a significant increase in the total abundance of supernatant proteins upon exposure to 300 mM NaCl (**Figure 8**). Furthermore, the amount of protein released into culture supernatants increased in a dose-dependent manner with increasing concentrations of NaCl. These data confirm that NaCl induces similar transcriptional and post-translational regulation of membrane proteins in MHB as in LB, providing the foundation for examining NaCl effects on antibiotic resistance in this medium. Moreover, these data expand upon previous results by demonstrating that the secretion of proteins into culture media increases in a dose-dependent manner with increasing NaCl.

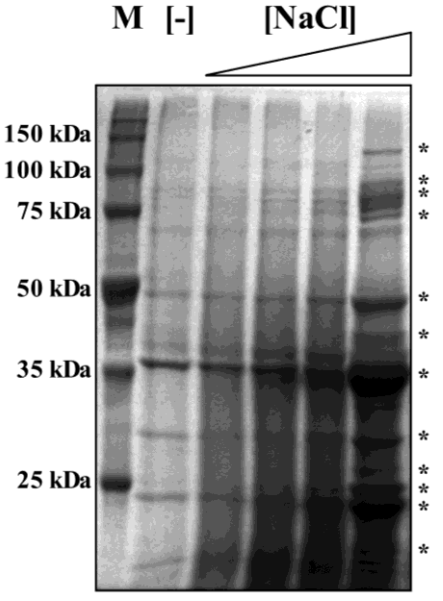

Figure 8. SDS-PAGE analyses of proteins released into culture supernatants.

Total protein was precipitated with trichloroacetic acid from filtered supernatants of *A. baumannii* grown to stationary phase in MHB [-] or MHB supplemented with NaCl to final concentrations of 50 mM, 90 mM, 150 mM and 300 mM and resolved by SDS-PAGE in 15 % polyacrylamide gels. M = molecular mass marker; * = bands that increase with increasing NaCl.

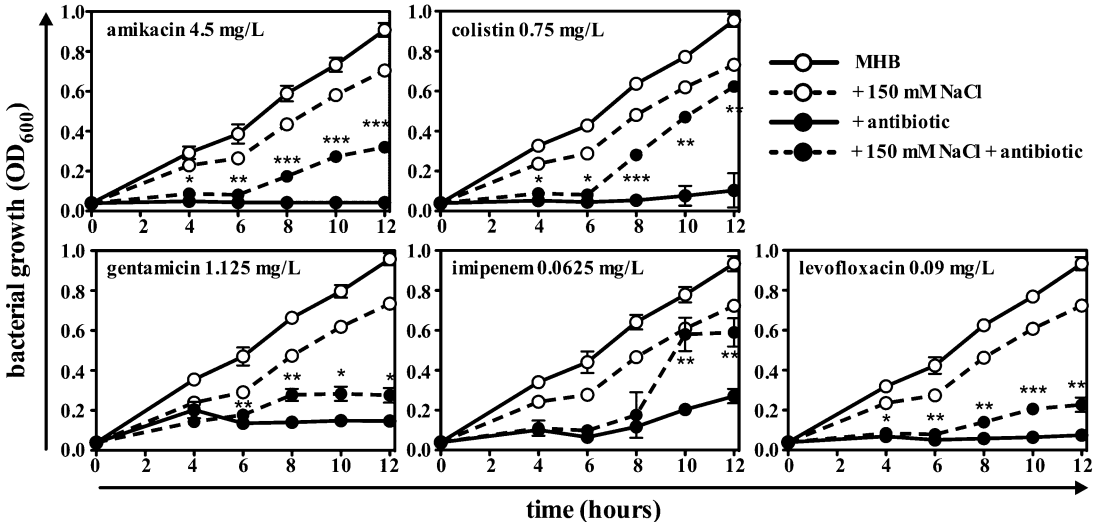

Figure 9. NaCl induces increased tolerance to distinct classes of antibiotics in *A. baumannii*.
A. baumannii strain ATCC 17978 was challenged with amikacin (4.5 mg/L), colistin (0.75 mg/L), gentamicin (1.125 mg/L), imipenem (0.0625 mg/L) or levofloxacin (0.09 mg/L) with (dashed lines) or without (solid lines) NaCl supplementation of culture media to a final concentration of 150 mM. Bacterial growth was monitored by measuring the optical density of the cultures at 600 nm with each point representing the mean ± SD of at least three cultures (error bars may be too small to be seen). Asterisks indicate statistically significant changes in growth upon antibiotic challenge in media containing NaCl compared to media lacking NaCl as determined by Student's *t* test (* $p < 0.05$; ** $p < 0.005$; *** $p < 0.0005$).

To determine whether NaCl impacts antibiotic resistance we determined minimum inhibitory concentrations for antibiotics from several distinct classes. These assays revealed modest increases in the minimum inhibitory concentrations for amikacin, levofloxacin and colistin (3, 1.5 and 2-fold increases, respectively). These changes were not sufficient to raise the MIC above clinical breakpoints for resistance to any of the drugs tested. However, the incremental increase in resistance nonetheless supported the hypothesis that the adaptive response to NaCl impacts susceptibility to antibiotics and suggested that NaCl may induce a tolerant phenotype in *A. baumannii*. To assess tolerance to antibiotics we monitored growth of *A. baumannii* challenged with sub-lethal concentrations of several classes of antibiotics in the presence or absence of NaCl. Growth curve analyses demonstrated that in the presence of physiologic NaCl

concentrations (150 mM), *A. baumannii* displays a significant increase in its ability to resist inhibition by antibiotics from four distinct classes: aminoglycosides (amikacin and gentamicin), quinolones (levofloxacin), carbapenems (imipenem) and polypeptides (colistin) (**Figure 9**). Given that growth is reduced slightly by NaCl alone, the effect of NaCl on antibiotic resistance is even more striking. The protective effect of NaCl is more apparent at late time points, which supports a model in which *A. baumannii* must first adapt to NaCl and this adaptive response results in increased tolerance to antibiotics. Together, the growth curve analyses demonstrate that NaCl induces tolerance to clinically relevant antibiotics.

To determine whether other cations similarly impact tolerance we performed growth curve analyses as above using KCl in the place of NaCl. KCl induces significant tolerance to amikacin, colistin and levofloxacin, comparable to the effect observed with NaCl (**Figure 10A**). Examination of supernatant proteins from *A. baumannii* cultured in KCl concentrations ranging from 50-300 mM revealed that KCl exposure results in increased abundance of proteins in culture supernatants in a similar pattern as that observed for NaCl (**Figure 10B**). We did not observe the same trend in supernatant protein profiles or increased antibiotic resistance upon treatment of *A. baumannii* with high concentrations of sucrose (data not shown). These results suggest that *A. baumannii* may respond to increased concentrations of monovalent ions, rather than to NaCl specifically or osmotic stress more generally.

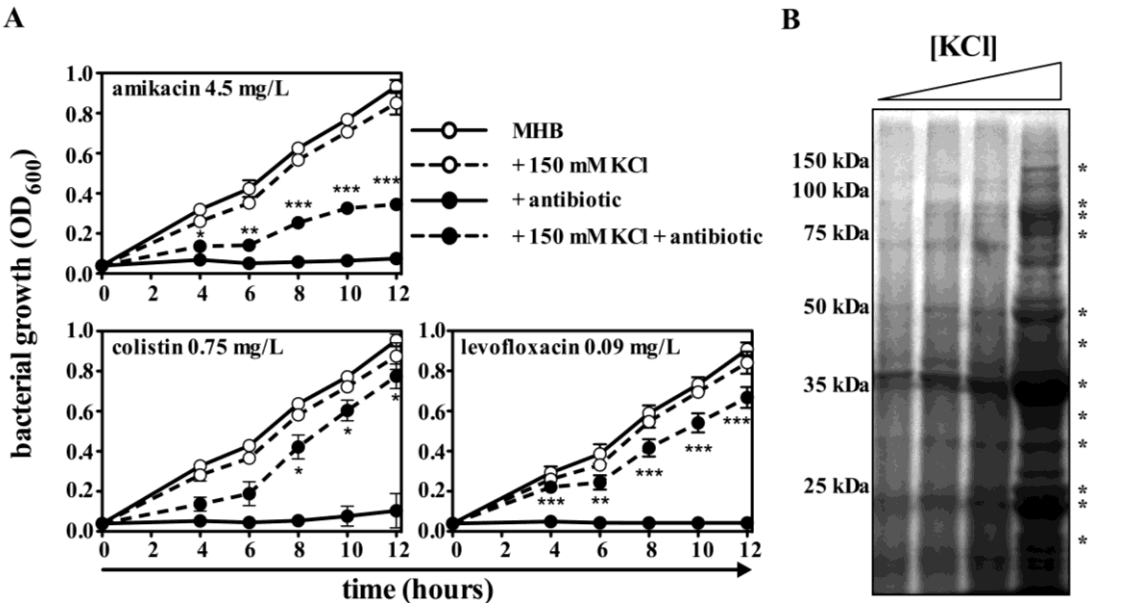

Figure 10. Effects of KCl on resistance to antibiotics and on release of proteins into culture media.

A) Growth curve analyses of *A. baumannii* challenged with antibiotics in MHB (solid lines) or MHB supplemented with 150 mM KCl (dashed lines) at the indicated concentrations. Error bars represent the mean ± 1 SD and may be obscured by the symbol in some cases. Asterisks indicate statistically significant changes in growth upon antibiotic challenge in media containing KCl compared to media lacking KCl as determined by Student's *t* test (* $p < 0.05$; ** $p < 0.005$; *** $p < 0.0005$). **B)** SDS-PAGE of TCA-precipitated proteins from *A. baumannii* culture supernatants. *A. baumannii* was grown to stationary phase in MHB supplemented with 50 mM, 86 mM, 154 mM or 308 mM KCl. * = bands that increase with increasing concentrations of KCl.

Inhibition of efflux reduces NaCl-induced resistance to amikacin and levofloxacin.

Effects of NaCl on resistance to aminoglycosides have been described for several species of both Gram-negative and Gram-positive bacteria (37, 283). While it has been proposed in previous studies that the observed NaCl-induced increase in antibiotic resistance may be the result of passive inhibition of antibiotic uptake by elevated external salt concentration, this has not been conclusively demonstrated (37, 283). In addition, the possibility that a regulated response to NaCl mediates antibiotic resistance has not previously been investigated. The observation that NaCl induces increased expression of efflux pumps introduces the intriguing possibility that the effect of NaCl on antibiotic resistance or tolerance is a regulated process, rather than a passive effect on antibiotic

uptake. Therefore, to determine the contribution of efflux to NaCl-induced antibiotic tolerance we tested whether the efflux pump inhibitor PAβN prevents the NaCl-induced response. PAβN is active against a broad spectrum of efflux pumps and its mechanism of action is thought to involve competitive inhibition (168). We pre-treated *A. baumannii* with 60 mg/L PAβN for 30 minutes in media with or without NaCl then challenged as above with amikacin, colistin, levofloxacin or imipenem. NaCl-induced tolerance to levofloxacin and amikacin were significantly reduced upon pre-treatment of *A. baumannii* with PAβN (**Figure 11**). However, we did not observe a difference in the effect of NaCl on tolerance to imipenem in the presence or absence of the efflux pump inhibitor (data not shown). It is possible that decreased permeation of imipenem into the cell, through loss or decreased expression of CarO and the 33-36 kDa Omp, is a more important mechanism in mediating tolerance to imipenem in response to NaCl. Paradoxically, tolerance to colistin is significantly increased in the presence of PAβN (**Figure 11**). At colistin concentrations of 1.5 mg/L, PAβN induces resistance to colistin regardless of the NaCl content of the media, restoring growth to approximately 75 % of that observed in the absence of colistin (**Figure 11**). Importantly, NaCl alone was not sufficient to induce protection of *A. baumannii* against challenge with 1.5 mg/L of colistin (**Figure 11**). NaCl induced significant resistance to colistin at lower concentrations (0.75 mg/L), preventing assessment of the effect of PAβN on colistin resistance below 1.5 mg/L (data not shown). Taken together, these data demonstrate that antibiotic efflux contributes significantly to NaCl-induced tolerance to levofloxacin and amikacin, while alternative mechanisms are necessary for mediating tolerance to imipenem and colistin.

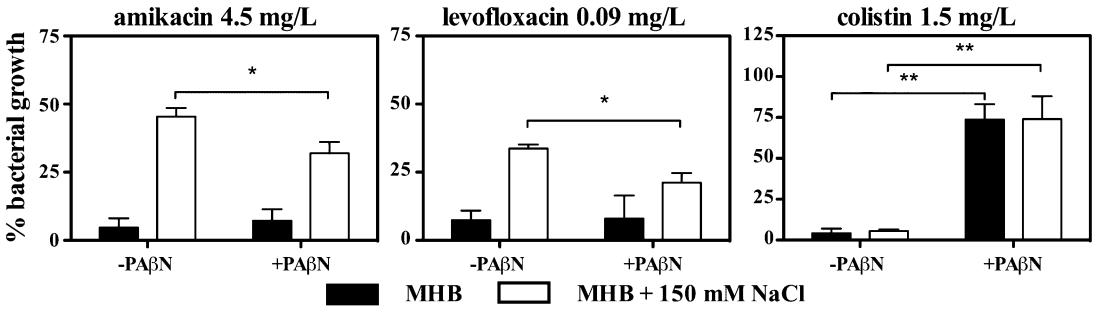

Figure 11. NaCl-induced resistance to levofloxacin and amikacin is due in part to increased antibiotic efflux.

A. baumannii was treated with amikacin, levofloxacin or colistin in MHB (filled bars) or MHB + 150 mM NaCl (white bars) in the presence or absence of 30 mg/L of the efflux pump inhibitor, PAβN. Bacterial growth was monitored for 12 hours and the optical densities of the cultures were normalized to the respective untreated (i.e. antibiotic-free) controls and expressed as the percent bacterial growth. Statistical analysis was performed by Student's *t* test comparing PAβN-treated with respective PAβN-untreated controls. Error bars = ± 1 SD from the mean; * $p < 0.05$, ** $p < 0.005$.

NaCl induces tolerance to colistin in multidrug resistant clinical isolates of *A. baumannii.*

Table 5: Antibiotic susceptibility profiles of clinical isolates obtained from the University of Nebraska Medical Center compared to the reference strain ATCC 17978.

Isolate[a]	Source	Site	Antibiotic Susceptibility																
			SAM	TZP	TIM	ATM	FEP	CTX	CAZ	CRO	AMK	GEN	TOB	CIP	LVX	IPM	MEM	SXT	TET
17978[b]	ATCC	CSF	S	S	-	R	S	-	-	I	S	S	S	S	-	S	S	R	-
510	UNMC	Sputum	R	R	R	R	R	R	R	R	R	R	R	R	I	S	S	R	-
2824	UNMC	Urine	S	R	R	R	R	R	R	R	R	R	R	R	R	S	S	R	R
2898	UNMC	Ankle	R	R	R	R	R	R	R	R	R	R	R	R	I	S	S	R	-
4860	UNMC	Urine	R	-	R	R	R	R	R	R	R	R	R	R	R	S	-	R	R
5191	UNMC	Urine	R	-	R	R	R	R	R	R	R	R	R	R	R	S	-	R	R

[a]Strains in bold are classified as multidrug resistant.
[b]Susceptibility data for the reference strain ATCC 17978 has been published previously (6).
ATCC = American Type Culture Collection, UNMC = University of Nebraska Medical Center, CDC = Centers for Disease Control and Prevention; R = resistant, S = susceptible, ND = not determined; SAM = ampicillin/sulbactam, TZP = piperacillin/tazobactam, TIM = ticarcillin/clavulanate, ATM = aztreonam, FEP = cefepime, CTX = cefotaxime, CAZ = ceftazidime, CRO = ceftriaxone, AMK = amikacin, GEN = gentamicin, TOB = tobramycin, CIP = ciprofloxacin, LVX = levofloxacin, IPM = imipenem, MEM = meropenem, SXT = trimethoprim-sulfamethoxazole, TET = tetracycline

The strain used in the experiments described in the previous sections is a drug-susceptible strain of *A. baumannii* isolated in 1951 (229). Given that recent clinical isolates of *A. baumannii* are resistant to most available antibiotics, we sought to

determine whether NaCl impacts resistance in recent MDR isolates of *A. baumannii.* We specifically investigated whether NaCl induces tolerance to drugs to which the clinical isolates were otherwise susceptible. MDR clinical isolates of *A. baumannii* were obtained from the University of Nebraska Medical Center (**Table 5**). Drug susceptibility profiles were reported by the University of Nebraska Medical Center clinical microbiology laboratory. The MDR phenotype was defined as resistance to three or more of the following antibiotic classes: β-lactam-β-lactamase inhibitor combinations, antipseudomonal cephalosporins (ceftazidime of cefepime), aminoglycosides (gentamicin, amikacin or tobramycin), quinolones (ciprofloxacin or levofloxacin), and carbapenems (imipenem or meropenem). Although MIC data were not available for colistin, resistance to colistin has only been reported in a handful of cases in the literature and colistin is increasingly used in the treatment of MDR *A. baumannii* (148, 223). We therefore sought to determine if NaCl could induce tolerance to colistin in each of the MDR clinical isolates. Growth curves performed in MHB with or without NaCl demonstrated that all of the isolates show similar susceptibility to colistin in the absence of NaCl as that observed with the reference strain. Likewise, all of the *A. baumannii* isolates were protected against 0.75 mg/L colistin in the presence of 150 mM NaCl (**Figure 12**). Similar to the results with the reference strain, the MIC for colistin was increased up to 2-fold in the presence of NaCl for the majority of clinical isolates tested (**Table 6**). Interestingly, UNMC 4860 shows more rapid tolerance to colistin in the presence of NaCl as demonstrated by the growth curve analyses, but the MIC (determined following 24 hours of exposure to drug) actually decreased slightly. To confirm that the conservation of the NaCl-induced response extended to clinical strains from distinct geographic locations, we

also performed MIC assays on two of the recently sequenced MDR isolates (AYE and AB0057) and two of the susceptible isolates (AB307-0294, AB900) all of which showed similar increases in the colistin MIC in response to NaCl (data not shown). These results demonstrate that NaCl-induced colistin tolerance is conserved among recent clinical isolates of MDR *A. baumannii*.

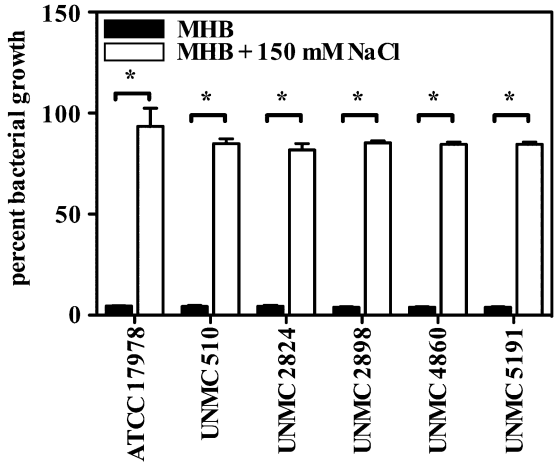

Figure 12. NaCl-induced resistance to colistin is conserved among drug susceptible and multidrug resistant *A. baumannii*.
A. baumannii 17978 and nine clinical isolates were treated with colistin (0.75 mg/L) with (solid bars) or without (open bars) NaCl-supplementation of culture media to a final concentration of 150 mM. Bacterial growth was monitored for 12 hours and the optical densities of the cultures were normalized to growth in the absence of colistin in the respective media (i.e. with or without NaCl). Statistically significant differences comparing media alone to media supplemented with NaCl were determined by Student's *t*-test. Error bars = ± 1 SD from the mean; * $p < 0.005$.

Table 6: Colistin MIC values determined in MHB (-) or MHB supplemented with 150 mM NaCl (+).

Isolate	Source	Site	NaCl	
			-	+
17978	ATCC	CSF	0.75	1.5
510	UNMC	Sputum	0.75	1.5
2824	UNMC	Urine	0.75	1.5
2898	UNMC	Ankle	1	1.5
4860	UNMC	Urine	2	1.5
5191	UNMC	Urine	0.75	1.5

Discussion

In this study we have taken a multifaceted approach to demonstrate that *A. baumannii* responds to extracellular NaCl by regulating membrane proteins through transcriptional and post-translational mechanisms. Furthermore, the response to NaCl results in tolerance to four distinct classes of antibiotics. Both NaCl and KCl were found to induce similar changes in protein secretion and antibiotic resistance, suggesting that the signal sensed by *A. baumannii* is not NaCl itself, but may be monovalent cations or anions. We have not directly tested whether it is the cationic or anionic component that is required for the NaCl/KCl-induced response; however it has been reported previously that Na^+ and K^+, but not Cl^- induce resistance to tobramycin in *Pseudomonas aeruginosa* and *Burkholderia cenocepacia* (283). We therefore hypothesize that monovalent cations are the relevant signal for *A. baumannii*.

Our data demonstrate that NaCl affects the expression of a large number of genes; however the transcriptional response does not support a model whereby NaCl induces an osmotic stress response at the concentrations evaluated. Up-regulation of a choline dehydrogenase (A1S_0925) may have a role in osmoprotection; however, apart from A1S_0925, the transcriptional changes observed did not resemble osmotic stress responses of *P. aeruginosa* or *Escherichia coli* (18, 298). In particular, the up-regulation of 18 genes encoding components of putative drug efflux pumps was distinctive. The transcriptional response to NaCl in *A. baumannii* therefore appears to be unique as a direct response to NaCl. Interestingly, the quality of the NaCl-response in *A. baumannii* bore similarity with the transcriptional changes described in *B. cenocepacia* upon culture

in sputum from patients with cystic fibrosis, including up-regulation of genes encoding putative efflux transporters, oxidoreductases and iron acquisition systems (75). It is unclear to what extent the NaCl concentration in sputum may have been responsible for inducing the transcriptional response in *B. cenocepacia*. It is interesting, however, that both responses appear to involve resistance to antibiotics as well as physiologic stress conditions such as oxidative stress and iron limitation.

Previous studies investigating the effect of NaCl on antibiotic resistance have shown that NaCl and KCl induce increased resistance to aminoglycosides while other antibiotics have not been evaluated (283). The mechanisms proposed for mediating NaCl-induced resistance involve passive effects of NaCl such as interference with antibiotic uptake. Our data reveal that NaCl-induced antibiotic tolerance may involve an active response mediated through a regulated transcriptional program as well as post-transcriptional or post-translational regulation of membrane protein expression and/or secretion.

As described above, our microarray analyses highlighted the up-regulation of 33 genes representing 25 putative transporters of which 12 are annotated as putative drug transporters. These include the membrane fusion component of the AdeABC efflux pump (AdeA), as well as the major facilitator superfamily transporter CraA. AdeABC mediates resistance to a number of antibiotics in *A. baumannii* although the function and regulation of this pump have not been investigated in *A. baumannii* strain ATCC 17978 (179, 181). It was recently determined that CraA is conserved among *A. baumannii* strains sequenced to date and mediates intrinsic chloramphenicol resistance (247). Given the number of putative efflux pumps that are up-regulated in response to NaCl, it is possible that the

antibiotic tolerance observed is the result of the combined action of several or all of these pumps.

The contribution of efflux to antibiotic tolerance in response to NaCl is supported by the fact that tolerance to levofloxacin and amikacin can be partially reversed upon the addition of a non-selective efflux pump inhibitor. Failure to see complete reversal of the resistance phenotype may be due to an inability to achieve complete efflux inhibition at the PAβN concentrations used; however increasing the concentration of PAβN leads to growth inhibition independent of antibiotic treatment. An alternative explanation for the failure to completely reverse NaCl-induced antibiotic resistance is that resistance to levofloxacin and amikacin may be mediated by multiple overlapping mechanisms, which is supported by our data that suggest that NaCl has a broad effect on gene expression.

Proteomic analyses of *A. baumannii* culture supernatants highlighted an increased abundance of several porins for which loss or inactivation has been associated with resistance to carbapenems. Based on the known functions of the putative 29 kDa porin (CarO) and the 33-36 kDa porin, their release in response to NaCl may result in decreased permeability to antibiotics. These proteins were down-regulated at the transcriptional level, suggesting that *A. baumannii* may shed these proteins to decrease their membrane abundance. Similarly, it was recently reported that *A. baumannii* down-regulates membrane expression of $OmpA_{32}$ (33-36kDa Omp), $OmpA_{38}$, CarO and OmpW in response to sub-MIC tetracycline, without alteration in transcript levels for the corresponding genes (310). Increased abundance of these Omps in culture supernatants suggested that down-regulation occurs through selective release from the membrane and the authors proposed that this might be related to tetracycline resistance, although

resistance was not directly evaluated (310). Consistent with the proposed model, we have demonstrated that *A. baumannii* is more resistant to several classes of antibiotics upon exposure to NaCl, including imipenem which would be predicted based on the known role of CarO and the 33-36kDa Omp in resistance to carbapenems (54, 163, 232, 269). In addition, the same group has recently published the results of proteomic analyses of outer membrane vesicles (OMVs) produced by *A. baumannii*. Proteins enriched in OMVs included homologues of CarO, OmpA and AmpC (152). The overlap between our proteomic results and the OMV proteome suggest that monovalent cations may induce increased membrane vesicle production, but this remains to be determined.

The finding that *A. baumannii* increases resistance to colistin upon exposure to NaCl is of considerable clinical interest as colistin is currently the last resort agent against MDR *A. baumannii*. Colistin resistance is uncommon clinically, with only a handful of case reports emerging out of Asia (148, 223). The mechanisms involved in mediating resistance to colistin have not been fully elucidated in *A. baumannii*. Proteomic profiles have been determined for *in vitro*-generated colistin-resistant *A. baumannii*; however these strains developed gross perturbations in general metabolic functions complicating interpretation of the results (87). A recent advancement in our understanding of colistin resistance in *A. baumannii* was the finding that mutations in the two-component system PmrAB lead to colistin resistance (7). The mechanism of PmrB-dependent colistin resistance is thought to result from increased expression of the lipid A-modifying phosphoethanolamine transferase, PmrC. In addition, low pH and ferric iron induce colistin resistance, yet this was not associated with increased expression of the *pmrCAB* operon, suggesting that additional mechanisms exist for mediating colistin resistance in *A.*

baumannii (7). Earlier studies in *E. coli* have suggested there may be a relationship between osmotic stress responses and responses to polymyxin antibiotics (161, 211). While the transcriptional response presented herein does not support a typical osmotic stress response, it is possible that the intersection of osmotic adaptation and polymyxin resistance may converge on an as-yet-unidentified pathway in *A. baumannii.* Notably, we did not observe increased tolerance to colistin in the presence of NaCl with *E. coli* (data not shown), further suggesting that the response to NaCl in *A. baumannii* may be distinct. Perhaps more intriguing is the observation that the efflux pump inhibitor PAβN induced significant resistance to colistin over and above that induced by NaCl. Importantly, we have determined that the combined effect of PAβN and NaCl results in an increase in the MIC to ≥ 4 mg/L, which is the breakpoint for colistin resistance in *A. baumannii* (data not shown). The mechanism of PAβN-induced colistin resistance remains elusive. It is possible that the interaction of PAβN with efflux transporters promotes stability of the outer membrane or that inhibition of efflux itself stabilizes the flux of solutes and water that would otherwise contribute to colistin-mediated cell death. Alternatively, PAβN may induce additional transcriptional changes that confer protection against colistin. Further elucidation of the mechanisms of both cation-induced antibiotic tolerance as well as PAβN-mediated colistin resistance may provide insight into the normal resistance response to colistin in *A. baumannii*.

Clinical implications of cation-induced antibiotic tolerance.

NaCl is ubiquitous within the hospital environment suggesting that *A. baumannii* encounters this signal within its hospital niche. The finding that *A. baumannii* becomes

more resistant to clinically relevant antibiotics in response to NaCl concentrations encountered within the human host highlights intriguing questions regarding the implications of these findings to the clinical setting. Our data suggest that MIC determined *in vitro* might be discrepant with the inducible tolerance of *A. baumannii* when exposed to NaCl or KCl within the human body. Although the magnitude of change in resistance to antibiotics was not as large as that described with constitutive over-expression of a broad-specificity efflux pump, the incremental increase in resistance may be sufficient to promote tolerance among otherwise susceptible isolates within the body. In this way, the response to NaCl might enhance the bacterium's ability to persist until conditions are more favorable for growth or until additional resistance determinants can be accumulated. In addition, local concentrations of electrolytes such as NaCl or KCl in specific tissues such as the urinary tract may exceed serum concentrations and may complicate eradication of *A. baumannii* from these sites. Finally, given that NaCl induces tolerance to a broad spectrum of antibiotics and that the response to colistin appears to be conserved among multidrug-resistant clinical isolates, targeting the regulatory systems responsible for mediating antibiotic resistance in response to NaCl may have therapeutic potential in combination with conventional antibiotics. This strategy might be particularly beneficial in combination with drugs such as colistin that possess narrow therapeutic windows by decreasing the dose required for efficacy thus limiting associated toxicity.

This work demonstrates that an extracellular signal encountered by *A. baumannii* results in increased antibiotic tolerance. This extends previous observations regarding the effects of NaCl on aminoglycoside resistance by demonstrating that in *A. baumannii* NaCl and KCl induce tolerance not only to aminoglycosides but also to levofloxacin,

imipenem (NaCl) and colistin. We have also demonstrated that *A. baumannii* regulates membrane protein expression and secretion at transcriptional and post-translational levels in response to a ubiquitous, non-antibiotic signal, and we demonstrate that this response results in increased antibiotic resistance. Further work to identify the systems responsible for sensing and adapting to NaCl or other monovalent cations and translating this signal into an increased resistance phenotype will provide valuable insight into the intrinsic mechanisms of adaptation and resistance in *A. baumannii* and holds promise in identifying novel therapeutic targets.

III. Genetic determinants of intrinsic colistin tolerance in *Acinetobacter baumannii*

Introduction

Colistin, or polymyxin E, is a cationic peptide antibiotic that is increasingly used to treat multidrug resistant infections. In many cases, colistin is the only remaining antibiotic effective in treating MDR *A. baumannii*. Resistance to colistin is currently rare in *A. baumannii*; however, heteroresistance and complete resistance to colistin have been reported clinically (128, 148, 170, 191). It is feared that the increasing use of colistin coupled with clonal spread of colistin-resistant isolates will quickly lead to widespread resistance to this drug. As evidence of this possibility, in Korea, rates of colistin resistance as high as 27.9% have been noted (148). These facts underscore the need to define the mechanisms mediating colistin resistance in *A. baumannii*. Mutations in the two-component system PmrAB are thought to induce colistin resistance by activating the two-component system ultimately leading to increased phosphoethanolamine modification of lipid A (7, 24, 169, 222). This modification reduces the net negative charge of the outer membrane thus reducing the affinity of colistin for this subcellular target. Colistin resistance can also be mediated by complete loss of LPS production through mutations or insertions in the genes encoding the lipid A biosynthesis machinery (105, 191). Notably, colistin resistance is most commonly mediated by adaptive and occasionally reversible mutations rather than by acquisition of resistance determinants (7, 24). Moreover, evolution of resistant isolates through adaptive mutations during antibiotic therapy is well documented in *A. baumannii* (114, 170). Taken together, these

facts highlight the adaptability of this organism to the hospital environment and suggest that *A. baumannii* possesses intrinsic mechanisms to resist the initial onslaught of antibiotic therapy until adaptive mutations or resistance determinants can be acquired. However, the molecular basis for these intrinsic resistance mechanisms in *A. baumannii* is largely unknown.

In *Chapter II* the data demonstrating that *A. baumannii* increases tolerance to four distinct classes of antibiotics, including colistin, in response to physiologic concentrations of monovalent cations were discussed (112). In this chapter I describe the identification of over 30 genes involved in this inducible colistin tolerance in *A. baumannii*. A majority of these genes converge on pathways and systems involved in osmotolerance including those involved in compatible solute and cell envelope biosynthesis as well as in protein folding. We further define the function of one of these genes, *lpsB*, and demonstrate the role for LpsB in cationic antimicrobial peptide resistance and pathogenesis in the lung.

Methods

Bacterial strains and reagents

A. baumannii strain ATCC 17978 (Ab7978) was obtained from the American Type Culture Collection and was used for all experiments unless otherwise noted. Primers and plasmids used in this study are listed in **Table 7**. Colistin sulfate was obtained from Sigma-Aldrich (St. Louis, MO). LL-37 was purchased from Phoenix Pharmaceuticals.

Table 7. Primers and plasmids used in this work.

Primers		
lpsbKO1	CCCGGATATCGTGATGCAATTTGGTATAGTCC	
lpsbKO2	CCCGCATATGACTGATGACCTTGTGCAACC	
lpsbKO3	CCCGCATATGCCTCAGCACAGTGGTTTAACC	
lpsbKO4	CCCGGATATCTAACGCGCTTGCTGTACTTG	
lpsbKO6	TTACCAATGCACAAGCTCAAG	
lpsbKO7	TAACCTTGACGGTTCTACGC	
X430F	GCCCGAATTCGCTTCGTATCGCACCAACTC	
X430R	CCCGGATATCTCAATTCAATACACTTTGATATAGCTC	
Plasmids		
pKOlpsB	*lpsB* inactivation vector in pEX100T	This work
plpsB	*lpsB* complementation vector	This work
pWH1266	*E. coli-A. baumannii* shuttle vector	(117)
pAB001	Derivative of pMU125 lacking *gfp*	This work
pMU125	Derivative of pWH1266 containing *gfp*	(73)
pEX100T	*sacB* conjugative plasmid for gene replacement	(74)

Transposon library screen and mutant identification

A transposon library was generated in Ab17978 using the EZ-Tn5 <R6Kγ*ori*-KAN-2> transposome system (Epicentre) as described previously (125). A total of 8,000 mutants were screened for loss of NaCl-induced colistin resistance by challenging with

1.5 mg/L colistin in Mueller Hinton Broth (MHB) with or without supplementation with 150 mM NaCl. Mutants that demonstrated no growth after 24 hours in NaCl-supplemented media were selected for further analysis. Phenotypes were confirmed by growth curve analysis in MHB ± NaCl ± colistin as described previously (112). With selected mutants, minimum inhibitory concentrations for colistin and LL-37 were determined by broth microdilution in MHB using established methods (1).

The locations of transposon insertions were determined by rescue cloning as described previously (74). Functional predictions for the disrupted genes were based on annotations in NCBI and The SEED (219). The SEED viewer was used to analyze genomic contexts surrounding the transposon integration sites. Predicted operons are based on proximity and orientation of predicted open reading frames as well as conservation of the genetic organization in multiple species.

Metabolic pathway analysis

Metabolic pathway analysis was carried out using the Kyota Encyclopedia of Genes and Genomes (KEGG) pathways program (http://www.genome.jp/kegg/). The database was filtered for genes and pathways predicted to be present in *A. baumannii* 17978 based on gene annotations in NCBI since there is limited experimental data available on this organism.

LPS analysis

Bacteria were harvested from LB agar plates in 150 mM NaCl, normalized to an OD_{600} of 1.5, pelleted and resuspended in lysing buffer (2% SDS, 4% 2-mercaptoethanol,

10% glycerol, 0.1 M Tris-HCl, pH 6.8). Samples were then boiled for 10 min, cooled to 60°C and treated with proteinase K for 1 hour. These samples were electrophoresed through a 15 % acrylamide gel and stained with Pro-Q Emerald 300 LPS stain according to the manufacturer's recommendations (Invitrogen).

Complementation of the LPS synthesis defect in 5A7

The *E. coli-A. baumannii* GFP expression vector pMU125 was modified by digesting with EcoRV to excise GFP and self-ligated to produce pAb001. A 1500 bp fragment including *lpsB* and 500 bp of flanking sequence was amplified from WT genomic DNA using primers X430F and X430R. The product was digested with EcoRI and EcoRV and cloned into the cognate sites of pAb001 to produce p*lpsB*. The complementation vector p*lpsB* was introduced into 5A7 by electroporation as previously described (123).

Site-directed insertional mutagenesis of *lpsB*

In order to assess the contribution of LpsB to pathogenesis in vivo, a strain was first generated in which the gene encoding LpsB was inactivated by allelic replacement. Approximately 1000 bp of DNA sequence on each side of *lpsB* were amplified using primers lpsbKO1 and lpsbKO2 (lpsB-up) or lpsbKO3 and lpsbKO4 (lpsB-down). The flanking sequences, lpsB-up and lpsB-down, were cloned separately into pCR2.1 (Invitrogen) using the TA cloning method specified by the manufacturer. LpsB-down was excised by digesting with NdeI and XhoI and cloned into the cognate sites of pCR2.1-lpsB-up. The combined flanking regions were then excised by digestion with EcoRV and

cloned into SmaI-digested pEX100T to yield pKO-lpsB-UD. The kanamycin resistance gene, *aph*, was amplified from pKAN-2 (Epicentre), digested with NdeI and cloned into the NdeI sites of pKO-lpsB-UD. The resulting vector, pKO-lpsB was introduced into Ab17978 by electroporation and integration of the plasmid was selected by plating on LB agar supplemented with 40 μg/ml kanamycin. Kanamycin-resistant colonies were counter selected on LB agar supplemented with 40 μg/ml kanamycin and 2% w/v sucrose. Loss of the plasmid backbone was confirmed based on positive growth on sucrose-containing plates and failure to grow on LB agar supplemented with 500 μg/ml ampicillin. Integration of *aph* into *lpsB* was confirmed by PCR using primers that anneal outside the region contained in pKO-lpsB (lpsbKO6 and lpsbKO7) and observing a shift in molecular weight corresponding to the insertion of *aph*. Disruption of *lpsB* function was confirmed by SDS-PAGE analysis of LPS from Δ*lpsB*.

Microarray analysis.

Bacterial cultures were grown overnight in Luria-Bertani (LB) medium supplemented with the appropriate antibiotic, diluted in fresh medium and grown at 37°C for 3.5 hours. Cultures were then mixed with an equal volume of ice-cold ethanol-acetone (1:1) and stored at −80°C for RNA processing. For RNA extraction, samples were thawed on ice and total bacterial RNA was released by mechanical disruption and purified using Qiagen RNeasy columns (Qiagen, Valencia, CA), as previously described (112). For microarray analysis, ten micrograms of each RNA sample were reverse transcribed, fragmented and 3′biotinylated as previously reported (25). Resulting labeled cDNA (1.5 μg) was hybridized to custom-made *A. baumannii* GeneChip (PMDACBA1)

according to the manufacturer's recommendations for antisense prokaryotic arrays (Affymetrix, Inc., Santa Clara, CA). Data from three independent biological replicates were analyzed as described in Hood *et al*. (2010). RNA species exhibiting ≥ 2-fold change in expression with titers above background as determined by Affymetrix algorithms in Δ*lpsB* and were found to be statistically differentially expressed (*t*-test $p \leq 0.05$) were reported.

Preparation of bacterial cultures for *in vivo* studies

Bacteria were harvested from log-phase cultures of Ab17978 or Δ*lpsB*, washed and resuspended in phosphate-buffered saline (PBS) and adjusted to 1 x 10^7 CFU/μl. Bacterial cell counts were confirmed post-infection by plating serial dilutions of each inoculation.

***A. baumannii* pneumonia model**

All animal experiments were approved by the Vanderbilt Institutional Animal Care and Use Committee. We have previously established a murine *Acinetobacter* pneumonia model in our laboratory (123). Briefly, six to eight week old, female C57BL/6 mice were anesthetized and infected intranasally with 30 μl of bacterial suspension. Mice were euthanized at 36 hours post infection (hpi) and lungs were aseptically removed, weighed and homogenized in 1 ml sterile PBS. Serial dilutions were plated on LB agar and/or LB agar containing kanamycin (40 μg/ml).

Results

Identification of genes involved in NaCl-induced colistin tolerance

Based on our previous studies demonstrating that NaCl induces increased resistance to colistin, we designed a transposon mutant screen to identify genes involved in mediating this resistance (**Figure 13**). In the primary screen, over 8,000 mutants were tested for loss of NaCl-induced colistin resistance by challenging with 1.5 mg/L colistin in the presence or absence of 150 mM NaCl (**Figure 13a**). Approximately 300 mutants were identified that failed to grow in the presence of NaCl and these mutants were confirmed for their colistin sensitivity by growth curve analyses (**Figure 13b**). The transposon integration sites were determined for all of the mutants that consistently demonstrate increased sensitivity to colistin despite NaCl-supplementation of media (**Figure 13b**). These genomic loci were compared with data from the SEED to assess whether the disrupted genes were found within predicted operons and putative functions were assigned based on annotations in NCBI and the SEED (**Table 8**). These analyses resulted in the identification of 31 mutants with loss of NaCl-induced colistin-resistance.

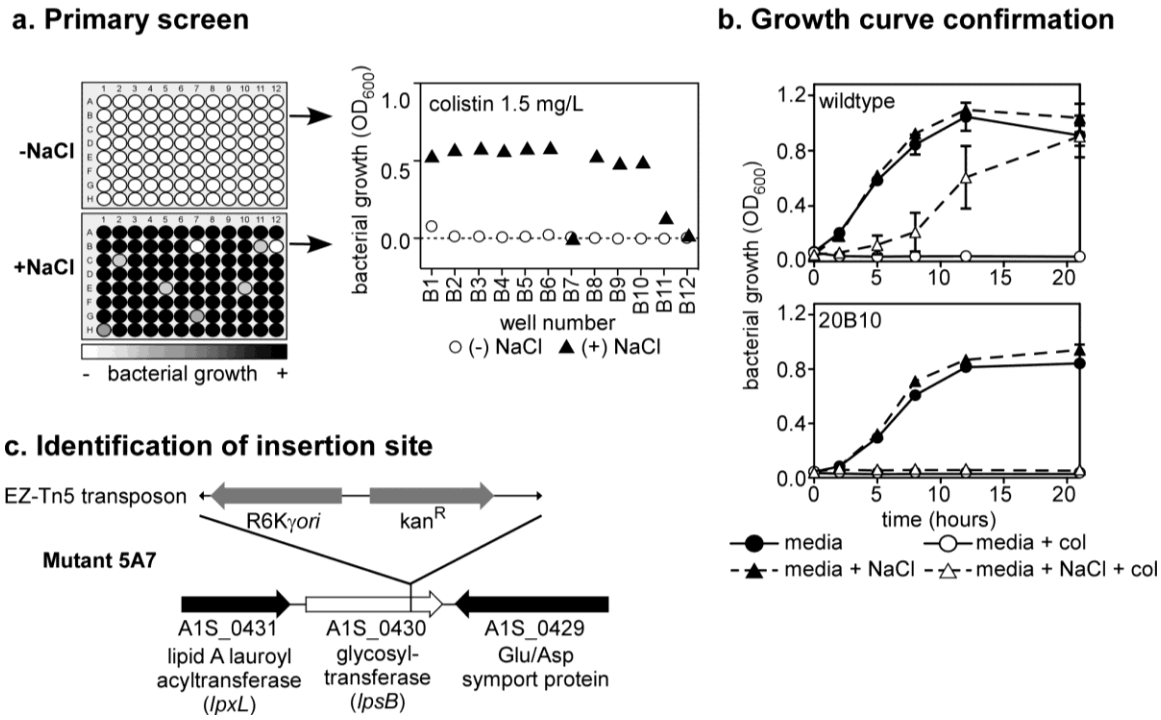

Figure 13. Schematic overview of the transposon library screen to identify genes involved in NaCl-induced colistin resistance.

(a) Bacteria were challenged with 1.5 mg/L colistin in Mueller Hinton Broth (MHB) with or without 150 mM NaCl. Data from a representative plate are shown. (b) Mutants that failed to grow in NaCl-supplemented MHB were confirmed by growth curve analyses. A representative mutant is shown that is inhibited by colistin (col) in the presence of NaCl. (c) The transposon insertion sites were determined for all confirmed mutants. The genomic locus for *lpsB* (5A7) is shown with a schematic of the EZ-Tn5 transposon.

Upon further analysis, it was found that the predicted functions fell into several broad categories (**Table 8**) In particular, genes involved in amino acid transport and metabolism, protein folding, phosphate metabolism and cell envelope biogenesis were over-represented. Interestingly, the genes with predicted roles in amino acid biosynthesis and energy production cluster into three interconnected pathways (**Figure 14**) The amino acid biosynthesis genes are found in pathways leading to production of osmolytes that mediate osmotic tolerance through membrane and protein stabilization (67, 119, 308). These genes include those involved in proline biosynthesis from glutamate and in aspartate metabolism. Genes involved in the citrate cycle were also identified, which can

mediate interconversion of aspartate and glutamate. Taken together, these analyses highlight critical contributions to intrinsic colistin resistance of genes involved directly in maintenance of membrane integrity and protein folding as well as those indirectly involved in these processes through compatible solute synthesis.

Table 8. Transposon mutants with reduced NaCl-induced colistin resistance.

Name	Insertion site	Acc. #	Gene annotation
Phosphate metabolism			
2F12	intergenic	A1S_2445	High-affinity phosphate transport protein (PstB)
		A1S_2444	Putative periplasmic protease
18G3	gene	A1S_3030	Phosphate-inducible protein, phoH-like
22F11	gene	A1S_0462	Putative phosphatase
42F6	gene	A1S_0607	exopolyphosphatase
Envelope biogenesis			
6D2	gene	A1S_2982	YidD
11E4	gene	A1S_2250	Zn-dependent protease with chaperone function
20A5	intergenic	A1S_3424	Putative lipoprotein-34 precursor (NlpB)
5A7	gene	A1S_0430	Putative glycosyltransferase (LpsB)
23E5	gene	A1S_1030	DNA-binding ATP-dependent protease La
19C4	gene	A1S_0499	Putative Fe-S-cluster redox enzyme (Ribosomal RNA large subunit methyltransferase N)
RNA synthesis, processing, modification and degradation			
20A5	intergenic	A1S_3425	Phosphoribosylaminoimidazole-succinocarboxamide
18G3	intergenic	A1S_0531	Putative GTPase
		A1S_0532	Oligoribonuclease
19C4	gene	A1S_0499	Putative Fe-S-cluster redox enzyme (Ribosomal RNA large subunit methyltransferase N)
6D2	gene	A1S_2982	YidD
Amino acid transport and metabolism (Glutamate, Apartate, Alanine), Urea cycle			
22E8	gene	A1S_3185	Glutamate synthase subunit alpha
17H6	intergenic	A1S_1142	Aspartate kinase
		A1S_1143	Hypothetical protein
20B10	gene	A1S_2793	Putative amino-acid transport protein
41C12	gene	A1S_2454	Diaminobutyrate-2-oxoglutarate transaminase
20A2	intergenic	A1S_2023	Hypothetical protein
		A1S_2024	Glutamate 5-kinase
20A1	gene	A1S_3025	Malate dehydrogenase
TCA cycle			
6H4	gene	A1S_2477	monomeric isocitrate dehydrogenase
31A2	gene	A1S_2710	Citrate synthase
Cofactor biosynthesis			
14G3	gene	A1S_0807	8-amino-7-oxononanoate synthase
Multidrug efflux system			
18D2	gene	A1S_0909	Multidrug resistance protein B
20A11	intergenic	A1S_1231	Major facilitator superfamily transporter
		A1S_1232	EsvB
Lipid metabolism			
20B2	intergenic	A1S_3159	Lipase chaperone
		A1S_3160	Lipase
Phage			
37A5	intergenic	A1S_1585	Putative replicative DNA helicase
		A1S_1586	EsvKI
1A1	rDNA		23S ribosomal RNA
20C2	rDNA		16S ribosomal RNA
4A5	rDNA		16S ribosomal RNA
4G1	rDNA		23S ribosomal RNA
6A3	rDNA		16S ribosomal RNA
6H5	rDNA		16S ribosomal RNA

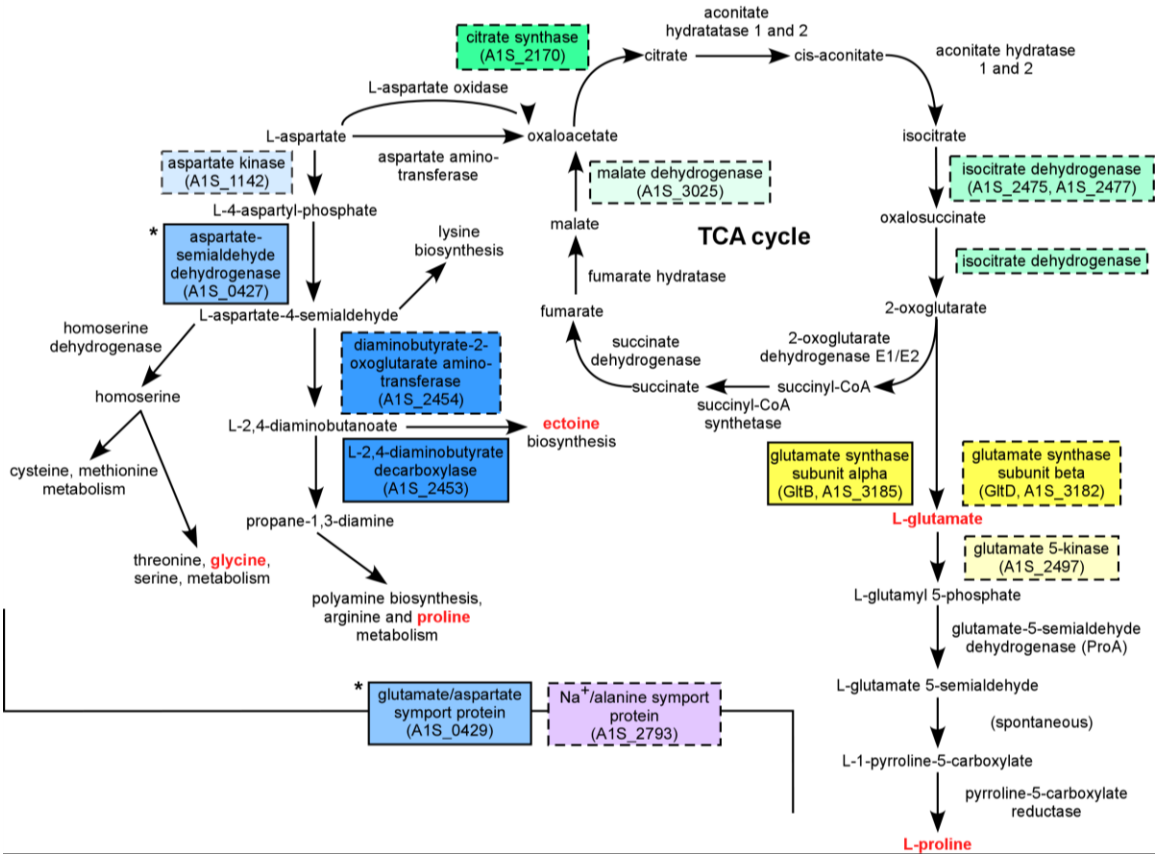

Figure 14. Metabolic pathways disrupted in colistin-sensitive mutants of *A. baumannii*.

Colored boxes indicate enzymes or transporters whose gene or predicted operon was disrupted in one of the colistin-sensitive transposon mutants. Dashed borders indicate genes that were directly disrupted by the transposon insertion or the immediate downstream genes if the insertion was intergenic. Boxes of the same color indicate genes in the same predicted operon. Asterisks indicate genes in a predicted operon upstream of a transposon insertion site. Names of amino acids or compatible solutes that contribute to osmotic protection are indicated with red lettering.

LpsB contributes to colistin resistance.

In mutant 5A7, the transposon disrupts *lpsB*, which encodes a glycosyltransferase involved in synthesis of the lipopolysaccharide (LPS) core (173). SDS-PAGE analyses of LPS from wildtype and 5A7 confirmed that this strain produces a truncated LPS, which is complemented by providing a wildtype copy of *lpsB* in trans (**Figure 15a-b**) (173). The core region of LPS is important for maintaining the structure and integrity of the outer membrane (32). To confirm the role for *A. baumannii* LPS core in mediating resistance to

colistin, we performed kill curve analyses in the presence of increasing concentrations of colistin with or without NaCl. These analyses demonstrate that 5A7 is more susceptible to colistin than WT and that 5A7 lacks NaCl-induced colistin resistance (**Figure 15c**).

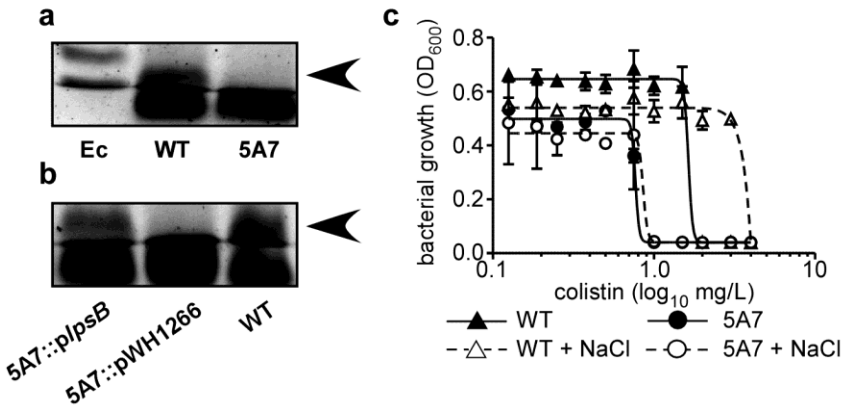

Figure 15. Demonstration of the LPS synthesis defect and colistin sensitivity of 5A7.

(a) SDS-PAGE analysis of LPS purified from WT and 5A7. LPS isolated from *E. coli* (Ec), WT *A. baumannii* and 5A7 was electrophoresed in a 12 % polyacrylamide gel and stained with Pro-Q Emerald 300 LPS stain. A higher molecular weight band is present in the WT lane (arrow), but this band is absent in 5A7. (b) Complementation of the LPS synthesis defect by providing *lpsB* in trans. LPS samples were electrophoresed and stained as in (a). (c) Kill curves comparing colistin sensitivities of WT with 5A7 in media with or without NaCl supplementation (150 mM). The data are presented as the mean ± one S.D. from the mean of at least three biological replicates. In some cases error bars may be obscured by the symbols. Curves were generated by non-linear regression analysis using a least squares fitting method.

Adaptation to chronic membrane instability

Disruption of core LPS biosynthesis in *A. baumannii* leads to increased sensitivity to human serum and detergents (173). These facts suggest that inactivation of *lpsB* compromises outer membrane integrity. Given that colistin acts through disruption of the bacterial membrane, an *lpsB* mutant can serve as a tool to probe the adaptations that allow *A. baumannii* to survive in the presence of chronic membrane perturbation. In order to determine how *A. baumannii* responds to the chronic membrane instability resulting from loss of LpsB function, we first generated a targeted deletion of *lpsB* in Ab17978 (Δ*lpsB*) and confirmed that this mutant produced a truncated LPS molecule similar to

5A7 (**Figure 16a**). We next performed microarray analyses comparing WT Ab17978 with Δ*lpsB* during exponential growth (*Appendix II*, **Table 14**).

A significant proportion of the genes whose expression is altered in Δ*lpsB* are involved in metabolic processes and energy generation within the cell. For example, we observed down-regulation of genes encoding for numerous ribosomal proteins suggesting that protein synthesis may be decreased in the mutant. We also observed down-regulation of genes encoding enzymes involved in fatty acid biosynthesis pathways. Strikingly, some of the most highly up-regulated genes are those involved in phenylacetic acid (PAA) degradation, pyruvate metabolism and the TCA cycle. Overall, these changes suggest a decrease in biosynthetic processes and an overall increase in catabolism and energy generation. These data demonstrate that disruption of *lpsB* profoundly impacts critical cellular processes.

Involvement of LpsB in the pathogenesis of pneumonia.

Colistin shares a similar mechanism of action with antimicrobial peptides of the innate immune system. Cationic antimicrobial peptides (AMPs) are known to be important mediators of host defense at mucosal surfaces. *A. baumannii* LPS stimulates the release of AMPs from respiratory epithelial cells in vitro, suggesting that AMPs may be an important component of host defenses that *A. baumannii* must overcome during infection of the lung (180). We therefore hypothesized that the mechanisms involved in colistin resistance would likewise confer resistance to antimicrobial peptides and contribute to virulence. Furthermore, our microarray analyses demonstrate that disruption of *lpsB* significantly alters critical cellular processes, which may also impact *A.*

baumannii growth within the host. To test the role for LpsB in pathogenesis, we first determined whether disruption of *lpsB* increases sensitivity to antimicrobial peptides of the innate immune system. To do this, we performed kill curves with the human antimicrobial peptide, LL-37. These analyses revealed a significant reduction in the minimum inhibitory concentration of LL-37 for *ΔlpsB* as compared to wildtype (**Figure 16b**). These data establish that LpsB contributes to protection against cationic AMPs of the innate immune system.

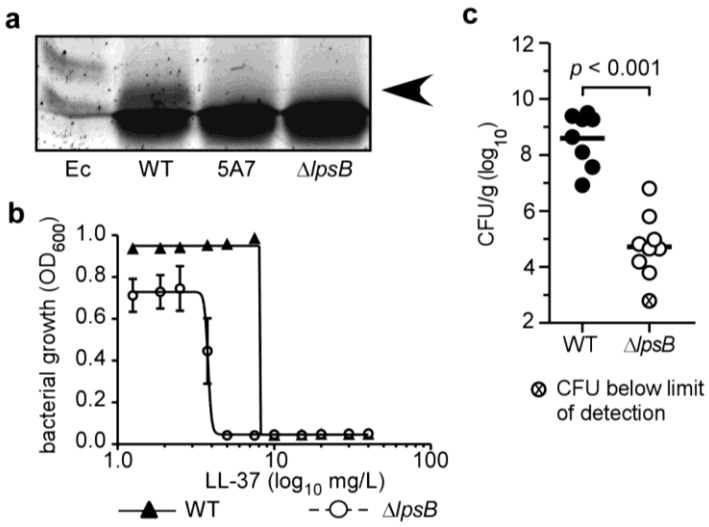

Figure 16. *A. baumannii* strains lacking LpsB are attenuated for virulence in the lung.

(a) SDS-PAGE analysis of LPS from WT, 5A7 and an *lpsB*-deleted strain (Δ*lpsB*). (b) Kill curves comparing LL-37 sensitivities of WT with Δ*lpsB.* The data are presented as the mean ± one S.D. from the mean of at least three biological replicates. In some cases error bars may be obscured by the symbols. Curves were generated by non-linear regression analysis using a least squares fitting method. (c) Bacterial burdens in lungs of mice infected with WT or Δ*lpsB* harvested at 36 hpi. Data are combined from two independent experiments with n = 4-5 mice per group in each experiment. *** $p < 0.001$ as determined by two-tailed, unpaired Student's *t* test. Horizontal bars indicate means for each data set. Red symbols indicate CFU below the limit of detection.

A. baumannii LPS is important in activating the inflammatory response in the lung (147, 180). However, the role for LPS in the pathogenesis of pulmonary infections has not been demonstrated for *A. baumannii*. To elucidate the contribution of *A.*

baumannii LPS to pulmonary infection we intranasally infected mice with WT or Δ*lpsB* and allowed the infection to proceed for 36 hours. Quantification of bacteria in lungs revealed a nearly 4-log reduction in bacterial burden in Δ*lpsB*-infected mice compared to WT (**Figure 16c**). These data establish that LpsB plays a critical role in the pathogenesis of *A. baumannii* pulmonary infections.

Discussion

A. baumannii is emblematic of the looming public health crisis threatening nearly all facets of medical practice. Namely, *A. baumannii* represents the growing burden of infections caused by organisms resistant to most, if not all, conventional antibiotics. This organism has proven particularly challenging due to its ability to persist in the hospital environment, its resistance to both antibiotics and common disinfectants and its propensity to acquire resistance to new antimicrobial agents. The latter fact underscores the adaptability of this organism to the hospital environment and suggests that *A. baumannii* possesses intrinsic mechanisms to respond and adapt to antibiotic treatment.

Colistin resistance in *A. baumannii* is currently rare and typically arises through adaptation of a previously susceptible isolate often during treatment with colistin in vivo. The fact that colistin resistance arises without the acquisition of horizontally transferred resistance determinants suggests that *A. baumannii* possesses intrinsic mechanisms to resist colistin. Furthermore, recent evidence suggests that strains that adapt to colistin treatment must undergo significant changes in physiologic processes in order to maintain the resistance phenotype (105, 170). Taken together, these facts underscore the need to

better understand the inherent mechanisms that contribute to colistin resistance in order to identify possible targets for therapeutic intervention.

We have previously demonstrated that *A. baumannii* increases resistance to colistin in response to physiologic concentrations of NaCl. We have now identified over 30 genes involved in this adaptation in *A. baumannii*. Colistin like other polymyxins, acts by disrupting the cell envelope leading to osmotic lysis of the bacterium by dysregulating the permeability of the bacterial membrane (162, 212, 213). Given the action of colistin it is not surprising that many of the genes identified are involved in processes that protect the bacterium from osmotic stress. For example, we identified several genes with roles in the synthesis of compatible solutes such as proline [Fig. 2]. Importantly, certain compatible solutes not only act as neutral osmolytes, but also exert protective effects by preventing protein misfolding (67, 119, 308). Proline, in particular, is known to protect protein structure at physiologically attainable concentrations. Furthermore, proline synthesis and uptake are typically induced by NaCl (67). Taken together, the results of the transposon mutagenesis screen suggest that bacteria exposed to colistin experience osmotic stress, which can be alleviated through synthesis of compatible solutes and expression of proteases that presumably degrade misfolded proteins. When these systems are inactivated, *A. baumannii* is more susceptible to colistin and NaCl no longer exerts a protective effect.

Upon loss of LpsB function some of the most highly up-regulated genes in Δ*lpsB* are those involved in the tricarboxylic acid cycle and in the phenylacetic acid (PAA) degradation pathway. It is not clear what the source of PAA is in Δ*lpsB*. Protein synthesis appears to be down regulated based on the reduced expression of many genes encoding

for ribosomal proteins. Furthermore, genes encoding for several proteases are up regulated. It is possible that endogenous phenylalanine is being converted to PAA to serve as a substrate for this degradation pathway. Furthermore, we observed up-regulation of a gene encoding for a polyhydroxyalcanoate (PHA) granule-associated protein. These granules are known to be reservoirs for carbon and energy within the cell and some of the PHAs can provide substrates for PAA degradation (92). The significance of this up-regulation is also unclear for *A. baumannii* although the PAA pathway has been implicated in antibiotic resistance in *B. cenocepacia* and it is known to be up-regulated during growth in cystic fibrosis sputum (103, 258). Furthermore, we have demonstrated that the efflux pump inhibitor phenylalanine-beta-naphthylamide (PAβN) paradoxically induces resistance to colistin (112). Although the mechanism has not been determined, it is possible that PAβN is cleaved to yield phenylalanine as a substrate for PAA degradation and that activation of this pathway provides protection against membrane-destabilizing agents.

It has been demonstrated previously that an *lpsB* mutant of *A. baumannii* exhibits decreased competitive fitness during co-infection with WT bacteria in a soft tissue model of infection (173). However, in the soft tissue model the mutant does not exhibit a virulence defect in a single strain infection. The striking difference between the phenotypes of the *lpsB* mutants in pulmonary and soft tissue models of infection suggests that *A. baumannii* has different virulence requirements depending on the infection site. These differences may stem from physical characteristics of the infection site, variation in innate immune factors and differing nutrient availability. It has been established, for example, that *A. baumannii* induces production of antimicrobial peptides at mucosal sites

like the lung (180). The increased sensitivity of Δ*lpsB* to these defense peptides likely contributes to this strain's reduced virulence in the lung. Moreover, we have defined significant changes in genes involved in nutrient acquisition and metabolism in Δ*lpsB*. It is possible that nutritional requirements and availability in the lung may also restrict growth of Δ*lpsB*, particularly if this strain lacks the flexibility to adapt to the host environment. The possibility that nutrient availability impacts both pathogenesis and antibiotic resistance in *A. baumannii* is particularly intriguing as further work in this area may elucidate novel targets for therapeutic intervention.

The rise of extensively drug resistant bacteria that are capable of causing lethal infections is rapidly creating a public health crisis yet therapeutic development has failed to keep pace. *A. baumannii* poses a particular challenge due to the ability of this bacterium to readily acquire resistance to new antibiotics. This fact underscores the adaptability of *A. baumannii* within the hospital and host environments. Targeting mechanisms that mediate the intrinsic antibiotic resistance of *A. baumannii* is therefore a viable strategy in developing novel inhibitors that could serve as adjuncts to our current antibiotic armamentarium.

IV. *Acinetobacter baumannii* transposon mutants redirect host inflammation to promote pathogen clearance.

Introduction

The clinical burden of *A. baumannii* infections is greatly compounded by the high rates of antibiotic resistance observed in this organism. Moreover, as discussed in *Chapters II* and *III, A. baumannii* readily adapts to the hospital environment and readily acquires resistance to new antimicrobial. Considering the propensity of *A. baumannii* to develop resistance to small molecule therapies, development of immune-enhancing therapeutics represents a viable alternative strategy to combat this important emerging pathogen. In order to design therapeutics that augment the host response to infection, it is necessary to understand the components of the immune system that are critical for promoting bacterial clearance. Toward this end, the work described herein addresses this need through the identification of transposon mutants of *A. baumannii* that attenuate WT infection *in vivo*. These strains represent a valuable to tool to understand the host response to *A. baumannii* infection. Moreover, these strains may be valuable as a new class of biologic therapeutic for the treatment or prevention of *A. baumannii* pneumonia.

Methods

Bacterial strains

A. baumannii strain ATCC 17978 (Ab7978) was obtained from the American Type Culture Collection and was used for all experiments unless otherwise noted. *A. baumannii* strain Ab307 was a gift from Dr. Anthony Campagnari (Buffalo, NY).

Transposon library screen and mutant identification

A transposon library was generated in Ab17978 using the EZ-Tn5 <R6Kγ*ori*-KAN-2> transposome system (Epicentre) as described previously (125). A total of 8,000 mutants were screened for loss of NaCl-induced colistin resistance by challenging with 1.5 mg/L colistin in Mueller Hinton Broth (MHB) with or without supplementation with 150 mM NaCl. Mutants that demonstrated no growth after 24 hours in NaCl-supplemented media were selected for further analysis. Phenotypes were confirmed by growth curve analysis in MHB +/- NaCl +/- colistin as described previously (112). The locations of transposon insertions were determined by rescue cloning (74).

Preparation of bacterial cultures for *in vivo* studies

Bacteria were harvested from log-phase cultures of Ab17978, Tn5A7 or Ab307, washed and resuspended in phosphate-buffered saline (PBS) and adjusted to 1 x 10^7 CFU/μl. Bacterial cell counts were confirmed post-infection by plating serial dilutions of each inoculation. For co-infections, equal amounts of wildtype and *ΔlpsB* were combined to yield 3 x 10^8 CFU/30 μl (total). For treatment experiments, bacteria were killed by

adding an equal volume of ethanol: acetone (1:1) to the culture. Killed bacteria were pelleted, washed once with ethanol: acetone then washed and resuspended in PBS as described above. Efficiency of killing was confirmed by plating. In addition, plating mixtures of killed bacteria with live wildtype bacteria confirmed that this method did not affect the viability of wildtype bacteria *in vitro*.

A. baumannii pneumonia model

All animal experiments were approved by the Vanderbilt Institutional Animal Care and Use Committee. We have previously established a murine *Acinetobacter* pneumonia model in our laboratory (125). Six to eight week old, female C57BL/6 mice were used for all experiments unless otherwise noted. C3H/HeJ mice were obtained from Jackson Laboratories. C3H control mice were obtained from Charles River Laboratories. MyD88$^{-/-}$ mice were a gift from Sebastian Joyce (Vanderbilt University). Mice were anesthetized and infected intranasally with 30 μl of bacterial suspension. For pre-treatment experiments, mice were anesthetized and 30 μl of killed bacteria were administered intranasally 24 hours prior to infection. At the indicated times mice were euthanized and lungs were aseptically removed, weighed and homogenized in 1 ml sterile PBS. Serial dilutions were plated on LB agar and/or LB agar containing kanamycin (40 μg/ml). Bacterial dissemination was assessed either by plating blood or by measuring bacterial burdens in spleens. In some experiments, right lungs were used for determination of bacterial burdens, while left lungs were used for RNA isolation or flow cytometry as described below. In all cases CFU were normalized to the mass of the tissue analyzed.

Tissue preparation for histology

Histopathology was assessed at 36 hpi in at least two mice per experimental group. Lungs were inflated and fixed with 10 % neutral buffered formalin. Lungs were paraffin embedded, sectioned and stained with hematoxylin and eosin or Gram-stained according to standard procedures. Lung sections were examined by a veterinary pathologist blinded to infection groups. Representative images are presented.

RNA isolation and PCR array

Lungs from infected animals were aseptically removed, transferred to RNAlater solution (Ambion) and stored at -20 °C until subsequent analyses. Approximately 30 mg of lung tissue was lysed and homogenized in 600 µl buffer RLT (Qiagen) in lysing matrix D tubes using a FastPrep tissue lyser (2 x 45 s at setting 6.0). RNA was isolated from tissue lysates using an RNeasy kit according to the manufacturer's recommendations for animal tissues (Qiagen). Reverse transcription was performed with the SABiosciences RT^2 cDNA synthesis kit according to the manufacturer's recommendations using 2.5 µg total RNA as template. Gene expression analysis was carried out using the SABiosciences mouse inflammatory cytokine/chemokine RT^2 Profiler^{TM} PCR array using RT^2 SYBR green PCR master mix according to the manufacturer's recommendations. A complete list of genes and controls included in the array are listed in Supplementary Table 1 online. Data were analyzed by the ΔΔCt method using the RT^2 Profiler^{TM} PCR Array Data Analysis tool (http://www.sabiosciences.com/pcr/arrayanalysis.php?target=upload). Genes that demonstrated greater than 2-fold regulation compared to uninfected controls

were further analyzed for differences in expression between wildtype and *ΔlpsB*-infected animals.

Flow cytometric analysis of neutrophils in infected lungs

Flow cytometric analyses were performed with total erythrocyte-free lung cells isolated at 24 hpi from individual mice infected as described above with Ab17978 or Δ*lpsB*. Antibodies and reagents for cell surface staining were purchased from BD Pharmingen. Analyses were carried out with a FACSCalibur® instrument (Becton Dickinson) and the data were analyzed using FlowJo software (Treestar Inc.) as described previously (55).

Neutrophil depletion experiments

Neutrophil depletion was achieved by intraperitoneal injection of 250 μg rat IgG2b anti-Gr-1 mAb RB6-8C5 (anti-neutrophil antibody) in 100μl PBS 24 hours prior to infection and again at the time of infection. Control mice were treated in the same way with an isotype control antibody. The bacterial inoculation was reduced to 3×10^7 CFU in order to reduce mortality associated with infection of neutrophil depleted mice. The infections were carried out as above using WT bacteria and killed Tn5A7.

Macrophage depletion

Liposomal encapsulation of clodronate (dichloromethylene diphosphonate) was performed as described previously (207). Briefly, a mixture of 8 mg cholesterol (Avanti, Alabaster, AL) and 86 mg egg-phosphatidylcholine (dioleoyl-phosphatidylcholine,

Avanti, Alabaster, AL) dissolved in chloroform were evaporated under nitrogen. Chloroform was further removed by placing under low vacuum in a speedvac the concentrator. Clodronate was prepared by dissolving 1.2 g dichloromethylene diphosphonic acid (Sigma) in 5 ml sterile PBS. The clodronate solution (5 ml) was added to the evaporated lipid preparation and mixed thoroughly. Control liposomes were prepared by adding 5 ml PBS to an identical lipid preparation. The solutions were sonicated and ultracentrifuged at 100,000 *g* for 1 h at 4°C. The liposome pellet was washed in 5 ml PBS, and ultracentrifuged at 100,000 *g* for 1 h at 4°C. Liposomes were resuspended in 5 ml PBS and stored at 4 °C for no more than 24 hours before use. Mice were anesthetized with isoflurane and treated intranasally with 50 µl of clodronate or control liposomes 48 hours prior to infection. Infections were then carried out as described above using WT bacteria and killed Tn5A7 or Tn20A11.

Microarray analysis.

Bacterial cultures were grown overnight in Luria-Bertani (LB) medium supplemented with the appropriate antibiotic, diluted in fresh medium and grown at 37°C for 3.5 hours. Cultures were then mixed with an equal volume of ice-cold ethanol-acetone (1:1) and stored at −80°C for RNA processing. For RNA extraction, samples were thawed on ice and total bacterial RNA was released by mechanical disruption and purified using Qiagen RNeasy columns (Qiagen, Valencia, CA), as previously described (112). For microarray analysis, ten micrograms of each RNA sample were reverse transcribed, fragmented and 3′biotinylated as previously reported (25). Resulting labeled cDNA (1.5 µg) was hybridized to custom-made *A. baumannii* GeneChip (PMDACBA1)

according to the manufacturer's recommendations for antisense prokaryotic arrays (Affymetrix, Inc., Santa Clara, CA) and data were analyzed as described in Hood *et al*. (2010). RNA species exhibiting ≥ 2-fold change in expression with titers above background as determined by Affymetrix algorithms in Δ*lpsB* and were found to be statistically differentially expressed (*t*-test $p \leq 0.05$) were reported.

Generation of new transposon mutants and mock-mutagenized strains

Transposon mutants were generated using the EZTn5 transposome kit as previously described and plated on LBA supplemented with kanamycin. Eight of the resulting colonies were picked and saved for future analyses. For mock transposon mutagenesis, the same mutagenesis protocol was followed except that the transposon DNA was omitted from the reaction. Bacteria were then plated on LBA and pooled into a single stock. For *in vivo* experiments, the transposon mutants were cultured independently then pooled, killed with ethanol: acetone and washed as described above. The mock treated strains were grown as a single, pooled culture, then killed and treated as above for the transposon mutants.

Whole genome sequencing

Genomic DNA was isolated from Ab17978S, Ab17978D (parent strain for the transposon mutants), Tn5A7, Tn20A11 and six of the newly derived transposon mutants described in the preceding section (Tn1-4, 7-8) using the Wizard genomic kit (Promega) according to the manufacturer's protocol for Gram-negative bacteria. Whole genome sequencing was carried out on an Illumina Genome Analyzer II using paired end, 100bp reads. Sample

preparation and sequencing was carried out by the Vanderbilt Genome Sciences Resource core laboratory.

Results

A. baumannii Tn5A7 attenuates wildtype infection.

In Chapter III I described the identification of a transposon mutant (Tn5A7) in which the transposon disrupts *lpsB*. The precise mechanism governing the reduced pathogenesis of LPS core biosynthesis mutants has not been defined. Serum resistance contributes to bacterial virulence and serum sensitivity has been proposed as the mechanism for the reduced pathogenesis of mutants defective in LPS core biosynthesis (173). However, we have previously demonstrated that a serum-sensitive Phospholipase D mutant of *A. baumannii* is attenuated for extra-pulmonary dissemination but fully virulent in the murine lung (125). These data suggest that serum sensitivity alone does not portend attenuation in pulmonary infection. Given the importance of LPS in triggering inflammation, we hypothesized that the dramatic attenuation of *lpsB* mutants in the lungs results from an altered inflammatory response. In keeping with this hypothesis I tested whether co-infection with wildtype bacteria would alter the virulence phenotype of Tn5A7. Mice were infected with 3×10^8 CFU of either wildtype, Tn5A7 or a 1:1 mixture of wildtype and Tn5A7. Unexpectedly, co-infection of wildtype and Tn5A7 resulted in significant attenuation of wildtype bacteria. Lung histopathology in co-infected mice resembled results obtained with Tn5A7 alone (**Figure 17a**). In addition, co-infection leads to a greater than 4-log reduction in wildtype bacterial burden in lungs compared to

wildtype administered alone ($1.66 \times 10^5 \pm 11.99$ CFU/g versus $4.09 \times 10^9 \pm 4.27$ CFU/g) (**Figure 17b**). The Tn5A7-mediated attenuation of wildtype is not due to the two-fold reduction in wildtype inoculum (data not shown). Moreover, co-infection prevents extra-pulmonary dissemination (**Figure 17c**). Taken together these data demonstrate that Tn5A7 attenuates the virulence of wildtype *A. baumannii* upon infection of the murine lung.

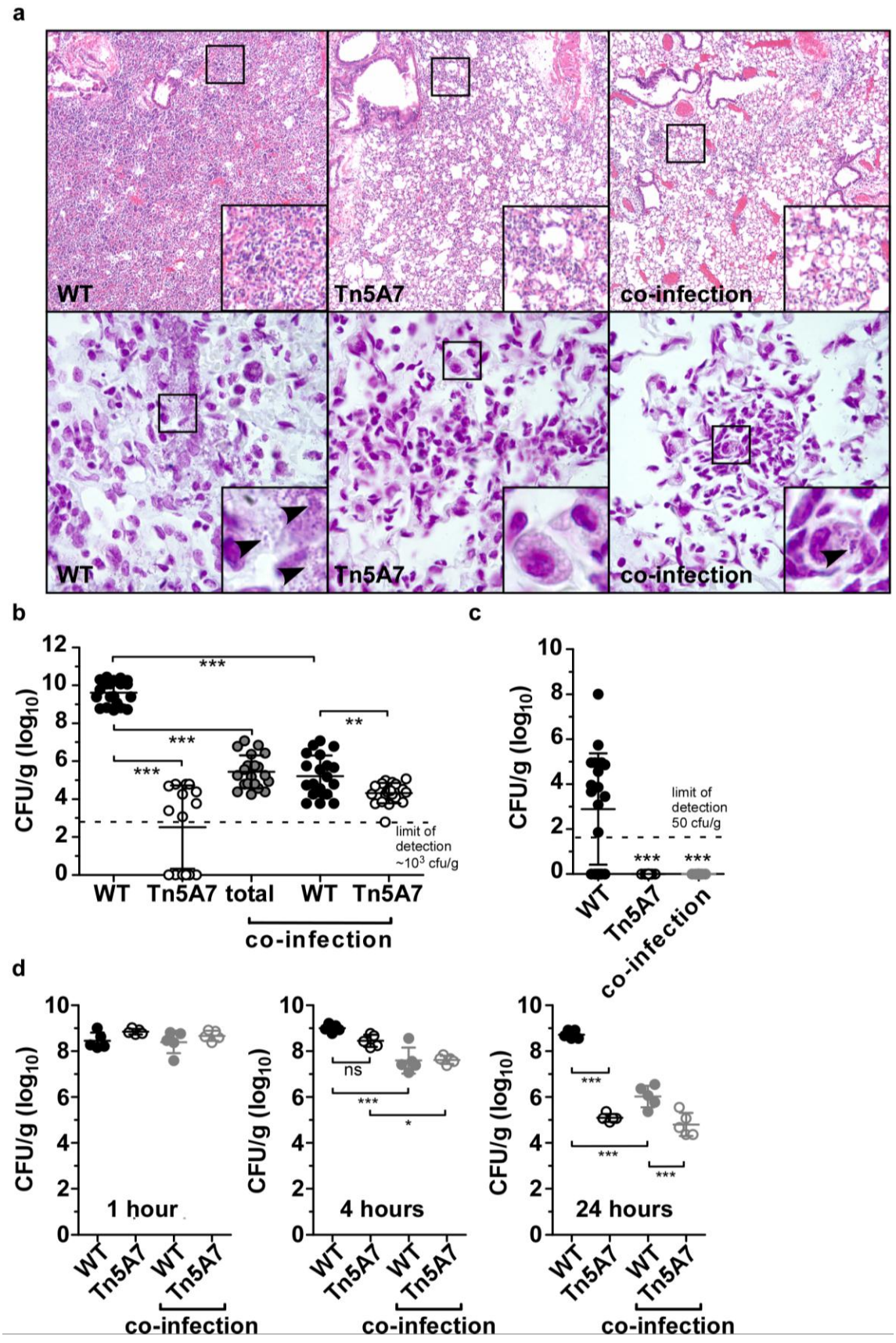
a
WT
Tn5A7
co-infection
WT
Tn5A7
co-infection
b
CFU/g (log10)
limit of detection ~10^3 cfu/g
WT
Tn5A7
total
WT
Tn5A7
co-infection
c
CFU/g (log10)
limit of detection 50 cfu/g
WT
Tn5A7
co-infection
d
CFU/g (log10)
1 hour
4 hours
24 hours
ns
WT
Tn5A7
WT
Tn5A7
co-infection

Figure 17. *A. baumannii* strains lacking LpsB are attenuated for virulence and promote bacterial clearance *in vivo*.
(a) Histological sections from lungs harvested at 36 hpi. Top row: Hematoxylin and eosin staining, original magnification = 10x. Bottom row: Gram staining showing bacteria in alveolar spaces (WT) and within macrophages (WT and co-infection; arrows, inset). Original magnification = 100x. **(b)** Bacterial burden in lungs of mice infected with wildtype (WT), Tn5A7 or co-infected with WT and Tn5A7 at 36 hpi. Bacterial burdens for the co-infection are graphed as the total bacterial burden (WT and Tn5A7) and the respective counts for WT and Tn5A7 as determined by plating on selective media. n = 20 (WT) or 15 (Tn5A7 and co-infection). **(c)** Bacterial burden in blood of mice infected with WT, Tn5A7 or co-infected with both strains at 36 hpi. n = 20 (WT) or 15 (Tn5A7 and co-infection). **(d)** Bacterial burden in lungs of mice infected with WT, Tn5A7 or co-infected with both strains during a time course of infection. For co-infections, individual WT and Tn5A7 bacterial counts, as determined by plating on selective media, are shown. n = 5 mice per group at each time point. * $p < 0.05$, ** $p < 0.005$, *** $p < 0.001$ as determined by two-tailed, unpaired Student's *t* test. Bars indicated the mean ± 1 SD from the mean.

Tn5A7 attenuates wildtype infection by inducing increased bacterial clearance from the lung.

The significant attenuation of wildtype bacteria upon co-infection with Tn5A7 suggests that Tn5A7 either promotes bacterial clearance or prevents wildtype bacteria from establishing infection in the lung. However, it is also possible that Tn5A7 directly inhibits wildtype growth. Growth curves of wildtype and Δ*lpsB in vitro* did not show any effect of Tn5A7 on wildtype growth, confirming that the effect of Tn5A7 requires the host environment (data not shown). To distinguish between increased clearance of wildtype bacteria and a decreased ability to establish infection in the lung, we examined bacterial burdens in lungs during a time course of infection. At 1 hpi, bacterial burdens were equivalent in mice infected with either wildtype, Tn5A7 or co-infected with both strains. This result suggests that Tn5A7 does not prevent WT from establishing infection in the lung. Similar results were obtained for wildtype and Tn5A7 at 4 hpi. By this time point, bacterial burdens began to decrease in co-infected mice. At 24 hpi, we observed a 4-log reduction in bacterial burden in Tn5A7-infected mice compared to wildtype. Similarly, in co-infected mice, we observed a 3-log reduction in wildtype bacterial

burden and a 4-log reduction for Tn5A7 (**Figure 17d**). Taken together, these data suggest that Tn5A7 interfaces with the host to promote increased clearance of wildtype bacteria.

Chemically inactivated Tn5A7 is effective in inhibiting WT *A. baumannii* infection.

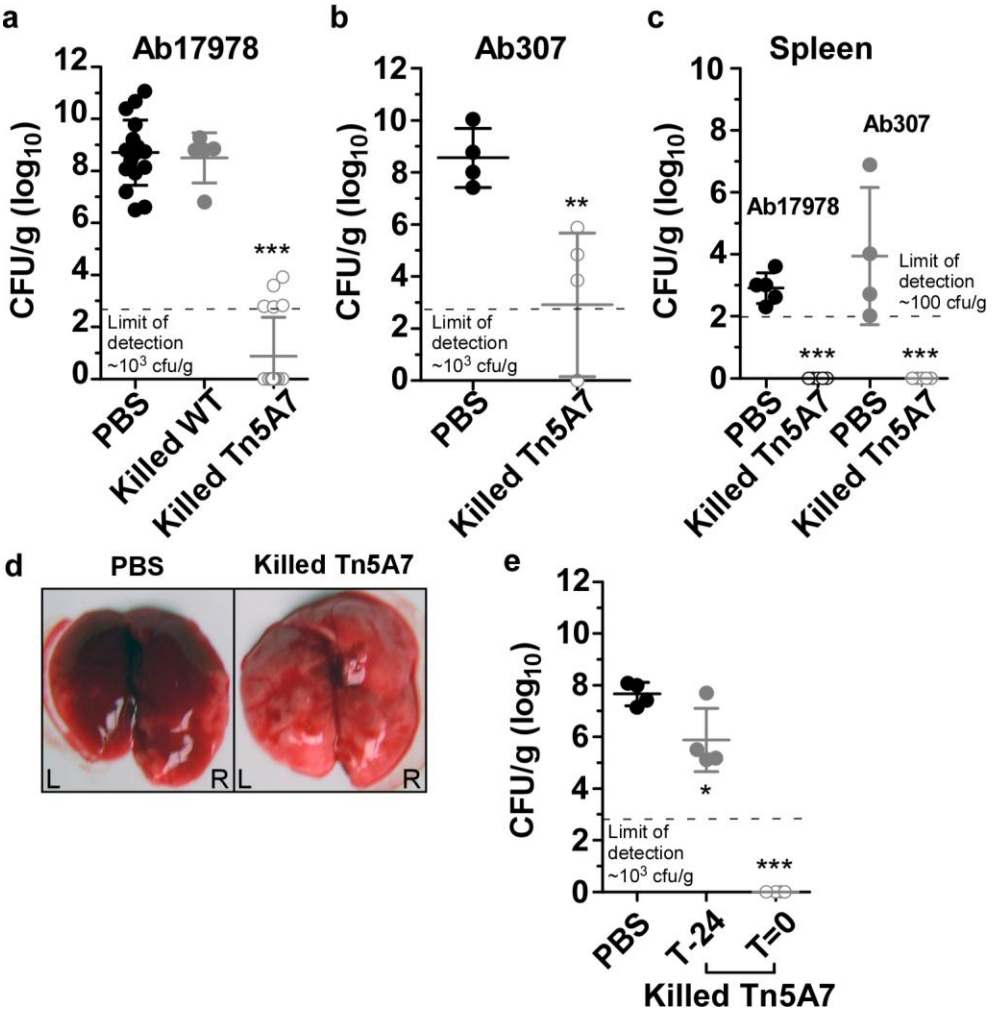

Figure 18. Application of Tn5A7 to the treatment of *A. baumannii* pneumonia.

(a) Bacterial burden at 36 hpi in lungs of mice infected with Ab17978 and treated with vehicle (PBS), chemically-killed Ab17978 (killed WT) or chemically-killed Tn5A7 (killed Tn5A7). (b) Bacterial burden at 36 hpi in lungs of mice infected with Ab307 and treated with vehicle (PBS) or killed Tn5A7. (c) Bacterial burden in spleens of mice infected with Ab17978 or Ab307 and mock-treated (PBS) or treated with killed Tn5A7. (d) Dorsal view of representative whole lungs harvested at 36 hpi showing large areas of hemorrhage and disease affecting nearly the whole lung of an untreated mouse compared to mild hyperemia and focal disease in a treated mouse. R = right lung, L = left lung. (e) Bacterial burden at 36 hpi in lungs of mice infected with Ab17978 and mock-treated (PBS) or treated with killed Tn5A7 24 hours prior to infection (T-24) or at the time of infection (T=0). * $p < 0.05$, ** $p < 0.005$, *** $p < 0.001$ as determined by two-tailed, unpaired Student's *t* test.

The results described above raise the intriguing possibility that the immune response elicited by Tn5A7 could be harnessed therapeutically for the treatment of *A. baumannii* infections. As an initial proof of concept, it was necessary to determine whether live bacteria were required for the attenuating effect of Tn5A7. To test this possibility, we infected mice with wildtype and co-administered an equal inoculation of chemically killed Tn5A7 or PBS as a vehicle control. By 36 hpi, bacterial burdens in mice treated with killed Tn5A7 were nearly 8-logs less than those of PBS-treated controls ($5.12 \times 10^8 \pm 17.9$ CFU/g versus $7.66 \times 10^0 \pm 30.9$ CFU/g) (**Figure 18a**). In fact, *A. baumannii* was undetectable in the majority of animals treated with the killed Tn5A7 preparation. This effect was specific for Tn5A7 since treatment with killed wildtype *A. baumannii* did not reduce bacterial burdens below those of untreated controls (**Figure 18a**). To determine if killed Tn5A7 is efficacious against other *A. baumannii* strains, we infected mice with Ab307, a blood isolate obtained from a patient at Erie County Medical Center in 1994. This strain has previously been shown to be virulent in rat pneumonia and soft tissue infection models (254). Similar to Ab17978, we found that treatment of Ab307-infected mice with killed Tn5A7 significantly reduced Ab307 bacterial burdens by 36 hpi (**Figure 18b**). Treatment with killed Tn5A7 prevented extra-pulmonary dissemination as demonstrated by undetectable bacterial loads in the spleens of both Ab17978 and Ab307-infected mice (**Figure 18c**). The beneficial effects of treatment with Tn5A7 were evident on gross examination of lungs, where lungs from untreated mice showed large areas of hemorrhage affecting both lungs, compared to only mild hyperemia present in focal areas of treated lungs (**Figure 18d**). Finally, we assessed the ability of Tn5A7 to prevent *A. baumannii* infection by pre-treating mice with killed

Tn5A7 24 hours prior to infection. Pre-treatment of mice produced a 2-log reduction in bacterial burden in the lungs at 36 hpi (**Figure 18e**). Taken together, these experiments establish that Tn5A7 has potential as a whole cell therapeutic for the treatment and prevention of *A. baumannii* pneumonia.

Tn5A7 blunts the inflammatory response to *A. baumannii*.

Few studies have examined the host inflammatory response to *A. baumannii* infection *in vivo*. Tn5A7 therefore serves as a valuable tool to define an inflammatory that is effective in rapidly clearing an *A. baumannii* infection. We therefore employed a mouse inflammatory gene array to measure the expression of 84 inflammatory genes in lung tissue harvested from mice infected with WT or Tn5A7. RNA was isolated from the lungs of infected mice at 1, 4 and 24 hpi. Uninfected controls were also taken at 24 hpi. A total of 14 genes were up-regulated greater than 2-fold in wildtype-infected mice compared to uninfected controls at 1 hpi, and this number increased to 31 genes at 4 hpi (**Figure 19, 20 a-b**). These up-regulated factors consisted primarily of pro-inflammatory cytokines, chemokines and their respective receptors (**Figure 20a-b and Figure 21a**). Interestingly, we did not observe significant up-regulation of interferon-γ upon infection with wildtype *A. baumannii* at any time point (**Figure 20a-b**). In fact, at 24 hpi there was significant down-regulation of the interferon-γ-inducing cytokines IL-18 and IL-15, and significant up-regulation of the anti-inflammatory cytokine IL-10 (**Figure 21b**). Another unexpected finding was the significant down-regulation of the neutrophil chemoattractant CXCL15 at 24 hpi (**Figure 21b**). The up-regulation of anti-inflammatory cytokines together with down-regulation of pro-inflammatory cytokines/chemokines in the face of

persistently elevated bacterial burdens, suggests that *A. baumannii* maintains its foothold in the lung by inducing an anti-inflammatory response.

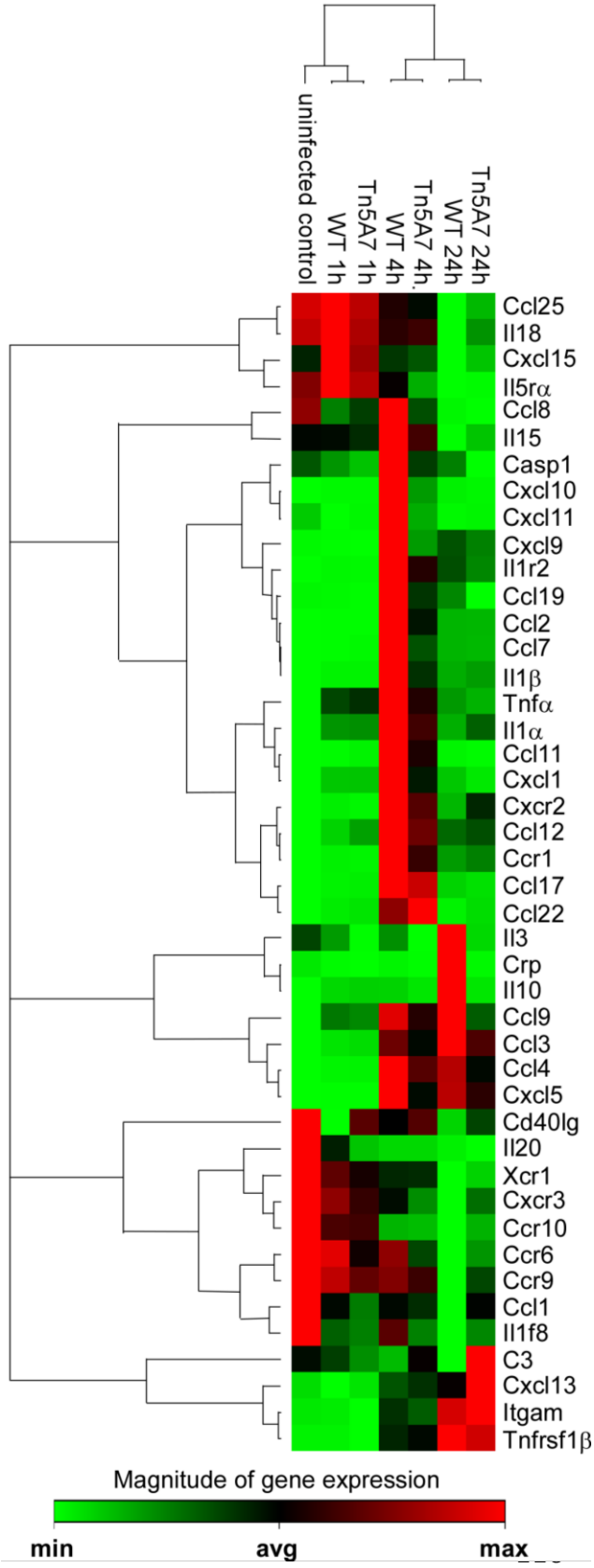

Figure 19. Cluster analysis of all genes regulated at least 5-fold in at least one experimental group compared to uninfected control.

PCR array data were analyzed using the SABiosciences data analysis software package. Genes and data sets were clustered according to overall expression patterns.

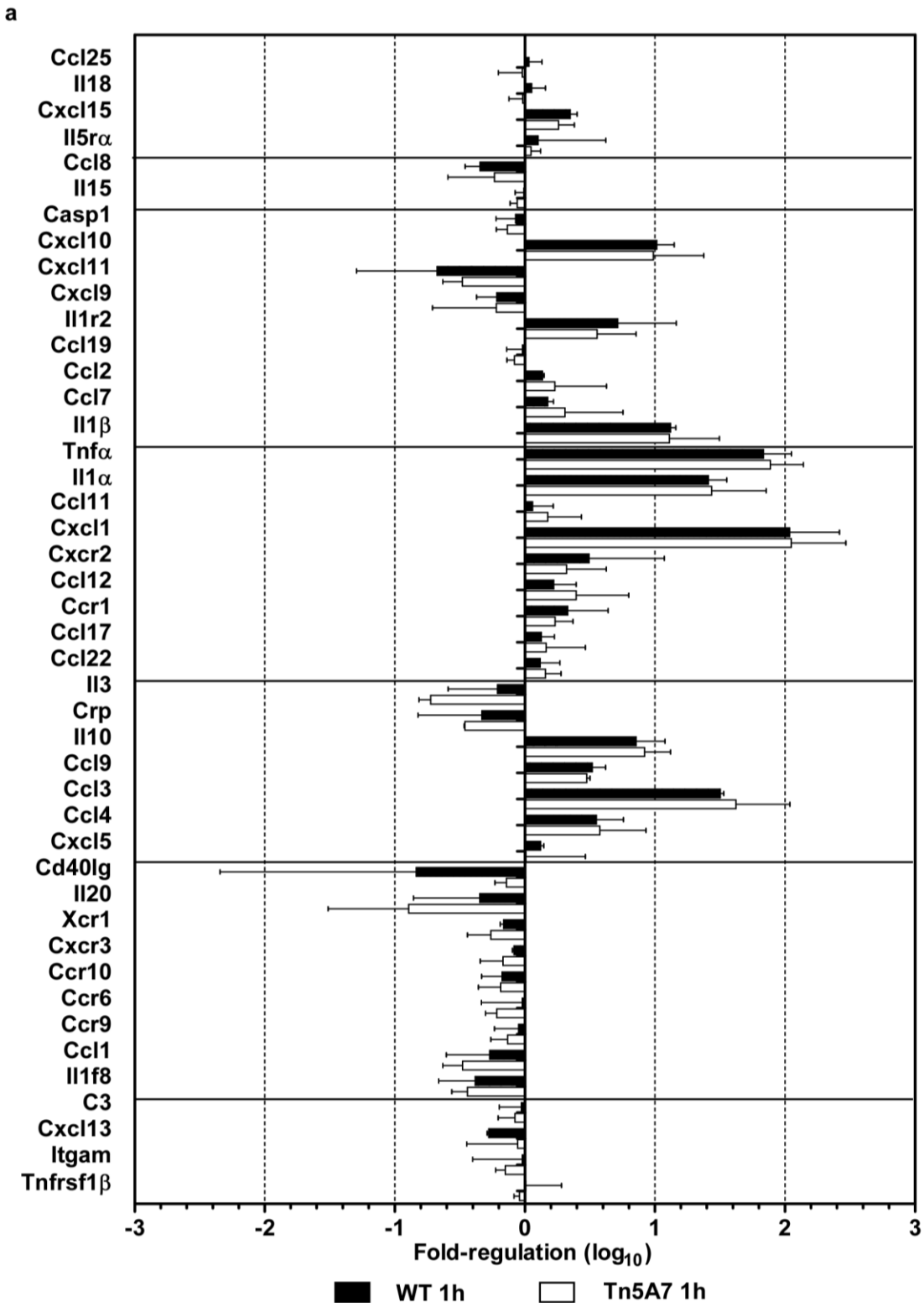
a
Ccl25
Il18
Cxcl15
Il5rα
Ccl8
Il15
Casp1
Cxcl10
Cxcl11
Cxcl9
Il1r2
Ccl19
Ccl2
Ccl7
Il1β
Tnfα
Il1α
Ccl11
Cxcl1
Cxcr2
Ccl12
Ccr1
Ccl17
Ccl22
Il3
Crp
Il10
Ccl9
Ccl3
Ccl4
Cxcl5
Cd40lg
Il20
Xcr1
Cxcr3
Ccr10
Ccr6
Ccr9
Ccl1
Il1f8
C3
Cxcl13
Itgam
Tnfrsf1β
-3
-2
-1
0
1
2
3
Fold-regulation (log10)
WT 1h
Tn5A7 1h

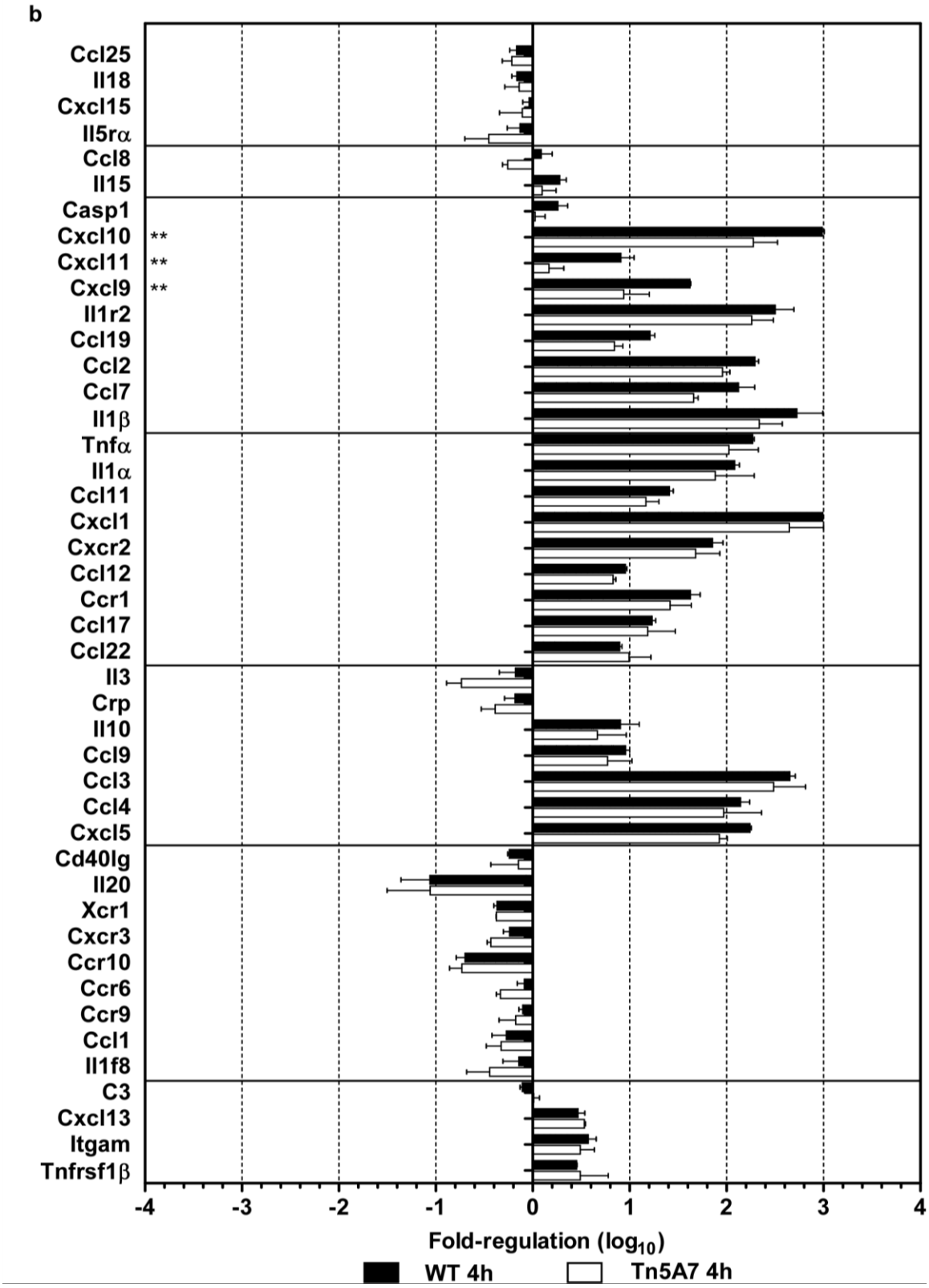
b
Ccl25
Il18
Cxcl15
Il5rα
Ccl8
Il15
Casp1
Cxcl10 **
Cxcl11 **
Cxcl9 **
Il1r2
Ccl19
Ccl2
Ccl7
Il1β
Tnfα
Il1α
Ccl11
Cxcl1
Cxcr2
Ccl12
Ccr1
Ccl17
Ccl22
Il3
Crp
Il10
Ccl9
Ccl3
Ccl4
Cxcl5
Cd40lg
Il20
Xcr1
Cxcr3
Ccr10
Ccr6
Ccr9
Ccl1
Il1f8
C3
Cxcl13
Itgam
Tnfrsf1β
-4
-3
-2
-1
0
1
2
3
4
Fold-regulation (log10)
WT 4h
Tn5A7 4h

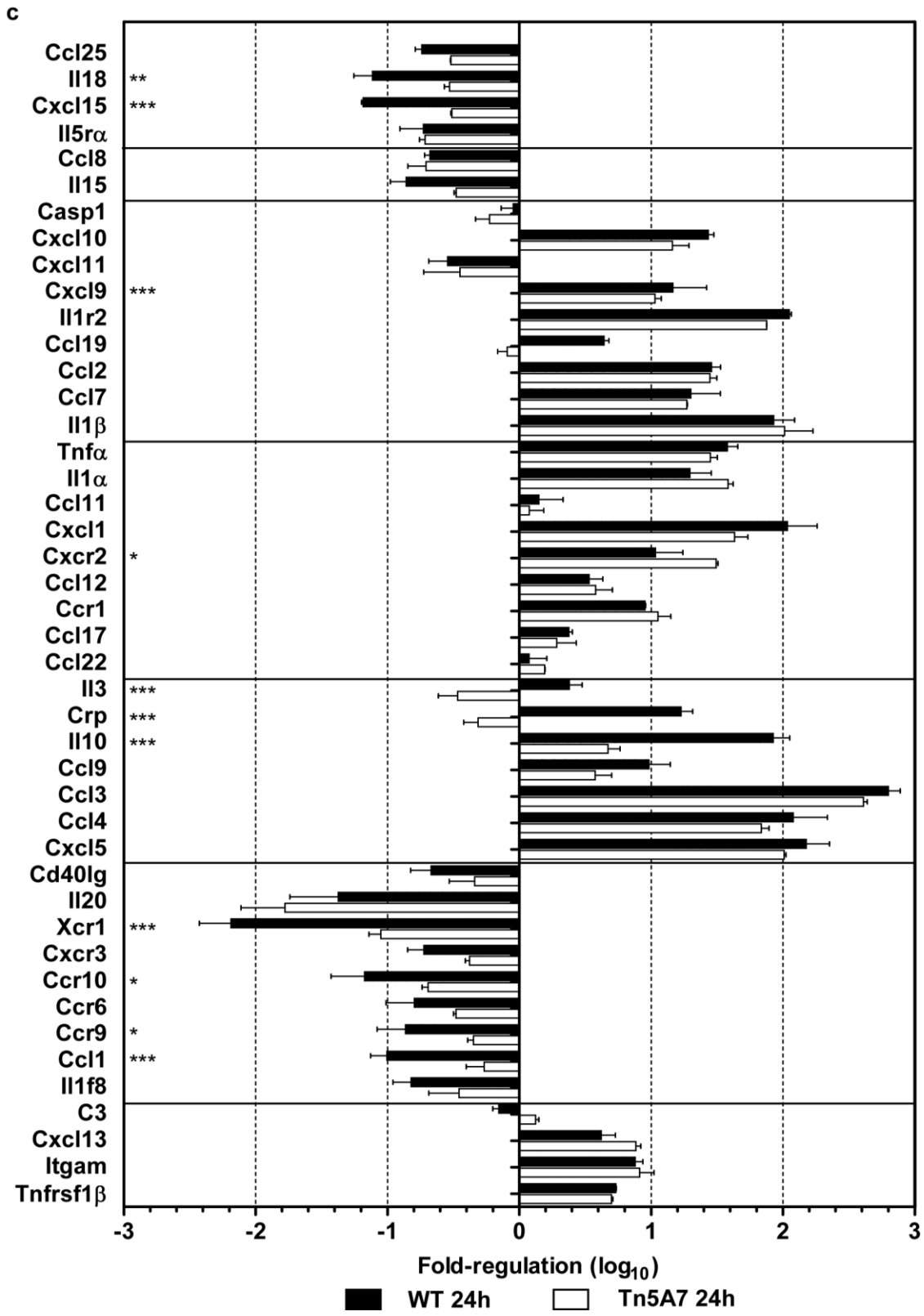

Figure 20. PCR array data for all genes that demonstrated at least 5-fold regulation in at least one experimental group compared to uninfected control.

RNA was isolated from lungs harvested at the indicated time points from animals infected with WT or Tn5A7. Gene expression analyses were carried out with the Mouse Inflammatory Gene RT^2 PCR Array (SABiosciences). Data are presented as the fold-regulation (log_{10}) compared to uninfected controls. Statistically significant differences between WT and Tn5A7 are indicated by asterisks (*p<0.05, **p<0.005, ***p<0.001) and were determined by two-way ANOVA with Bonferroni post-tests to compare WT and Tn5A7 at each time point. C reactive protein, Crp; caspase 1, Casp1; CC chemokine ligand, Ccl; CC chemokine receptor, Ccr; CD40 ligand, CD40lg; Chemokine (C motif) receptor, Xcr; CXC chemokine ligand, Cxcl; CXC chemokine receptor, Cxcr; integrin alpha M, Itgam; interferon-γ, Ifn-γ; interleukin, Il; TNF receptor sub-family, Tnfrsf; tumor necrosis factor, Tnf.

Significant differences in inflammatory gene expression were observed between wildtype- and Tn5A7-infected mice (**Figures 19, 20 and 21a-b**). Specifically, the magnitude of gene regulation was decreased in Tn5A7 compared to wildtype even at early time points when bacterial burdens in lungs were similar (Fig. 19e Figures 20-21). In particular, Tn5A7 induced only mild down-regulation of certain pro-inflammatory molecules (IL-18, IL-15, CXCL-15) and little up-regulation of IL-10 (**Figure 21b**). IL-3 and C-reactive protein (Crp) were down-regulated throughout the time course in Tn5A7-infected mice whereas these two genes were up-regulated in wildtype-infected lungs (**Figure 21b**). Interestingly, at 24 hpi IL-1α and IL-1β expression were persistently elevated in Tn5A7-infected mice compared to wildtype, although these differences did not reach statistical significance (**Figure 21b**). Finally, CXCR-2 was up-regulated in Tn5A7-infected mice compared to wildtype (**Figure 21b**). CXCR-2 is the receptor for neutrophil chemotactic cytokines such as CXCL-1 and CXCL-15, suggesting increased neutrophil recruitment to Tn5A7-infected lungs (46, 59, 107, 253). To test this hypothesis, we determined neutrophil numbers in lungs of wildtype and Tn5A7-infected mice at 24 hpi by flow cytometry. These analyses revealed a 2-fold increase in total neutrophil numbers in the lungs of Tn5A7-infected mice compared to wildtype (**Figure 21c**). Taken together, these data demonstrate that wildtype *A. baumannii* elicits a potent pro-inflammatory response early in infection but initiates an anti-inflammatory response

by 24 hpi. Infection with Tn5A7 reduces the magnitude of the anti-inflammatory response leading to increased neutrophil recruitment and persistent pro-inflammatory cytokine expression consistent with the ability of this strain to attenuate wildtype infection.

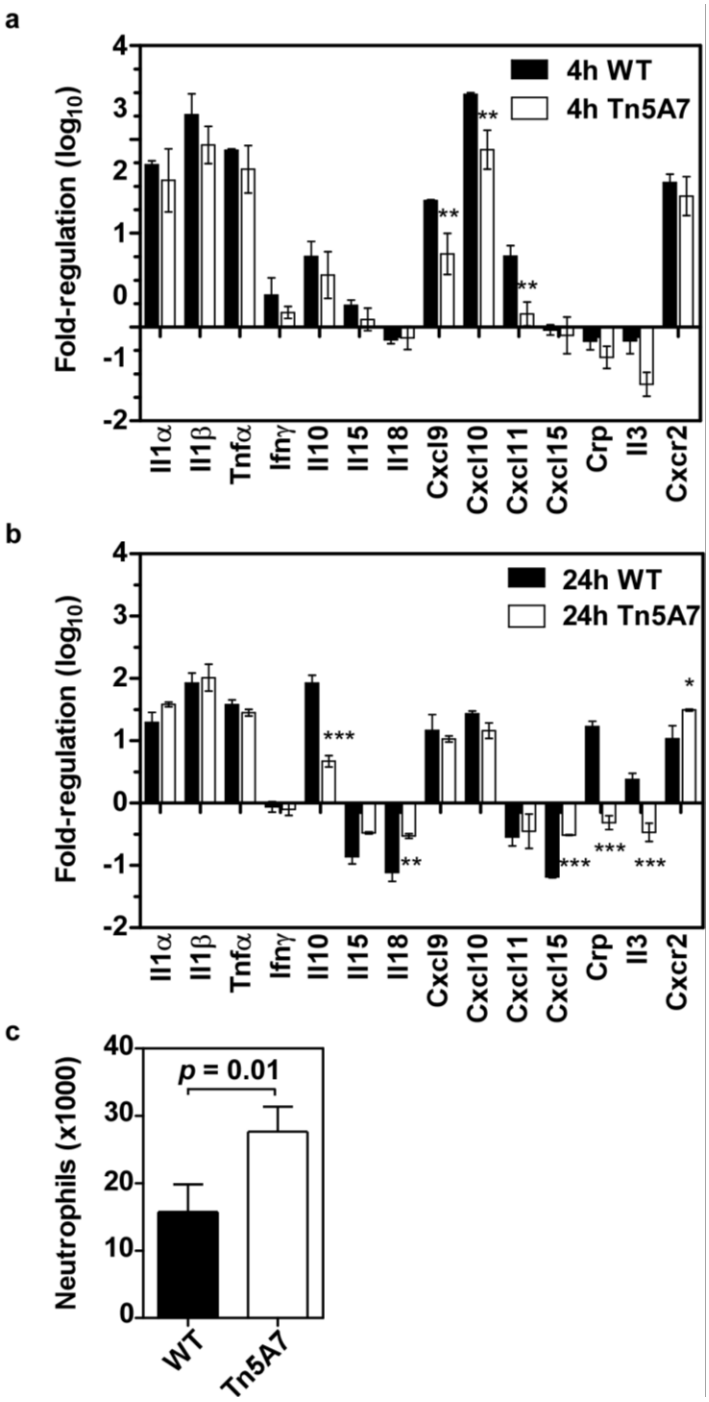

Figure 21. Measurement of the inflammatory response to WT and Tn5A7.

(a-b) PCR array data for a subset of inflammatory genes whose expression exhibited at least 5-fold regulation compared to uninfected controls at 4 hpi (a) or 24 hpi (b). Data are presented as the fold-regulation (log_{10}) compared to uninfected controls. Statistical significance was determined by two-way ANOVA with Bonferroni post-tests. Asterisks indicate statistically significant differences between WT and Tn5A7 where * $p < 0.05$, ** $p < 0.005$ and *** $p < 0.001$. (c) Neutrophil counts measured in lung tissue of mice infected with WT or Tn5A7. Statistical significance was determined by two-tailed, unpaired Student's *t* test. C reactive protein, Crp; CXC chemokine ligand, Cxcl; CXC chemokine receptor, Cxcr; interferon-γ, Ifn-γ; interleukin, Il; tumor necrosis factor-α, Tnfα.

Attenuation of WT bacteria by treatment with Tn5A7 does not depend on neutrophils or macrophages.

Since neutrophil recruitment appears to be increased in mice infected with Tn5A7, we hypothesize that neutrophils are a key mediator in the response to Tn5A7. In order to define the contribution of neutrophils to the attenuating effect of Tn5A7, mice were depleted of neutrophils using an antibody raised against Ly6G (RB6-8C5). Control mice were treated with an isotype control antibody. Despite the increase in the number of neutrophils observed in mice infected with Tn5A7 demonstrated above, depletion of neutrophils did not reverse the attenuating phenotype (**Figure 22**).

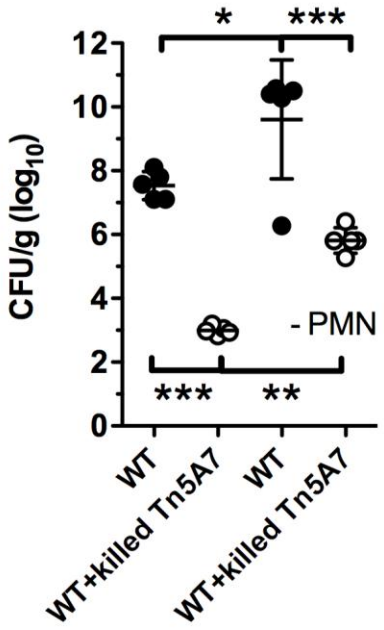

Figure 22. Effect of neutrophil depletion on the attenuating effect of Tn5A7.

Bacterial burden at in lungs of mice treated with isotype control or anti-neutrophil antibody (-PMN) measured at 36 hpi with WT bacteria with or without treatment with killed Tn5A7.

A role for macrophages in *A. baumannii* infection has not been demonstrated previously. However, given that important role that macrophages play in other bacterial infections, and the fact that alveolar macrophages are present in the lung and poised to

respond to bacterial invaders, we determined whether macrophages play a role in the response to Tn5A7. In order to assess the contribution of macrophages to the attenuating phenotype, mice were treated with clodronate-loaded liposomes 48 hours prior to infection to deplete macrophages. Consistent with the neutrophil depletion experiments, the total bacterial burden was increased in macrophage-depleted mice but the transposon mutants still dramatically attenuate WT infection. These data demonstrate that macrophages are important in protection against *A. baumannii* infections, but not for the attenuating phenotype of Tn5A7. Taken together with the results of the neutrophil depletion experiments, these data suggest that neutrophils and macrophages are not the primary cell types mediating the attenuating effect of the transposon mutants (**Figure 23**).

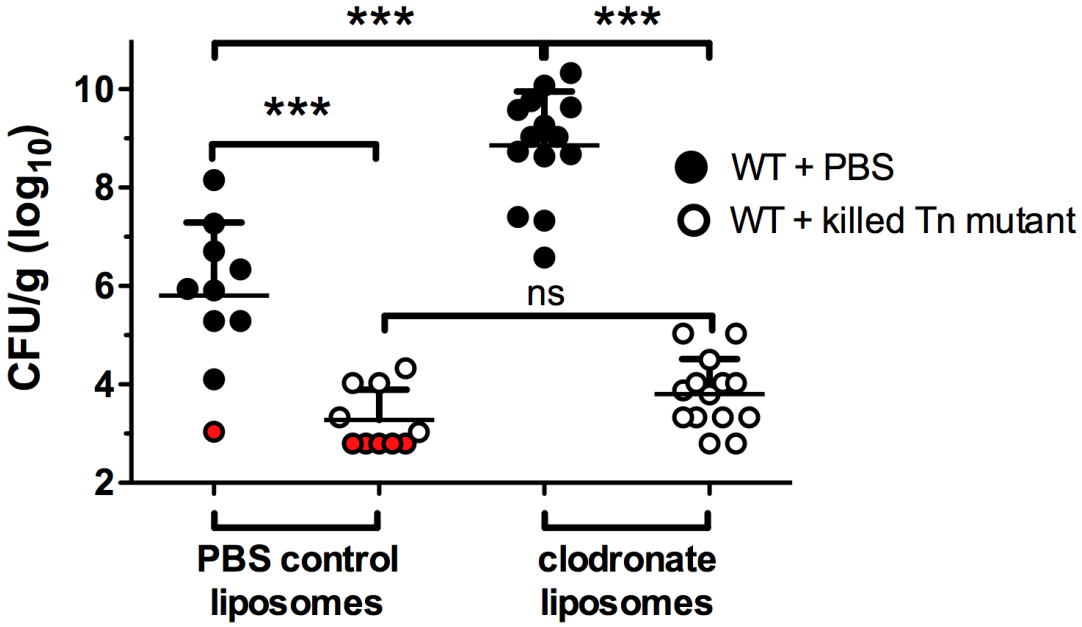

Figure 23. Macrophages contribute to defense against *A. baumannii* but are not required for the attenuating phenotype.

Macrophages were depleted by intranasal administration of clodronate-loaded liposomes. Additional mice were treated with PBS loaded control liposomes. The bacterial burdens in lungs of mice at 36 hpi with WT bacteria with or without treatment with killed transposon mutant are depicted. Red symbols indicate CFU below the limit of detection. *** $p < 0.001$ as determined by one-way ANOVA.

TLR4 is not required for the dominant negative effect of the transposon mutants.

Neither neutrophils nor macrophages appear to be the primary cell types mediating the attenuating phenotype of Tn5A7. We demonstrate above that inflammatory gene expression changes as a result of infection with Tn5A7 compared to WT. Moreover, bacterial clearance is increased in Tn5A7-infected animals very early post infection. These findings suggest that Tn5A7 is recognized by resident cells in the lung in order initiate a rapid response to the infection. In *P. aeruginosa* infections, the respiratory epithelium is itself critical in responding to bacterial infection and activating the immune response. It is therefore possible that Tn5A7 is recognized by pattern recognition receptors (PRRs) expressed on the lung epithelium. As a first step in determining how Tn5A7 is recognized by the host, we sought to evaluate the necessity of individual PRRs in the response to Tn5A7. In order to select a candidate PRR, we considered the fact that attenuation of WT infection by Tn5A7 does not require live bacteria, suggesting that Tn5A7 expresses a surface-exposed ligand that is recognized by the host to activate the immune response. Moreover, this ligand is not disrupted by treatment with ethanol and acetone. Given that the transposon disrupts a gene involved in LPS biosynthesis, I hypothesize that the truncated LPS produced by this strain may be responsible for the attenuating phenotype. In $TLR4^{-/-}$ (C3H/HeJ) mice infected with WT bacteria, co-infection with Tn5A7 exerts an equal magnitude of protective effect compared to the same co-infection in WT C3H mice (**Figure 24**). These data suggest that while $TLR4^{-/-}$ mice are more susceptible to infection with *A. baumannii* they maintain the ability to respond to Tn5A7 and clear WT infection.

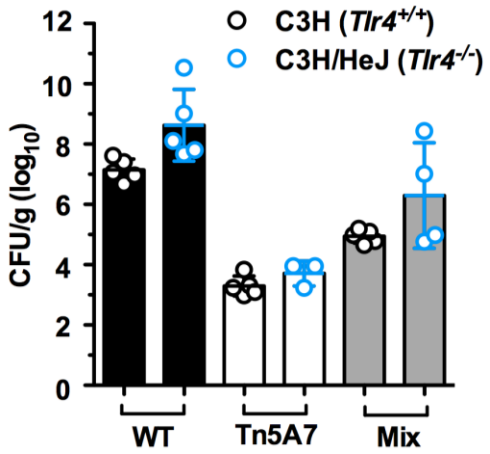

Figure 24. TLR4 is not required for the attenuating phenotype of Tn5A7.

Bacterial burdens in lungs of C3H (*Tlr4*$^{+/+}$) and C3H/HeJ (TLR4$^{-/-}$) infected with WT *A. baumannii*, Tn5A7 or a 1:1 mixture of both strains.

The attenuating phenotype of Tn5A7 is not due to disruption of *lpsB*.

In mutant Tn5A7 the transposon inserts into *lpsB* causing a disruption in LPS core biosynthesis. However, TLR4 is not necessary for the attenuating phenotype of Tn5A7. This result can be explained by the fact that the LPS core is not directly recognized by TLR4, and it also suggests that Tn5A7, which elicits the attenuating phenotype, must express another protein or molecule. Since transposon mutagenesis can induce secondary mutations or polar effects on other genes it was necessary to determine whether disruption of *lpsB* is responsible for the attenuating phenotype. The LPS biosynthesis phenotype of Tn5A7 can be rescued by providing a WT copy of *lpsB* on a plasmid (Tn5A7::p*lpsB*). Treatment of WT bacteria with chemically inactivated Tn5A7::p*lpsB* resulted in the same level of attenuation as treatment with Tn5A7 alone (**Figure 25**). Furthermore, co-infection of WT with the targeted deletion mutant, Δ*lpsB*, does not lead to attenuation of the WT infection (**Figure 25**). Taken together, these data demonstrate

that disruption of *lpsB* is not directly responsible for the attenuating effect of Tn5A7 on WT bacteria.

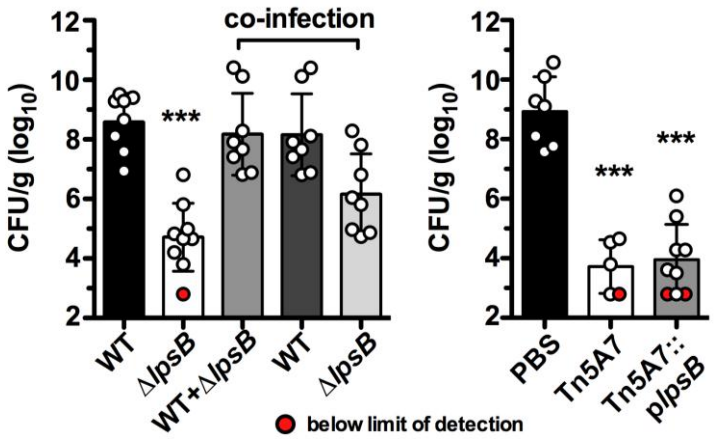

Figure 25. Disruption of *lpsB* is not responsible for the attenuating phenotype of Tn5A7.

A. Bacterial burden in lungs harvested at 36 hpi from mice infected with WT, Δ*lpsB* or co-infected with both strains. B. Bacterial burden in lungs of mice infected with WT and mock treated (PBS) or treated with killed Tn5A7 or killed Tn5A7::p*lpsB*. *** $p < 0.001$ as determined by Student's *t* test.

Transposon mutagenesis induces the attenuating phenotype with a high frequency.

There are several possible ways in which transposon mutagenesis can induce a phenotype that is not the direct result of gene disruption by the transposon itself. These possibilities include polar effects on the expression of genes near the site of integration, secondary mutations that arise during the process of mutagenesis, or the transposon itself may exert unexpected effects on the host bacterium. As an initial experiment to differentiate between these possibilities, I selected another mutant from the transposon library and repeated the treatment experiments with chemically inactivated bacteria as before. In mutant 20A11, the transposon disrupts the gene for a putative major facilitator family transporter that is not related to LPS biosynthesis. When WT are bacteria are

treated with chemically killed 20A11, this treatment attenuates the WT infection similar to treatment with Tn5A7 (**Figure 26**). These data suggest a role for the transposon itself in mediating the attenuating effect. However, this experiment does not rule out the possibility that the process of transposon mutagenesis induces this phenotype at a high frequency.

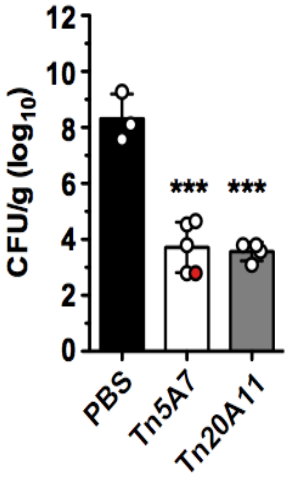

Figure 26. Demonstration of the attenuating phenotype in a separate transposon mutant.

Bacterial burden in lungs harvested at 36hpi from mice infected with WT A. *baumannii* and mock treated (PBS) or treated with killed Tn5A7 or killed Tn20A11. Tn20A11 is a transposon mutant in which the transposon integration disrupts a predicted MFS family transporter that is not involved in LPS biosynthesis.

To address the possibility that the process of transposon mutagenesis induces this phenotype at a high frequency, I generated new transposon mutants following the same mutagenesis procedure that was used to generate the original library. In addition, a mock mutagenesis protocol was carried out in which bacteria were transformed with the transposase but the transposon DNA was excluded from the reaction. Eight colonies were picked from the transposon mutagenized bacteria. Since there is no method for selecting bacteria that have taken up the transposase without the transposon DNA, following electroporation, the bacteria from the mock mutagenesis were plated and the pooled without selection. Mice were infected with WT bacteria mixed with chemically-killed, pooled transposon mutants or mock mutagenized bacteria. Treatment with the pooled transposon mutants reduced WT bacterial burdens but not to the same extent as treatment

with either Tn5A7 or Tn20A11 (**Figure 27**). In contrast, the mock treated cells had no effect on WT bacterial growth. The intermediate effect of the pooled mutants suggests that only a subset of the mutants have the attenuating phenotype. Taken together, the infections with multiple transposon mutants suggest that the process of transposon mutagenesis induces the attenuating phenotype. Moreover, this phenotype arises with high frequency, since at least one out eight mutants must have the phenotype in order for the pooled mixture to have an effect on WT infection.

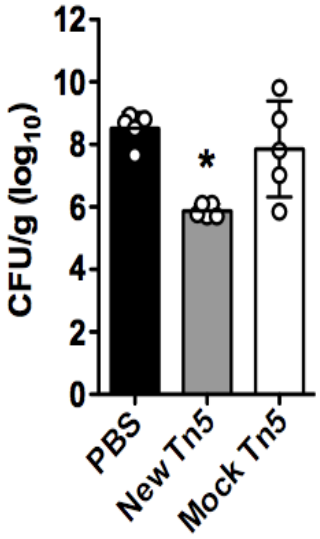

Figure 27. Induction of the therapeutic phenotype by transposon mutagenesis.

Bacterial burden in lungs harvested at 36 hpi from mice infected with WT bacteria and mock treated (PBS) or treated with a mixture of eight newly derived transposon mutants (New Tn5) or a mixture of mock transposon mutants.

Attenuating mutants do not share any common secondary mutations.

To determine if the process of transposon mutagenesis induced common mutations at sites secondary to the transposon integration site, whole genome sequencing was carried out on Tn5A7, Tn20A11 and a subset of the pooled mutants described above. In addition, the Ab17978 parent strain and a separate stock of Ab17978 were also sequenced. The parent strain for the transposon mutants is designated as Ab17978D, while the other is

referred to as Ab17978S. Unexpectedly, sequencing did not identify any point mutations, insertions or deletions that were common to the transposon mutants. In fact, although there were five point mutations identified in Tn5A7 and Tn20A11 compared to Ab17978D, these mutations were not found in the more recently derived transposon mutants. Given that the same five nucleotide changes were found in both Tn5A7 and Tn20A11, these mutations are most likely present in all of the mutants from the library. Since these mutations are not conserved in the other transposon mutants, these changes are not likely to be the cause for the attenuating phenotype.

Attenuating mutants share a common pattern of gene dysregulation.

Transcriptional analyses were undertaken to compare the expression profiles of WT, 20A11, 5A7 and Δ*lpsB*. Expression profiles in each of the transposon mutants was compared to WT. Expression changes that were common between Tn5A7 and Δ*lpsB* were thought to derive from disruption of *lpsB* and were therefore ignored. Likewise, gene expression changes common between all three mutants are likely the result of kanamycin treatment, so those changes were also filtered out. Finally, Expression changes common between Tn5A7 and Tn20A11 result from the transposon mutagenesis. The bacterial cultures for the microarray experiments were grown exactly as if they were for the infection studies. I therefore hypothesize that one or a combination of genes that change in expression in these two mutants is responsible for the attenuating phenotype. These transcriptional analyses are summarized in **Figure 28** and *Appendix* III, **Tables 17 and 18**. We focused our attention on genes that were up regulated in the transposon mutants compared to WT. This decision is based on the fact that the mutants exert a

dominant negative effect on WT bacteria. It is therefore more likely that the mutants overexpress a surface-exposed pathogen-associated molecular pattern (PAMP), which augments recognition and response by the host.

Among the genes that are most highly up-regulated are those that encode genes involved in horizontal gene transfer (A1S_0663, A1S_0664, A1S_0665 and A1S_0666). These genes appear to be encoded within a horizontally acquired DNA element. Moreover, several transposases or transposase-associated genes are also modestly up-regulated (A1S_0211, A1S_0773, A1S_0774, A1S_0777, A1S_1172). Other genes that encode proteins with possible bacterial surface accessibility include two outer membrane or inner and outer membrane-spanning transporters (A1S_1241, A1S_1771, A1S_1772 and A1S_1773). Taken together, the microarray analyses define a conserved transcriptional program in two transposon mutants when compared to WT bacteria.

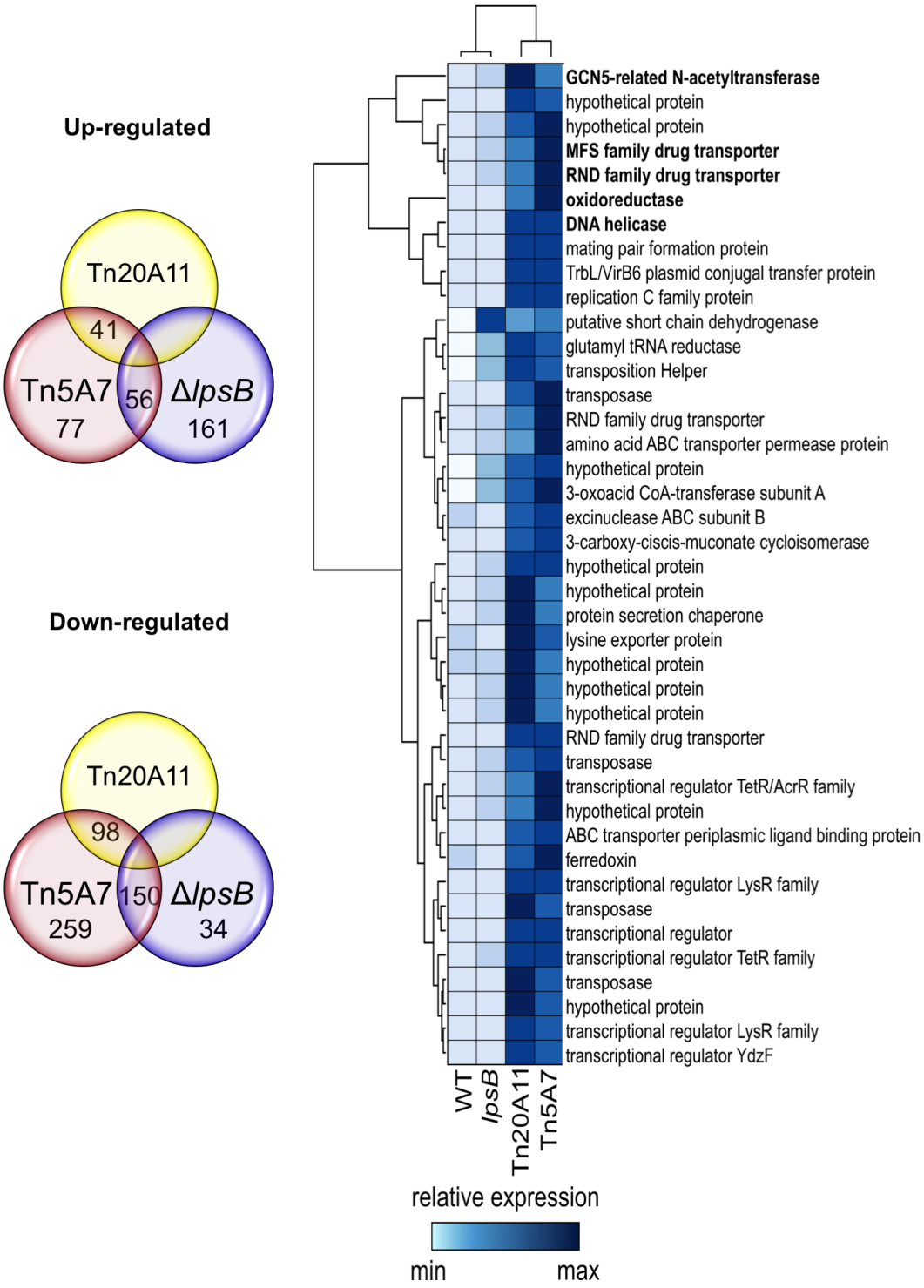

Figure 28. Subtractive microarray defining a conserved pattern of gene expression in attenuating strains.

A. Number of genes whose expression differed in Tn5A7, Tn20A11 and Δ*lpsB* relative to WT by microarray analysis. Numbers in overlapping circles indicate the number of genes common to the two strains. B. Heat map displaying relative expression of genes that were significantly upregulated in Tn5A7 and Tn20A11 compared to WT. Data are clustered according to similarity in expression profiles. Bold type face indicates genes or transcriptional units targeted for inactivation.

The attenuating effect of the transposon mutants requires signaling through MyD88.

The data presented above suggest that immune signaling is disrupted by treatment with the transposon mutants. In addition, as discussed above, the fact that killed bacteria are sufficient to induce the curative immune response strongly suggests that these mutants express a PAMP that is readily accessible to its cognate PRR *in vivo*. To test this hypothesis, we performed the infection and treatment experiments in MyD88$^{-/-}$ mice since these mice would lack responsiveness to several of the major bacterial PAMPs. MyD88$^{-/-}$ mice are more susceptible to *A. baumannii* infection than their heterozygous littermates and WT controls (**Figure 29**). Importantly, Mice infected with WT bacteria and treated with killed Tn20A11 only exhibit a modest reduction in bacterial burden compared to untreated mice. These data establish a role for MyD88 signaling in the response to the transposon mutants. Moreover, these data further support the hypothesis that the attenuating effect of the mutants involves recognition of a PAMP.

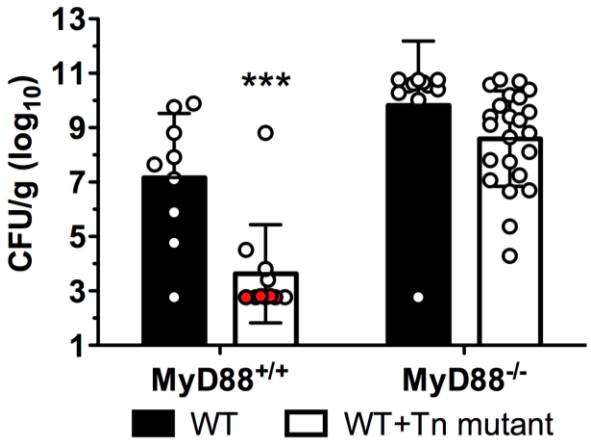

Figure 29. Involvement of MyD88 in the attenuating phenotype of the transposon mutants.
Bacterial burden in lungs of WT or MyD88-/- mice at 36 hpi with Ab17978+PBS or Ab17978+killed Tn mutant.

The microarray analyses above demonstrate up regulation of a locus possibly involved in horizontal gene transfer in Tn5A7 and Tn20A11. We hypothesized that up-

regulation of these genes may lead to increased exposure of bacterial DNA to PRRs *in vivo*. In order to define the contribution of surface-exposed DNA to the attenuating effect of the transposon mutants, the mutants were treated with DNase prior to treatment with ethanol and acetone. Proteinase K treatment, alone or in combination with DNase treatment, was also included in order to determine whether a surface exposed protein is responsible for the attenuation. Mice were infected with WT bacteria and treated at the time of infection with killed Tn20A11 that had been treated with DNase, Proteinase K, or sequentially with both enzymes. A partial reduction in the attenuating phenotype of Tn20A11 was observed with each of the three treatment conditions (**Figure 30**). Addition of DNase and proteinase K followed by immediate treatment with ethanol and acetone did not reduce the attenuating phenotype establishing that the reduction observed above cannot be accounted for simply by the addition of DNase and Proteinase K. Failure to completely reduce the phenotype may result from incomplete digestion.

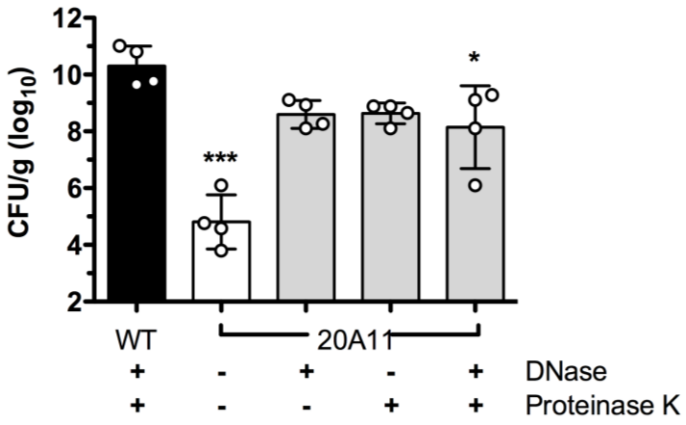

Figure 30. Effect of DNase and proteinase K pre-treatment on the therapeutic effect of Tn20A11.

Bacterial burden in lungs of mice infected with WT bacteria and treated with killed 20A11 treated with DNase and/or proteinase K or left untreated. * $p < 0.05$, *** $p < 0.001$ by one-way ANOVA.

Discussion

Mammals have evolved elegant mechanisms to recognize invading pathogens and mobilize an infantry of soluble and cellular effectors capable of controlling and clearing the invading microbe. Likewise, pathogens have also evolved means to evade these defenses and proliferate in their mammalian hosts. The intricate balance that underlies the host-pathogen interaction is exemplified by the finding that transposon mutagenesis of *A. baumannii* results in strains that tailor the host response to induce pathogen clearance. The precise mechanism governing this attenuating effect is not known, however the fact that attenuating mutants share a common pattern of gene dysregulation suggests that the aberrant expression of a bacterial PAMP triggers host inflammation *in vivo*. Notably, in mice treated with the transposon mutants, WT *A. baumannii* is rapidly cleared from the lungs without residual histopathology. This demonstrates that these strains do not merely induce a robust immune response, but that the immune response is tailored for both pathogen elimination from the lung and protection of tissue integrity.

Inflammatory dysregulation contributes to disease susceptibility in infections of critically ill patients (188, 189). Consistent with this clinical observation, the pattern of gene expression reported here following infection with wildtype *A. baumannii* bears numerous features typical of the immunosuppressive phase of sepsis (27, 197). Notably, sepsis develops during the course of primary lung infection with *A. baumannii* and the observed immunosuppression, which is dependent on full-length LPS, results in failure to clear this initial infection. This is a clinically relevant situation and one that is associated with high mortality in hospitalized patients (81, 246, 268). The hallmarks of post-septic

immunosuppression, namely lack of interferon-γ expression and up-regulation of IL-10, are observed throughout wildtype *A. baumannii* infection. However, while many studies focus on the IL-10/IFNγ axis in sepsis, therapeutic modulation of these cytokines *in vivo* has had mixed results (132, 197, 198). It is therefore notable that *A. baumannii* infection results in the regulation of a broad panel of pro- and anti-inflammatory cytokines, many of whom have demonstrated roles in host defense against pulmonary infections (46, 107, 120, 132, 153, 197, 253, 303). Furthermore, the expression of numerous genes differs significantly between wildtype and Tn5A7 infections and these patterns associate with drastically different disease outcomes. These data underscore the fact that coordinated regulation of the full complement of inflammatory genes contributes to the outcome of bacterial infections.

The inflammatory gene expression data provide possible mechanisms for the attenuating effect of the transposon mutants *in vivo.* One potential confounding factor however, is the fact that there are vast differences in bacterial burden at the time points at which we observe the greatest changes in gene expression. It is therefore not clear to what extent these changes are responsible for the increase in bacterial clearance, or whether these changes are the result of lower bacterial burdens at these time points. Furthermore, the time course infection data demonstrate that bacterial clearance begins very quickly following the initiation of the infection. The latter point, together with a lack of a role for neutrophils and macrophages, suggest that the respiratory epithelium itself or other resident cells within the lungs must respond to the infection and initiate the response. Future work will address these points and is discussed in *Chapter VIII*.

It is notable that neither neutrophils nor macrophages were required for the attenuating phenotype of the transposon mutants. While these data imply another cell type such as the respiratory epithelium or dendritic cells in activating the response, it is necessary to consider that the depletion experiments likely do not remove all of the targeted cells. It is therefore possible that a sufficient number of cells remain to carry out their effector function. Regardless of the cell type responsible for recognition of the transposon mutants, it is clear that MyD88 is necessary for the attenuating effect of these strains. This implies that a PAMP is expressed by the bacteria and recognized by host TLRs. However, MyD88 is also involved in IL-1 and TNF receptor signaling, so it is not possible to rule out involvement of these receptors at this time. Interestingly, genes involved in either the synthesis or export of known PAMPs were not found to be upregulated in the transposon mutants. One possible exception to this finding is the up-regulation of four genes that make up part of a putative competence locus (**Figure 31**). Bacterial DNA activates the immune response through recognition by TLR9. It is possible that DNA associated with these competence proteins is exposed to the immune system. However, it is also possible that the phenotype induced by the transposon mutants results from recognition of a previously uncharacterized bacterial PAMP.

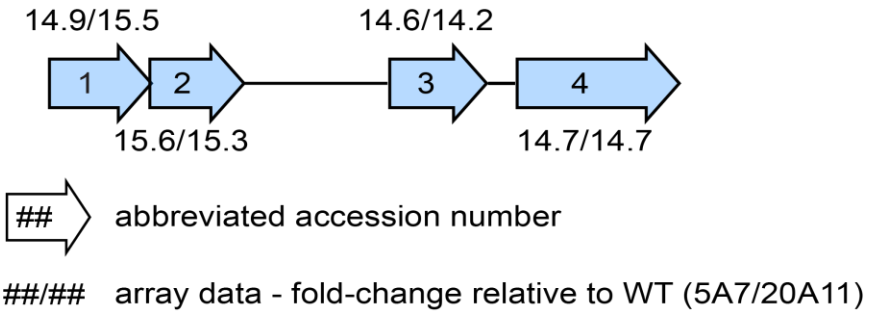

Figure 31. Schematic diagram of a highly upregulated locus in Tn5A7 and Tn20A11.

The four most highly upregulated genes in the array encode a putative competence locus consisting of a putative DNA helicase (1), replication C family protein (2), putative mating pair formation protein (3) and TrbL/VirB6 plasmid conjugal transfer protein (4).

The rise of extensively drug resistant bacteria that are capable of causing lethal infections is rapidly creating a public health crisis yet therapeutic development has failed to keep pace. *A. baumannii* poses a particular challenge due to the intrinsic drug resistance imparted by its impermeable outer membrane. Furthermore, up-regulation of efflux pumps and down-regulation of outer membrane porins leads to rapid acquisition of resistance to new antibiotics (112, 179, 181, 224, 255). Based on these facts, reliance solely on small molecule antibiotics is unlikely to provide a lasting solution to the growing burden of *A. baumannii* infections. Novel strategies for the treatment and prevention of these infections are therefore desperately needed. Toward this end, the work described herein demonstrates that Tn5A7 restores the host's ability to mount an effective immune response and clear a wildtype *A. baumannii* infection. Notably, Tn5A7 exerts a magnitude of effect that is equal to or greater than virtually all published reports of antibiotic therapy in murine models of *A. baumannii* pneumonia (48, 131, 149, 192, 228, 306, 309). Illustrating this point, in a comparable pneumonia model, tigecycline elicits only a 2- to 5-log reduction in bacterial burden by 48 hpi, compared to complete bacterial clearance in nearly all animals treated with Tn5A7 by 36 hpi (**Figure 19**) (228). Notably, tigecycline is the only new drug that has been approved for the treatment of *A. baumannii* infections in recent years and resistance to this drug has already been reported (224, 255). These facts underscore the potential for further elucidation of the mechanism of the attenuating effect in order to harness this host response for the treatment for *A. baumannii* pneumonia. Moreover, this treatment strategy has advantages over selective modulation of individual cytokines since the transposon mutants marshal the full

complement of host defenses required for effective pathogen clearance. Taken together, this work demonstrates that the bacterial pathogens can be engineered to harness innate host defenses and to attenuate *A. baumannii* infections. Thus, innate immune enhancing biologics may represent a novel class of antimicrobials that can be developed for the treatment of a variety of infectious diseases.

V. ZnuB contributes to zinc acquisition, resistance to calprotectin and pathogenesis of *Acinetobacter baumannii* infections

Introduction

Despite the growing clinical burden of *A. baumannii* disease there remains relatively little known about the basic mechanisms of *A. baumannii* pathogenesis. It is well established that all bacteria require certain transition metals in order to carry out basic physiologic functions. Mammalian hosts take advantage of this requirement by limiting the availability of metals in a process referred to as nutritional immunity. Although this term was first used to describe the withholding of iron from invading bacteria, more recently it was established that mammalian hosts likewise sequester other metals including manganese and zinc. As a result, bacterial pathogens need efficient mechanisms to acquire nutrient metals from their hosts in order to cause infection. In the case of *A. baumannii*, several mechanisms for iron acquisition have been elucidated. These include siderophore biosynthesis and transport machinery, which have been shown to play a role during infection. However, there is currently nothing known about the roles for other essential metals such as manganese or zinc during *A. baumannii* infection. Moreover, mechanisms for acquiring these metals have not been elucidated.

Herein we describe the role for the host protein calprotectin in protection against *A. baumannii* pneumonia. Calprotectin (calgranulin A/B, MRP 8/14) is an S100 family protein consisting of a heterodimer of S100A8 and S100A9. Calprotectin is an important inflammatory marker and exhibits antimicrobial activity through the chelation of Mn and Zn (26, 116, 186, 278). Although the role for this protein has been demonstrated in systemic and gastrointestinal infections, the role for this protein in bacterial pneumonia

has not been examined previously. In addition to investigating the contribution of calprotectin to host defense against *A. baumannii* we further utilize CP-mediated metal chelation to define bacterial processes that are affected by Mn and Zn limitation. Finally, we describe a zinc acquisition system in *A. baumannii* and define the role for this system in *A. baumannii* pathogenesis.

Materials and Methods

Bacterial strains and reagents

All experiments were performed using *A. baumannii* strain ATCC 17978 or its derivatives unless otherwise noted. The transposon mutant library was constructed using the EZ-Tn5 transposome system as described previously (123). *A. baumannii* strain AB0057 is a carbapenemase-producing strain with an imipenem MIC of >12 μg/ml (6). This strain was a gift from Robert Bonomo. Chemicals and antibiotics were purchased from Sigma unless otherwise noted. Recombinant human calprotectin was used for all *in vitro* experiments and was expressed and purified as described previously (56).

In vitro growth inhibition assays with calprotectin

Overnight cultures of *A. baumannii* were diluted 1:20 in chelex-treated RPMI (ChxRPMI) without metals added back and incubated for 1 hour at 37°C. Following incubation, the cultures were further diluted 1:50 in CP growth media, which consists of 20 percent CP diluted in CP buffer (20 mM Tris, pH 7.5, 100 mM NaCl, 10 mM beta-mercaptoethanol, 3 mM $CaCl_2$), and 80 percent ChxRPMI to which was added 0.1 mM

$CaCl_2$, 1mM $MgSO_4$ and 10 μM $FeSO_4$. In some assays, Mn and/or Zn were also added at the indicated concentrations. Bacteria were incubated at 37 °C and growth was monitored at 1 to 2-hour intervals throughout the time course.

A. baumannii infections

Wildtype C57BL/6 mice were obtained from Jackson Laboratories and allowed at least one week of acclimation time prior to infections. $S100A9^{-/-}$ mice, which are functionally calprotectin-deficient were a gift from Wolfgang Nacken (Institute of Experimental Dermatology, University of Münster, 48149 Münster, Germany). All of the infection experiments were approved by the Vanderbilt University Institutional Animal Care and Use Committee. In *vivo* studies utilized the *A. baumannii* pneumonia previously developed in our laboratory with a few modifications (123). Briefly, mice were infected with 3-5 x 10^8 CFU *A. baumannii* in 50 μl PBS. At the indicated times post infection mice were euthanized and CFU were enumerated in lungs and livers. We initially performed time course studies comparing male C57BL/6 with $S100A9^{-/-}$ mice for their susceptibilities to *A. baumannii* infection to determine the optimal age at which to perform subsequent experiments (data not shown). Based on these studies, 9 week-old male mice were used for subsequent experiments. For co-infection experiments, equal numbers of WT and Δ*znuB* were mixed to yield a total of 5 x 10^{10} CFU/ml and mice were infected with 50 μl of the combined mixture. At 36 hours post infection (hpi), mice were euthanized and differential bacterial counts were determined in lungs and livers by plating organ homogenates on LBA or LBA supplemented with 40 μg/ml kanamycin.

Transposon mutant library screen

A transposon library was constructed using the EZ-Tn5 transposome system as described previously (123). Since growth of WT bacteria is significantly attenuated in ChxRPMI without Mn or Zn added back, the growth conditions were modified for the primary screen in order to facilitate rapid screening of over 4000 mutants. Mutants were inoculated directly from frozen stocks into LB and incubated at 37 °C overnight. Bacteria were then sub-cultured at a 1:20 dilution in ChxRPMI for 1 hour at room temperature. Following the 1-hour subculture, bacteria were diluted 1:50 into 96-well plates containing 100 μl of CP screening media, which consisted of 50 percent RPMI (not chelex-treated) without supplemental metals and 50 percent CP (40 μg/ml) in CP buffer. The plates were incubated at 37 °C with shaking at 180 rpm for 10-12 hours and growth was monitored by measuring the optical density of the cultures at 600 nm. Mutants whose growth in the presence of CP differed by more than two standard deviations from the plate average were confirmed by repeating the inhibition assay as described above for the primary screen. Mutants that exhibited growth comparable to WT in media without CP but whose growth in the presence of CP differed significantly from that of WT bacteria were selected for insert identification. The transposon insertion sites were determined by inverse PCR or by sequencing directly from chromosomal DNA using primers KAN-1 and KAN-2.

Identification of a putative zur-binding consensus sequence and zur-regulated genes

The intergenic region between *znuA* and *zur* was searched for possible Zur binding motifs using the consensus 19 bp zur box (AATGTTATAWTATAACATT)

derived from the analysis of 13 genes from several gamma-Proteobacteria (135). BLAST analysis was then employed to search for this *A. baumannii* zur box in the Ab17978 genome. Once possible zur-regulated genes were identified, 300bp of 5' flanking sequence was collected from each gene. These sequences were searched for motifs using the Multiple Em for Motif Elicitation (MEME) tool, which confirmed the putative zur boxes from the majority of genes analyzed (154). Each of the zur box sequences was then input into WebLogo 2.0 to generate a sequence logo that graphically represents the degree of sequence conservation at each nucleotide position (82).

Construction of Δ*znuB*

Approximately 1000 bp of flanking DNA sequence was amplified from the immediate 5' and 3' regions surrounding *znuB.* The kanamycin resistance gene *aph* was amplified from pUCK1 and the three PCR products were stitched by overlap extension PCR as described previously (248). This PCR product was cloned into pCR2.1 (Invitrogen) and sequence verified. The product was then re-amplified and the resulting linear DNA product was transformed into Ab17978 to generate an in-frame allelic replacement of *znuB* with *aph*. Transformants were selected on LBA supplemented with 40 μg/ml kanamycin. The resulting colonies were screened for integration of the kanamycin cassette into the correct locus using locus-specific primers that anneal outside the region contained within the knock out construct.

ICP-MS analyses of intracellular zinc concentrations

Bacteria were cultured overnight in chxRPMI with 0.1 mM $CaCl_2$, 1mM $MgSO_4$ and 10 μM $FeSO_4$ added. Bacteria were sub-cultured 1:20 in fresh chxRPMI for 1 hour. For experiments with CP, the bacteria were then sub-cultured 1:50 into 10 mL CP growth media with 37.5 μg/ml CP and 50 μM Mn. Since Δ*znuB* grows very poorly under these conditions, WT bacteria were harvested after approximately 6 hours (OD_{600} = 0.6), while Δ*znuB* cultures were harvested after approximately 10 hours (OD_{600} = 0.4). For the experiments without CP, the bacteria were sub-cultured 1:50 into fresh media similar to the overnight conditions except that Mn and ^{68}Zn were added to final concentrations of 100 μM and 1 μM, respectively. The bacteria were harvested after approximately 8 hours (OD_{600} = 0.6). In all cases, at the indicated time points, bacteria from the overnight cultures or the sub-cultures were pelleted by centrifugation (10 minutes, 6,000 x *g*), washed twice with water and transferred to Teflon vials. Bacterial pellets were dried by incubation at 50 °C overnight then digested by boiling in nitric acid for 6 hours at 130 °C.

Elemental quantification was performed on the Thermo Element 2 HR-ICPMS (Thermo Fisher Scientific, Bremen, Germany) coupled with ESI auto sampler (Elemental Scientific, Omaha, NE). The HR-ICPMS is equipped with a PFA microflow nebulizer (Elemental Scientific, Omaha, NE), a double channel spray chamber (at room temperature), a magnetic sector followed by an electric sector, and a second electron multiplier. The sample uptake was achieved through self-aspiration via 0.25 mm ID sample probe and sample capillary. The operation parameters are listed in **Table 9**.

Table 9. HR-ICP-MS parameters.

Instrument	Element 2 HR-IC-MS
RF power	1200 W
Cool gas	16.00 L min^{-1}
Auxiliary gas	0.8 L min^{-1}
Sample gas	1.05 L min^{-1}
Resolution mode	Medium resolution (4000)
Isotopes measured	^{55}Mn, ^{57}Fe, ^{63}Cu, ^{65}Cu, ^{66}Zn, ^{68}Zn
Runs	10
Passes	1
Samples per peak	20
Sample time	0.01 s

Imipenem inhibition assays

Bacteria were cultured in Mueller Hinton Broth (MHB) overnight then sub-cultured 1:1000 in MHB containing 25 μM TPEN and imipenem (0 – 20 μg/ml). Where indicated, $ZnSO_4$ was added to a final concentration of 100 μM. Bacteria were cultured for 24 hours while the optical densities of the cultures were monitored at 600 nm. Minimum inhibitory concentrations were determined as the concentration in the first well in which no bacterial growth was observed.

Results

Calprotectin contributes to defense against *A. baumannii* infection.

Calprotectin has been implicated in defense against bacterial pathogens through chelation of manganese and zinc (56, 136, 164). This protein makes up approximately 50 percent of the neutrophil cytoplasmic protein content, which facilitates accumulation of CP at sites of infection. Neutrophils are a critical component of the innate response to *A.*

baumannii infection; however, the role for CP in *A. baumannii* infection has not been demonstrated previously (238, 287). As a first step toward elucidating a possible role for CP in *A. baumannii* infection, growth inhibition assays were performed with increasing concentrations of CP (**Figure 32a**). These assays demonstrate that CP inhibits *A. baumannii* growth with an IC_{50} of approximately 60 μg/ml under these conditions. Importantly, the inhibitory effect of CP is completely reversed by the addition of excess Mn and Zn. Moreover, a variant of CP in which the Mn and Zn binding sites are mutated is unable to inhibit *A. baumannii* growth (data not shown). Finally, treatment with CP reduces intracellular accumulation of Mn and Zn (**Figure 32b**). Taken together, these results establish that CP inhibits *A. baumannii* growth through chelation of Mn and Zn.

In order to determine if CP contributes to host defense against *A. baumannii* pneumonia, we obtained $S100A9^{-/-}$ mice and compared their susceptibility to *A. baumannii* infection with wildtype C57BL/6 mice. $S100A9^{-/-}$ mice are functionally CP-deficient because S100A8 does not form stable homodimers. Although *A. baumannii* is rarely causes lethal infection in immunocompetent mice, a significant increase in mortality was observed over a 72-hour time course in $S100A9^{-/-}$ mice (**Figure 32c**). Consistent with this observation, bacterial burdens were significantly higher at 36 hpi in the lungs of $S100A9^{-/-}$ mice compared to WT. Moreover, dissemination to secondary sites was also increased in CP-deficient mice as evidenced by an increase in bacterial burden in livers. We did not see a significant increase in bacterial burden at 72 hpi suggesting that those mice that survive to 72 hours are eventually able to control their infection. Taken together, these data demonstrate that CP is an important component of the innate immune response to *A. baumannii* pulmonary infections.

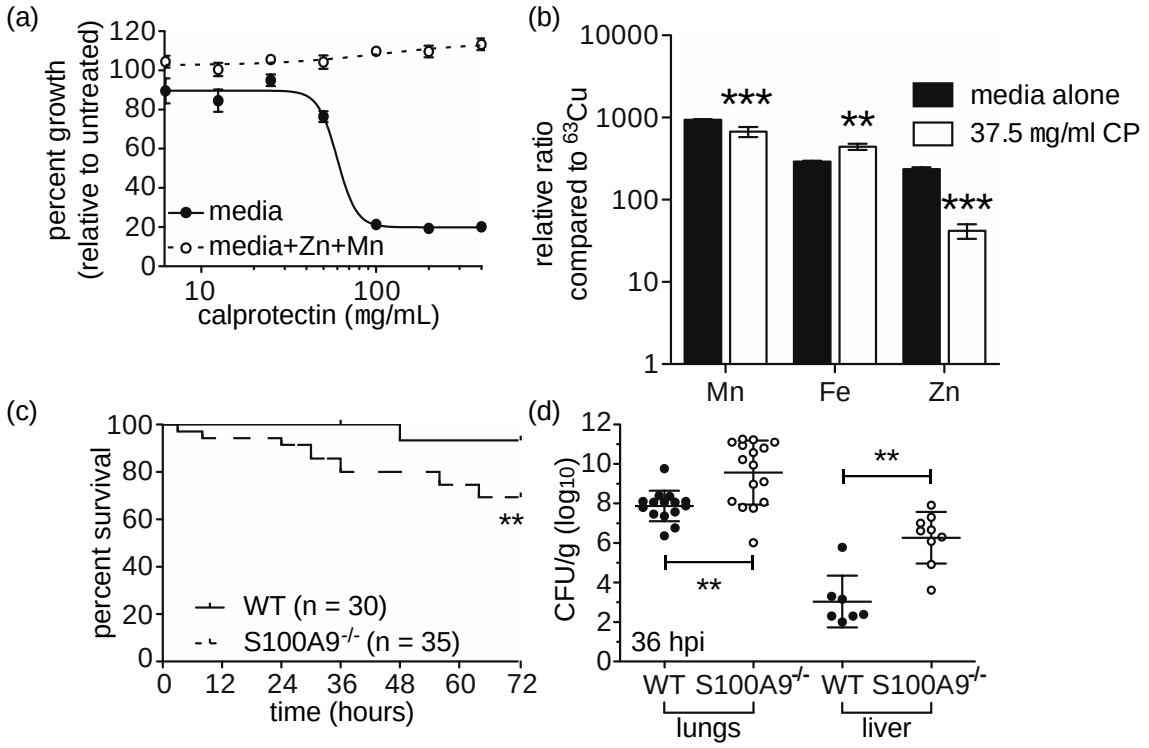

Figure 32. CP inhibits *A. baumannii* growth *in vitro* and contributes to protection against *A. baumannii* infection.

(a) CP-mediated inhibition of *A. baumannii* growth *in vitro* is Mn and Zn dependent. *A. baumannii* growth in the presence of increasing concentrations of CP with (dashed lines) or without (solid lines) excess Mn and Zn added back. Data represent the average of three biological replicates. (b) Treatment with CP reduces intracellular Mn and Zn accumulation. (c-d) CP contributes to host defense against *A. baumannii* infection. (c) Survival of WT or CP-deficient mice following infection with *A. baumannii*. Data were averaged from three independent experiments with 8-16 mice per group in each experiment. ** $p < 0.01$ as determined by Gehan-Breslow-Wilcoxon Test. (d) Bacterial burden in lungs and livers of WT or CP-deficient mice 36 hpi with *A. baumannii*. Data were averaged from three independent experiments with 5-10 mice per group in each experiment. ** $p < 0.01$ as determined by Student's *t* test.

Identification of *A. baumannii* mutants with altered sensitivity to CP

The contribution of CP to defense against *A. baumannii* infection suggests that *A. baumannii* requires Mn and/or Zn in order to maximally colonize the murine lung. To date, no Mn or Zn acquisition systems have been described in *A. baumannii* and specific bacterial processes that require either of these metals have not been described in this organism. In order to determine the impact of Mn and Zn limitation on *A. baumannii* physiological processes, we performed a transposon library screen to identify mutants with either increased or decreased resistance to CP (**Figure 33a**). We screened

approximately 4000 mutants and selected 40 whose growth was significantly different from WT in the presence of CP, but unchanged compared to WT in media without CP. Many of these mutants had transposon insertions into ribosomal RNA-encoding genes. We have observed the same pattern in previous transposon library screens (*Chapter III*). It is possible that these sites represent areas of the chromosome into which the transposon preferentially integrates and we therefore did not follow up on any of these mutants. Of the remaining mutants, approximately half were mutants with increased sensitivity to CP, while the others demonstrate increased resistance. Interestingly, a majority of the mutants cluster into a few common categories based on the putative functions of the proteins encoded by the genes disrupted by transposon integration (**Figure 33b and Table 10**). These functions include biofilm formation and polysaccharide production, inorganic ion transport and DNA replication or repair.

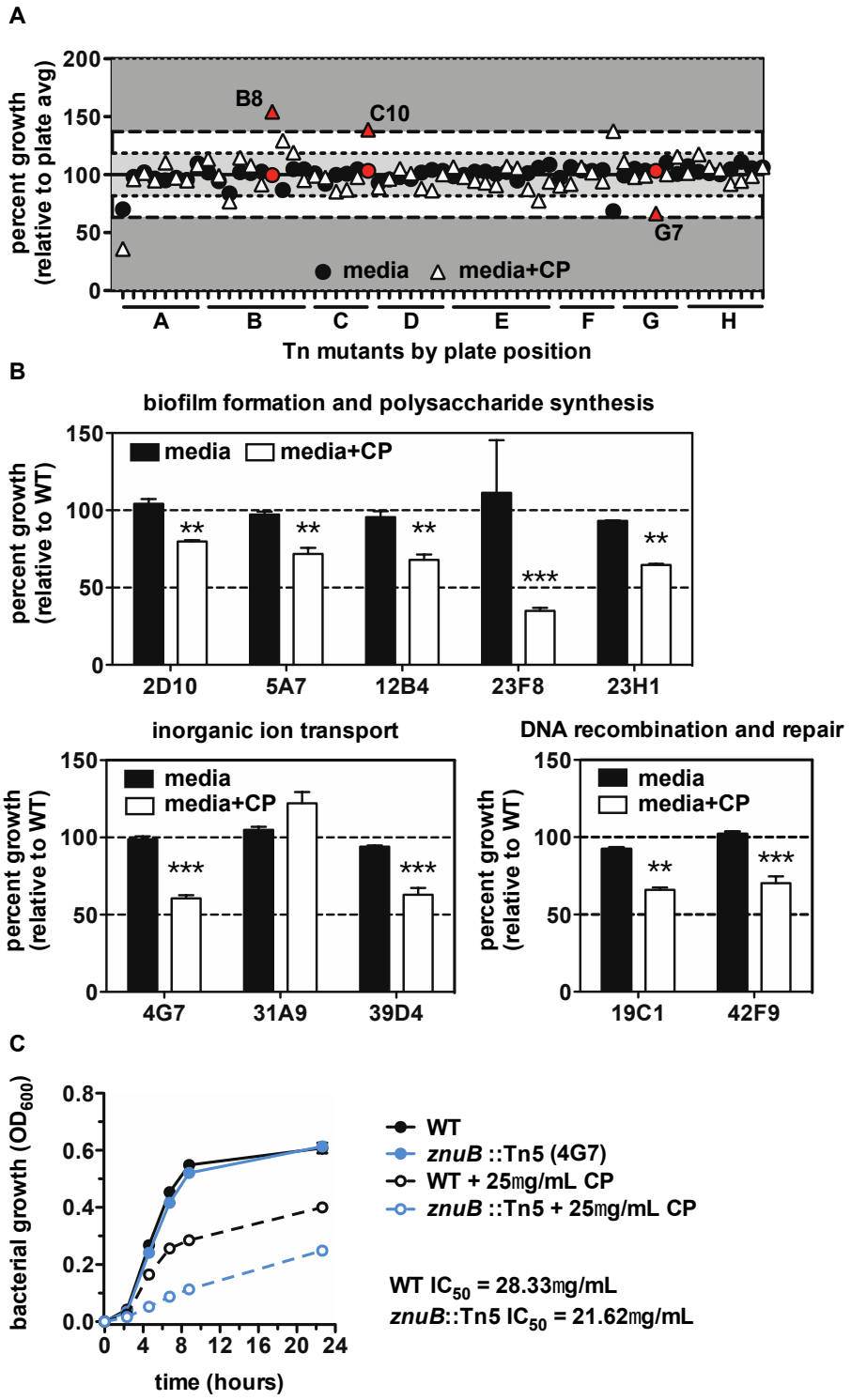

Figure 33. Transposon library screen to identify bacterial processes affected by CP treatment.
(a) Bacterial growth from a representative plate of mutants cultured in media alone or media with 40 μg/ml CP. **(b)** Growth of selected mutants relative to WT bacteria cultured in media alone or media containing 40 μg/ml CP. Mutants are classified according to the predicted functional category of the gene disrupted by the transposon. ** $p < 0.01$, *** $p < 0.001$ for relative growth in the presence of CP compared to media alone, as determined by two-way ANOVA. **(c)** Growth curves comparing WT *A. baumannii* and *znuB*::Tn5 in the presence or absence of 25 μg/ml CP.

Table 10. Transposon mutants with altered sensitive to CP.

Mutant ID	Locus tag	Description	Phenotype	Insert type
PDL05G12	A1S_2148	flavin reductase-like protein; putative acetyl-CoA synthetase/AMP-(fatty) acid ligase	resistant	intergenic
PDL31A10	A1S_0352	hypothetical protein	resistant	intergenic
PDL02D10	A1S_2505; A1S_2506	hypothetical protein (110bp 5`); putative GGDEF family protein (290bp 3`)	sensitive	intergenic
PDL23H1	A1S_2841; A1S_2842	putative type 4 fimbrial biogenesis protein FimT (not present in the SEED); Acetyl-CoA C-acyltransferase	sensitive	intergenic
PDL15F1	A1S_3277	putative pirin-like protein	sensitive	intergenic
PDL03F9	A1S_0367	glutathione-regulated potassium-efflux system protein (K(+)/H(+) antiporter) (KefB)	resistant	intragenic
PDL03H9	A1S_0367	glutathione-regulated potassium-efflux system protein (K(+)/H(+) antiporter)	resistant	intragenic
PDL03H10	A1S_0367	glutathione-regulated potassium-efflux system protein (K(+)/H(+) antiporter)	resistant	intragenic
PDL05D12	A1S_0196	Long-chain-fatty-acid-CoA ligase	resistant	intragenic
PDL06C3	A1S_3463	Cro-like protein (pAb1)	resistant	intragenic
PDL26D12	A1S_2040	putative phage integrase	resistant	intragenic
PDL31A11	A1S_1053	hypothetical protein	resistant	intragenic
PDL31A9	A1S_0118	hypothetical protein	resistant	intragenic
PDL11C6	A1S_3142	putative membrane protein	resistant	intragenic
PDL04G7	A1S_0143	high affinity Zn transport protein	sensitive	intragenic
PDL06H4	A1S_2477	isocitrate dehydrogenase	sensitive	intragenic
PDL09F4	A1S_0076	aconitate hydratase	sensitive	intragenic
PDL05A7	A1S_0430	Putative glycosyltransferase	sensitive	intragenic
PDL19C1	A1S_2588	Holliday junction DNA helicase RuvB	sensitive	intragenic
PDL22A12	A1S_0023	putative malic acid transport protein	sensitive	intragenic
PDL23E2	A1S_3472	DNA replication protein (pAB2)	sensitive	intragenic
PDL23F8	A1S_0060	hypothetical protein	sensitive	intragenic
PDL12B4	A1S_0749	BfmS	sensitive	intragenic
PDL42C3	A1S_3352; A1S_3353	putative OHCU decarboxylase; putative transthyretin-like protein precursor	sensitive	intragenic
PDL42F9	A1S_0696	putative MutT/nudix family protein	sensitive	intragenic
PDL39D4	A1S_0118	hypothetical protein	sensitive	intragenic

Identification of a Zn uptake system in *A. baumannii*

In mutant 4G7 the transposon disrupts a predicted *znuB* orthologue. In other bacteria, ZnuB is a cytoplasmic membrane permease involved in Zn uptake (9, 38, 62,

65). This protein is part of an ABC-family transporter where ZnuC is the cognate ATPase and ZnuA is the periplasmic substrate-binding protein (9, 38, 62, 65). Consistent with a role for the putative *A. baumannii* ZnuB in Zn transport, disruption of *znuB* by integration of the transposon leads to increased sensitivity to CP (**Figure 33c**). Since transposon mutagenesis can cause polar effects on neighboring genes, we generated a targeted deletion mutant in which *znuB* was replaced by an in-frame copy of the kanamycin resistance gene, *aph*, which was used for all subsequent experiments. In order to confirm that Δ*znuB* was more sensitive to CP than WT bacteria, the CP growth inhibition assays were repeated with Δ*znuB* in CP growth media. CP growth media was chosen over the transposon screening media since this medium allows for better titration of the Zn and Mn concentrations and would allow for differentiation between the effects of Zn- and Mn-chelation on Δ*znuB*. Interestingly, Δ*znuB* did not exhibit a significant defect in growth compared to WT bacteria grown in the presence of CP in CP growth media without Mn or Zn added (**Figure 34**). Similarly, when either Zn alone or Zn and Mn were added back to CP growth media, both WT and Δ*znuB* exhibit similar growth levels and are no longer inhibited by CP. However, if only Mn is added back to CP growth media, growth of Δ*znuB* is significantly inhibited in the presence of increasing concentrations of CP, while WT growth is not. The observation that growth of Δ*znuB* cannot be rescued by supplementation with Mn alone confirms that this mutant is sensitive to growth in Zn limiting conditions. The fact that Δ*znuB* does not exhibit reduced growth compared to WT when neither Mn nor Zn were added back was unexpected given the previous results with 4G7. However, given that both WT and Δ*znuB* are significantly inhibited under these conditions, it is possible that the low basal level of Mn and Zn in the media is

sufficient to reduce WT growth to similar levels as Δ*znuB*. Consistent with this hypothesis, Δ*znuB* exhibits impaired growth compared to WT in rich media (LB) in the presence of the Zn-selective chelator, TPEN (**Figure 35**). The latter finding supports a role for ZnuB in Zn acquisition since this mutant is particularly sensitive to growth in low Zn concentrations and Zn addition is necessary to rescue Δ*znuB* from CP-mediated growth inhibition.

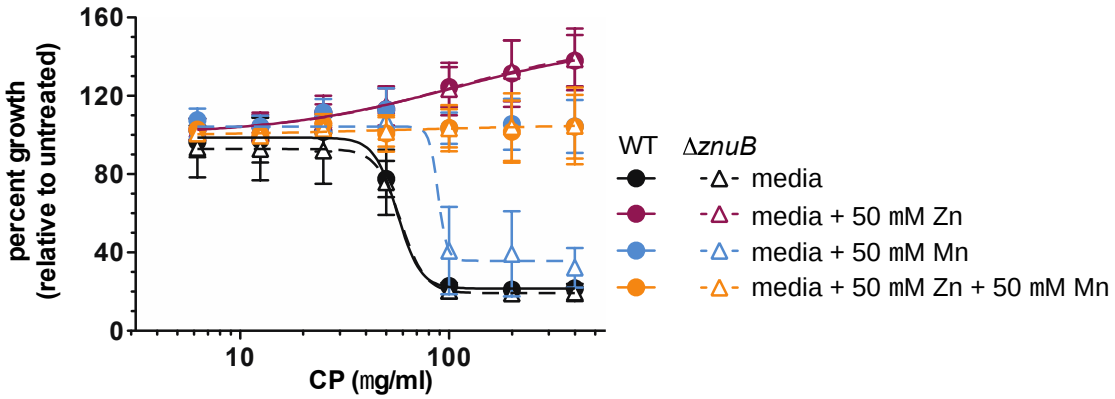

Figure 34. CP growth inhibition assays comparing WT with Δ*znuB*.

Bacteria were cultured in CP growth media in the presence of increasing concentrations of CP with or without addition of Zn, Mn or Zn and Mn. Data are presented as the percent growth relative to bacteria growth without CP. Curve fit was performed using a non-linear regression with variable slope.

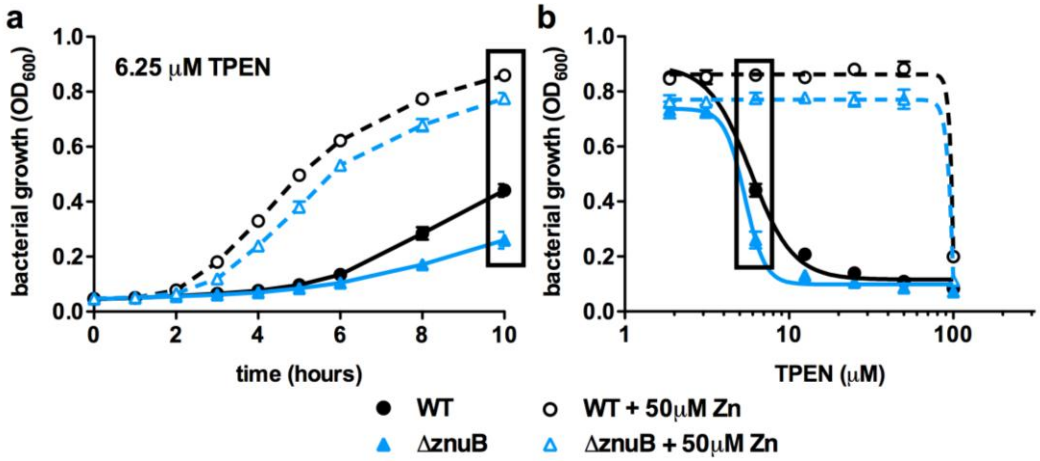

Figure 35. Comparison of the effect of TPEN on inhibition of WT and Δ*znuB* with or without addition of excess Zn.

(a) Growth curves comparing WT (black) and Δ*znuB* (blue) in the presence of 6.25 μM TPEN with (dashed lines) or without (solid lines) addition of 50 μM Zn. (b) Growth inhibition assays in increasing concentrations of TPEN.

Regulation of *znuB* in Zn-limiting conditions

In a number of bacteria, the expression of high affinity Zn acquisition systems like ZnuABC is repressed in the presence of Zn by the Zn uptake regulator, Zur (9, 38, 135, 267). To determine whether *znuB* is under similar transcriptional control in *A. baumannii* we first determined whether Ab17978 encodes a *zur* homologue. The genomic context surrounding *znuB* is illustrated in **Figure 36a**. Homologues of both *zur* and *znuC* are present within the same predicted operon as *znuB*, while *znuA* is divergently transcribed, but still encoded within the same locus. In other bacteria, Zur is a Zn-dependent repressor that binds to a 19 bp consensus sequence in the presence of Zn to repress transcription of genes involved in Zn uptake (135). The intragenic region between *znuA* and *zur* was searched for a possible Zur-binding site using the consensus sequence from γ-Proteobacteria. This search yielded a possible Zur-binding sequence within 100 bp of the *znuA* translational start site (**Figure 36b**). Since a second site was not identified in the region between *znuA* and *zur* it is likely that binding at this sequence leads to repression of both *znuA* and *zurznuCB*.

Using the putative *A. baumannii* zur box sequence, we next conducted a BLAST search against the *A. baumannii* genome in order to identify additional putative Zur-regulated genes (**Figure 36c** and **Table 11**). These candidate Zur-regulated genes were further validated by searching for sequence motifs within their 5' flanking sequences. The latter analysis, which employed the MEME analysis tool, independently identified the zur box in a majority of the genes analyzed. Based on these results a list of putative Zur-regulated genes was constructed (**Table 11**). A number of the predicted Zur-regulated genes in *A. baumannii* are regulated by Zur in other bacteria. These include the

ribosomal L31 protein, carbonic anhydrase and the Znu system (53, 135, 175, 196, 267). While the functional significance of Zur-regulation has been elucidated for some of these genes, in many cases the function of the encoded proteins and their roles in Zn homeostasis have not been defined. Interestingly, Ab17978 encodes two predicted TonB-dependent receptors with highly conserved Zur-binding sequences immediately upstream. One of these genes, A1S_2892 is found within the chromosome, while A1S_3475 is found within one of this strain's native plasmids. These transporters have homology (include percentages) to ZnuD, a Zur-regulated receptor involved in Zn and heme transport in *N. meningitidis* (274). Based on their homology and putative zur-regulation, we have designated these genes as *znuD1* (A1S_2892) and *znuD2* (A1S_3475).

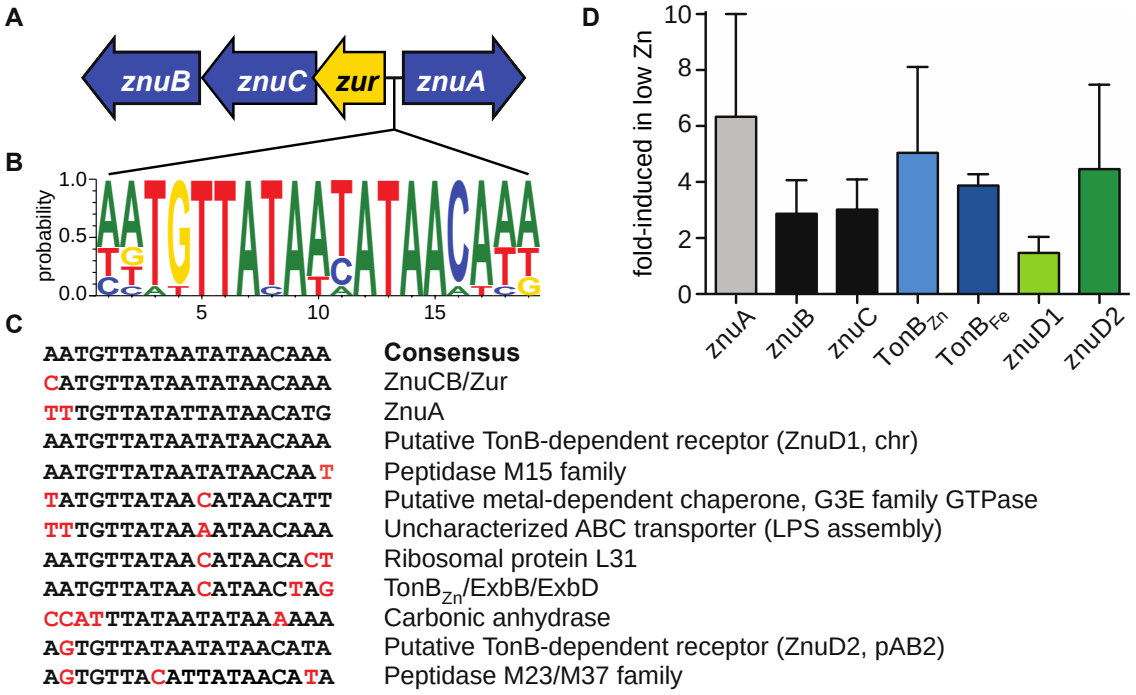

Figure 36. Genetic characterization of a putative Zn uptake system in *A. baumannii*

(a) Schematic representation of the genomic locus containing *znuA* and the *zurznuCB* operon. (c) Consensus Zur operator sequence. (d) Predicted Zur-regulated genes. (e) qPCR analysis of the expression of genes predicted to be involved in Zn uptake across the outer (znuD1, znuD2, TonB) and inner (znuA, znuB, znuC) membranes.

To determine whether these genes are regulated under Zn-limiting conditions, *A. baumannii* was grown in LB or LB supplemented with the Zn-chelator, TPEN, at a concentration of 25 μM. This concentration was selected because at this concentration of TPEN Δ*znuB* begins to exhibit decreased growth compared to WT bacteria. This suggests that the Znu system is required for optimal growth under these conditions and is therefore likely to be induced under these conditions in WT bacteria. Consistent with this hypothesis, transcripts for *znuA, znuB, znuC, znuD1* and *znuD2* were all increased in TPEN-containing media compared to media without TPEN (**Figure 34D**). These data support the hypothesis that ZnuABC, ZnuD1 and ZnuD2 are involved in Zn acquisition.

Table 11. Locus tags and descriptions of predicted Zur-regulated genes

Locus tag	Description
A1S_0144	Zur (ZnuB, ZnuC)
A1S_0145	ZnuA
A1S_0391	LSU ribosomal protein L31p
A1S_0452	TonB (ExbB, ExbD)
A1S_2892	Putative TonB-dependent receptor, ZnuD1 (Pld)
A1S_3103	Uncharacterized ABC transporter (LPS assembly)
A1S_3225	Carbonic anhydrase
A1S_3329	Peptidase, M23/M37 family
A1S_3411	Putative metal chaperone involved in Zn homeostasis
A1S_3412	Hypothetical protein, putative signal peptide (Peptidase M15)
A1S_3475	Putative tonB dependent receptor protein, ZnuD2 (plasmid pAB2)

The outer membrane of Gram-negative bacteria represents a significant permeability barrier for ions and small molecules. In many bacteria, transport of transition metal ions across the outer membrane is thought to occur by diffusion through non-selective porins. However, the expression of two TonB-dependent receptors in *A. baumannii* under Zn-limiting conditions suggests that transport of Zn across the outer membrane of this organism may be an energy dependent process similar to the case in *N.*

meningitidis. Transport through TonB-dependent receptors requires the TonB-ExbB-ExbD system, which harnesses energy from the proton motive force generated at the inner membrane to facilitate transport across the outer membrane. Interestingly, *A. baumannii* encodes two predicted TonB-ExbB-ExbD systems, one of which appears to be under transcriptional control by Zur, based on the presence of a Zur-binding consensus sequence upstream. We have designated the putative Zur-regulated system TonB1-ExbB1-ExbB2, based on its location within the chromosome relative to the position of the predicted Fur-regulated system. Although this system was previously shown to be up-regulated in the presence of the iron chelator 2,2-dipyridyl, we sought to determine whether Zn-limiting conditions induce expression of either of the *tonBexbBexbD* operons (124). In the presence of 25μM TPEN, transcripts for both *tonB* genes were up-regulated 4 to 5-fold (**Figure 36d**). Given that TPEN can also bind Fe with high affinity, up-regulation of both genes does not rule out the possibility that one system responds preferentially to depletion of one metal compared to the other. Taken together, these data further suggest that translocation of Zn across the outer membrane is an energy-dependent process in *A. baumannii*.

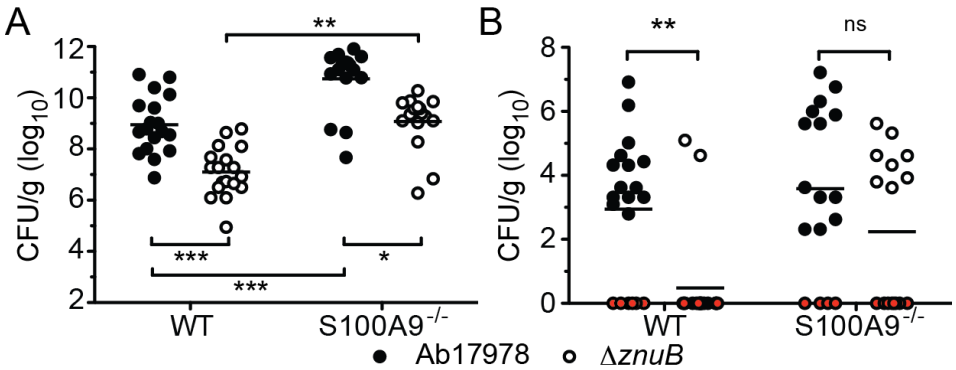

Figure 37. Contribution of the Znu system to pathogenesis *in vivo*.

Bacterial burden in lungs (a) and livers (b) of mice co-infected with WT *A. baumannii* and Δ*znuB*. Red symbols indicate CFU below the limit of detection. * $p < 0.05$, ** $p < 0.01$, *** $p < 0.001$ as determined by one-way ANOVA.

ZnuB contributes to the pathogenesis of *A. baumannii* pulmonary infections.

Based on the finding that CP contributes to host defense against *A. baumannii* infection and that Δ*znuB* is more sensitive to CP-mediated Zn chelation *in vitro*, we hypothesized that disruption of Zn acquisition would reduce *A. baumannii* virulence. To define the contribution of Δ*znuB* to pulmonary infections, WT and S100A9$^{-/-}$ mice were co-infected with an equal mixture of WT and Δ*znuB* and bacterial burdens were quantified at 36 hpi in lungs and livers. WT *A. baumannii* significantly outcompetes Δ*znuB* for colonization of the lungs of both WT and CP-deficient mice (**Figure 37a**). Of particular interest is the finding that Δ*znuB* could only be detected in the livers of two mice (10 percent) (**Figure 37b**). Moreover, dissemination of Δ*znuB* to the liver is nearly rescued in S100A9$^{-/-}$ mice. These data suggest that CP-mediated Zn-chelation is particularly important in limiting bacterial dissemination from the primary site of infection in the lung. Taken together, the results of the *in vivo* studies demonstrate that Zn acquisition through ZnuB contributes to *A. baumannii* pathogenesis.

Zn chelation reverses carbapenem resistance in MDR *A. baumannii*.

Multidrug resistance is a common problem complicating the treatment of *A. baumannii* infections. One of the few remaining antibiotic classes available for the treatment of *A. baumannii* infections is the carbapenems. However, carbapenem resistance is becoming increasingly common primarily through dissemination of genes encoding carbapenem hydrolyzing enzymes or carbapenemases. Currently there are no carbapenemase inhibitors available for combination therapy. Interestingly, many of these enzymes are metalloenzymes that require Zn for their hydrolyzing activity. This fact led us to

hypothesize that Zn limitation may serve as a valuable adjunct to carbapenem therapy. To test this hypothesis, we determined the imipenem MIC against the carbapenem resistant clinical isolate, Ab0057, in the presence or absence of 25 μM TPEN. Treatment with TPEN reduced the imipenem MIC to below the clinical breakpoint for imipenem resistance in *A. baumannii* and this effect was reversed by addition of excess Zn (**Figure 38**). The same experiments were performed with levofloxacin since resistance to levofloxacin is mediated by mutation of the drug's target and therefore should not be impacted by Zn chelation. Consistently, the levofloxacin MIC was unchanged by Zn limitation and remained above the breakpoint for clinically defined resistance (**Figure 38**). These results highlight Zn-limitation as a possible mechanism to combat carbapenem resistance in *A. baumannii*.

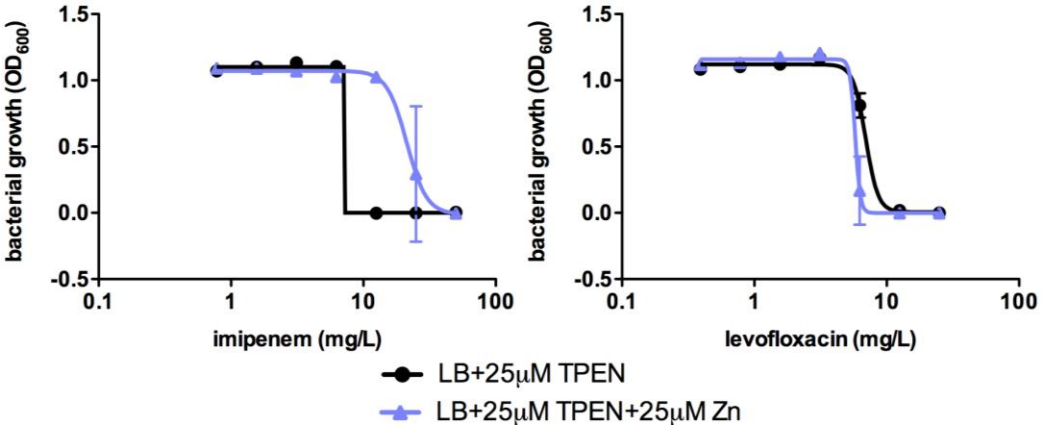

Figure 38. Effect of Zn chelation on resistance to imipenem and levofloxacin an MDR isolate of *A. baumannii.*

Bacterial growth measured at 24 hours in LB medium in the presence of increasing concentrations of imipenem or levofloxacin and TPEN, with or without addition of excess Zn.

Discussion

Transition metals occupy an essential niche within biological systems. The essentiality of transition metals to invading bacterial pathogens has been exploited by vertebrate hosts as an innate defense strategy against these infections. Most work has focused on iron sequestration as a mechanism of nutritional immunity; however, it is now known that nutritional immunity includes strategies to withhold other essential metals such as Mn and Zn. In this *Chapter*, I have demonstrated that Mn and Zn chelation by CP inhibits *A. baumannii* growth *in vitro* and that CP is important for defense against *A. baumannii* pulmonary infections. Moreover, I have used CP to elucidate physiological processes that are impacted by Mn and Zn chelation by screening a transposon library for mutants with increased or decreased susceptibility to CP. This screen identified over 40 mutants with altered sensitivity to CP. The putative contributions of the genes identified in the screen to Mn and Zn homeostasis are discussed below. Finally, I have identified a Zn acquisition system in *A. baumannii* and defined its Zn-dependent regulation and its roles in Zn uptake and pathogenesis.

By comparing the results of the transposon mutagenesis screen with the putative *A. baumannii* Zur regulon it is possible to identify a number of physiological processes that are impacted by Zn and/or Mn concentrations. For example, a number of genes identified in the transposon screen encode proteins with known or potential roles in biofilm formation. While some of these genes may be involved in biofilm formation directly (e.g. A1S_0749, bfmS; A1S_2841), others have potential roles in signaling (A1S_2506), or polysaccharide production (A1S_0060, A1S_0430) (90, 281). Although the proteins

encoded by the latter subset of genes are predicted to be involved in LPS biosynthesis, LPS biosynthesis and exopolysaccharide biosynthesis machinery often overlap. Nonetheless, one cannot rule out that CP impacts LPS biosynthesis directly and that this effect rather than potential contributions to biofilm formation is the reason for identifying the polysaccharide synthesis genes in the screen. In support of a direct impact on LPS biosynthesis, LpxC, which catalyzes a critical step in lipid A biosynthesis, is a Zn-dependent enzyme. Taking all of these data into consideration, we can conclude that biofilm formation and polysaccharide production are regulated in response to Zn or Mn-limitation.

The results of the transposon screen also highlight DNA replication and repair as processes that are impacted by calprotectin treatment. Since DNA polymerases require Zn for function it is not surprising that Zn-limitation would impact DNA replication. However, it is not clear why disrupting a DNA replication protein encoded on the pAB2 plasmid would result in decreased resistance to CP. It is interesting to note, however, that this plasmid also carries *znuD2*. It is possible that disruption of the replication protein encoded on this plasmid causes a polar effect on *znuD2*, either directly impacting its expression or perhaps by reducing the copy number of the plasmid. In contrast, the effect of disrupting *ruvB* is perhaps more clear. RuvB is a DNA helicase which functions with RuvA in the repair of stalled replication forks. Since DNA polymerases require Zn, Zn-limitation may lead to stalling of the replication fork. A similar process has been shown for *Salmonella typhimurium* where treatment with nitric oxide displaces Zn from Zn-containing enzymes (241). This disruption then leads to stalled replication forks, which

require RuvAB for repair. Disruption of *ruvB* sensitizes bacteria to Zn-limitation by CP, presumably because these stalled replication forks are no longer efficiently repaired.

A mutant in which *mutT* is disrupted is more sensitive to CP treatment. In other bacteria, MutT is important for the repair of oxidative DNA damage. Oxidative damage to DNA involves the formation of oxidized guanine, which is highly mutagenic due to ambiguous base pairing with either cytosine or adenine. MutT specifically hydrolyzes both 8-oxo-deoxyguanosine triphosphate (8-oxo-dGTP) and 8-oxo-guanosine triphosphate (8-oxo-rGTP), which are otherwise incorporated in DNA and RNA opposite template A. This activity therefore prevents misincorporation of these nucleotides into DNA and RNA, respectively (24). Mn contributes directly to protection from oxidative stress in other bacteria. Mn can replace Fe in some proteins, preventing oxidative damage to these proteins. Moreover, some bacteria encode Mn-dependent superoxide dismutases (SODs), which directly protect against oxidative damage by detoxifying superoxide by dismutation to hydrogen peroxide, which is then converted to water by catalase. Based on these roles for Mn in oxidative stress resistance, CP treatment perpetuates oxidative stress (136). *A. baumannii* does not have Mn-dependent SODs; rather it has one Cu/Zn-dependent SOD and one Fe-dependent SOD. Interestingly, the gene immediately upstream from the Cu/Zn-dependent SOD was hit in the transposon screen. This gene encodes a putative PerR-regulated outer membrane protein of unknown function and disruption of this gene increases resistance to CP. It is not yet known whether disruption of this omp is directly responsible for the decreased susceptibility to CP. Taken together, the results of the transposon screen suggest that CP treatment indirectly induces DNA

damage through oxidative stress or inhibition of replication machinery and that repair of this damage is necessary to resist the effects of CP.

A final category of genes identified in the screen that should be mentioned are those classified in the COG functional category of inorganic ion transport and metabolism. ZnuB will be discussed in greater detail below. In addition to *znuB*, two mutants were identified in which the transposon inserts into a gene encoding a non-ribosomal peptide synthetase (NRPS). The transposon inserts into a different site in each of the mutants. While their phenotypes initially appeared to be opposing, subsequent analyses have demonstrated that at later time points, both mutants appear to be slightly more resistant to CP (data not shown). The function of this NRPS is not yet known, however it is annotated as part of a pyoverdine biosynthesis cluster. Identification of these mutants could have several implications. Intracellular concentrations of transition metals are carefully regulated in bacteria in order to meet physiologic needs and avoid toxicity. Moreover, the relative abundance of individual metals can influence the toxicity of others (126, 187, 289). As a result, it is not only the absolute abundance of a given metal that is important, but also its ratio with respect to other metals. The fact that the two NRPS mutants appear to be more resistant to CP suggests that reducing iron uptake may be beneficial under Zn and/or Mn-limiting conditions. Further work is necessary to define the contribution of this NRPS to transition metal homeostasis.

Additional genes that encode proteins with putative roles in inorganic ion transport and metabolism were identified within the putative Zur regulon. In particular, the genes encoding the remaining components of the Znu inner membrane transporter, as well as two ZnuD homologues and a TonB system were all up-regulated in Zn-limiting

conditions. Although it was previously thought that transition metal ions such as Zn^{2+} and Mn^{2+} freely diffuse through non-selective porins, the identification of ZnuD in *Neisseria spp.* suggests that in some bacteria transport of Zn across the outer membrane may be an energy-dependent process (274). *A. baumannii* strain 17978 has two putative ZnuD homologues, one encoded on the chromosome and the other on a plasmid. In contrast to *N. meningitidis, A. baumannii* also encodes a TonB/ExbB/ExbD system, which is up-regulated in low Zn conditions. Notably, a Zn-regulated TonB system has not been described previously. It appears that Zn transport across the outer membrane of *A. baumannii* is energy dependent. Recently, the ZnuD from *N. meningitidis* was shown to contribute to heme acquisition when expressed in *E. coli* (151). This finding suggests that ZnuD is either a heme transporter that is up-regulated in low Zn conditions, or that ZnuD transports more than one substrate. Although Zn-dependent regulation of a heme transporter has not been shown previously, several key enzymes involved in heme biosynthesis require Zn. It is therefore possible that under low Zn conditions, bacteria are unable to synthesize sufficient quantities of heme and must up-regulate transporters for exogenous heme acquisition. It remains to be determined whether either of the ZnuD transporters in *A. baumannii* directly transport Zn or heme.

As summarized above, we identified a transposon mutant in which the transposon integrates into *znuB.* A targeted deletion of *znuB* is more sensitive to CP and other Zn chelators, particularly in the presence of excess Mn. This latter finding is interesting and supports the idea that transition metal toxicity is highly dependent on the relative abundances of each essential metal, not just on the absolute concentration of any individual metal. Notably, the phenotype of the *znuB* mutant can be rescued by addition

of excess Zn, suggesting that *A. baumannii* possesses an additional mechanism to transport Zn across the inner membrane. Although we did not identify additional inorganic ion transporters in the analysis of the putative Zur regulon, it is possible that Zn is being transporter through a low affinity or non-specific transporter. Based on the observation that excess Mn potentiates the effects of Zn chelation on Δ*znuB*, it is also possible that Zn acquisition in this mutant depends on an inner membrane Mn transporter. If this is the case, in the presence of excess Mn the transporter would translocate its preferred substrate, further reducing Zn acquisition by Δ*znuB*.

In addition to the role for ZnuB in Zn acquisition and resistance to CP *in vitro*, this protein also contributes to pathogenesis *in vivo*. Although infections with Δ*znuB* alone did not result in a significant virulence defect in this mutant (data not shown), co-infection with WT demonstrates that Δ*znuB* is less able to compete with WT *in vivo*. Notably, in the lung, Δ*znuB* exhibits reduced competitive fitness in both WT and CP-deficient mice, suggesting that other factors in addition to CP may contribute to Zn limitation within the lung. In contrast, the ability of Δ*znuB* to disseminate past the primary site of infection was nearly completely abrogated during co-infection with WT *A. baumannii* in WT mice. However, in CP-deficient mice, Δ*znuB* disseminated efficiently to the liver where bacterial burdens for the mutant approached those for WT bacteria. These data suggest that CP is particular important in defending against dissemination to secondary sites like the liver. Previous studies have demonstrated an important role for CP in limiting bacterial replication and abscess formation in liver during *S. aureus* systemic infections (56). This finding would support a possible role for CP in specifically limiting replication in the liver. However, it remains to be determined for *A. baumannii*

infections whether CP inhibits bacterial growth in the bloodstream or whether CP is important for protecting against colonization of the liver itself.

Another notable observation with regard to CP treatment in the presence of excess metals was the observation that in the presence of excess Zn or Mn, *A.* baumannii actually grows better with increasing concentrations of CP (**Figure 34**). The mechanism for the increased CP-dependent growth has not been elucidated. However, it does not appear to depend on the metal-binding capacity of CP since a mutant of CP that no longer binds Mn or Zn also enhances growth of *A. baumannii* in the presence of excess Mn and Zn (data not shown). It is possible that CP is degraded by a Mn or Zn dependent protease allowing the resulting peptides to be taken up as a carbon source. Interestingly, *S. aureus* abscesses are Zn deplete despite the presence of abundant CP. This suggests that metal-bound CP is removed from the site of infection. Given that we observe increased growth in the presence of increased concentrations of CP in metal-replete conditions, it is possible that removal of CP from the site of infection is necessary to prevent bacteria from utilizing CP as a nutrient (amino acid or metal) source. Elemental imaging of Zn in *A. baumannii* infected lungs does not show the same pattern of Zn depletion as that seen in *S. aureus* abscesses (**Figure 39**) However, given the substantial structural differences between lung and liver, particularly the fact that healthy lung is primarily open airways, it is difficult to make direct comparisons regarding the distribution of Zn in these two models. Perhaps as the technologies improve to allow low or sub-micrometer resolution in LA-ICP-MS analyses it will be possible to more accurately define elemental distribution in lungs in response to infection.

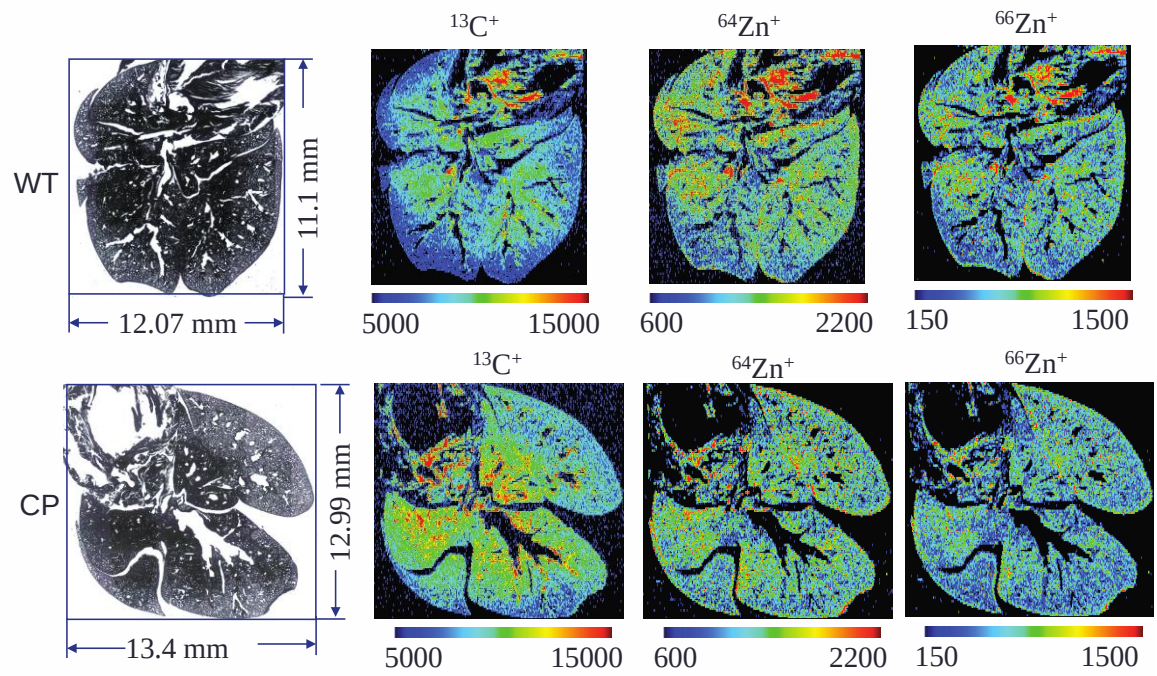

Figure 39. Elemental imaging by LA-ICP-MS analysis of lungs during *A. baumannii* infection.

Elemental distribution in lungs of C57BL/6 (WT) or S100A9-/- (CP) mice harvested at 36 hpi with *A. baumannii*. Lungs were perfused with NaS sulfide for 30 min to precipitate Zn *in situ* and prevent washing out of this ion during fixation. Lungs were then fixed in paraformaldehyde, embedded in paraffin sectioned at 30 μm thickness. Prior to LA-ICP-MS analysis tissue sections were deparaffinized in xylene. Regions of greater ion intensity correspond with areas of increased inflammation and infiltration of the lungs based on histological analyses of serial sections.

Vertebrate hosts have evolved elegant mechanisms to withhold essential metals from invading pathogens. Likewise, bacterial pathogens have evolved efficient means to acquire metals from their vertebrate hosts. Based on these important roles for transition metals at the pathogen-host interface, bacterial metal acquisition systems represent possible targets for therapeutic development. Given that Δ*znuB* exhibits only a modest virulence defect in the lung, targeting this system may not be effective alone for the treatment of *A. baumannii* infections. However, the observation that Zn-limitation reverses imipenem resistance in a carbapenem-producing clinical isolate suggests that Zn chelation may be a viable strategy to use in combination with existing antimicrobial compounds. Given the dire need for new antibiotics effective against MDR *A. baumannii*,

combination strategies like this one may be critical in the battling this important public health threat.

Vi. Circadian variation in susceptibility to *Acinetobacter baumannii* pulmonary infections.

Introduction

Circadian rhythms control numerous physiologic processes including sleep/wake cycles, feeding behaviors and metabolism (147, 180, 308). Disruption of circadian rhythms, such as that observed in shift workers, has been associated with a large number of disease states. Recently, the impact of circadian rhythms on immune function has been described (32, 93, 103, 106, 169, 172). People have observed alterations in immune function with respect to time of day for a long time. However, many studies have focused primarily circadian variation in the responsiveness to pro-inflammatory stimuli, or in the expression of various immune effectors. Few studies have examined whether these variations in the immune response impact susceptibility to bacterial infections or the outcome of those infections.

I have made the anecdotal observation that mice seem to differ in their susceptibility to *A. baumannii* infection based on the time of day that the infection is initiated. I sought to confirm these observations in a controlled setting in order to determine the effect of circadian cycles on *A. baumannii* infection. *A. baumannii* is a particular problem in hospitalized patients and these patients frequently suffer from disruption of their circadian rhythms. By understanding the influence of circadian rhythms on susceptibility to infection it may be possible to modify the clinical environment in order to reduce *A. baumannii* infections.

Methods

A. baumannii infection model and housing conditions

The *A. baumannii* pneumonia model described in previous chapters was used for all of the studies except that the housing conditions were modified as described below in order to control light exposure. Mice were housed in standard cages, which were placed inside a ventilated box with an internal light source. The walls of the box are painted black to prevent transmission of external light. The mice were either exposed to a 12h: 12h light: dark (LD) cycle or to constant dim red light (RR). Fresh bacterial cultures were prepared for each infection. The infections were initiated at the indicated times and allowed to proceed for 48 hours at which point lungs were harvested for enumeration of CFU.

Infections with *A. baumannii* Δ*blsA*

Bls1 is a blue light sensing domain containing protein which mediates light-dependent regulation of motility and biofilm formation (67). We obtained a knockout of *blsA* as a gift from Luis Actis (Miami University) and tested the virulence of this mutant in the *A. baumannii* pneumonia model. Bacteria were grown planktonically at room temperature in constant darkness or in the presence of white light. Bacteria that were cultured in light were then used to infect mice housed in RR conditions, while bacteria cultured in the dark were used to infect mice housed in LD conditions. This experimental setup was selected to distinguish between contribution of light sensing in the culture conditions prior to infection and light sensing *in vivo*. Infections were performed as described above and bacterial CFU in lungs were enumerated at 48 hpi.

Results and Discussion

Mice are most susceptible to infection near the onset of their active period.

In order to determine if mice differ in their susceptibility to infection based on the time of infection initiation, we housed mice in a controlled 12:12 LD cycle and infected at 6-hour intervals beginning at ZT = 10 (two hours prior to activity onset). Since mice are nocturnal, ZT = 12, which is the beginning of the dark cycle, is the time of activity onset. A significant difference in bacterial burden was observed at 48 hpi when mice were infected at ZT = 10, compared to any other time point. The lowest bacterial burdens were observed at ZT = 22 and ZT = 4 (**Figure 40A**). Notably the magnitude of the change in bacterial burden between the highest and lowest points is roughly equivalent to the difference observed with depletion of neutrophils (**Figure 40A**). These data demonstrate a significant daily variation in susceptibility to infection based on the time of infection initiation.

By definition, in order for a process to be considered circadian in nature, it must vary over a 24-hour period and this cyclical variation must remain intact in constant conditions. Since the experiments described above only demonstrate diurnal variation in susceptibility to infection, we repeated the experiments in constant conditions (RR). Although the amplitude of the cycle decreased compared to the LD conditions, there remained a peak bacterial burden in mice infected at CT = 10 compared to other time points (**Figure 40B)**. These data demonstrate that susceptibility to *A. baumannii* infections is regulated by the circadian cycle.

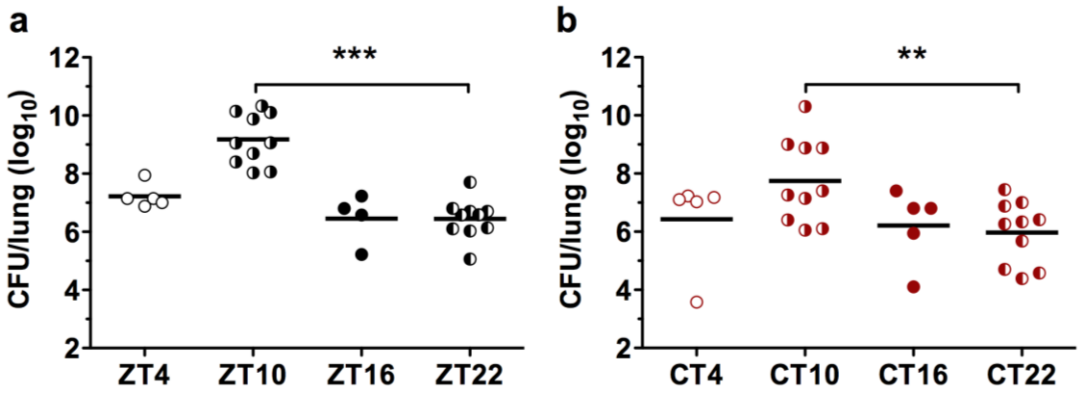

Figure 40. Susceptibility to *A. baumannii* infection is under circadian regulation.

(a) Bacterial burdens in lungs of mice housed in 12:12 light: dark cycles (LD) and infected at ZT 4, 10, 16 and 22 and harvested at 48 hpi. ZT = zeitgeber time where ZT = 0 is the beginning of the light phase, which in our experiments was approximately 6:00 am. (b) Bacterial burdens in lungs of mice housed in constant dim red light and infected at CT 4, 10, 16 and 22. CT = circadian time, where CT = 12 is the onset of the active phase for nocturnal animals, which corresponds to ZT = 12 or the onset of the dark phase when the mice are housed in LD conditions. Lungs were harvested at 48 hpi. ** $p < 0.01$, *** $p < 0.001$ as determined by one-way ANOVA.

Contribution of a bacterial light sensing protein to *A. baumannii* infection

The results described above demonstrate circadian variation in susceptibility to *A. baumannii* infection. However, it is possible that at least some of this difference could be the result of light sensing or circadian rhythmicity within the bacterium itself. *A. baumannii* possess a blue-light sensing domain-containing protein, which mediates regulation of biofilm formation and motility in response to blue light. In order to determine whether this protein contributes to the circadian variation in *A. baumannii* infection, we obtained a mutant in which *blsA* is deleted (Δ*blsA*). Since light sensing modulates phenotypes that might be important at the initiation of infection (e.g. motility), it was necessary to differentiate between light sensing prior to infection and during infection. To do this, the bacteria were in white light or in the dark. Bacteria cultured in the dark were then used to infect mice housed in LD conditions, while bacteria cultured in the light were used to infect mice housed in RR. Regardless of the culture conditions,

Δ*blsA* did not exhibit a change in bacterial burden in the lungs of mice compared to WT bacteria (**Figure 41**). These data suggest that *blsA* does not play a role during infection in this model. Moreover, these data reinforce the conclusion that susceptibility to *A. baumannii* infection is regulated by the host's circadian clock.

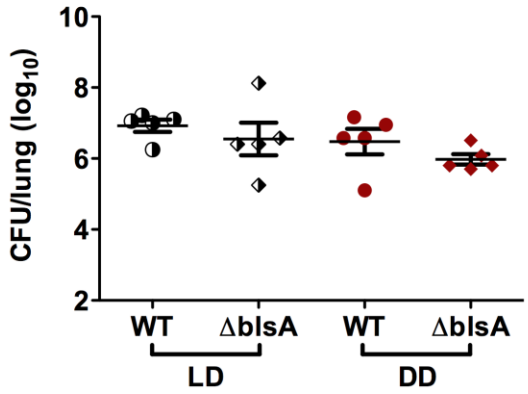

Figure 41. Contribution of *blsA* to *A. baumannii* pathogenesis.

Bacterial burdens in lungs of mice housed in 12: 12 light dark cycles (LD) or constant dim red light (DD) and infected with WT or Δ*blsA*. No statistically significant differences were observed between any of the groups.

Vii. Summary and significance

As infections due to multidrug resistant organisms become increasingly common, therapeutic development to treat these infections languishes. *Acinetobacter baumannii* poses a particular challenge due to the intrinsic drug resistance imparted by its impermeable outer membrane. Furthermore, up-regulation of efflux pumps and down-regulation of outer membrane porins leads to rapid acquisition of resistance to new antibiotics (113, 255). While rates of multi- and pan-drug resistant *A. baumannii* increase, the antibacterial development pipeline remains virtually devoid of agents effective against MDR Gram-negative pathogens. LpxC inhibitors have been highlighted recently as promising new drugs for Gram-negatives. However, these drugs may have little efficacy against *A. baumannii* since LPS is not essential in at least some clinical and laboratory strains of *A. baumannii* (105, 170, 191). These facts further suggest that innovative strategies for the identification of new therapeutic targets are desperately needed to counter the growing burden of *A. baumannii* infections. Toward this end, my work has focused on basic bacterial physiological processes and pathogenesis with the ultimate goal of elucidating new targets for therapeutic intervention.

There are a number of ways to approach therapeutic development for challenging MDR pathogens such as *A. baumannii*. The strategies addressed in my work fall into two broad categories:

1. Restoring the utility of currently available therapeutics.

2. “Outside the box” strategies including interventions that target the host response to infection and attempts to modulate the host response in order to modify disease outcome.

Restoring the utility of currently available antibiotics by targeting antibiotic resistance determinants in *A. baumannii*.

Targeting intrinsic and inducible resistance in *A. baumannii*

Acinetobacter baumannii poses a formidable therapeutic challenge due to its numerous antibiotic resistance determinants and its ability to acquire resistance to new antibiotics through adaptation or mutation. In *Chapter II*, the ability of *A.* baumannii to adapt to signals encountered within the hospital environment in order to augment antibiotic resistance was discussed. The mechanisms underlying NaCl-induced resistance to colistin was further elucidated in *Chapter III* where screening of a transposon mutant library identified over 30 genes involved in inducible colistin resistance in *A. baumannii*. One of the genes identified was *lpsB*, which encodes a glycosyltransferase involved in LPS synthesis. We demonstrate that loss of LpsB function results in increased sensitivity to both colistin and cationic antimicrobial peptides of the innate immune system. Moreover, LpsB is critical for pathogenesis in a pulmonary model of infection. Taken together, the data presented in *Chapters II* and *III* define bacterial processes required for intrinsic antibiotic tolerance in *A. baumannii* and underscore the importance of outer membrane structure in both antibiotic resistance and pathogenesis of *A. baumannii.*

Targeting Zn acquisition to combat imipenem resistance

The data presented in Chapter V establish the role for a newly identified Zn transporter in *A. baumannii* Zn acquisition *in vitro* and pathogenesis *in vivo*. Interestingly, we determined that Zn chelation *in vitro* reverses imipenem resistance in a carbapenemase-expressing clinical isolate of *A. baumannii*. Since carbapenemases are Zn-dependent metalloenzymes, reversal of the imipenem resistance phenotype is most likely due to inhibition of the catalytic activity of the carbapenemase. Carbapenems are currently one of the last remaining classes of antibiotics with activity against *A. baumannnii*. However, resistance to carbapenems is increasingly common in this organism. In parts of Latin America and Africa, resistance rates to imipenem exceed 40 percent. Importantly, none of the available beta lactamase inhibitors are effective against carbapenemases meaning that there are currently no carbapenemase inhibitors available for combination therapy. These facts highlight the significance of our results demonstrating the synergistic activity of a Zn chelator with imipenem. Additional work will be necessary to determine the *in vivo* efficacy of Zn chelation as a combination therapy for carbapenem-resistant *A. baumannii*.

Alternative therapeutic strategies that enhance host defenses to prevent or reduce the severity of *A. baumannii* infections.

Dominant negative mutants of *A. baumannii*

As discussed above, *A. baumannii* rapidly acquires resistance to new antimicrobials. Based on this fact, reliance solely on small molecule antibiotics is

unlikely to provide a lasting solution to the growing burden of *A. baumannii* infections. Novel strategies for the treatment and prevention of these infections are therefore desperately needed. Toward this end, we have identified therapeutic strains of *A. baumannii* that augment the vertebrate host's ability to mount an effective immune response and cure a WT *A. baumannii* infection. Notably, treatment with these strains exerts a therapeutic effect equal to or greater than virtually all published reports of antibiotic therapy in murine models of *A. baumannii* pneumonia (48). Illustrating this point, in a comparable pneumonia model, tigecycline elicits only a 2- to 5-log reduction in bacterial burden. In comparison, we observe complete bacterial clearance in animals co-treated with Tn5A7 (**Figure 18**) (228). These facts underscore the potential for further development of these strains as biologic therapy for *A. baumannii* pneumonia. In order for this strategy to be realized, however, further elucidation of the mechanisms mediating attenuation in this model is necessary. An experimental approach to address this point is discussed in *Chapter VIII*.

Beyond a direct therapeutic application of the transposon mutants, these strains also serve as valuable tool for the understanding host responses to bacterial pneumonia. Mammals have evolved elegant mechanisms to recognize invading pathogens and mobilize an infantry of soluble and cellular effectors capable of controlling and eliminating the invading microbe. Likewise, pathogens have evolved means to evade these defenses and proliferate in their mammalian hosts. The work described in *Chapter IV* lays the foundation for delineating critical factors on both sides of the pathogen-host interaction using mutants of *A. baumannii* that shift the balance toward a host response that favors pathogen elimination. The idea of recruiting host responses to combat

infection is well established in the area of acquired immunity with the use of vaccines. However, immune-enhancing strategies are not well established in the area of innate immunity or in the treatment of acute bacterial infections. Most strategies have applied individual cytokines to promote host defenses, but this strategy has had minimal and mixed results. Innate defenses rely on the orchestration of a full panel of cellular and molecular effectors. Administration of the transposon mutants, therefore, has advantages over selective modulation of individual cytokines since these strains marshal the full complement of host defenses required for effective pathogen clearance. As such, the work described herein together with the opportunities provided by this foundational work move the field forward by providing critical innovations for the study of host pathogen interactions. Defining the specific bacterial products expressed by the bacteria that induce the attenuating phenotype will lead to the identification of bacterial factors that promote effective host responses. This work thus lays the foundation for engineering bacterial strains or recombinant proteins that elicit a protective host response to infection. In addition, these strains can be applied to the understanding of the host immune response by elucidating the full spectrum of host effectors elicited by the mutants.

Manipulation of circadian rhythms to reduce susceptibility to *A. baumannii* infection.

A. baumannii is an important cause of infections in hospitalized patients. Importantly, hospitalized patients frequent suffer from circadian disruption as result of medical procedures, medications or underlying medical conditions. Our data demonstrate that mice exhibit significant variation in their susceptibility to infection based on the time

of infection initiation. While the immunological mechanisms governing this variation in susceptibility are yet to be determined, these data nonetheless have important implications for the treatment and prevention of *A. baumannii* infections. For example, it may be possible in some cases to monitor treatment practices in order to minimize susceptibility to infection during the more susceptible periods within the circadian cycle. Minimizing invasive procedures that increase infection risk during susceptible periods in the circadian cycle could potentially reduce transmission of *A. baumannii* during these procedures. Moreover, it may be possible to manipulate specific aspects of the immune response once the immune effectors that contribute to circadian susceptibility to infection are identified.

Acinetobacter baumannii transposon mutants and implications for genetic manipulation and investigation of pathogenesis.

Transposon mutagenesis is a widely used technology in bacterial genetics since it provides a means to generate large libraries of mutants that can be screened for phenotypes of interest. However, transposon mutagenesis has disadvantages including the possibility of causing polar effects on genes adjacent to the integration site or the introduction of secondary mutations that have global effects on gene expression. For example, it is well established that transposon mutagenesis of *Staphylococcus aureus* frequently leads to point mutations in the *sae* or *agr* loci, which encode global virulence regulators. Until this problem was recognized, numerous genes were assigned functions in virulence factor regulation only to later discover that the phenotypes were the result of secondary mutations. We have identified a conserved pattern of gene dysregulation induced upon transposon mutagenesis in *A. baumannii*, which appears to occur with fairly high frequency. This is a critical finding in *A. baumannii* research. Methods for genetic manipulation of *A. baumannii* are in their early stages of development. As such, most investigators rely on transposon mutagenesis to establish the genetic basis for phenotypes of interest. Therefore, further characterization of the transposon mutants will elucidate the consequences of transposon mutagenesis in *A. baumannii*. In so doing, this work will be critical for progress in *A. baumannii* research by providing methods to prevent the off-target effects of transposon mutagenesis or to screen out mutants in which these effects have occurred.

Viii. Future directions

Redirection of host inflammation to promote bacterial clearance

It is becoming increasingly clear that small molecule antibiotics alone will not provide a lasting solution to the growing burden of MDR *A. baumannii*. Based on this fact, therapeutic strategies that augment the host response to infection represent a viable strategy for the treatment or prevention of *A. baumannii* infections. The work described in Chapter IV represents the initial identification and characterization of *A. baumannii* transposon mutants that induce an inflammatory response *in vivo* that is effective in clearing a WT *A. baumannii* infection. There remain a number of critical questions to address with regard to these mutants and their mechanism of action within the host.

1. **Identify the bacterial product responsible for inducing the attenuating phenotype of the transposon mutants.**

The striking attenuation of WT infection elicited by the transposon mutants warrants further investigation into the mechanisms underlying this phenotype. To date, identification of the specific bacterial product has been hampered by the recalcitrance of these strains to targeted genetic manipulation. I therefore propose a multifaceted approach to identify the bacterial factors responsible for the attenuating phenotype.

1a. Develop an in vitro system that recapitulates the pattern of attenuation observed in vivo.

Currently, the only methods for testing candidate mutants or bacterial products for their attenuating activity is to test these candidates *in vivo*. We have previously hesitated to develop an *in vitro* system for screening purposes because bacterial clearance *in vivo* is likely a multifactorial process that cannot be completely recapitulated *in vitro.* This makes it unclear what the readout for such an *in vitro* system should be. However, it is clear that as this project moves forward, an *in vitro* system would not only allow for screening of candidate bacterial products, but would also be of tremendous value for future therapeutic development. Specifically, if an *in vitro* phenotype accurately predicts *in vivo* activity, the *in vitro* system could be screened for chemical compounds that elicit the same response. Such compounds could have therapeutic value without requiring administration of the bacterial product. In order to develop an *in vitro* assay system I propose to screen the major cell types that are present in the lung for differences in bacterial invasion and cytotoxicity in response to infection with WT, Tn mutants, or a combination of WT and the Tn mutants. These cell types would include respiratory epithelial cells, dendritic cells, macrophages and mast cells. To supplement these assays, proinflammatory cytokine production in response to infection can also be measured since a specific pattern of cytokine production may serve as a molecular signature for the attenuating phenotype. These data would then be compared to *in vivo* attenuating activity and cytokine profiles to determine the predictive value of the *in vitro* system. These experiments would result in an *in vitro* system to evaluate candidate mutants or bacterial

products for their attenuating activity. Moreover, the system could be adapted for high throughput screening of therapeutic compounds that likewise have attenuating activity.

1b. Identify bacterial products that are recognized by the host upon treatment with the transposon mutants.

Proteinase K treatment partially reverses the phenotype of the transposon mutants suggesting that a surface exposed protein is either recognized by the host directly or that is required for recognition of another ligand. Both possibilities suggest that the protein is accessible to the host during infection. It is therefore possible that antibodies could be raised against this product in mice infected with the transposon mutants. As an initial proof of concept, mice treated with the transposon mutants should be allowed to recover from their infection and then re-challenged with WT bacteria with or without treatment with the transposon mutant. If antibodies are generated against the bacterial product necessary for the attenuating effect, the transposon mutant should lose its therapeutic activity in the WT challenge. It may be necessary to use a different WT strain for the second infection, since antibodies generated against the transposon mutant may protect against WT infection if they recognize conserved antigens between the two strains. In order to identify the protein component necessary for the attenuating phenotype, we can fractionate the transposon mutant and separate the proteins from these fractions by 2D-DIGE. Serum from convalescent mice infected with the transposon mutant can then be used to probe the resulting proteins for those that were accessible and immunogenic *in vivo*. Proteins recognized by antibodies in the convalescent serum can then be identified by mass spectrometry. These proteins can be cross-referenced with the microarray data to

generate a focused candidate list for the protein required for the attenuating phenotype. To identify the specific protein responsible for the effect, genetic approaches, outlined below, can be attempted to knock out or knock down the gene of interest. In addition, depending on the number of candidates identified, antibodies can be raised against each candidate and this antiserum can be used to block recognition of the bacterial product by the host.

1c. Define the genetic element encoding the bacterial product that elicits the attenuating immune response.

The transposon mutants have proven recalcitrant to targeted manipulation of the chromosome such as targeted deletion of candidate genes. Nonetheless, defining the genetic basis of the attenuating phenotype is critical to our understanding of the mechanism of the *in vivo* attenuation as well as for our understanding of the mechanism through which transposon mutagenesis induces this phenotype. An alternative to making targeted deletions in the transposon mutants is to knock down the expression of candidate genes using anti-sense RNA. This strategy would be beneficial regardless of whether the above experiments are successful in identifying the bacterial product necessary for the attenuating phenotype. We know that we can express genes *in trans* in the transposon mutants based on the fact that we can complement the LPS synthesis defect of Tn5A7 by providing a WT copy of *lpsB* on a plasmid. It is therefore conceivable that anti-sense constructs specific for the candidate genes of interest can be generated and evaluated for their ability to inhibit the attenuating phenotype of the transposon mutants. One complicating factor in this approach is that we do not currently have antibodies to the

proteins of interest. However, the antisera generated above could be used to probe for loss of a protein band corresponding to the predicted size of the targeted protein.

2. Elucidate the host factors necessary for recognizing the transposon mutants and mediating bacterial clearance.

We have demonstrated that MyD88 is necessary for the attenuating effect of the transposon mutants on WT *A. baumannii* infection. Based on the results of the DNase and proteinase K experiments, I hypothesize that signaling through TLR9 and/or TLR2 are required for the attenuating phenotype. Others have previously shown synergy between activation of TLR9 and the TLR2/6 heterodimer in protecting against bacterial pneumonia (128). The role for TLR9 in defense against *A. baumannii* infection has not been demonstrated previously. However, infection of $TLR2^{-/-}$ mice actually leads to reduced bacterial burdens as compared to WT. The mechanism behind this paradoxical observation is not defined and does not preclude a role for signaling through TLR2 in our model. I propose to define the roles for TLR9 and TLR2 in mediating the host response to the transposon mutants by performing the infection and treatment experiments in mice that lack one or both of these PRRs.

$TLR9^{-/-}$ mice are not commercially available so as a preliminary experiment we treated mice with oligonucleotides (ODN) that inhibit signaling through TLR9 or a control oligonucleotide with neither inhibitory nor stimulatory activity. Mice treated with anti-TLR9 ODN exhibit a 100-fold increase in bacterial burden compared to mice treated with control ODN (**Figure 42**). While a similar increase is observed in the Tn20A11-treated groups, Tn20A11 still dramatically attenuates the WT infection. These data

suggest that TLR9 may not be required for the attenuating phenotype. However, in the absence of a complete knockout of TLR9, we cannot conclude with certainty that TLR9 is not involved. It is possible that the level of TLR9 inhibition was not sufficient to reverse the transposon-mediated effect. Work is ongoing to determine the effectiveness of the anti-TLR9 ODN treatment. In addition future work will also determine whether TLR2 is required for the attenuating phenotype and to more clearly demonstrate whether or not TLR9 is involved in response to the transposon mutants.

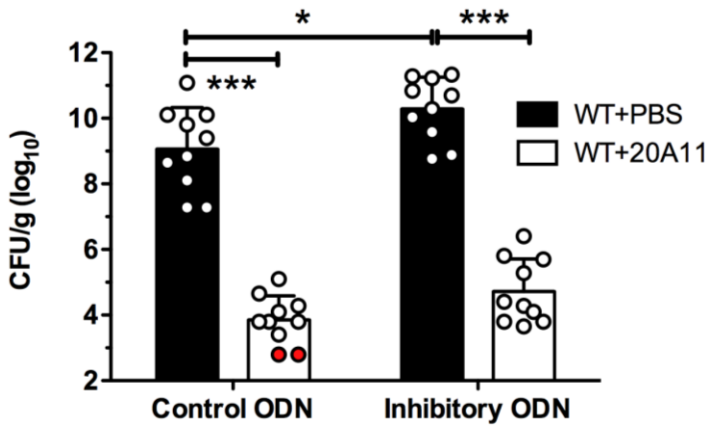

Figure 42. Contribution of TLR9 to the attenuating effect of the transposon mutants.

Mice were treated with 30 μg of anti-TLR9 or control ODN 24 hours prior to infection and at the time of infection. Bacterial burden are shown for lungs harvested at 36 hpi from mice infected with WT *A. baumannii* with or without co-treatment with killed Tn20A11 are shown.

3. Define the mechanism through which transposon mutagenesis induces the attenuating phenotype.

Our sequence analyses did not identify any conserved mutations across all of the transposon mutants. However, these analyses unexpectedly identified evidence of large chromosomal duplications and rearrangements. In some cases, these changes were present in all strains that were sequenced, suggesting that these may simply be errors in the original, published sequence. Although copy number has not yet been confirmed, it is

intriguing to speculate that variation in the copy number of some genes might lead to changes in expression or regulation of the affected genes. One region of the chromosome where this is particularly interesting is within a putative endogenous transposon at approximately 200 kb. A schematic representation of this locus is given in **Figure 43**.

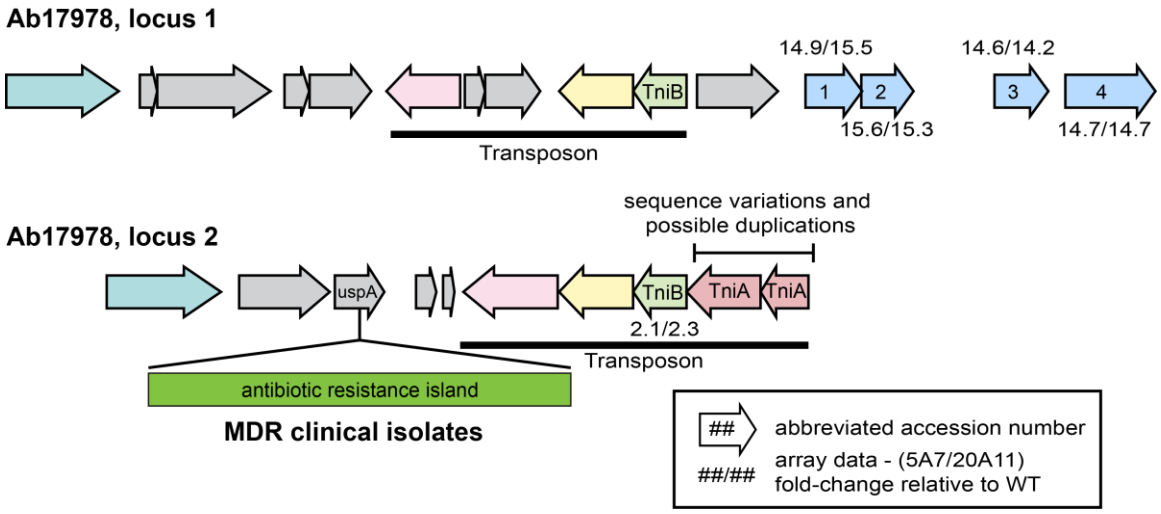

Figure 43. Genomic loci encoding the competence-related genes up-regulated in the array (locus 1) and two related transposons.

Genes are represented by arrows where homologous genes are the same color. Whole genome sequencing identified TniA as a locus with significant variation including possible variation in copy number. Interestingly, the gene encoding the transposition helper protein, TniB is upregulated in the transposon mutants and a homologue of this gene lies immediately upstream of the competence locus. Moreover, locus 2 is a frequent site for integration of large antibiotic resistance islands in MDR clinical isolates. Taken together, these data suggest that locus 2 may be a hotspot for recombination and that activation of the transposition helper protein, TniB, may contribute to the transposon-induced phenotype.

The sequence coverage in locus 1 is greater than four times the coverage observed in other areas of the genome. Moreover, in at least four of the sequenced transposon mutants there was evidence for allelic variation within this locus. The latter conclusion is based on the fact that there were numerous point mutation within this site that were only present in a subset of the sequence reads generated from the high throughput sequencing. It is also interesting to not that TniB is upregulated in the transposon mutants that were included in the microarray. Finally, a locus with partial homology to locus 1 is located at

approximately 700 kb and the region of homology lies immediately adjacent to the four most highly upregulated genes in the microarray. Taken together, these data suggest that expression of the putative competence locus may be affected by copy number variation at a distant, homologous locus.

While the hypothesis outlined above remains to be tested, it is important to note that genomic plasticity and large chromosomal amplifications are not unprecedented in *Acinetobacter spp.* In fact, genome amplification has been described extensively in *Acinetobacter* sp. strain ADP1 (243, 262). In this organism, amplification of large regions of the chromosome that encode genes involved in metabolism of aromatic substrates can arise at high frequency even in the absence of selective pressure. Based on phenotypic analyses of the resulting mutants, it is proposed that spontaneous duplication of chromosomal segments allows for a copy-number dependent increase in the expression of the duplicated genes (243, 262). Interestingly, long-range interactions between distant chromosomal sites have also been described (262). In the mutants that arise through amplification, genomic duplications can result in over 100 copies of a given amplicon. Moreover, amplifications can each be as large as 300 kb and can account for up 1 Mb of the resulting genome (262). Under non-selective conditions, the duplication frequency was estimated at between $10^{-4} – 10^{-5}$, suggesting that genome amplification can serve as a major source of genetic variation within a species (243). Although genomic amplification has not been described for *A. baumannii* the results of our sequencing data strongly suggest that certain regions of the chromosome may be duplicated in our strains. Based on these results, a first step toward understanding how transposon mutagenesis induces the attenuating phenotype will be to define the copy number variations and allelic

variations present in all of our sequenced strains. From there it will be possible to determine whether there are common features, such as higher copy number, in the transposon mutants as compared to either WT strain. Finally, Southern hybridization can be used to screen for large chromosomal rearrangements and duplications. We can then utilize the transposon mutagenesis protocol to determine whether chromosomal rearrangements occur as a consequence of mutagenesis. Alternatively, transient expression of the transposase enzyme may induce the genomic rearrangements. This can be tested by expressing a transposase from a constitutive promoter on a plasmid and determining whether expression of the transposase induces chromosomal rearrangement.

Nutrient metal acquisition and metal dependent processes in *A. baumannii*

1. Elucidate the mechanisms for Zn acquisition in *A. baumannii*.

Chapter IV presents data identifying a Zn uptake system in *A. baumannii* and the initial characterization of this system and its role in Zn uptake and pathogenesis. These results determined that A1S_0142 encodes ZnuB, the permease component of an ABC transporter that contributes to Zn acquisition *in vitro* and pathogenesis *in vivo*. Moreover, additional genes encoding proteins predicted to be involved in outer membrane transport were also identified. This work highlights several important areas for future investigation into the mechanisms for Zn acquisition in *A. baumannii*.

1a. Define the inner membrane Zn transport machinery in A. baumannii.

Zn supplementation rescues the growth of Δ*znuB* suggesting that additional transporters exist that are capable of transporting Zn across the inner membrane. However, additional inner membrane Zn transporters have not yet been identified in *A. baumannii*. To address this gap in our current knowledge, the transporters that compensate for loss of *znuB* function should be identified by performing transcriptional analyses of Δ*znuB* compared to WT in Zn-replete and Zn-deplete conditions. These studies would identify transporters that are up-regulated in response to Zn-starvation in Δ*znuB*. Once the transporters are identified, it will be possible to generate deletion mutants of these genes in order to determine their contribution to Zn uptake. In addition, ICP-MS analyses of the resulting mutants, combined with growth assays in combinations of various metal concentrations can be used to determine the primary substrate for the transporter. Together, these

analyses will determine whether these transporters primarily transport Zn, or whether other metals or other compounds are preferentially transported.

1b. Elucidate the mechanism for translocation of Zn across the outer membrane.

In many bacteria, transport of Zn across the outer membrane is thought to occur by passive diffusion through non-selective channels. In contrast, *A. baumannii* has two predicted Zur-regulated, TonB-dependent receptors, as well as a predicted Zur-regulated TonB/ExbB/ExbD system. Moreover, all of the genes encoding these components are induced in Zn-replete conditions. These results suggest that Zn transport across the outer membrane is an energy dependent process, but this remains to be experimentally confirmed. In order to determine the mechanism of Zn transport across the outer membrane, deletion mutants of the two ZnuD-encoding genes as well as for the predicted Zur-regulated TonB system should be generated. The contribution of these systems to Zn acquisition can then be assessed by measuring the growth of the resulting mutants in Zn-limiting conditions. In addition, direct interactions between TonB and each of the outer membrane receptors can be measured by immunoprecipitation using a tagged version of TonB. This type of analysis has been employed to define the interaction between *P. aeruginosa* TonB1 and the pyoverdine receptor, FpvA (5). Alternatively, interactions between these proteins can be determined by cysteine substitution of key residues predicted to form part of the TonB-box of the receptors and conserved receptor-interaction residues in TonB. This method has likewise been successful in defining the interaction between *E. coli* TonB and FepA (66). Together, these experiments would

define the mechanism for Zn uptake from the external environment, across the outer membrane, periplasm and inner membrane to reach the cytoplasm.

2. Define the *A. baumannii* Zur regulon and the roles for Zur-regulated genes in Zn uptake and homeostasis.

Initial *in silico* data have identified a number of candidate Zur-regulated genes. While several of the genes involved in Zn acquisition are induced in Zn-limiting conditions (*Chapter V*, **Figure 36D**), a direct role for Zur in regulating these genes has not been demonstrated.

2a. Elucidate the transcriptional profiles of a zur deletion mutant compared to WT bacteria in Zn-replete and Zn-deplete conditions.

In order to validate the *in silico* analyses described above, a *zur* deletion mutant will be generated. Transcriptional analyses of this strain compared to WT bacteria in Zn-replete and Zn-deplete conditions will identify genes whose expression is no longer Zn-responsive in the absence of Zur. Direct measurement of Zur binding to target promoters would further confirm the direct role for Zur in regulation of the putative targets.

2b. Determine the function of Zur-regulated genes and define their roles in Zn homeostasis.

Based on the results of 1a, genes can be prioritized based on those with known functions in other bacteria and those without known functions. Based on the *in silico* analyses,

several promising candidates have already been identified, and the role for Zur in regulating these genes can be determined directly even without a *zur* deletion mutant. Candidates that are particularly interesting include a putative metallochaperone that may be involved in metallocenter formation as well as a carbonic anhydrase. The former is of particular interest because of its possible role in metallocenter formation. Determining the specific target of this protein, together with the metals with which it associates should provide valuable information regarding the regulation of metalloprotein synthesis under Zn limiting conditions. The carbonic anhydrase is particular interesting based on several factors. First, several gamma-proteobacteria encode putative Zur-regulated carbonic anhydrases, suggesting an important physiological role for this protein under Zn-limiting conditions. Secondly, several genes were identified in the transposon mutagenesis screen that encode proteins with roles in maintaining intracellular pH. Carbonic anhydrases regulate pH by the conversion of bicarbonate to CO_2. Among all of the biologically active transition metals, Zn displays the strongest Lewis acid character. It is therefore intriguing to speculate about the interplay between intracellular pH and the catalytic activity and stability of Zn-dependent enzymes or proteins under Zn-limiting conditions.

3. Elucidate the *A. baumannii* metalloproteome and define changes to the metalloproteome as a result of nutrient metal limitation.

Predicted metalloproteins make up a significant proportion of the proteins encoded within bacterial genomes. Predicted Zn-binding proteins, for example, account for 4-8 percent of the proteins encoded within the genomes of Gram-negative and Gram-positive bacteria

(11). However, the majority of these proteins have not been experimentally validated for their metal-binding capacity, or for the role for the associated metal in protein function. Moreover, changes in the expressed metalloproteome in response to nutrient metal starvation have not been described. Understanding such changes would provide valuable insight into the physiological processes that are critical under nutrient limited conditions as well as into the basic mechanisms through which bacteria respond to nutrient limitation. Given that vertebrate hosts represent nutrient limiting environments for invading bacteria, understanding the physiologic response to nutrient limitation may identify novel avenues for therapeutic development. In order to define the metalloproteome of *A. baumannii*, fractionation of native proteins and separation by gel electrophoresis can be combined with laser-ablation inductively coupled plasma mass spectrometry (LA-ICP-MS). Proteins that are found associated with transition metals can then be identified by mass spectrometry. These analyses can then be combined with analyses of proteins isolated from bacteria grown under nutrient-metal restricted conditions to evaluate resulting changes in the total proteome and the metalloproteome.

4. Determine the contribution of transition metal intoxication to *A. baumannii* pathogenesis.

The work discussed in Chapter V focused on Zn acquisition and the effects of Zn sequestration on *A. baumannii*. However, as discussed in the *Chapter I*, Zn intoxication is recognized as a component of the innate immune response to certain bacterial pathogens. I have identified a transposon mutant in which the gene encoding a putative Cd/Zn/Cu efflux transporter is disrupted by integration of the transposon. This mutant is extremely

sensitive to growth in high Zn concentrations, suggesting that the transporter is important in mediating resistance to Zn intoxication **(Figure 44).** Future work will determine the contribution of this transporter to resistance to other toxic metals such as Cu and Cd, as well as its role in pathogenesis.

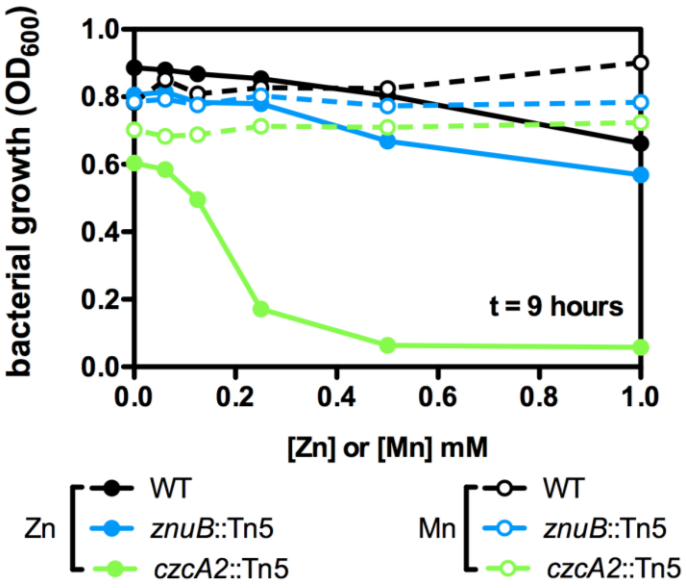

Figure 44. Mn and Zn intoxication of *A. baumannii*.

WT *A. baumannii* and isogenic derivatives with Tn insertions in *znuB* or *czcA2* were cultured in LB medium supplemented with Mn or Zn at final concentrations ranging from 0 to 1 mM. While modest growth inhibition is observed in WT and *znuB*::Tn5 in the presence of 0.5 and 1 mM Zn, *czcA2*::Tn5 is significantly inhibited in by concentrations as low as 100 mM Zn. In contrast, Mn was not inhibitory at any of the concentrations tested.

REFERENCES

1. 2006. Methods for dilution antimicrobial susceptibility tests for bacteria that grow aerobically; approved standard, 7 ed, vol. 26. Clinical and Laboratory Standards Institute, Wayne, Pennsylvania.

2. **Abergel, R. J., M. K. Wilson, J. E. L. Arceneaux, T. M. Hoette, R. K. Strong, B. R. Byers, and K. N. Raymond.** 2006. Anthrax pathogen evades the mammalian immune system through stealth siderophore production. Proc Natl Acad Sci U S A **103:**18499-18503.

3. **Achard, M. E. S., J. J. Tree, J. A. Holden, K. R. Simpfendorfer, O. L. C. Wijburg, R. A. Strugnell, M. A. Schembri, M. J. Sweet, M. P. Jennings, and A. G. McEwan.** 2010. The multi-copper-ion oxidase CueO of *Salmonella enterica* serovar Typhimurium is required for systemic virulence. Infect Immun **78:**2312-2319.

4. **Actis, L. A., M. E. Tolmasky, L. M. Crosa, and J. H. Crosa.** 1993. Effect of iron-limiting conditions on growth of clinical isolates of *Acinetobacter baumannii*. J Clin Microbiol **31:**2812-5.

5. **Adams, H., G. Zeder-Lutz, I. Schalk, F. Pattus, and H. Celia.** 2006. Interaction of TonB with the Outer Membrane Receptor FpvA of *Pseudomonas aeruginosa*. J Bacteriol **188:**5752-5761.

6. **Adams, M. D., K. Goglin, N. Molyneaux, K. M. Hujer, H. Lavender, J. J. Jamison, I. J. MacDonald, K. M. Martin, T. Russo, A. A. Campagnari, A. M. Hujer, R. A. Bonomo, and S. R. Gill.** 2008. Comparative genome sequence analysis of multidrug-resistant *Acinetobacter baumannii*. J Bacteriol **190:**8053-8064.

7. **Adams, M. D., G. C. Nickel, S. Bajaksouzian, H. Lavender, A. R. Murthy, M. R. Jacobs, and R. A. Bonomo.** 2009. Resistance to colistin in *Acinetobacter baumannii* associated with mutations in the PmrAB two-component system. Antimicrob Agents Chemother **53:**3628-34.

8. **Allegranzi, B., S. Bagheri Nejad, C. Combescure, W. Graafmans, H. Attar, L. Donaldson, and D. Pittet.** 2011. Burden of endemic health-care-associated infection in developing countries: systematic review and meta-analysis. Lancet **377:**228-41.

9. **Ammendola, S., P. Pasquali, C. Pistoia, P. Petrucci, P. Petrarca, G. Rotilio, and A. Battistoni.** 2007. High-affinity Zn2+ uptake system ZnuABC is required for bacterial zinc homeostasis in intracellular environments and contributes to the virulence of *Salmonella enterica.* Infect Immun **75:**5867-5876.

10. **Anderson, E. S., J. T. Paulley, J. M. Gaines, M. W. Valderas, D. W. Martin, E. Menscher, T. D. Brown, C. S. Burns, and R. M. Roop.** 2009. The manganese transporter MntH is a critical virulence determinant for *Brucella abortus* 2308 in experimentally infected mice. Infect Immun **77:**3466-3474.

11. **Andreini, C., L. Banci, I. Bertini, and A. Rosato.** 2006. Zinc through the three domains of life. Journal of Proteome Research **5:**3173-3178.

12. **Andreini, C., I. Bertini, G. Cavallaro, G. L. Holliday, and J. M. Thornton.** 2008. Metal ions in biological catalysis: from enzyme databases to general principles. Journal of Biological Inorganic Chemistry **13:**1205-1218.

13. **Andreini, C., I. Bertini, and A. Rosato.** 2009. Metalloproteomes: a bioinformatic approach. Accounts of chemical research **42:**1471-1479.

14. **Andresen, E., C. Lange, D. Strodthoff, T. Goldmann, N. Fischer, H. Sahly, D. Branscheid, and H. Heine.** 2011. S100A7/psoriasin expression in the human lung: unchanged in patients with COPD, but upregulated upon positive *S. aureus detection*. BMC pulmonary medicine **11:**10.

15. **Anjem, A., S. Varghese, and J. A. Imlay.** 2009. Manganese import is a key element of the OxyR response to hydrogen peroxide in *Escherichia coli.* Mol Microbiol **72:**844-858.

16. **Apisarnthanarak, A., and L. M. Mundy.** 2009. Mortality associated with Pandrug-resistant *Acinetobacter baumannii* infections in Thailand. Am J Infect Control **37:**519-20.

17. **Aranda, J., P. Cortés, M. E. Garrido, N. Fittipaldi, M. Llagostera, M. Gottschalk, and J. Barbé.** 2009. Contribution of the FeoB transporter to *Streptococcus suis* virulence. Int Microbiol **12:**137-143.

18. **Aspedon, A., K. Palmer, and M. Whiteley.** 2006. Microarray analysis of the osmotic stress response in Pseudomonas aeruginosa. J Bacteriol **188:**2721-5.

19. **Bajmoczi, M., M. Gadjeva, S. L. Alper, G. B. Pier, and D. E. Golan.** 2009. Cystic fibrosis transmembrane conductance regulator and caveolin-1 regulate epithelial cell internalization of Pseudomonas aeruginosa. American journal of physiology Cell physiology **297:**C263-77.

20. **Balasubramanian, R., G. E. Kenney, and A. C. Rosenzweig.** 2011. Dual pathways for copper uptake by methanotrophic bacteria. J Biol Chem **286:**37313-37319.

21. **Balasubramanian, R., and A. C. Rosenzweig.** 2008. Copper methanobactin: a molecule whose time has come. Curr Opin Chem Biol **12:**245-249.

22. **Bayle, L., S. Chimalapati, G. Schoehn, J. Brown, T. Vernet, and C. Durmort.** 2011. Zinc uptake by *Streptococcus pneumoniae* depends on both AdcA and AdcAII and is essential for normal bacterial morphology and virulence. Mol Microbiol **82:**904-916.

23. **Beasley, F. C., E. D. Vinés, J. C. Grigg, Q. Zheng, S. Liu, G. A. Lajoie, M. E. P. Murphy, and D. E. Heinrichs.** 2009. Characterization of staphyloferrin A biosynthetic and transport mutants in *Staphylococcus aureus*. Mol Microbiol **72:**947-963.

24. **Beceiro, A., E. Llobet, J. Aranda, J. A. Bengoechea, M. Doumith, M. Hornsey, H. Dhanji, H. Chart, G. Bou, D. M. Livermore, and N. Woodford.** 2011. Phosphoethanolamine modification of lipid A in colistin-resistant variants of *Acinetobacter baumannii* mediated by the PmrAB two-component regulatory system. Antimicrob Agents Chemother **55:**3370-9.

25. **Beenken, K. E., P. M. Dunman, F. McAleese, D. Macapagal, E. Murphy, S. J. Projan, J. S. Blevins, and M. S. Smeltzer.** 2004. Global gene expression in *Staphylococcus aureus* biofilms. J Bacteriol **186:**4665-4684.

26. **Bianchi, M., M. J. Niemiec, U. Siler, C. F. Urban, and J. Reichenbach.** 2011. Restoration of anti-Aspergillus defense by neutrophil extracellular traps in human chronic granulomatous disease after gene therapy is calprotectin-dependent. J Allergy Clin Immunol **127:**1243-52.e7.

27. **Biswas, S. K., and E. Lopez-Collazo.** 2009. Endotoxin tolerance: new mechanisms, molecules and clinical significance. Trends Immunol **30:**475-87.

28. **Bonomo, R. A., and D. Szabo.** 2006. Mechanisms of multidrug resistance in Acinetobacter species and Pseudomonas aeruginosa. Clin Infect Dis **43 Suppl 2:**S49-56.

29. **Borkow, G., and J. Gabbay.** 2005. Copper as a biocidal tool. Curr Med Chem **12:**2163-2175.

30. **Botella, H., P. Peyron, F. Levillain, R. Poincloux, Y. Poquet, I. Brandli, C. Wang, L. Tailleux, S. Tilleul, G. M. Charrière, S. J. Waddell, M. Foti, G. Lugo-Villarino, Q. Gao, I. Maridonneau-Parini, P. D. Butcher, P. R. Castagnoli, B. Gicquel, C. de Chastellier, and O. Neyrolles.** 2011. Mycobacterial P1-type ATPases mediate resistance to zinc poisoning in human macrophages. Cell Host Microbe **10:**248-259.

31. **Boucher, H. W., G. H. Talbot, J. S. Bradley, J. E. Edwards, D. Gilbert, L. B. Rice, M. Scheld, B. Spellberg, and J. Bartlett.** 2009. Bad bugs, no drugs: no ESKAPE! An update from the Infectious Diseases Society of America. Clin Infect Dis **48:**1-12.

32. **Boyce, J. D., M. Harper, F. St Michael, M. John, A. Aubry, H. Parnas, S. M. Logan, I. W. Wilkie, M. Ford, A. D. Cox, and B. Adler.** 2009. Identification of novel glycosyltransferases required for assembly of the *Pasteurella multocida* A:1 lipopolysaccharide and their involvement in virulence. Infect Immun **77:**1532-42.

33. **Brandel, J., N. Humbert, M. Elhabiri, I. J. Schalk, G. L. A. Mislin, and A.-M. Albrecht-Gary.** 2012. Pyochelin, a siderophore of *Pseudomonas aeruginosa*: Physicochemical characterization of the iron(iii), copper(ii) and zinc(ii) complexes. Dalton Transactions **41:**2820-2834.

34. **Brandtzaeg, P., T. O. Gabrielsen, I. Dale, F. Müller, M. Steinbakk, and M. K. Fagerhol.** 1995. The leucocyte protein L1 (calprotectin): a putative nonspecific defence factor at epithelial surfaces. Adv Exp Med Biol **371A:**201-206.

35. **Braun, V., and K. Hantke.** 2011. Recent insights into iron import by bacteria. Curr Opin Chem Biol **15:**328-334.

36. **Bryant, C. E., D. R. Spring, M. Gangloff, and N. J. Gay.** 2010. The molecular basis of the host response to lipopolysaccharide. Nat Rev Microbiol **8:**8-14.

37. **Campos, J. M., C. J. Gill, R. S. Hare, and G. H. Miller.** 1986. Effect of NaCl supplementation of Mueller-Hinton broth on susceptibility of staphylococci to aminoglycosides. Antimicrob Agents Chemother **29:**152-4.

38. **Campoy, S., M. Jara, N. Busquets, A. M. Pérez De Rozas, I. Badiola, and J. Barbé.** 2002. Role of the high-affinity zinc uptake znuABC system in *Salmonella enterica* serovar Typhimurium virulence. Infect Immun **70:**4721-4725.

39. **Caricato, A., L. Montini, G. Bello, V. Michetti, R. Maviglia, M. G. Bocci, G. Mercurio, S. M. Maggiore, and M. Antonelli.** 2009. Risk factors and outcome of Acinetobacter baumanii infection in severe trauma patients. Intensive Care Med **35:**1964-1969.

40. **Cartron, M. L., S. Maddocks, P. Gillingham, C. J. Craven, and S. C. Andrews.** 2006. Feo – Transport of ferrous iron into bacteria. Biometals **19:**143-157.

41. **Casey, A. L., D. Adams, T. J. Karpanen, P. A. Lambert, B. D. Cookson, P. Nightingale, L. Miruszenko, R. Shillam, P. Christian, and T. S. J. Elliott.** 2010. Role of copper in reducing hospital environment contamination. J Hosp Infect **74:**72-77.

42. **Cassat, J. E., and E. P. Skaar.** 2011. Metal ion acquisition in *Staphylococcus aureus*: overcoming nutritional immunity. Seminars in Immunopathology**:**1-21.

43. **Cescau, S., H. Cwerman, S. Létoffé, P. Delepelaire, C. Wandersman, and F. Biville.** 2007. Heme acquisition by hemophores. Biometals **20:**603-613.

44. **Champion, O. L., A. Karlyshev, I. A. M. Cooper, D. C. Ford, B. W. Wren, M. Duffield, P. C. F. Oyston, and R. W. Titball.** 2011. *Yersinia pseudotuberculosis* mntH functions in intracellular manganese accumulation, which is essential for virulence and survival in cells expressing functional Nramp1. Microbiology **157:**1115-1122.

45. **Chan, P.-C., L.-M. Huang, H.-C. Lin, L.-Y. Chang, M.-L. Chen, C.-Y. Lu, P.-I. Lee, J.-M. Chen, C.-Y. Lee, H.-J. Pan, J.-T. Wang, S.-C. Chang, and Y.-C. Chen.** 2007. Control of an outbreak of pandrug-resistant *Acinetobacter baumannii* colonization and infection in a neonatal intensive care unit. Infect Control Hosp Epidemiol **28:**423-9.

46. **Chen, S. C., B. Mehrad, J. C. Deng, G. Vassileva, D. J. Manfra, D. N. Cook, M. T. Wiekowski, A. Zlotnik, T. J. Standiford, and S. A. Lira.** 2001. Impaired pulmonary host defense in mice lacking expression of the CXC chemokine lungkine. J Immunol **166:**3362-8.

47. **Cheung, J., F. C. Beasley, S. Liu, G. A. Lajoie, and D. E. Heinrichs.** 2009. Molecular characterization of staphyloferrin B biosynthesis in *Staphylococcus aureus*. Mol Microbiol **74:**594-608.

48. **Chiang, S.-R., Y.-C. Chuang, H.-J. Tang, C.-C. Chen, C.-H. Chen, N.-Y. Lee, C.-H. Chou, and W.-C. Ko.** 2009. Intratracheal colistin sulfate for BALB/c mice with early pneumonia caused by carbapenem-resistant *Acinetobacter baumannii*. Crit Care Med **37:**2590-5.

49. **Chim, N., A. Iniguez, T. Q. Nguyen, and C. W. Goulding.** 2010. Unusual diheme conformation of the heme-degrading protein from *Mycobacterium tuberculosis.* J Mol Biol **395:**595-608.

50. **Choi, C. H., S. H. Hyun, J. Y. Lee, J. S. Lee, Y. S. Lee, S. A. Kim, J. P. Chae, S. M. Yoo, and J. C. Lee.** 2008. *Acinetobacter baumannii* outer membrane protein A targets the nucleus and induces cytotoxicity. Cell Microbiol **10:**309-19.

51. **Choi, C. H., E. Y. Lee, Y. C. Lee, T. I. Park, H. J. Kim, S. H. Hyun, S. A. Kim, S. K. Lee, and J. C. Lee.** 2005. Outer membrane protein 38 of *Acinetobacter baumannii* localizes to the mitochondria and induces apoptosis of epithelial cells. Cell Microbiol **7:**1127-38.

52. **Choi, C. H., J. S. Lee, Y. C. Lee, T. I. Park, and J. C. Lee.** 2008. Acinetobacter baumannii invades epithelial cells and outer membrane protein A mediates interactions with epithelial cells. BMC Microbiol **8:**216.

53. **Choi, E. H., P. A. Zimmerman, C. B. Foster, S. Zhu, V. Kumaraswami, T. B. Nutman, and S. J. Chanock.** 2001. Genetic polymorphisms in molecules of innate immunity and susceptibility to infection with Wuchereria bancrofti in South India. Genes Immun **2:**248-253.

54. **Clark, R. B.** 1996. Imipenem resistance among *Acinetobacter baumannii:* association with reduced expression of a 33-36 kDa outer membrane protein. J Antimicrob Chemother **38:**245-51.

55. **Corbin, B. D., E. H. Seeley, A. Raab, J. Feldmann, M. R. Miller, V. J. Torres, K. L. Anderson, B. M. Dattilo, P. M. Dunman, R. Gerads, R. M. Caprioli, W. Nacken, W. J. Chazin, and E. P. Skaar.** 2008. Metal chelation and inhibition of bacterial growth in tissue abscesses. Science **319:**962-5.

56. **Corbin, B. D., E. H. Seeley, A. Raab, J. Feldmann, M. R. Miller, V. J. Torres, K. L. Anderson, B. M. Dattilo, P. M. Dunman, R. Gerads, R. M. Caprioli, W. Nacken, W. J. Chazin, and E. P. Skaar.** 2008. Metal chelation and inhibition of bacterial growth in tissue abscesses. Science **319:**962-965.

57. **Cornelis, P.** 2010. Iron uptake and metabolism in *pseudomonads.* Appl Microbiol Biotechnol **86:**1637-1645.

58. **Corvec, S., N. Caroff, E. Espaze, C. Giraudeau, H. Drugeon, and A. Reynaud.** 2003. AmpC cephalosporinase hyperproduction in *Acinetobacter baumannii* clinical strains. J Antimicrob Chemother **52:**629-635.

59. **Craig, A., J. Mai, S. Cai, and S. Jeyaseelan.** 2009. Neutrophil recruitment to the lungs during bacterial pneumonia. Infect Immun **77:**568-75.

60. **Crooks, G. E., G. Hon, J. M. Chandonia, and S. E. Brenner.** 2004. WebLogo: a sequence logo generator. Genome Res **14:**1188-1190.

61. **Dashper, S. G., C. A. Butler, J. P. Lissel, R. A. Paolini, B. Hoffmann, P. D. Veith, N. M. O'Brien-Simpson, S. L. Snelgrove, J. T. Tsiros, and E. C. Reynolds.** 2005. A novel *Porphyromonas gingivalis* FeoB plays a role in manganese accumulation. The Journal of Biological Chemistry **280:**28095-28102.

62. **Davis, L. M., T. Kakuda, and V. J. DiRita.** 2009. A *Campylobacter jejuni znuA* orthologue is essential for growth in low-zinc environments and chick colonization. J Bacteriol **191:**1631-1640.

63. **Dellagi, A., D. Segond, M. Rigault, M. Fagard, C. Simon, P. Saindrenan, and D. Expert.** 2009. Microbial siderophores exert a subtle role in *Arabidopsis* during infection by manipulating the immune response and the iron status. Plant Physiol **150:**1687-1696.

64. **Desai, A., D. K. Maheshwari, and G. Archana (ed.).** 2011. Bacteria in agrobiology: Plant nutrient management. Springer Berlin Heidelberg, Berlin, Heidelberg.

65. **Desrosiers, D. C., S. W. Bearden, I. Mier, J. Abney, J. T. Paulley, J. D. Fetherston, J. C. Salazar, J. D. Radolf, and R. D. Perry.** 2010. Znu is the predominant zinc importer in *Yersinia pestis* during *in vitro* growth but is not essential for virulence. Infect Immun **78:**5163-5177.

66. **Devanathan, S., and K. Postle.** 2007. Studies on colicin B translocation: FepA is gated by TonB. Mol Microbiol **65:**441-453.

67. **Diamant, S., N. Eliahu, D. Rosenthal, and P. Goloubinoff.** 2001. Chemical chaperones regulate molecular chaperones in vitro and in cells under combined salt and heat stresses. J Biol Chem **276:**39586-91.

68. **Dintilhac, A., G. Alloing, C. Granadel, and J.-P. Claverys.** 1997. Competence and virulence of *Streptococcus pneumoniae*: Adc and PsaA mutants exhibit a requirement for Zn and Mn resulting from inactivation of putative ABC metal permeases. Mol Microbiol **25:**727-739.

69. **Djoko, K. Y., J. A. Franiek, J. L. Edwards, M. L. Falsetta, S. P. Kidd, A. J. Potter, N. H. Chen, M. A. Apicella, M. P. Jennings, and A. G. McEwan.** 2012. Phenotypic characterization of a *copA* mutant of *Neisseria gonorrhoeae* identifies a link between copper and nitrosative stress. Infect Immun **80:**1065-1071.

70. **Doerks, T., R. R. Copley, J. Schultz, C. P. Ponting, and P. Bork.** 2002. Systematic identification of novel protein domain families associated with nuclear functions. Genome Res **12:**47-56.

71. **Doi, Y., S. Husain, B. A. Potoski, K. R. McCurry, and D. L. Paterson.** 2009. Extensively drug-resistant *Acinetobacter baumannii*. Emerging Infect Dis **15:**980-2.

72. **Dorsey, C. W., M. S. Beglin, and L. A. Actis.** 2003. Detection and analysis of iron uptake components expressed by *Acinetobacter baumannii* clinical isolates. J Clin Microbiol **41:**4188-93.

73. **Dorsey, C. W., A. P. Tomaras, and L. A. Actis.** 2002. Genetic and phenotypic analysis of *Acinetobacter baumannii* insertion derivatives generated with a transposome system. Appl Environ Microbiol **68:**6353-60.

74. **Dorsey, C. W., A. P. Tomaras, P. L. Connerly, M. E. Tolmasky, J. H. Crosa, and L. A. Actis.** 2004. The siderophore-mediated iron acquisition systems of

Acinetobacter baumannii ATCC 19606 and *Vibrio anguillarum* 775 are structurally and functionally related. Microbiology **150:**3657-67.

75. **Drevinek, P., M. T. Holden, Z. Ge, A. M. Jones, I. Ketchell, R. T. Gill, and E. Mahenthiralingam.** 2008. Gene expression changes linked to antimicrobial resistance, oxidative stress, iron depletion and retained motility are observed when Burkholderia cenocepacia grows in cystic fibrosis sputum. BMC Infect Dis **8:**121.

76. **Dryla, A., B. Hoffmann, D. Gelbmann, C. Giefing, M. Hanner, A. Meinke, A. S. Anderson, W. Koppensteiner, R. Konrat, A. von Gabain, and E. Nagy.** 2007. High-affinity binding of the *staphylococcal* HarA protein to haptoglobin and hemoglobin involves a domain with an antiparallel eight-stranded beta-barrel fold. J Bacteriol **189:**254-264.

77. **Echenique, J. R., H. Arienti, M. E. Tolmasky, R. R. Read, R. J. Staneloni, J. H. Crosa, and L. A. Actis.** 1992. Characterization of a high-affinity iron transport system in *Acinetobacter baumannii*. J Bacteriol **174:**7670-9.

78. **Edwards, J. L.** 2010. *Neisseria gonorrhoeae* survival during primary human cervical epithelial cell infection requires nitric oxide and is augmented by progesterone. Infect Immun **78:**1202-1213.

79. **Eisenreich, W., T. Dandekar, J. Heesemann, and W. Goebel.** 2010. Carbon metabolism of intracellular bacterial pathogens and possible links to virulence. Nat Rev Microbiol **8:**401-412.

80. **El Ghazouani, A., A. Baslé, S. J. Firbank, C. W. Knapp, J. Gray, D. W. Graham, and C. Dennison.** 2011. Copper-binding properties and structures of methanobactins from *Methylosinus trichosporium* OB3b. Inorg Chem **50:**1378-1391.

81. **Erbay, A., A. Idil, M. G. Gözel, I. Mumcuoğlu, and N. Balaban.** 2009. Impact of early appropriate antimicrobial therapy on survival in Acinetobacter baumannii bloodstream infections. Int J Antimicrob Agents **34:**575-9.

82. **Erdem, I., A. Ozgultekin, A. Sengoz Inan, E. Dincer, G. Turan, N. Ceran, D. Ozturk Engin, S. Senbayrak Akcay, N. Akgun, and P. Goktas.** 2008. Incidence, etiology, and antibiotic resistance patterns of gram-negative microorganisms isolated from patients with ventilator-associated pneumonia in a

medical-surgical intensive care unit of a teaching hospital in istanbul, Turkey (2004-2006). Jpn J Infect Dis **61:**339-42.

83. **Expert, D.** 1999. Withholding and exchanging iron: interactions between *Erwinia spp.* and their plant hosts. Annu Rev Phytopathol **37:**307-334.

84. **Fabian, M., E. Solomaha, J. S. Olson, and A. W. Maresso.** 2009. Heme transfer to the bacterial cell envelope occurs via a secreted hemophore in the Gram-positive pathogen *Bacillus anthracis*. J Biol Chem **284:**32138-32146.

85. **Falagas, M. E., and I. A. Bliziotis.** 2007. Pandrug-resistant Gram-negative bacteria: the dawn of the post-antibiotic era? Int J Antimicrob Agents **29:**630-6.

86. **Falagas, M. E., P. I. Rafailidis, D. K. Matthaiou, S. Virtzili, D. Nikita, and A. Michalopoulos.** 2008. Pandrug-resistant *Klebsiella pneumoniae, Pseudomonas aeruginosa* and *Acinetobacter baumannii* infections: characteristics and outcome in a series of 28 patients. Int J Antimicrob Agents **32:**450-4.

87. **Fernandez-Reyes, M., M. RodrÌguez-FalcÛn, C. Chiva, J. PachÛn, D. Andreu, and L. Rivas.** 2009. The cost of resistance to colistin in <B><I>Acinetobacter baumannii</I></B>: a proteomic perspective. Proteomics **9:**1632-1645.

88. **Festa, R. A., M. B. Jones, S. Butler-Wu, D. Sinsimer, R. Gerads, W. R. Bishai, S. N. Peterson, and K. H. Darwin.** 2010. A novel copper-responsive regulon in *Mycobacterium tuberculosis*. Mol Microbiol **79:**133-148.

89. **Flo, T. H., K. D. Smith, S. Sato, D. J. Rodriguez, M. A. Holmes, R. K. Strong, S. Akira, and A. Aderem.** 2004. Lipocalin 2 mediates an innate immune response to bacterial infection by sequestrating iron. Nature **432:**917-921.

90. **Gaddy, J. A., and L. A. Actis.** 2009. Regulation of Acinetobacter baumannii biofilm formation. Future Microbiol **4:**273-8.

91. **Gaddy, J. A., A. P. Tomaras, and L. A. Actis.** 2009. The Acinetobacter baumannii 19606 OmpA Protein Plays a Role in Biofilm Formation on Abiotic Surfaces and in the Interaction of This Pathogen with Eukaryotic Cells. Infect Immun **77:**3150-3160.

92. **García, B., E. R. Olivera, B. Miñambres, M. Fernández-Valverde, L. M. Cañedo, M. A. Prieto, J. L. García, M. Martínez, and J. M. Luengo.** 1999. Novel biodegradable aromatic plastics from a bacterial source. Genetic and biochemical studies on a route of the phenylacetyl-coa catabolon. J Biol Chem **274:**29228-41.

93. **Garza-González, E., J. M. Llaca-Díaz, F. J. Bosques-Padilla, and G. M. González.** 2010. Prevalence of multidrug-resistant bacteria at a tertiary-care teaching hospital in Mexico: special focus on *Acinetobacter baumannii*. Chemotherapy **56:**275-9.

94. **Gaynes, R., J. R. Edwards, and N. N. I. S. System.** 2005. Overview of nosocomial infections caused by gram-negative bacilli. Clin Infect Dis **41:**848-54.

95. **Geiser, D. L., and J. J. Winzerling.** 2012. Insect transferrins: Multifunctional proteins. Biochim Biophys Acta **1820:**437-451.

96. **Gerhard, G. S., K. A. Levin, J. P. Goldstein, M. M. Wojnar, M. J. Chorney, and D. A. Belchis.** 2001. *Vibrio vulnificus* septicemia in a patient with the hemochromatosis *HFE* C282Y Mutation. Arch Pathol Lab Med **125:**1107-9.

97. **Ghigo, J. M., S. Létoffé, and C. Wandersman.** 1997. A new type of hemophore-dependent heme acquisition system of *Serratia marcescens* reconstituted in *Escherichia coli.* J Bacteriol **179:**3572-3579.

98. **Gläser, R., J. Harder, H. Lange, J. Bartels, E. Christophers, and J.-M. Schröder.** 2005. Antimicrobial psoriasin (S100A7) protects human skin from *Escherichia coli* infection. Nat Immunol **6:**57-64.

99. **Hakemian, A. S., and A. C. Rosenzweig.** 2007. The biochemistry of methane oxidation. Annu Rev Biochem **76:**223-241.

100. **Hakemian, A. S., C. E. Tinberg, K. C. Kondapalli, J. Telser, B. M. Hoffman, T. L. Stemmler, and A. C. Rosenzweig.** 2005. The copper chelator methanobactin from *Methylosinus trichosporium* OB3b binds copper(I). J Am Chem Soc **127:**17142-17143.

101. **Haley, K. P., E. M. Janson, S. Heilbronner, T. J. Foster, and E. P. Skaar.** 2011. *Staphylococcus lugdunensis* IsdG liberates iron from host heme. J Bacteriol **193:**4749-4757.

102. **Haley, K. P., and E. P. Skaar.** 2011. A battle for iron: host sequestration and *Staphylococcus aureus* acquisition. Microb Infect**:**1-11.

103. **Hamlin, J. N. R., R. A. M. Bloodworth, and S. T. Cardona.** 2009. Regulation of phenylacetic acid degradation genes of Burkholderia cenocepacia K56-2. BMC Microbiol **9:**222.

104. **Hantke, K.** 2005. Bacterial zinc uptake and regulators. Curr Opin Microbiol **8:**196-202.

105. **Henry, R., N. Vithanage, P. Harrison, T. Seemann, S. Coutts, J. H. Moffatt, R. L. Nation, J. Li, M. Harper, B. Adler, and J. D. Boyce.** 2011. Colistin-resistant, lipopolysaccharide-deficient *Acinetobacter baumannii* responds to lipopolysaccharide loss through increased expression of genes involved in the synthesis and transport of lipoproteins, phospholipids and poly-{beta}-1,6-N-acetylglucosamine. Antimicrob Agents Chemother **56:**59-69.

106. **Henry, R., N. Vithanage, P. Harrison, T. Seemann, S. Coutts, J. H. Moffatt, R. L. Nation, J. Li, M. Harper, B. Adler, and J. D. Boyce.** 2011. Colistin-resistant, lipopolysaccharide-deficient *Acinetobacter baumannii* responds to lipopolysaccharide loss through increased expression of genes involved in the synthesis and transport of lipoproteins, phospholipids and poly-{beta}-1,6-N-acetylglucosamine. Antimicrob Agents Chemother.

107. **Herbold, W., R. Maus, I. Hahn, N. Ding, M. Srivastava, J. W. Christman, M. Mack, J. Reutershan, D. E. Briles, J. C. Paton, C. Winter, T. Welte, and U. A. Maus.** 2010. Importance of CXC chemokine receptor 2 in alveolar neutrophil and exudate macrophage recruitment in response to pneumococcal lung infection. Infect Immun.

108. **HÈritier, C., L. Poirel, and P. Nordmann.** 2006. Cephalosporinase over-expression resulting from insertion of IS*Aba1* in *Acinetobacter baumannii*. Clinical Microbiology & Infection **12:**123-130.

109. **Hoffman, L. R., A. R. Richardson, L. S. Houston, H. D. Kulasekara, W. Martens-Habbena, M. Klausen, J. L. Burns, D. A. Stahl, D. J. Hassett, F. C. Fang, and S. I. Miller.** 2010. Nutrient availability as a mechanism for selection of antibiotic tolerant *Pseudomonas aeruginosa* within the CF airway. PLoS Path **6:**e1000712.

110. **Hohle, T. H., W. L. Franck, G. Stacey, and M. R. O'Brian.** 2011. Bacterial outer membrane channel for divalent metal ion acquisition. Proc Natl Acad Sci U S A **108:**15390-15395.

111. **Honsa, E. S., and A. W. Maresso.** 2011. Mechanisms of iron import in anthrax. Biometals **24:**533-545.

112. **Hood, M. I., A. C. Jacobs, K. Sayood, P. M. Dunman, and E. P. Skaar.** *Acinetobacter baumannii* Increases Tolerance to Antibiotics in Response to Monovalent Cations. Antimicrob Agents Chemother **54:**1029-1041.

113. **Hood, M. I., A. C. Jacobs, K. Sayood, P. M. Dunman, and E. P. Skaar.** 2010. *Acinetobacter baumannii* increases tolerance to antibiotics in response to monovalent cations. Antimicrob Agents Chemother **54:**1029-1041.

114. **Hornsey, M., N. Loman, D. W. Wareham, M. J. Ellington, M. J. Pallen, J. F. Turton, A. Underwood, T. Gaulton, C. P. Thomas, M. Doumith, D. M. Livermore, and N. Woodford.** 2011. Whole-genome comparison of two *Acinetobacter baumannii* isolates from a single patient, where resistance developed during tigecycline therapy. J Antimicrob Chemother **66:**1499-1503.

115. **Hou, Z. J., S. Narindrasorasak, B. Bhushan, B. Sarkar, and B. Mitra.** 2001. Functional analysis of chimeric proteins of the Wilson Cu(I)-ATPase (ATP7B) and ZntA, a Pb(II)/Zn(II)/Cd(II)-ATPase from *Escherichia coli*. The Journal of Biological Chemistry **276:**40858-40863.

116. **Hsu, K., C. Champaiboon, B. D. Guenther, B. S. Sorenson, A. Khammanivong, K. F. Ross, C. L. Geczy, and M. C. Herzberg.** 2009. Anti-infective protective properties of S100 calgranulins. Antiinflamm Antiallergy Agents Med Chem **8:**290-305.

117. **Hunger, M., R. Schmucker, V. Kishan, and W. Hillen.** 1990. Analysis and nucleotide sequence of an origin of an origin of DNA replication in *Acinetobacter calcoaceticus* and its use for *Escherichia coli* shuttle plasmids. Gene **87:**45-51.

118. **Iacono, M., L. Villa, D. Fortini, R. Bordoni, F. Imperi, R. J. Bonnal, T. Sicheritz-Ponten, G. De Bellis, P. Visca, A. Cassone, and A. Carattoli.** 2008. Whole-genome pyrosequencing of an epidemic multidrug-resistant *Acinetobacter baumannii* strain belonging to the European clone II group. Antimicrob Agents Chemother **52:**2616-25.

119. **Ignatova, Z., and L. M. Gierasch.** 2006. Inhibition of protein aggregation in vitro and in vivo by a natural osmoprotectant. Proc Natl Acad Sci USA **103:**13357-61.

120. **Inoue, S., J. Unsinger, C. G. Davis, J. T. Muenzer, T. A. Ferguson, K. Chang, D. F. Osborne, A. T. Clark, C. M. Coopersmith, J. E. Mcdunn, and R. S. Hotchkiss.** 2010. IL-15 Prevents Apoptosis, Reverses Innate and Adaptive Immune Dysfunction, and Improves Survival in Sepsis. The Journal of Immunology **184:**1401-1409.

121. **Isidor, B., S. Poignant, N. Corradini, M. Fouassier, P. Quartier, J. Roth, and G. Picherot.** 2009. Hyperzincemia and hypercalprotectinemia: unsuccessful treatment with tacrolimus. Acta paediatrica (Oslo, Norway : 1992) **98:**410-412.

122. **Jabado, N., A. Jankowski, S. Dougaparsad, V. Picard, S. Grinstein, and P. Gros.** 2000. Natural resistance to intracellular infections: natural resistance-associated macrophage protein 1 (Nramp1) functions as a pH-dependent manganese transporter at the phagosomal membrane. The Journal of Experimental Medicine **192:**1237-1248.

123. **Jacobs, A. C., I. Hood, K. L. Boyd, P. D. Olson, J. Morrison, S. Carson, K. Sayood, P. C. Iwen, E. P. Skaar, and P. M. Dunman.** 2010. Inactivation of Phospholipase D diminishes *Acinetobacter baumannii* pathogenesis. Infect Immun **78:**1952-62.

124. **Jacobs, A. C., I. Hood, K. L. Boyd, P. D. Olson, J. Morrison, S. Carson, K. Sayood, P. C. Iwen, E. P. Skaar, and P. M. Dunman.** 2010. Inactivation of phospholipase D diminishes *Acinetobacter baumannii* pathogenesis. Infect Immun **78:**1952-1962.

125. **Jacobs, A. C., I. Hood, K. L. Boyd, P. D. Olson, J. M. Morrison, S. Carson, K. Sayood, P. C. Iwen, E. P. Skaar, and P. M. Dunman.** Inactivation of Phospholipase D Diminishes *Acinetobacter baumannii* Pathogenesis. Infect Immun **78:**1952-1962.

126. **Jacobsen, F. E., K. M. Kazmierczak, J. P. Lisher, M. E. Winkler, and D. P. Giedroc.** 2011. Interplay between manganese and zinc homeostasis in the human pathogen *Streptococcus pneumoniae.* Metallomics **3:**38-41.

127. **Jawad, A., H. Seifert, A. M. Snelling, J. Heritage, and P. M. Hawkey.** 1998. Survival of *Acinetobacter baumannii* on dry surfaces: comparison of outbreak and sporadic isolates. J Clin Microbiol **36:**1938-1941.

128. **Jean, S.-S., and P.-R. Hsueh.** 2011. High burden of antimicrobial resistance in Asia. Int J Antimicrob Agents **37:**291-5.

129. **Jean, S.-S., P.-R. Hsueh, W.-S. Lee, H.-T. Chang, M.-Y. Chou, I.-S. Chen, J.-H. Wang, C.-F. Lin, J.-M. Shyr, W.-C. Ko, J.-J. Wu, Y.-C. Liu, W.-K. Huang, L.-J. Teng, and C.-Y. Liu.** 2009. Nationwide surveillance of antimicrobial resistance among non-fermentative Gram-negative bacteria in Intensive Care Units in Taiwan: SMART programme data 2005. Int J Antimicrob Agents **33:**266-71.

130. **Jin, B., S. M. C. Newton, Y. Shao, X. Jiang, A. Charbit, and P. E. Klebba.** 2006. Iron acquisition systems for ferric hydroxamates, haemin and haemoglobin in *Listeria monocytogenes.* Mol Microbiol **59:**1185-1198.

131. **Joly-Guillou, M. L., M. Wolff, R. Farinotti, A. Bryskier, and C. Carbon.** 2000. In vivo activity of levofloxacin alone or in combination with imipenem or amikacin in a mouse model of Acinetobacter baumannii pneumonia. J Antimicrob Chemother **46:**827-30.

132. **Kalechman, Y., U. Gafter, R. Gal, G. Rushkin, D. Yan, M. Albeck, and B. Sredni.** 2002. Anti-IL-10 therapeutic strategy using the immunomodulator AS101 in protecting mice from sepsis-induced death: dependence on timing of immunomodulating intervention. J Immunol **169:**384-92.

133. **Kallifidas, D., B. Pascoe, G. A. Owen, C. M. Strain-Damerell, H.-J. Hong, and M. S. B. Paget.** 2010. The zinc-responsive regulator Zur controls expression of the coelibactin gene cluster in *Streptomyces coelicolor*. J Bacteriol **192:**608-611.

134. **Källman, O., C. Lundberg, B. Wretlind, and A. Ortqvist.** 2006. Gram-negative bacteria from patients seeking medical advice in Stockholm after the tsunami catastrophe. Scand J Infect Dis **38:**448-50.

135. **Kammler, M., C. Schon, and K. Hantke.** 1993. Characterisation of the ferrous iron uptake system of *Escherichia coli*. J Bacteriol **175:**6212-6219.

136. **Kehl-Fie, T. E., S. Chitayat, M. I. Hood, S. Damo, N. Restrepo, C. Garcia, K. A. Munro, W. J. Chazin, and E. P. Skaar.** 2011. Nutrient metal sequestration by calprotectin inhibits bacterial superoxide defense, enhancing neutrophil killing of *Staphylococcus aureus.* Cell Host Microbe **10:**158-164.

137. **Kehl-Fie, T. E., and E. P. Skaar.** 2010. Nutritional immunity beyond iron: a role for manganese and zinc. Curr Opin Chem Biol **14:**218-224.

138. **Kenney, G. E., and A. C. Rosenzweig.** 2011. Chemistry and biology of the copper chelator methanobactin. ACS Chemical Biology**:**120124121712008.

139. **Keven, K., K. Ates, M. S. Sever, M. Yenicesu, B. Canbakan, T. Arinsoy, N. Ozdemir, M. Duranay, B. Altun, and E. Erek.** 2003. Infectious complications after mass disasters: the Marmara earthquake experience. Scand J Infect Dis **35:**110-3.

140. **Kiani, Q. H., M. Amir, M. A. Ghazanfar, and M. Iqbal.** 2009. Microbiology of wound infections among hospitalised patients following the 2005 Pakistan earthquake. J Hosp Infect **73:**71-8.

141. **Kim, B.-E., T. Nevitt, and D. J. Thiele.** 2008. Mechanisms for copper acquisition, distribution and regulation. Nat Chem Biol **4:**176-185.

142. **Kim, H. J.** 2004. Methanobactin, a copper-acquisition compound from methane-oxidizing bacteria. Science **305:**1612-1615.

143. **Kim, H. W., Q. Chan, S. E. Afton, J. A. Caruso, B. Lai, N. L. Weintraub, and Z. Qin.** 2011. Human macrophage ATP7A is localized in the trans-Golgi apparatus, controls intracellular copper levels, and mediates macrophage responses to dermal wounds. Inflammation.

144. **Kim, J. S., M. H. Kim, M. H. Joe, S. S. Song, I. S. Lee, and S.-Y. Choi.** 2002. The sctR of *Salmonella enterica* serova Typhimurium encoding a homologue of MerR protein is involved in the copper-responsive regulation of *cuiD*. FEMS Microbiol Lett **210:**99-103.

145. **Klein, J. S., and O. Lewinson.** 2011. Bacterial ATP-driven transporters of transition metals: physiological roles, mechanisms of action, and roles in bacterial virulence. Metallomics **3:**1098.

146. **Knapp, C. W., D. A. Fowle, E. Kulczycki, J. A. Roberts, and D. W. Graham.** 2007. Methane monooxygenase gene expression mediated by methanobactin in the presence of mineral copper sources. Proc Natl Acad Sci U S A **104:**12040-12045.

147. **Knapp, S., C. W. Wieland, S. Florquin, R. Pantophlet, L. Dijkshoorn, N. Tshimbalanga, S. Akira, and T. van der Poll.** 2006. Differential roles of CD14 and toll-like receptors 4 and 2 in murine *Acinetobacter pneumonia*. Am J Respir Crit Care Med **173:**122-9.

148. **Ko, K. S., J. Y. Suh, K. T. Kwon, S.-I. Jung, K.-H. Park, C. I. Kang, D. R. Chung, K. R. Peck, and J.-H. Song.** 2007. High rates of resistance to colistin and polymyxin B in subgroups of *Acinetobacter baumannii* isolates from Korea. J Antimicrob Chemother **60:**1163-7.

149. **Koomanachai, P., A. Kim, and D. P. Nicolau.** 2009. Pharmacodynamic evaluation of tigecycline against *Acinetobacter baumannii* in a murine pneumonia model. J Antimicrob Chemother **63:**982-7.

150. **Krishna Kumar, K., D. A. Jacques, G. Pishchany, T. Caradoc-Davies, T. Spirig, G. R. Malmirchegini, D. B. Langley, C. F. Dickson, J. P. Mackay, R. T. Clubb, E. P. Skaar, J. M. Guss, and D. A. Gell.** 2011. Structural basis for hemoglobin capture by *Staphylococcus aureus* cell-surface protein, IsdH. J Biol Chem **286:**38439-38447.

151. **Kumar, P., S. Sannigrahi, and Y.-L. Tzeng.** 2012. The *Neisseria meningitidis* ZnuD zinc receptor contributes to interactions with epithelial cells and supports heme utilization when expressed in *Escherichia coli*. Infect Immun **80:**657-667.

152. **Kwon, S.-O., Y. S. Gho, J. C. Lee, and S. I. Kim.** 2009. Proteome analysis of outer membrane vesicles from a clinical *Acinetobacter baumannii* isolate. FEMS Microbiol Lett **297:**150-156.

153. **Lauw, F. N., J. Branger, S. Florquin, P. Speelman, S. J. H. van Deventer, S. Akira, and T. van der Poll.** 2002. IL-18 improves the early antimicrobial host response to pneumococcal pneumonia. J Immunol **168:**372-8.

154. **Law, R. J., J. N. R. Hamlin, A. Sivro, S. J. McCorrister, G. A. Cardama, and S. T. Cardona.** 2008. A functional phenylacetic acid catabolic pathway is required for full pathogenicity of *Burkholderia cenocepacia* in the *Caenorhabditis elegans* host model. J Bacteriol **190:**7209-18.

155. **Lawrence, M. C., P. A. Pilling, V. C. Epa, A. M. Berry, A. D. Ogunniyi, and J. C. Paton.** 1998. The crystal structure of pneumococcal surface antigen PsaA reveals a metal-binding site and a novel structure for a putative ABC-type binding protein. Structure **6:**1553-1561.

156. **Lee, A. C. W., and C. H. Li.** 2004. Age as a factor in severe bacterial infection in transfusion-dependent patients with thalassemia major. Clin Infect Dis **38:**1194-5; author reply 1195.

157. **Lee, H. W., Y. M. Koh, J. Kim, J. C. Lee, Y. C. Lee, S. Y. Seol, and D. T. Cho.** 2008. Capacity of multidrug-resistant clinical isolates of *Acinetobacter baumannii* to form biofilm and adhere to epithelial cell surfaces. Clin Microbiol Infect **14:**49-54.

158. **Lemanceau, P., P. Bauer, S. Kraemer, and J.-F. Briat.** 2009. Iron dynamics in the rhizosphere as a case study for analyzing interactions between soils, plants and microbes. Plant Soil **321:**513-535.

159. **Lemanceau, P., D. Expert, F. Gaymard, P. A. H. M. Bakker, and J. F. Briat.** 2009. Chapter 12 - Role of iron in plant-microbe interactions. Plant Innate Immunity **51:**491-549.

160. **Li, J. M., C. S. Russell, and S. D. Cosloy.** 1989. The structure of the *Escherichia coli hemB* gene. Gene **75:**177-184.

161. **Liechty, A., J. Chen, and M. K. Jain.** 2000. Origin of antibacterial stasis by polymyxin B in Escherichia coli. Biochimica et Biophysica Acta (BBA) - Biomembranes **1463:**55-64.

162. **Liechty, A., J. Chen, and M. K. Jain.** 2000. Origin of antibacterial stasis by polymyxin B in *Escherichia coli*. Biochimica et Biophysica Acta **1463:**55-64.

163. **Limansky, A. S., M. A. Mussi, and A. M. Viale.** 2002. Loss of a 29-kilodalton outer membrane protein in *Acinetobacter baumannii* is associated with imipenem resistance. J Clin Microbiol **40:**4776-8.

164. **Liu, J. Z., S. Jellbauer, A. Poe, V. Ton, M. Pesciaroli, T. Kehl-Fie, N. A. Restrepo, M. Hosking, R. A. Edwards, A. Battistoni, P. Pasquali, T. E. Lane, W. J. Chazin, T. Vogl, J. Roth, E. P. Skaar, and M. Raffatellu.** 2012. Zinc

sequestration by the neutrophil protein calprotectin enhances *Salmonella* growth in the inflamed gut. Cell Host Microbe **11:**227-39.

165. **Liu, M., W. N. Tanaka, H. Zhu, G. Xie, D. M. Dooley, and B. Lei.** 2008. Direct hemin transfer from IsdA to IsdC in the iron-regulated surface determinant (Isd) heme acquisition system of *Staphylococcus aureus.* The Journal of Biological Chemistry **283:**6668-6676.

166. **Liu, T., A. Ramesh, Z. Ma, S. K. Ward, L. Zhang, G. N. George, A. M. Talaat, J. C. Sacchettini, and D. P. Giedroc.** 2006. CsoR is a novel *Mycobacterium tuberculosis* copper-sensing transcriptional regulator. Nat Chem Biol **3:**60-68.

167. **Lockhart, S. R., M. A. Abramson, S. E. Beekmann, G. Gallagher, S. Riedel, D. J. Diekema, J. P. Quinn, and G. V. Doern.** 2007. Antimicrobial Resistance among Gram-Negative Bacilli Causing Infections in Intensive Care Unit Patients in the United States between 1993 and 2004. J Clin Microbiol **45:**3352-3359.

168. **Lomovskaya, O., M. S. Warren, A. Lee, J. Galazzo, R. Fronko, M. Lee, J. Blais, D. Cho, S. Chamberland, T. Renau, R. Leger, S. Hecker, W. Watkins, K. Hoshino, H. Ishida, and V. J. Lee.** 2001. Identification and characterization of inhibitors of multidrug resistance efflux pumps in *Pseudomonas aeruginosa*: novel agents for combination therapy. Antimicrob Agents Chemother **45:**105-16.

169. **López-Rojas, R., J. Domínguez-Herrera, M. J. McConnell, F. Docobo-Peréz, Y. Smani, M. Fernández-Reyes, L. Rivas, and J. Pachón.** 2011. Impaired virulence and in vivo fitness of colistin-resistant *Acinetobacter baumannii*. J Infect Dis **203:**545-8.

170. **López-Rojas, R., M. E. Jiménez-Mejías, J. A. Lepe, and J. Pachón.** 2011. *Acinetobacter baumannii* resistant to colistin alters its antibiotic resistance profile: a case report from Spain. J Infect Dis **204:**1147-8.

171. **Lu, Z. H., C. T. Dameron, and M. Solioz.** 2003. The *Enterococcus hirae* paradigm of copper homeostasis: copper chaperone turnover, interactions, and transactions. Biometals **16:**137-143.

172. **Luengo, J. M., J. L. García, and E. R. Olivera.** 2001. The phenylacetyl-CoA catabolon: a complex catabolic unit with broad biotechnological applications. Mol Microbiol **39:**1434-42.

173. **Luke, N. R., S. L. Sauberan, T. A. Russo, J. M. Beanan, R. Olson, T. W. Loehfelm, A. D. Cox, F. St. Michael, E. V. Vinogradov, and A. A. Campagnari.** Identification and Characterization of a Glycosyltransferase Involved in *Acinetobacter baumannii* Lipopolysaccharide Core Biosynthesis. Infect Immun **78:**2017-2023.

174. **M Höpfner, R. N. A. R. D. H. S. S. U. R. F.** 2001. *Yersinia enterocolitica* infection with multiple liver abscesses uncovering a primary hemochromatosis. Scand J Gastroenterol **36:**220-4.

175. **Maciag, A., E. Dainese, G. M. Rodriguez, A. Milano, R. Provvedi, M. R. Pasca, I. Smith, G. Palù, G. Riccardi, and R. Manganelli.** 2007. Global analysis of the *Mycobacterium tuberculosis* Zur (FurB) regulon. J Bacteriol **189:**730-740.

176. **Mack, J., C. Vermeiren, D. E. Heinrichs, and M. J. Stillman.** 2004. *In vivo* heme scavenging by *Staphylococcus aureus* IsdC and IsdE proteins. Biochem Biophys Res Commun **320:**781-788.

177. **MacLean, L. L., M. B. Perry, W. Chen, and E. Vinogradov.** 2009. The structure of the polysaccharide O-chain of the LPS from *Acinetobacter baumannii* strain ATCC 17961. Carbohydr Res **344:**474-478.

178. **Macomber, L., and J. A. Imlay.** 2009. The iron-sulfur clusters of dehydratases are primary intracellular targets of copper toxicity. Proc Natl Acad Sci U S A **106:**8344-8349.

179. **Magnet, S., P. Courvalin, and T. Lambert.** 2001. Resistance-Nodulation-Cell Division-type efflux pump involved in aminoglycoside resistance in *Acinetobacter baumannii* strain BM4454. Antimicrob Agents Chemother **45:**3375-3380.

180. **March, C., V. Regueiro, E. Llobet, D. Moranta, P. Morey, J. Garmendia, and J. A. Bengoechea.** 2010. Dissection of host cell signal transduction during *Acinetobacter baumannii*-triggered inflammatory response. PLoS ONE **5:**e10033.

181. **Marchand, I., L. Damier-Piolle, P. Courvalin, and T. Lambert.** 2004. Expression of the RND-Type efflux pump AdeABC in *Acinetobacter baumannii* is regulated by the AdeRS two-component system. Antimicrob Agents Chemother **48:**3298-3304.

182. **Maresso, A. W., T. J. Chapa, and O. Schneewind.** 2006. Surface protein IsdC and Sortase B are required for heme-iron scavenging of *Bacillus anthracis.* J Bacteriol **188:**8145-8152.

183. **Marlovits, T. C.** 2002. The membrane protein FeoB contains an intramolecular G protein essential for Fe(II) uptake in bacteria. Proceedings of the National Academy of Sciences **99:**16243-16248.

184. **Martin, J. E., and J. A. Imlay.** 2011. The alternative aerobic ribonucleotide reductase of *Escherichia coli*, NrdEF, is a manganese-dependent enzyme that enables cell replication during periods of iron starvation. Mol Microbiol **80:**319-334.

185. **Mazmanian, S. K., E. P. Skaar, A. H. Gaspar, M. Humayun, P. Gornicki, J. Jelenska, A. Joachmiak, D. M. Missiakas, and O. Schneewind.** 2003. Passage of heme-iron across the envelope of *Staphylococcus aureus.* Science **299:**906-909.

186. **McCormick, A., L. Heesemann, J. Wagener, V. Marcos, D. Hartl, J. Loeffler, J. Heesemann, and F. Ebel.** 2010. NETs formed by human neutrophils inhibit growth of the pathogenic mold *Aspergillus fumigatus.* Microb Infect **12:**928-936.

187. **McDevitt, C. A., A. D. Ogunniyi, E. Valkov, M. C. Lawrence, B. Kobe, A. G. McEwan, and J. C. Paton.** 2011. A molecular mechanism for bacterial susceptibility to zinc. PLoS Path **7:**e1002357.

188. **Meduri, G. U., G. Kohler, S. Headley, E. Tolley, F. Stentz, and A. Postlethwaite.** 1995. Inflammatory cytokines in the BAL of patients with ARDS. Persistent elevation over time predicts poor outcome. Chest **108:**1303-1314.

189. **Meduri, G. U., R. C. Reddy, T. Stanley, and F. El-Zeky.** 1998. Pneumonia in acute respiratory distress syndrome. A prospective evaluation of bilateral bronchoscopic sampling. Am J Respir Crit Care Med **158:**870-5.

190. **Mikolay, A., S. Huggett, L. Tikana, G. Grass, J. Braun, and D. H. Nies.** 2010. Survival of bacteria on metallic copper surfaces in a hospital trial. Appl Microbiol Biotechnol **87:**1875-1879.

191. **Moffatt, J. H., M. Harper, B. Adler, R. L. Nation, J. Li, and J. D. Boyce.** 2011. Insertion sequence ISAba11 is involved in colistin resistance and loss of

lipopolysaccharide in *Acinetobacter baumannii*. Antimicrob Agents Chemother **55:**3022-4.

192. **Montero, A., J. Ariza, X. Corbella, A. Doménech, C. Cabellos, J. Ayats, F. Tubau, C. Ardanuy, and F. Gudiol.** 2002. Efficacy of colistin versus beta-lactams, aminoglycosides, and rifampin as monotherapy in a mouse model of pneumonia caused by multiresistant Acinetobacter baumannii. Antimicrob Agents Chemother **46:**1946-52.

193. **Morgan, D. J., S. A. Weisenberg, M. H. Augenbraun, D. P. Calfee, B. P. Currie, E. Y. Furuya, R. Holzman, M. C. Montecalvo, M. Phillips, B. Polsky, and K. A. Sepkowitz.** 2009. Multidrug-resistant Acinetobacter baumannii in New York City - 10 years into the epidemic. Infection control and hospital epidemiology : the official journal of the Society of Hospital Epidemiologists of America **30:**196-197.

194. **Moroz, O. V., A. A. Antson, S. J. Grist, N. J. Maitland, G. G. Dodson, K. S. Wilson, E. Lukanidin, and I. B. Bronstein.** 2003. Structure of the human S100A12-copper complex: implications for host-parasite defence. Acta crystallographica Section D, Biological crystallography **59:**859-867.

195. **Moroz, O. V., W. Burkitt, H. Wittkowski, W. He, A. Ianoul, V. Novitskaya, J. Xie, O. Polyakova, I. K. Lednev, A. Shekhtman, P. J. Derrick, P. Bjoerk, D. Foell, and I. B. Bronstein.** 2009. Both Ca2+ and Zn2+ are essential for S100A12 protein oligomerization and function. BMC Biochem **10:**11.

196. **Mortensen, B. L., and E. P. Skaar.** 2012. Host-microbe interactions that shape the pathogenesis of *Acinetobacter baumannii* infection. Cell Microbiol.

197. **Muenzer, J. T., C. G. Davis, K. Chang, R. E. Schmidt, W. M. Dunne, C. M. Coopersmith, and R. S. Hotchkiss.** 2010. Characterization and Modulation of the Immunosuppressive Phase of Sepsis. Infect Immun **78:**1582-1592.

198. **Murphey, E. D., and E. R. Sherwood.** 2006. Bacterial clearance and mortality are not improved by a combination of IL-10 neutralization and IFN-gamma administration in a murine model of post-CLP immunosuppression. Shock **26:**417-24.

199. **Murray, C. K., K. Wilkins, N. C. Molter, H. C. Yun, M. A. Dubick, M. A. Spott, D. Jenkins, B. Eastridge, J. B. Holcomb, L. H. Blackbourne, and D. R.**

Hospenthal. 2009. Infections in combat casualties during Operations Iraqi and Enduring Freedom. The Journal of trauma **66:**S138-44.

200. **Muryoi, N., M. T. Tiedemann, M. Pluym, J. Cheung, D. E. Heinrichs, and M. J. Stillman.** 2008. Demonstration of the iron-regulated surface determinant (Isd) heme transfer pathway in *Staphylococcus aureus.* The Journal of Biological Chemistry **283:**28125-28136.

201. **Mussi, M. A., A. S. Limansky, and A. M. Viale.** 2005. Acquisition of resistance to carbapenems in multidrug-resistant clinical strains of Acinetobacter baumannii: natural insertional inactivation of a gene encoding a member of a novel family of beta-barrel outer membrane proteins. Antimicrob Agents Chemother **49:**1432-40.

202. **Nesper, J., A. Kraiss, S. Schild, J. Blass, K. E. Klose, J. Bockemühl, and J. Reidl.** 2002. Comparative and genetic analyses of the putative Vibrio cholerae lipopolysaccharide core oligosaccharide biosynthesis (wav) gene cluster. Infect Immun **70:**2419-2433.

203. **Newton, S. M. C., P. E. Klebba, C. Raynaud, Y. Shao, X. Jiang, I. Dubail, C. Archer, C. Frehel, and A. Charbit.** 2005. The *svpA-srtB* locus of *Listeria monocytogenes*: fur-mediated iron regulation and effect on virulence. Mol Microbiol **55:**927-940.

204. **Nielubowicz, G. R., S. N. Smith, and H. L. T. Mobley.** 2010. Zinc uptake contributes to motility and provides a competitive advantage to *Proteus mirabilis* during experimental urinary tract infection. Infect Immun **78:**2823-2833.

205. **Nobles, C. L., and A. W. Maresso.** 2011. The theft of host heme by Gram-positive pathogenic bacteria. Metallomics **3:**788-796.

206. **Noinaj, N., N. C. Easley, M. Oke, N. Mizuno, J. Gumbart, E. Boura, A. N. Steere, O. Zak, P. Aisen, E. Tajkhorshid, R. W. Evans, A. R. Gorringe, A. B. Mason, A. C. Steven, and S. K. Buchanan.** 2012. Structural basis for iron piracy by pathogenic *Neisseria*. Nature.

207. **Nordmann, P., L. Poirel, T. R. Walsh, and D. M. Livermore.** 2011. The emerging NDM carbapenemases. Trends Microbiol **19:**588-595.

208. **Nudel, C., R. Gonzalez, N. Castaneda, G. Mahler, and L. A. Actis.** 2001. Influence of iron on growth, production of siderophore compounds, membrane

proteins, and lipase activity in Acinetobacter calcoaceticus BD 413. Microbiol Res **155:**263-9.

209. **Nygaard, T. K., G. C. Blouin, M. Liu, M. Fukumura, J. S. Olson, M. Fabian, D. M. Dooley, and B. Lei.** 2006. The mechanism of direct heme transfer from the streptococcal cell surface protein Shp to HtsA of the HtsABC transporter. The Journal of Biological Chemistry **281:**20761-20771.

210. **Ogunniyi, A. D., L. K. Mahdi, M. P. Jennings, A. G. McEwan, C. A. McDevitt, M. B. Van der Hoek, C. J. Bagley, P. Hoffmann, K. A. Gould, and J. C. Paton.** 2010. Central role of manganese in regulation of stress responses, physiology, and metabolism in *Streptococcus pneumoniae*. J Bacteriol **192:**4489-4497.

211. **Oh, J.-T., T. K. Van Dyk, Y. Cajal, P. S. Dhurjati, M. Sasser, and M. K. Jain.** 1998. Osmotic Stress in ViableEscherichia colias the Basis for the Antibiotic Response by Polymyxin B. Biochem Biophys Res Commun **246:**619-623.

212. **Oh, J. T., Y. Cajal, E. M. Skowronska, S. Belkin, J. Chen, T. K. Van Dyk, M. Sasser, and M. K. Jain.** 2000. Cationic peptide antimicrobials induce selective transcription of micF and osmY in *Escherichia coli*. Biochim Biophys Acta **1463:**43-54.

213. **Oh, J. T., T. K. Van Dyk, Y. Cajal, P. S. Dhurjati, M. Sasser, and M. K. Jain.** 1998. Osmotic stress in viable *Escherichia coli* as the basis for the antibiotic response by polymyxin B. Biochem Biophys Res Commun **246:**619-23.

214. **Ong, C. W. M., D. C. B. Lye, K. L. Khoo, G. S. W. Chua, S. F. Yeoh, Y. S. Leo, P. A. Tambyah, and A. C. Chua.** 2009. Severe community-acquired Acinetobacter baumannii pneumonia: an emerging highly lethal infectious disease in the Asia-Pacific. Respirology **14:**1200-5.

215. **Ong, S. T., J. Z. Shan Ho, B. Ho, and J. L. Ding.** 2006. Iron-withholding strategy in innate immunity. Immunobiology **211:**295-314.

216. **Osman, D., K. J. Waldron, H. Denton, C. M. Taylor, A. J. Grant, P. Mastroeni, N. J. Robinson, and J. S. Cavet.** 2010. Copper homeostasis in *Salmonella* is atypical and copper-CueP is a major periplasmic metal complex. J Biol Chem **285:**25259-25268.

217. **Ouattara, M., E. B. Cunha, X. Li, Y.-S. Huang, D. Dixon, and Z. Eichenbaum.** 2010. Shr of group A streptococcus is a new type of composite NEAT protein involved in sequestering haem from methaemoglobin. Mol Microbiol **78:**739-756.

218. **Outten, F. W., D. L. Huffman, J. A. Hale, and T. V. O'Halloran.** 2001. The independent *cue* and *cus* systems confer copper tolerance during aerobic and anaerobic growth in *Escherichia coli*. The Journal of Biological Chemistry **276:**30670-30677.

219. **Overbeek, R., T. Begley, R. M. Butler, J. V. Choudhuri, H.-Y. Chuang, M. Cohoon, V. de Crécy-Lagard, N. Diaz, T. Disz, R. Edwards, M. Fonstein, E. D. Frank, S. Gerdes, E. M. Glass, A. Goesmann, A. Hanson, D. Iwata-Reuyl, R. Jensen, N. Jamshidi, L. Krause, M. Kubal, N. Larsen, B. Linke, A. C. McHardy, F. Meyer, H. Neuweger, G. Olsen, R. Olson, A. Osterman, V. Portnoy, G. D. Pusch, D. A. Rodionov, C. Rückert, J. Steiner, R. Stevens, I. Thiele, O. Vassieva, Y. Ye, O. Zagnitko, and V. Vonstein.** The Subsystems Approach to Genome Annotation and its Use in the Project to Annotate 1000 Genomes. Nucleic Acids Research **33:**5691-5702.

220. **Panciera, R., D. Marlow, and A. Stintzi.** 2006. Major role for FeoB in *Campylobacter jejuni* ferrous iron acquisition, gut colonization, and intracellular survival. Infect Immun **74:**5433-44.

221. **Pandey, A., and R. V. Sonti.** 2010. Role of the FeoB protein and siderophore in promoting virulence of *Xanthomonas oryzae* pv. oryzae on rice. J Bacteriol **192:**3187-3203.

222. **Park, Y. K., J. Y. Choi, D. Shin, and K. S. Ko.** 2011. Correlation between overexpression and amino acid substitution of the PmrAB locus and colistin resistance in *Acinetobacter baumannii*. Int J Antimicrob Agents **37:**525-30.

223. **Park, Y. K., S.-I. Jung, K.-H. Park, H. S. Cheong, K. R. Peck, J.-H. Song, and K. S. Ko.** 2009. Independent emergence of colistin-resistant Acinetobacter spp. isolates from Korea. Diagn Microbiol Infect Dis **64:**43-51.

224. **Peleg, A. Y., J. Adams, and D. L. Paterson.** 2007. Tigecycline Efflux as a Mechanism for Nonsusceptibility in Acinetobacter baumannii. Antimicrob Agents Chemother **51:**2065-2069.

225. **Peleg, A. Y., H. Seifert, and D. L. Paterson.** 2008. Acinetobacter baumannii: emergence of a successful pathogen. Clin Microbiol Rev **21:**538-82.

226. **Perry, R. D., S. K. Craig, J. Abney, A. G. Bobrov, O. Kirillina, I. Mier, H. Truszczynska, and J. D. Fetherston.** 2012. Manganese transporters Yfe and MntH are Fur regulated and important for the virulence of *Yersinia pestis.* Microbiology **158:**804-15.

227. **Petersen, K., M. S. Riddle, J. R. Danko, D. L. Blazes, R. Hayden, S. A. Tasker, and J. R. Dunne.** 2007. Trauma-related infections in battlefield casualties from Iraq. Ann Surg **245:**803-11.

228. **Pichardo, C., M. E. Pachón-Ibañez, F. Docobo-Perez, R. López-Rojas, M. E. Jiménez-Mejías, A. Garcia-Curiel, and J. Pachon.** 2010. Efficacy of tigecycline vs. imipenem in the treatment of experimental Acinetobacter baumannii murine pneumonia. Eur J Clin Microbiol Infect Dis **29:**527-31.

229. **Piechaud, M., and L. Second.** 1951. [Studies of 26 strains of Moraxella Iwoffi.]. Ann Inst Pasteur (Paris) **80:**97-9.

230. **Pishchany, G., A. L. McCoy, V. J. Torres, J. C. Krause, J. E. Crowe, M. E. Fabry, and E. P. Skaar.** 2010. Specificity for human hemoglobin enhances *Staphylococcus aureus* infection. Cell Host Microbe **8:**544-550.

231. **Pluym, M., N. Muryoi, D. E. Heinrichs, and M. J. Stillman.** 2008. Heme binding in the NEAT domains of IsdA and IsdC of *Staphylococcus aureus.* J Inorg Biochem **102:**480-488.

232. **Poirel, L., S. Marque, C. Heritier, C. Segonds, G. Chabanon, and P. Nordmann.** 2005. OXA-58, a novel class D {beta}-lactamase involved in resistance to carbapenems in Acinetobacter baumannii. Antimicrob Agents Chemother **49:**202-8.

233. **Ponton, F., K. Wilson, S. C. Cotter, D. Raubenheimer, and S. J. Simpson.** 2011. Nutritional immunology: A multi-dimensional approach. PLoS Path **7:**e1002223.

234. **Posey, J. E., and F. C. Gherardini.** 2000. Lack of a role for iron in the Lyme disease pathogen. Science **288:**1651-1653.

235. **Pournaras, S., A. Markogiannakis, A. Ikonomidis, L. Kondyli, K. Bethimouti, A. N. Maniatis, N. J. Legakis, and A. Tsakris.** 2006. Outbreak of multiple

clones of imipenem-resistant Acinetobacter baumannii isolates expressing OXA-58 carbapenemase in an intensive care unit. J Antimicrob Chemother **57:**557-61.

236. **Price, C. T. D., T. Al-Quadan, M. Santic, I. Rosenshine, and Y. Abu Kwaik.** 2011. Host proteasomal degradation generates amino acids essential for intracellular bacterial growth. Science **334:**1553-1557.

237. **Puri, S., and M. R. O'Brian.** 2006. The *hmuQ* and *hmuD* genes from *Bradyrhizobium japonicum* encode heme-degrading enzymes. J Bacteriol **188:**6476-6482.

238. **Qiu, H., R. KuoLee, G. Harris, and W. Chen.** 2009. Role of NADPH phagocyte oxidase in host defense against acute respiratory *Acinetobacter baumannii* infection in mice. Infect Immun **77:**1015-1021.

239. **Queenan, A. M., C. M. Pillar, J. Deane, D. F. Sahm, A. S. Lynch, R. K. Flamm, J. Peterson, and T. A. Davies.** 2012. Multidrug resistance among *Acinetobacter spp.* in the USA and activity profile of key agents: results from CAPITAL Surveillance 2010. Diagn Microbiol Infect Dis **73:**267-270.

240. **Raetz, C., R. Ulevitch, S. Wright, C. Sibley, A. Ding, and C. Nathan.** 1991. Gram-negative endotoxin: an extraordinary lipid with profound effects on eukaryotic signal transduction. FASEB J **5:**2652-2660.

241. **Rahman, S. M. J., A. L. Gonzalez, M. Li, E. H. Seeley, L. J. Zimmerman, X. J. Zhang, M. L. Manier, S. J. Olson, R. N. Shah, A. N. Miller, J. B. Putnam, Y. E. Miller, W. A. Franklin, W. J. Blot, D. P. Carbone, Y. Shyr, R. M. Caprioli, and P. P. Massion.** 2011. Lung cancer diagnosis from proteomic analysis of preinvasive lesions. Cancer Res **71:**3009-3017.

242. **Ran, Y.-C., X.-X. Ao, L. Liu, Y.-L. Fu, H. Tuo, and F. Xu.** 2010. Microbiological study of pathogenic bacteria isolated from paediatric wound infections following the 2008 Wenchuan earthquake. Scand J Infect Dis.

243. **Reams, A. B., and E. L. Neidle.** 2004. Gene Amplification Involves Site-specific Short Homology-independent Illegitimate Recombination in Acinetobacter sp. Strain ADP1. J Mol Biol **338:**643-656.

244. **Reniere, M. L., G. N. Ukpabi, S. R. Harry, D. F. Stec, R. Krull, D. W. Wright, B. O. Bachmann, M. E. Murphy, and E. P. Skaar.** 2010. The IsdG-family of

haem oxygenases degrades haem to a novel chromophore. Mol Microbiol **75:**1529-1538.

245. **Ressner, R. A., C. K. Murray, M. E. Griffith, M. S. Rasnake, D. R. Hospenthal, and S. E. Wolf.** 2008. Outcomes of bacteremia in burn patients involved in combat operations overseas. J Am Coll Surg **206:**439-44.

246. **Robenshtok, E., M. Paul, L. Leibovici, A. Fraser, S. Pitlik, I. Ostfeld, Z. Samra, S. Perez, B. Lev, and M. Weinberger.** 2006. The significance of Acinetobacter baumannii bacteraemia compared with Klebsiella pneumoniae bacteraemia: risk factors and outcomes. J Hosp Infect **64:**282-7.

247. **Roca, I., S. Marti, P. Espinal, P. Martinez, I. Gibert, and J. Vila.** 2009. CraA, a Major Facilitator Superfamily Efflux Pump Associated with Chloramphenicol Resistance in Acinetobacter baumannii. Antimicrob Agents Chemother **53:**4013-4014.

248. **Rodrigues, P. M. d. A., E. do Carmo Neto, L. R. d. C. Santos, and M. F. Knibel.** 2009. Ventilator-associated pneumonia: epidemiology and impact on the clinical evolution of ICU patients. Jornal brasileiro de pneumologia : publicaçẫo oficial da Sociedade Brasileira de Pneumologia e Tisilogia **35:**1084-91.

249. **Rodriguez-Bano, J., S. Marti, S. Soto, F. Fernandez-Cuenca, J. M. Cisneros, J. Pachon, A. Pascual, L. Martinez-Martinez, C. McQueary, L. A. Actis, and J. Vila.** 2008. Biofilm formation in Acinetobacter baumannii: associated features and clinical implications. Clin Microbiol Infect **14:**276-8.

250. **Rohmer, L., D. Hocquet, and S. I. Miller.** 2011. Are pathogenic bacteria just looking for food? Metabolism and microbial pathogenesis. Trends Microbiol **19:**341-348.

251. **Rokhbakhsh-Zamin, F., D. Sachdev, N. Kazemi-Pour, A. Engineer, K. R. Pardesi, S. Zinjarde, P. K. Dhakephalkar, and B. A. Chopade.** 2011. Characterization of plant-growth-promoting traits of *Acinetobacter* species isolated from rhizosphere of *Pennisetum glaucum.* Journal of Microbiology and Biotechnology **21:**556-566.

252. **Rosch, J. W., G. Gao, G. Ridout, Y.-D. Wang, and E. I. Tuomanen.** 2009. Role of the manganese efflux system *mntE* for signalling and pathogenesis in *Streptococcus pneumoniae.* Mol Microbiol **72:**12-25.

253. **Rossi, D. L., S. D. Hurst, Y. Xu, W. Wang, S. Menon, R. L. Coffman, and A. Zlotnik.** 1999. Lungkine, a novel CXC chemokine, specifically expressed by lung bronchoepithelial cells. J Immunol **162:**5490-7.

254. **Russo, T. A., J. M. Beanan, R. Olson, U. Macdonald, N. R. Luke, S. R. Gill, and A. A. Campagnari.** 2008. Rat pneumonia and soft-tissue infection models for the study of Acinetobacter baumannii biology. Infect Immun **76:**3577-86.

255. **Ruzin, A., D. Keeney, and P. A. Bradford.** 2007. AdeABC multidrug efflux pump is associated with decreased susceptibility to tigecycline in *Acinetobacter calcoaceticus-Acinetobacter baumannii* complex. J Antimicrob Chemother **59:**1001-1004.

256. **Saito, Y., K. Saito, Y. Hirano, K. Ikeya, H. Suzuki, K. Shishikura, S. Manno, Y. Takakuwa, K. Nakagawa, A. Iwasa, S. Fujikawa, M. Moriya, N. Mizoguchi, B. E. Golden, and M. Osawa.** 2002. Hyperzincemia with systemic inflammation: a heritable disorder of calprotectin metabolism with rheumatic manifestations? The Journal of pediatrics **140:**267-269.

257. **Samanovic, M. I., C. Ding, D. J. Thiele, and K. H. Darwin.** 2012. Copper in microbial pathogenesis: meddling with the metal. Cell Host Microbe **11:**106-115.

258. **Sass, A., A. Marchbank, E. Tullis, J. J. Lipuma, and E. Mahenthiralingam.** 2020. Spontaneous and evolutionary changes in the antibiotic resistance of Burkholderia cenocepacia observed by global gene expression analysis. BMC Genomics **12:**373.

259. **Schalk, I. J.** 2008. Metal trafficking via siderophores in Gram-negative bacteria: specificities and characteristics of the pyoverdine pathway. J Inorg Biochem **102:**1159-1169.

260. **Schroeder, T. H., M. M. Lee, P. W. Yacono, C. L. Cannon, A. A. Gerçeker, D. E. Golan, and G. B. Pier.** 2002. CFTR is a pattern recognition molecule that extracts Pseudomonas aeruginosa LPS from the outer membrane into epithelial cells and activates NF-kappa B translocation. Proc Natl Acad Sci U S A **99:**6907-6912.

261. **Schryvers, A. B., and L. J. Morris.** 1988. Identification and characterization of the transferrin receptor from *Neisseria meningitidis*. Mol Microbiol **2:**281-288.

262. **Seaton, S. C., K. T. Elliott, L. E. Cuff, N. S. Laniohan, P. R. Patel, and E. L. Neidle.** 2011. Genome-wide selection for increased copy number in Acinetobacter baylyi ADP1: locus and context-dependent variation in gene amplification. Mol Microbiol **83:**520-535.

263. **Segond, D., A. Dellagi, V. Lanquar, M. Rigault, O. Patrit, S. Thomine, and D. Expert.** 2009. *NRAMP* genes function in *Arabidopsis thaliana* resistance to *Erwinia chrysanthemi* infection. The Plant Journal **58:**195-207.

264. **Shafeeq, S., H. Yesilkaya, T. G. Kloosterman, G. Narayanan, M. Wandel, P. W. Andrew, O. P. Kuipers, and J. A. Morrissey.** 2011. The *cop* operon is required for copper homeostasis and contributes to virulence in *Streptococcus pneumoniae*. Mol Microbiol **81:**1255-1270.

265. **Sharan, R., S. Chhibber, and R. H. Reed.** 2011. A murine model to study the antibacterial effect of copper on infectivity of *Salmonella enterica* serovar Typhimurium. Int J Env Res Public Health **8:**21-36.

266. **Shin, H. J., H. Lee, J. D. Park, H. C. Hyun, H. O. Sohn, D. W. Lee, and Y. S. Kim.** 2007. Kinetics of binding of LPS to recombinant CD14, TLR4, and MD-2 proteins. Mol Cells **24:**119-124.

267. **Shin, J.-H., H. J. Jung, Y. J. An, Y.-B. Cho, S.-S. Cha, and J.-H. Roe.** 2011. Graded expression of zinc-responsive genes through two regulatory zinc-binding sites in Zur. Proc Natl Acad Sci U S A **108:**5045-5050.

268. **Siempos, I. I., K. Z. Vardakas, C. E. Kyriakopoulos, T. K. Ntaidou, and M. E. Falagas.** 2009. Predictors of mortality in adult patients with ventilator-associated pneumonia: a meta-analysis. Shock.

269. **Siroy, A., V. Molle, C. Lemaitre-Guillier, D. Vallenet, M. Pestel-Caron, A. J. Cozzone, T. Jouenne, and E. De.** 2005. Channel Formation by CarO, the Carbapenem Resistance-Associated Outer Membrane Protein of Acinetobacter baumannii. Antimicrob Agents Chemother **49:**4876-4883.

270. **Smith, M. G., T. A. Gianoulis, S. Pukatzki, J. J. Mekalanos, L. N. Ornston, M. Gerstein, and M. Snyder.** 2007. New insights into Acinetobacter baumannii pathogenesis revealed by high-density pyrosequencing and transposon mutagenesis. Genes Dev **21:**601-14.

271. **Sobota, J. M., and J. A. Imlay.** 2011. Iron enzyme ribulose-5-phosphate 3-epimerase in *Escherichia coli* is rapidly damaged by hydrogen peroxide but can be protected by manganese. Proc Natl Acad Sci U S A **108:**5402-5407.

272. **Souli, M., I. Galani, and H. Giamarellou.** 2008. Emergence of extensively drug-resistant and pandrug-resistant Gram-negative bacilli in Europe. Euro Surveill **13**.

273. **Srivastava, S., and N. Shetty.** 2007. Healthcare-associated infections in neonatal units: lessons from contrasting worlds. J Hosp Infect **65:**292-306.

274. **Stork, M., M. P. Bos, I. Jongerius, N. de Kok, I. Schilders, V. E. Weynants, J. T. Poolman, and J. Tommassen.** 2010. An outer membrane receptor of *Neisseria meningitidis* involved in zinc acquisition with vaccine potential. PLoS Path **6:**e1000969.

275. **Su, X. Z., J. Chen, T. Mizushima, T. Kuroda, and T. Tsuchiya.** 2005. AbeM, an H+-coupled Acinetobacter baumannii multidrug efflux pump belonging to the MATE family of transporters. Antimicrob Agents Chemother **49:**4362-4.

276. **Summer, K. H., J. Lichtmannegger, N. Bandow, D. W. Choi, A. A. DiSpirito, and B. Michalke.** 2011. The biogenic methanobactin is an effective chelator for copper in a rat model for Wilson disease. J Trace Elem Med Biol **25:**36-41.

277. **Tao, C., M. Kang, Z. Chen, Y. Xie, H. Fan, L. Qin, and Y. Ma.** 2009. Microbiologic study of the pathogens isolated from wound culture among Wenchuan earthquake survivors. Diagn Microbiol Infect Dis **63:**268-70.

278. **Terrin, G., A. Passariello, F. Manguso, G. Salvia, L. Rapacciuolo, F. Messina, F. Raimondi, and R. B. Canani.** 2011. Serum calprotectin: an antimicrobial peptide as a new marker for the diagnosis of sepsis in very low birth weight newborns. Clin Dev Immunol **2011:**291085.

279. **Thiennimitr, P., S. E. Winter, M. G. Winter, M. N. Xavier, V. Tolstikov, D. L. Huseby, T. Sterzenbach, R. M. Tsolis, J. R. Roth, and A. J. Bäumler.** 2011. Intestinal inflammation allows *Salmonella* to use ethanolamine to compete with the microbiota. Proc Natl Acad Sci U S A **108:**17480-17485.

280. **Tien, H. C., A. Battad, E. A. Bryce, J. Fuller, M. Mulvey, K. Bernard, R. Brisebois, J. J. Doucet, S. B. Rizoli, R. Fowler, and A. Simor.** 2007. Multi-drug

resistant Acinetobacter infections in critically injured Canadian forces soldiers. BMC Infect Dis **7:**95.

281. **Tomaras, A. P., M. J. Flagler, C. W. Dorsey, J. A. Gaddy, and L. A. Actis.** 2008. Characterization of a two-component regulatory system from Acinetobacter baumannii that controls biofilm formation and cellular morphology. Microbiology **154:**3398-409.

282. **Torres, V. J., G. Pishchany, M. Humayun, O. Schneewind, and E. P. Skaar.** 2006. *Staphylococcus aureus IsdB* is a hemoglobin receptor required for heme iron utilization. J Bacteriol **188:**8421-8429.

283. **Treerat, P., F. Widmer, P. G. Middleton, J. Iredell, and A. M. George.** 2008. In vitro interactions of tobramycin with various nonantibiotics against Pseudomonas aeruginosa and Burkholderia cenocepacia. FEMS Microbiol Lett **285:**40-50.

284. **Tseng, H. J., Y. Srikhanta, A. G. McEwan, and M. P. Jennings.** 2001. Accumulation of manganese in *Neisseria gonorrhoeae* correlates with resistance to oxidative killing by superoxide anion and is independent of superoxide dismutase activity. Mol Microbiol **40:**1175-1186.

285. **Urban, C. F., D. Ermert, M. Schmid, U. Abu-Abed, C. Goosmann, W. Nacken, V. Brinkmann, P. R. Jungblut, and A. Zychlinsky.** 2009. Neutrophil extracellular traps contain calprotectin, a cytosolic protein complex involved in host defense against *Candida albicans.* PLoS Path **5:**e1000639.

286. **Vallenet, D., P. Nordmann, V. r. Barbe, L. Poirel, S. Mangenot, E. Bataille, C. Dossat, S. Gas, A. Kreimeyer, P. Lenoble, S. Oztas, J. Poulain, B. a. Segurens, C. Robert, C. Abergel, J.-M. Claverie, D. Raoult, C. M√ ©digue, J. Weissenbach, and S. p. Cruveiller.** 2008. Comparative Analysis of Acinetobacters: Three Genomes for Three Lifestyles. PLoS ONE **3:**e1805.

287. **van Faassen, H., R. KuoLee, G. Harris, X. Zhao, J. W. Conlan, and W. Chen.** 2007. Neutrophils play an important role in host resistance to respiratory infection with *Acinetobacter baumannii* in mice. Infect Immun **75:**5597-5608.

288. **Velayudhan, J., N. J. Hughes, A. A. McColm, J. Bagshaw, C. L. Clayton, S. C. Andrews, and D. J. Kelly.** 2000. Iron acquisition and virulence in *Helicobacter*

pylori: a major role for FeoB, a high-affinity ferrous iron transporter. Mol Microbiol **37:**274-286.

289. **Veyrier, F. J., I. G. Boneca, M. F. Cellier, and M.-K. Taha.** 2011. A novel metal transporter mediating manganese export (MntX) regulates the Mn to Fe intracellular ratio and *Neisseria meningitidis* virulence. PLoS Path **7:**e1002261.

290. **Vila, J., S. Marti, and J. Sanchez-Cespedes.** 2007. Porins, efflux pumps and multidrug resistance in Acinetobacter baumannii. J Antimicrob Chemother **59:**1210-5.

291. **Vincent, J.-L., J. Rello, J. Marshall, E. Silva, A. Anzueto, C. D. Martin, R. Moreno, J. Lipman, C. Gomersall, Y. Sakr, K. Reinhart, and E. I. G. o. Investigators.** 2009. International study of the prevalence and outcomes of infection in intensive care units. JAMA **302:**2323-9.

292. **Vinogradov, E. V., J. Ø. Duus, H. Brade, and O. Holst.** 2002. The structure of the carbohydrate backbone of the lipopolysaccharide from Acinetobacter baumannii strain ATCC 19606. European journal of biochemistry / FEBS **269:**422-430.

293. **Vinogradov, E. V., B. O. Petersen, J. E. Thomas-Oates, J. Duus, H. Brade, and O. Holst.** 1998. Characterization of a novel branched tetrasaccharide of 3-deoxy-D-manno-oct-2-ulopyranosonic acid. The structure of the carbohydrate backbone of the lipopolysaccharide from Acinetobacter baumannii strain nctc 10303 (atcc 17904). The Journal of biological chemistry **273:**28122-28131.

294. **Wang, H., J. Head, P. Kosma, H. Brade, S. Müller-Loennies, S. Sheikh, B. McDonald, K. Smith, T. Cafarella, B. Seaton, and E. Crouch.** 2008. Recognition of heptoses and the inner core of bacterial lipopolysaccharides by surfactant protein d. Biochemistry (Mosc) **47:**710-720.

295. **Wang, S.-C., K.-H. Lin, J. P. S. Chern, M.-Y. Lu, S.-T. Jou, D.-T. Lin, and K.-S. Lin.** 2003. Severe bacterial infection in transfusion-dependent patients with thalassemia major. Clin Infect Dis **37:**984-988.

296. **Ward, S. K., B. Abomoelak, E. A. Hoye, H. Steinberg, and A. M. Talaat.** 2010. CtpV: a putative copper exporter required for full virulence of *Mycobacterium tuberculosis*. Mol Microbiol **77:**1096-1110.

297. **Watson, R. J., P. Millichap, S. A. Joyce, S. Reynolds, and D. J. Clarke.** 2010. The role of iron uptake in pathogenicity and symbiosis in Photorhabdus luminescens TT01. BMC Microbiol **10:**177.

298. **Weber, A., and K. Jung.** 2002. Profiling early osmostress-dependent gene expression in Escherichia coli using DNA macroarrays. J Bacteriol **184:**5502-7.

299. **Weinberg, E. D.** 1975. Nutritional immunity. Host's attempt to withold iron from microbial invaders. JAMA **231:**39-41.

300. **Weinberg, E. D.** 2008. Survival advantage of the hemochromatosis C282Y mutation. Perspect Biol Med **51:**98-102.

301. **Weinberg, E. D.** 2009. Iron availability and infection. Biochim Biophys Acta **1790:**600-605.

302. **White, C., J. Lee, T. Kambe, K. Fritsche, and M. J. Petris.** 2009. A role for the ATP7A copper-transporting ATPase in macrophage bactericidal activity. J Biol Chem **284:**33949-33956.

303. **Wieland, C. W., S. Florquin, and T. van der Poll.** 2007. Interleukin 18 participates in the early inflammatory response and bacterial clearance during pneumonia caused by nontypeable Haemophilus influenzae. Infect Immun **75:**5068-72.

304. **Wilks, A.** 2002. Heme oxygenase: evolution, structure, and mechanism. Antioxidants & Redox Signaling **4:**603-614.

305. **Winter, S. E., P. Thiennimitr, M. G. Winter, B. P. Butler, D. L. Huseby, R. W. Crawford, J. M. Russell, C. L. Bevins, L. G. Adams, R. M. Tsolis, J. R. Roth, and A. J. Bäumler.** 2010. Gut inflammation provides a respiratory electron acceptor for *Salmonella.* Nature **467:**426-429.

306. **Wolff, M., M. L. Joly-Guillou, R. Farinotti, and C. Carbon.** 1999. In vivo efficacies of combinations of beta-lactams, beta-lactamase inhibitors, and rifampin against Acinetobacter baumannii in a mouse pneumonia model. Antimicrob Agents Chemother **43:**1406-11.

307. **Wolschendorf, F., D. Ackart, T. B. Shrestha, L. Hascall-Dove, S. Nolan, G. Lamichhane, Y. Wang, S. H. Bossmann, R. J. Basaraba, and M. Niederweis.** 2011. Copper resistance is essential for virulence of *Mycobacterium tuberculosis.* Proc Natl Acad Sci U S A **108:**1621-1626.

308. **Yancey, P. H.** 2005. Organic osmolytes as compatible, metabolic and counteracting cytoprotectants in high osmolarity and other stresses. J Exp Biol **208:**2819-30.

309. **Yuan, Z., K. R. Ledesma, R. Singh, J. Hou, R. A. Prince, and V. H. Tam.** 2010. Quantitative assessment of combination antimicrobial therapy against multidrug-resistant bacteria in a murine pneumonia model. J Infect Dis **201:**889-97.

310. **Yun, S. H., C. W. Choi, S. H. Park, J. C. Lee, S. H. Leem, J. S. Choi, S. Kim, and S. I. Kim.** 2008. Proteomic analysis of outer membrane proteins from Acinetobacter baumannii DU202 in tetracycline stress condition. J Microbiol **46:**720-7.

311. **Zarantonelli, M.-L., M. Szatanik, D. Giorgini, E. Hong, M. Huerre, F. Guillou, J.-M. Alonso, and M.-K. Taha.** 2007. Transgenic mice expressing human transferrin as a model for meningococcal infection. Infect Immun **75:**5609-5614.

312. **Zhang, R., J. Zhang, H. Ding, D. Lu, Y. Hu, D.-C. Wang, and Q. Zou.** 2011. Crystallization and preliminary crystallographic studies of *Campylobacter jejuni* ChuZ, a member of a novel haem oxygenase family. Acta Crystallogr **67:**1228-1230.

313. **Zhang, R., J. Zhang, G. Guo, X. Mao, W. Tong, Y. Zhang, D.-C. Wang, Y. Hu, and Q. Zou.** 2011. Crystal structure of *Campylobacter jejuni* ChuZ: a split-barrel family heme oxygenase with a novel heme-binding mode. Biochem Biophys Res Commun **415:**82-87.

314. **Zhou, T., Y. Ma, X. Kong, and R. C. Hider.** 2012. Design of iron chelators with therapeutic application. Dalton transactions.

315. **Zhu, H., M. Liu, and B. Lei.** 2008. The surface protein Shr of *Streptococcus pyogenes* binds heme and transfers it to the streptococcal heme-binding protein Shp. BMC Microbiol **8:**15.

316. **Zimbler, D. L., W. F. Penwell, J. A. Gaddy, S. M. Menke, A. P. Tomaras, P. L. Connerly, and L. A. Actis.** 2009. Iron acquisition functions expressed by the human pathogen *Acinetobacter baumannii*. Biometals **22:**23-32.

317. **Zughaier, S., S. Agrawal, D. S. Stephens, and B. Pulendran.** 2006. Hexa-acylation and KDO(2)-glycosylation determine the specific immunostimulatory activity of Neisseria meningitidis lipid A for human monocyte derived dendritic cells. Vaccine **24:**1291-1297.

Appendix 1. Supplementary tables associated with Chapter II.

Table 12: Primers used for real-time PCR

Target gene	Primer Name	Sequence
A1S_2396	RT2396F	GCTGAATGATTGTGCCTTCC
	RT2396R	CCAACGCTTATCAAACCGC
A1S_2647	RT2647F	CTGAATGATTGTGCCTTCTACC
	RT2647R	AGAACACTAAAACCTGATGCCTC
A1S_1751	RT1751F	GGTGCTTTCCATGCTGCC
	RT1751R	AAGGTACAGCGGAAATTCGTC
A1S_1769	RT1769F	CCTGTGTAATATCGGCTTGACC
	RT1769R	TGATTACCCGTGCAGACTTGG
A1S_2198	RT2198F	GCCGCCCAGTCATTATTGC
	RT2198R	GAACAACATCGAAACATCTGAAGC
A1S_2377	RT2377F	TTGCTAATTGAACGACACCTTC
	RT2377R	CAACCTTACTGCGAGCACTTG
A1S_2642	RT2642F	CTACAGGTTACGGTGGTGCTTTG
	RT2642R	TTTGTTCCGTTAATTTTGATAGTACC
A1S_3146	RT3146F	ATAGCATTGAAACAGCAGCAGC
	RT3146R	CTTGCTTGTTAATAGGTATGACACTC
A1S_r01 (16S rRNA)	RTR01F	GCTAATAGATGAGCCTAAGTCGG
	RTR01R	CAGACCCGCTACAGATCGTC

Table 13: Transcripts that increased significantly upon NaCl exposure as determined by microarray analysis

Locus Tag	Description	Fold Induction[a]
Amino Acid Metabolism[b]		
A1S_0925	choline dehydrogenase	2.1
A1S_0956	L-aspartate dehydrogenase	4.3
A1S_1274	alcohol dehydrogenase GroES-like protein	8.9
A1S_1364	aminotransferase class V	2.2
A1S_1957	putative L-kynurenine hydrolase	18.2
Carbohydrate metabolism		
A1S_0804	trehalose-6-phosphate phophatase	3.0
Cell envelope biogenesis, outer membrane		
A1S_0494	putative glycosyl transferase	2.8
A1S_1792	nucleoside-diphosphate-sugar epimerase	29.4
A1S_3218	membrane fusion protein, EsvF1	2.1
Cell motility and secretion		
A1S_0464	Sec-independent protein translocase protein	2.6
A1S_2090	P pilus assembly protein, chaperone PapD	2.5
A1S_2214	P pilus assembly protein, CsuD	25.8
A1S_2215	P pilus assembly protein, CsuC	2.2
A1S_2216	type 1 pili protein, CsuB	2.9
A1S_3165	pilin like competence factor	2.5
Coenzyme Metabolism		
A1S_2397	molybdopterin biosynthesis enzyme, MoeA	5.5
A1S_2581	isochorismate synthetase	11.1
DNA replication, recombination and repair		
A1S_0657	transposase	3.1
A1S_1501	phage integrase	2.5
A1S_2015	DNA-directed DNA polymerase	2.4
Energy Production/Conversion		
A1S_0849	tartrate dehydrogenase	8.1
A1S_0950	putative ferredoxin reductase subunit of phenylpropionate dioxygenase	3.1
A1S_1528	hypothetical protein A1S_1528, Proline dehydrogenase	2.3
A1S_1719	4Fe-4S ferredoxin iron-sulfur binding	2.5
Inorganic ion transport and metabolism		
A1S_0092	putative ferric siderophore receptor protein	2.8
A1S_0947	putative vanillate O-demethylase oxygenase subunit (VanA-like)	4.7
A1S_1123	putative flavin-binding monooxygenase	3.7
A1S_1808	hypothetical protein, Di- and tricarboxylate transporters	12.8
A1S_2386	putative ferric acinetobactin binding protein	3.0

A1S_2387	BauE	2.7
A1S_2971	putative vanillate O-demethylase oxygenase subunit	2.6
Lipid Metabolism		
A1S_0112	acyl-CoA synthetase/AMP-acid ligase II	27.6
A1S_1108	acyl coenzyme A dehydrogenase	18.6
A1S_2229	putative acyl-CoA dehydrogenase-related protein	3.6
A1S_3326	hypothetical protein, predicted membrane protein	2.6
Post-translational modification, protein turnover, chaperones		
A1S_3415	maleylacetoacetate isomerase	2.7
Regulation		
A1S_0205	hypothetical protein A1S_0205, transcriptional regulator	5.8
A1S_0963	putative transcriptional regulator, AraC family	2.3
A1S_1081	putative transcriptional regulator, TetR family	3.1
A1S_1272	putative transcriptional regulator	21.9
A1S_1282	putative transcriptional regulator, CopG	2.9
A1S_1393	putative two-component sensor kinase	3.5
A1S_1763	putative transcriptional regulator	3.4
A1S_1775	transcriptional activator, LuxR family	26.4
A1S_2006	response regulator protein	3.3
A1S_2396	putative transcriptional regulator, TetR family	7.7
A1S_2396	putative transcriptional regulator	43.1
A1S_2647	putative transcriptional regulator, TetR family	37.3
A1S_2647	putative transcriptional regulator	15.7
A1S_2747	transcriptional regulator, LysR family	2.2
A1S_2771	putative transcriptional regulator, AraC family	2.3
A1S_3255	putative transcriptional regulator, AraC/XylS family	9.7
A1S_3271	putative transcriptional regulator, LysR family	2.1
Resistance/Defense Mechanisms		
A1S_1751	$AdeA_2$ membrane fusion protein	25.9
A1S_1752	$AdeA_1$ membrane fusion protein	8.7
A1S_2376	putative ABC-type antimicrobial peptide transport system	11.8
A1S_2377	putative ABC-type multidrug transport system	3.6
A1S_3420	MATE family drug transporter	12.1
A1S_3445	putative RND family cation/multidrug efflux pump	3.2
Secondary metabolites biosynthesis, transport and catabolism		
A1S_0948	putative short-chain dehydrogenase	11.5
A1S_1105	hypothetical protein A1S_1105	2.2
A1S_1125	putative transferase	13.2
A1S_1387	oxidoreductase	13.9
A1S_2227	putative methyltransferase	2.6
A1S_2373	putative acinetobactin biosynthesis protein	3.1
A1S_2381	putative acinetobactin biosynthesis protein	3.1
A1S_2382	non-ribosomal peptide synthetase, BasD	29.0
A1S_2382	non-ribosomal peptide synthetase, BasD	2.3

A1S_2383	putative acinetobactin biosynthesis protein	17.2
A1S_2576	putative non-ribosomal peptide synthetase	2.3
A1S_2580	23-dihydro-2,3-dihydroxybenzoate synthetase, isochorismatase	3.4
A1S_3414	fumarylacetoacetase	2.7
Translation, ribosomal structure and biogenesis		
A1S_0089	dual specificity pseudouridine synthase	2.2
Transporters and Permeases		
A1S_0565	hypothetical protein A1S_0565, DMT family permease	2.1
A1S_0596	putative transporter	2.2
A1S_0915	putative MFS transporter	3.2
A1S_1209	putative benzoate transport porin (BenP)	16.2
A1S_1284	ABC-type nitrate/sulfonate/bicarbonate transport systems	2.3
A1S_1286	binding-protein-dependent transport systems, inner membrane component	10.1
A1S_1287	ABC nitrate/sulfonate/bicarbonate family transporter	2.0
A1S_1323	hypothetical protein A1S_1323, DMT family permease	3.4
A1S_1331	major facilitator superfamily MFS_1	2.7
A1S_1361	ABC-type spermidine/putrescine transport system, ATPase component	2.2
A1S_1362	ABC-type Fe^{3+} transport system permease component	9.4
A1S_1722	putative ATP-binding component of ABC transporter	2.0
A1S_1739	major facilitator superfamily MFS_1	4.1
A1S_1769	putative RND family drug transporter	2.9
A1S_1814	putative transporter	2.5
A1S_1956	putative amino acid permease	2.0
A1S_1992	DMT family permease	2.6
A1S_2141	potassium-transporting ATPase A chain	2.4
A1S_2198	putative mutlidrug resistance protein, Major facilitator superfamily	2.4
A1S_2304	putative RND family drug transporter	2.9
A1S_2378	putative ABC transporter	14.3
A1S_2388	putative ferric acinetobactin transport system permease protein	4.0
A1S_2389	putative ferric acinetobactin transport system permease protein	23.2
A1S_2932	heavy metal efflux pump CzcA	2.6
A1S_2934	heavy metal RND efflux outer membrane protein, CzcC family	16.0
A1S_3146	multidrug efflux transport protein, major facilitator superfamily	17.6
A1S_3251	transporter, LysE family	3.9
Proteins with general function predictions/functions unknown		
A1S_0032	putative signal peptide	3.7
A1S_0110	hypothetical protein	3.0
A1S_0117	hypothetical protein	3.0
A1S_0211	transposition helper	2.5
A1S_0296	hypothetical protein	10.7
A1S_0301	predicted esterase of the alpha/beta hydrolase fold	2.1
A1S_0396	uncharacterized protein conserved in bacteria	2.6
A1S_0425	hypothetical protein, Neuromodulin	2.2
A1S_0440	hypothetical protein	2.1
A1S_0660	transposition helper	4.2
A1S_0673	putative transposase	2.6

A1S_0677	transposase	4.3
A1S_0740	putative phage related protein	2.4
A1S_0741	hypothetical protein	3.6
A1S_0847	putative signal peptide	3.5
A1S_0889	putative hemolysin	2.5
A1S_0946	hypothetical protein	4.0
A1S_0954	putative hydrolase	3.5
A1S_0959	putative signal peptide	5.5
A1S_1053	hypothetical protein, M protein trans-acting positive regulator	2.6
A1S_1148	hypothetical protein	3.8
A1S_1149	hypothetical protein	3.5
A1S_1150	hypothetical protein	4.0
A1S_1151	uncharacterized conserved protein	7.9
A1S_1167	uncharacterized conserved protein	2.7
A1S_1233	predicted outer membrane protein	5.4
A1S_1383	surface antigen	2.6
A1S_1385	hypothetical protein, Ribosomal protein L31e	2.4
A1S_1583	hypothetical protein	2.6
A1S_1588	phage terminase-like protein large subunit	13.7
A1S_1589	phage-related protein	2.1
A1S_1592	putative phage head-tail adaptor	9.7
A1S_1595	hypothetical protein	2.2
A1S_1744	putative electron transfer flavoprotein	21.4
A1S_1770	hypothetical protein, GH3 auxin-responsive promoter	2.2
A1S_1802	uncharacterized protein conserved in bacteria	3.3
A1S_1803	uncharacterized protein conserved in bacteria	2.4
A1S_1809	putative hydrolase transmembrane protein	3.6
A1S_1811	uncharacterized protein conserved in bacteria	2.4
A1S_1851	penicillin G amidase	2.4
A1S_1897	predicted membrane protein	2.0
A1S_1901	predicted metal-dependent hydrolase	2.1
A1S_1952	uncharacterized conserved protein	5.4
A1S_2032	hypothetical protein	3.2
A1S_2074	hypothetical protein, OB-fold nucleic acid binding domain	4.2
A1S_2228	uncharacterized proteins, LmbE homologs	2.8
A1S_2278	putative hydrolase of the alpha/beta superfamily	20.9
A1S_2400	predicted metal-dependent hydrolase	2.3
A1S_2889	putative signal peptide	4.3
A1S_3120	hypothetical protein	2.1
A1S_3338	uncharacterized conserved small protein	2.3

[a]Fold-induction in LB + 200 mM NaCl relative to LB without NaCl supplementation.
[b]Transcripts were divided into functional categories based on cluster of orthologous groups (COG) classifications.

Table 14: Transcripts that decreased significantly upon exposure to NaCl as determined by microarray analyses

Locus Tag	Description	Fold Repression[a]
Amino acid transport and metabolism[b]		
A1S_0071	tyrosine aminotransferase tyrosine repressible, PLP-dependent	5.1
A1S_0095	D-amino acid dehydrogenase	6.3
A1S_0177	cysteine synthase A/O-acetylserine sulfhydrolase A subunit PLP-dependent enzyme	8.1
A1S_0203	hypothetical protein	2.7
A1S_0227	aminopeptidase A	4.4
A1S_0238	threonine synthase pyridoxal-5'-phosphate-dependent enzyme	5.1
A1S_0239	homoserine dehydrogenase	5.1
A1S_0258	argininosuccinate lyase	3.6
A1S_0259	argininosuccinate lyase	3.5
A1S_0274	anthranilate synthase component I; TrpE	3.5
A1S_0346	hypothetical protein	3.2
A1S_0415	putative hydrolase haloacid dehalogenase-like family	2.1
A1S_0427	aspartate-semialdehyde dehydrogenase NAD(P)-binding	2.9
A1S_0471	homoserine O-acetyltransferase	2.0
A1S_0472	2-isopropylmalate synthase	6.1
A1S_0483	phosphogluconate dehydratase	4.6
A1S_0489	gamma-glutamyl phosphate reductase	4.3
A1S_0543	acetolactate synthase III large subunit	6.9
A1S_0544	acetolactate synthase isozyme III small subunit	7.7
A1S_0545	acetohydroxy acid isomeroreductase	6.4
A1S_0575	cysteine synthase B	4.1
A1S_0610	pyrroline-5-carboxylate reductase	3.1
A1S_0686	ATP-phosphoribosyltransferase	3.1
A1S_0687	histidinol dehydrogenase	5.4
A1S_0688	histidinol-phosphate aminotransferase	4.5
A1S_0712	hypothetical protein	4.0
A1S_0737	5-methyltetrahydropteroyltriglutamate-homocysteine methyltransferase	12.4
A1S_0888	acetylglutamate kinase	4.2
A1S_0905	putative D-amino acid oxidase	2.8
A1S_0912	ribosomal protein L22	3.4
A1S_0962	putative glutaminase	2.6
A1S_1000	sulfate adenylyltransferase subunit 2	6.1
A1S_1039	aminopeptidase P	3.2
A1S_1068	argininosuccinate synthetase	3.8
A1S_1069	argininosuccinate synthetase	6.9
A1S_1084	glycine/D-amino acid oxidases (deaminating)	2.8
A1S_1119	choline dehydrogenase and related flavoproteins	2.7
A1S_1142	aspartate kinase	3.0
A1S_1178	ATP phosphoribosyltransferase	3.8
A1S_1463	serine acetyltransferase	2.7
A1S_1473	putative aminotransferase	4.3
A1S_1532	glycine cleavage complex protein H	3.4
A1S_1610	Zn-dependent oligopeptidase	2.3

A1S_1632	cysteine desulfurase	6.0
A1S_1633	cysteine desulfurase	4.3
A1S_1664	phospho-2-dehydro-3-deoxyheptonate aldolase	5.0
A1S_1683	o-succinylhomoserine sulfhydrylase	3.4
A1S_1705	putative (RR)-butanediol dehydrogenase	3.3
A1S_1762	hypothetical protein	4.4
A1S_1913	N-acetyl-gamma-glutamyl-phosphate reductase	3.0
A1S_1916	threonine dehydratase	4.4
A1S_1936	acetylornithine aminotransferase	2.4
A1S_1980	ornithine carbamoyltransferase	3.6
A1S_1984	D-amino acid dehydrogenase small subunit	6.2
A1S_2009	3-dehydroquinate dehydratase type II	3.4
A1S_2044	putative ferredoxin-dependent glutamate synthase	2.1
A1S_2084	chorismate mutase	2.4
A1S_2092	aminopeptidase N	3.9
A1S_2274	aminoacyl-histidine dipeptidase	2.5
A1S_2276	hypothetical protein A1S_2276	2.9
A1S_2277	hypothetical protein A1S_2277	4.4
A1S_2281	putative anthranilate phosphoribosyltransferase	2.8
A1S_2307	serine hydroxymethyltransferase	6.4
A1S_2319	hypothetical protein A1S_2319	4.7
A1S_2335	510-methylenetetrahydrofolate reductase	3.9
A1S_2351	glutamine synthetase	5.8
A1S_2352	glutamine synthetase	5.5
A1S_2354	Peptidase M24	2.3
A1S_2355	anthranilate synthase component II	4.1
A1S_2359	anthranilate phosphoribosyltransferase	2.5
A1S_2360	indole-3-glycerol phosphate synthase (IGPS)	2.3
A1S_2426	lactoylglutathione lyase	5.8
A1S_2453	L-24-diaminobutyrate decarboxylase	3.7
A1S_2454	L-24-diaminobutyrate:2-ketoglutarate 4-aminotransferase	4.2
A1S_2496	putative phosphoserine phosphatase	3.5
A1S_2508	aspartate aminotransferase A	4.9
A1S_2631	diaminopimelate epimerase	2.4
A1S_2632	diaminopimelate decarboxylase	2.7
A1S_2686	carbamoyl-phosphate synthase small chain	7.4
A1S_2687	carbamoyl-phosphate synthase large subunit	5.7
A1S_2774	putative homoserine kinase (ThrH)	2.4
A1S_2775	3'-phosphoadenylylsulfate reductase	4.9
A1S_2875	tryptophan synthase beta chain	3.8
A1S_2876	N-(5'-phosphoribosyl)anthranilate isomerase	5.5
A1S_2904	branched-chain amino acid transferase	4.3
A1S_3046	oligopeptidase A	2.9
A1S_3047	oligopeptidase A	2.7
A1S_3109	dehydroshikimate reductase NAD(P)-binding	2.9
A1S_3128	succinylglutamate desuccinylase	2.1
A1S_3131	arginine succinyltransferase	2.7
A1S_3132	succinylornithine transaminase	3.2

A1S_3133	bifunctional N-succinyldiaminopimelate-aminotransferase/acetylornithine transaminase protein	5.1
A1S_3134	glutamate dehydrogenase (NAD(P)+) oxidoreductase protein	7.5
A1S_3152	D-3-phosphoglycerate dehydrogenase	5.2
A1S_3182	glutamate synthase small chain	3.0
A1S_3185	glutamate synthase large chain precursor	3.5
A1S_3187	3-dehydroquinate synthase	2.3
A1S_3190	shikimate-kinase	3.1
A1S_3222	homocysteine synthase	2.8
A1S_3234	hypothetical protein A1S_3234	4.5
A1S_3235	imidazole glycerol phosphate synthetase glutamine amidotransferase subunit	3.7
A1S_3245	imidazole glycerol phosphate synthase cyclase subunit	2.1
A1S_3302	putative two-component sensor	2.8
A1S_3370	putative aminotransferase	3.0
A1S_3405	histidine ammonia-lyase	5.6
A1S_3406	urocanate hydratase	7.6
A1S_3407	urocanase	9.0
A1S_3423	dihydrodipicolinate synthase	7.9
A1S_3442	dihydrodipicolinate reductase	3.6
A1S_3455	dihydroxy-acid dehydratase	4.3
	tryptophan synthase alpha chain	8.2
	aspartate ammonia-lyase (aspartase)	3.9
	succinylarginine dihydrolase	3.7
	gamma-glutamyl kinase	2.7
	tryptophan synthase subunit beta	2.6
	urease alpha subunit	2.6
	chorismate synthase	2.2

Carbohydrate transport and metabolism

A1S_0064	putative phosphoglucose isomerase	4.8
A1S_0066	hypothetical protein A1S_0066	2.0
A1S_0073	putative carboxyphosphonoenolpyruvate phosphonomutase or putative methylisocitrate lyase (PrpB)	5.1
A1S_0230	phosphoglycerate mutase III cofactor independent	3.5
A1S_0330	triosephosphate isomerase	2.7
A1S_0484	hypothetical protein A1S_0484	3.1
A1S_0486	thermoresistant gluconokinase	3.5
A1S_0492	beta-N-acetyl-D-glucosaminidase	2.2
A1S_0571	hydroxypyruvate isomerase	2.5
A1S_0589	phosphocarrier protein (HPr-like)	5.1
A1S_0705	D-ribulose-5-phosphate 3-epimerase	3.0
A1S_0887	phosphomannomutase	3.6
A1S_0965	mutarotase precursor	2.4
A1S_1520	transketolase	5.6
A1S_1521	transketolase	4.0
A1S_1543	phosphoglycerate kinase	2.4
A1S_1871	putative phosphoglycerate mutase related protein	2.5
A1S_1898	enolase	4.3
A1S_1915	ribose 5-phosphate isomerase	4.4

A1S_1922	putative sugar kinase protein	5.3
A1S_2052	hypothetical protein A1S_2052	4.1
A1S_2164	phosphoenolpyruvate synthase	5.7
A1S_2200	L-sorbosone dehydrogenase	2.4
A1S_2283	putative inorganic polyphosphate/ATP-NAD kinase	3.3
A1S_2450	putative pyruvate decarboxylase	2.9
A1S_2501	glyceraldehyde-3-phosphate dehydrogenase	3.9
A1S_2596	fructose-16-bisphosphatase	4.6
A1S_2847	glucose dehydrogenase	4.7
A1S_2848	glucose dehydrogenase	4.6
A1S_3105	inositol-1-monophosphatase	2.8
A1S_3248	glycerol uptake facilitator	4.3
A1S_3320	phosphoglucosamine mutase	6.5
	fructose-16-bisphosphate aldolase, class II	3.6
	Sequence 1 from Patent EP1367120	2.7

Cell cycle control, cell division, chromosome partitioning

A1S_0049	protein tyrosine kinase	2.7
A1S_0124	putative chromatin partitioning ATPase (ParA family ATPase)	3.8
A1S_0137	hypothetical protein A1S_0137	2.6
A1S_0246	cell division protein	3.1
A1S_0639	IncC protein	5.4
A1S_0780	putative ATP-binding protein	2.6
A1S_0798	putative cell division protein (ZipA-like)	5.4
A1S_0876	putative cell division protein (FstK)	5.8
A1S_0879	cell division topological specificity factor	4.1
A1S_0880	minC activating cell division inhibitor a membrane ATPase	6.1
A1S_0881	cell division inhibitor	2.5
A1S_1551	chromosome partitioning protein	2.3
A1S_1896	putative cell division protein (FtsB-like)	5.5
A1S_2182	glucose-inhibited division protein A	3.8
A1S_2656	hypothetical protein A1S_2656	2.8
A1S_2781	rod shape-determining protein	3.0
A1S_3141	putative partition-related protein	4.8
A1S_3205	cell division protein	3.5
A1S_3331	cell division protein tubulin-like GTP-binding protein and GTPase	4.8
A1S_3332	cell division protein	4.6

Cell wall/membrane/envelope biogenesis

A1S_0019	Signal peptidase II	3.8
A1S_0051	putative outer membrane protein	2.9
A1S_0052	WecC protein	2.8
A1S_0055	WecE protein	3.9
A1S_0059	putative glycosyltransferase	2.1
A1S_0060	hypothetical protein A1S_0060	2.4
A1S_0061	putative UDP-galactose phosphate transferase	5.4
A1S_0062	putative UTP-glucose-1-phosphate uridylyltransferase	5.5
A1S_0063	putative UDP-glucose 6-dehydrogenase	5.1
A1S_0065	putative UDP-glucose 4-epimerase	7.4

A1S_0096	alanine racemase 2 PLP-binding, catabolic	4.2
A1S_0237	D-alanyl-D-alanine endopeptidase penicillin-binding protein 7 and penicillin-binding protein 8	5.2
A1S_0245	UDP-N-acetylmuramoylalanine-D-glutamate ligase	2.8
A1S_0292	putative outer membrane protein W	8.7
A1S_0380	glutamate racemase	4.4
A1S_0431	lipid A biosynthesis lauroyl acyltransferase	2.6
A1S_0493	carboxy-terminal protease	3.4
A1S_0495	putative glycosyl transferase	3.2
A1S_0540	putative minor lipoprotein	4.3
A1S_0622	putative lipoprotein precursor (VacJ) transmembrane	4.5
A1S_0685	UDP-N-acetylglucosamine 1-carboxyvinyltransferase	3.4
A1S_0884	putative outer membrane protein	6.0
A1S_0989	monofunctional biosynthetic peptidoglycan transglycosylase	2.2
A1S_1009	putative lipoprotein	4.0
A1S_1020	penicillin-binding protein 2	2.1
A1S_1055	hypothetical protein A1S_1055	4.2
A1S_1193	OmpA/MotB	5.2
A1S_1236	D-arabinose 5-phosphate isomerase	3.3
A1S_1546	organic solvent tolerance protein precursor	3.0
A1S_1550	glucose-inhibited division protein B	2.9
A1S_1618	hypothetical protein A1S_1618	3.5
A1S_1919	putative phospholipase A1 precursor (PldA)	3.3
A1S_1965	UDP-acetylglucosamine acyltransferase	4.7
A1S_1967	hypothetical protein A1S_1967	4.9
A1S_1968	putative outer membrane protein (OmpH)	4.5
A1S_1969	putative outer membrane protein	3.5
A1S_1970	putative membrane-associated Zn-dependent proteases 1	2.7
A1S_1987	putative UDP-galactose 4-epimerase (GalE-like)	2.7
A1S_2050	UDP-N-acetylenolpyruvoylglucosamine reductase FAD-binding	2.4
A1S_2132	putative outer membrane protein	3.7
A1S_2202	aspartate racemase	22.8
A1S_2284	hypothetical protein A1S_2284	4.2
A1S_2317	putative lipoprotein precursor (RlpA-like)	2.2
A1S_2432	lipoprotein precursor	2.5
A1S_2435	D-ala-D-ala-carboxypeptidase; penicillin-binding protein 5 (precursor)	2.7
A1S_2479	putative D-ala-D-ala-carboxypeptidase penicillin-binding protein	3.0
A1S_2503	putative outer membrane lipoprotein	3.9
A1S_2522	GTP-binding protein	3.0
A1S_2595	peptidoglycan-associated lipoprotein precursor	4.6
A1S_2609	putative lipid A biosynthesis lauroyl acyltransferase	4.8
A1S_2657	putative transglycosylase	2.4
A1S_2780	rod shape-determining protein	2.2
A1S_2834	mechanosensitive channel	5.1
A1S_2849	putative glucose-sensitive porin (OprB-like)	5.3
A1S_2866	hypothetical protein A1S_2866	3.9
A1S_2900	putative lipopolysaccharide core biosynthesis glycosyl transferase LpsC	3.1
A1S_2962	putative membrane-bound lytic murein transglycosylase	4.1

A1S_2987	putative lipoprotein precursor	3.8
A1S_2995	hypothetical protein A1S_2995	2.8
A1S_3027	putative lytic murein transglycosylase soluble	2.5
A1S_3094	putative nucleoside-diphosphate-sugar epimerase	2.6
A1S_3176	hypothetical protein A1S_3176	3.6
A1S_3196	putative penicillin binding protein (PonA)	4.0
A1S_3197	putative penicillin binding protein (PonA)	3.7
A1S_3201	phospho-N-acetylmuramoyl-pentapeptide transferase	3.7
A1S_3203	UDP-N-acetylmuramoylalanyl-D-glutamate-2 6-diaminopimelate ligase	3.1
A1S_3204	septum formation penicillin binding protein 3, peptidoglycan synthetase	3.4
A1S_3206	S-adenosylmethionine methyltransferase	3.5
A1S_3311	hypothetical protein A1S_3311	2.1
A1S_3329	EsvJ	5.1
A1S_3330	UDP-3-O-acyl-N-acetylglucosamine deacetylase	2.8
A1S_3333	cell division protein	4.9
A1S_3334	D-alanine-D-alanine ligase B	4.1
A1S_3335	UDP-N-acetylmuramate--alanine ligase	3.5
A1S_3336	UDP-N-acetylglucosamine:N-acetylmuramyl- (pentapeptide) pyrophosphoryl-undecaprenol N-acetylglucosamine transferase	5.5
A1S_3393	hypothetical protein A1S_3393	3.5
A1S_3394	hypothetical protein A1S_3394	4.2
A1S_3395	glucosamine-fructose-6-phosphate aminotransferase	3.3
A1S_3396	glucosamine-fructose-6-phosphate aminotransferase	3.7
	2-dehydro-3-deoxyphosphooctonate aldolase	4.5
	3-deoxy-manno-octulosonate cytidylyltransferase	3.3

Cell motility

A1S_0271	putative general secretion pathway protein	2.3
A1S_0370	general secretion pathway protein G	4.6
A1S_0500	type 4 fimbrial biogenesis protein	4.8
A1S_0616	secretion protein XcpR	2.5
A1S_1510	Fimbrial protein	2.3
A1S_1559	type 4 fimbrial biogenesis protein	3.7
A1S_2020	hypothetical protein A1S_2020	2.5

Coenzyme transport and metabolism

A1S_0036	3-demethylubiquinone-9 3-methyltransferase and 2-octaprenyl-6-hydroxy phenol methylase	2.8
A1S_0221	hypothetical protein A1S_0221	3.0
A1S_0262	porphobilinogen deaminase	2.4
A1S_0350	S-adenosylmethionine : 2-DMK methyltransferase and 2-octaprenyl-6-methoxy-14-benzoquinone methylase	4.5
A1S_0457	dihydrofolate reductase	2.7
A1S_0584	2-amino-4-hydroxy-6-hydroxymethyldihydropteridine pyrophosphokinase	2.6
A1S_0585	3-methyl-2-oxobutanoate hydroxymethyltransferase	4.3
A1S_0586	3-methyl-2-oxobutanoate hydroxymethyltransferase	5.0
A1S_0587	pantoate-beta-alanine ligase	3.9

A1S_0713	quinolinate synthetase A	3.1
A1S_0821	hypothetical protein A1S_0821	2.4
A1S_0825	aspartate 1-decarboxylase precursor	4.2
A1S_0837	glutamyl tRNA reductase	2.9
A1S_0845	phosphopantetheine adenylyltransferase	6.2
A1S_0858	putative glutamine-dependent NAD(+) synthetase (NAD(+) synthase	2.7
A1S_0906	delta-aminolevulinic acid dehydratase	6.3
A1S_1040	ubiH protein 2-octaprenyl-6-methoxyphynol hydroxylase, FAD/NAD(P)-binding	3.2
A1S_1041	putative FAD-dependent monooxygenase	2.7
A1S_1345	PaaK	3.6
A1S_1346	phenylacetyl-CoA ligase	3.1
A1S_1356	p-hydroxybenzoate hydroxylase transcriptional activator	6.0
A1S_1511	biotin synthase	4.0
A1S_1519	methionine adenosyltransferase	3.9
A1S_1566	putative 6-pyruvoyl-tetrahydropterin synthase	3.0
A1S_1619	S-adenosylmethionine2-demethylmenaquinone methyltransferase	5.0
A1S_1660	nicotinate-nucleotide-dimethylbenzimidazole phosphoribosyltransferase	2.8
A1S_1696	hypothetical protein A1S_1696	2.6
A1S_1996	hypothetical protein A1S_1996	3.0
A1S_1997	molybdopterin converting factor large subunit	4.6
A1S_2134	putative ubiquinone biosynthesis protein	2.8
A1S_2144	dihydroneopterin aldolase	3.3
A1S_2146	molybdopterin biosynthesis protein	2.6
A1S_2264	ThiF/ThiS complex component	3.7
A1S_2334	S-adenosyl-L-homocysteine hydrolase	5.7
A1S_2349	4-hydroxybenzoate octaprenyltransferase	2.4
A1S_2350	chorismate pyruvate lyase	2.3
A1S_2464	glutamate-1-semialdehyde aminotransferase	5.1
A1S_2465	putative thiamin-phosphate pyrophosphorylase	2.3
A1S_2516	pyridoxal phosphate biosynthetic protein	2.7
A1S_2674	hypothetical protein A1S_2674	2.7
A1S_2697	multifunctional protein	3.0
A1S_2725	multifunctional protein	5.6
A1S_2732	solanesyl diphosphate synthase	2.7
A1S_2760	geranyltranstransferase	2.4
A1S_2867	hypothetical protein A1S_2867	5.0
A1S_2868	hypothetical protein A1S_2868	3.4
A1S_2877	vitamin B12 receptor precursor	3.8
A1S_2999	4-hydroxythreonine-4-phosphate dehydrogenase	3.7
A1S_3106	1-deoxyxylulose-5-phosphate synthase	2.4
A1S_3107	GTP cyclohydrolase II	2.5
A1S_3108	coproporphyrinogen III oxidase	8.5
A1S_3319	pyridoxamine 5'-phosphate oxidase	4.6
A1S_3337	glutathione synthetase	2.4
A1S_3388	hypothetical protein A1S_3388	4.7
A1S_3389	67-dimethyl-8-ribityllumazine synthase	5.4
A1S_3391	thiamin-monophosphate kinase	2.3

	lipoate synthase	8.3
	riboflavin synthase alpha chain	5.7
DNA replication, recombination and repair		
A1S_0001	DNA replication initiator protein	2.8
A1S_0002	DNA polymerase III	3.1
A1S_0004	DNA gyrase	6.1
A1S_0016	site-specific tyrosine recombinase	2.2
A1S_0209	transposase	6.5
A1S_0210	transposase	4.9
A1S_0222	putative DNA modification methylase	4.5
A1S_0226	DNA polymerase III chi subunit	3.6
A1S_0319	hypothetical protein A1S_0319	2.7
A1S_0356	exonuclease V beta chain	3.5
A1S_0357	exonuclease V beta chain	2.4
A1S_0414	(di)nucleoside polyphosphate hydrolase (Ap5A pyrophosphatase)	4.3
A1S_0439	DNA topoisomerase type I omega protein	2.7
A1S_0539	putative DNA polymerase III delta subunit	2.4
A1S_0576	hypothetical protein A1S_0576	2.2
A1S_0603	integration host factor alpha subunit	6.5
A1S_0612	DNA polymerase I	3.0
A1S_0661	phage integrase family protein	6.2
A1S_0672	resolvase	3.1
A1S_0697	putative MutT/nudix family protein	2.8
A1S_0838	DNA primase	2.1
A1S_0839	DNA primase	3.4
A1S_1052	putative NADH pyrophosphatase	2.5
A1S_1054	hypothetical protein A1S_1054	2.5
A1S_1065	ribonuclease T	4.1
A1S_1189	putative N-6 Adenine-specific DNA methylase	2.6
A1S_1206	ATP-dependent helicase	2.3
A1S_1207	ATP-dependent helicase	2.5
A1S_1251	mismatch repair protein	3.1
A1S_1252	methyl-directed mismatch repair	2.1
A1S_1465	DNA polymerase III alpha chain	3.0
A1S_1558	DNA polymerase III delta prime subunit	2.1
A1S_1560	putative deoxyribonuclease	2.9
A1S_1567	uracil-DNA glycosylase	4.2
A1S_1573	integration host factor beta subunit	6.1
A1S_1623	transcription-repair coupling protein	2.6
A1S_1637	DNA-binding protein HU-beta	7.0
A1S_1685	recombination protein gap repair	3.7
A1S_1962	DNA strand exchange and recombination protein	5.9
A1S_2056	DNA polymerase III tau and gamma subunits (DNA elongation factor III)	2.9
A1S_2114	methyl-directed mismatch repair enzyme	2.9
A1S_2115	methyl-directed mismatch repair enzyme	3.5
A1S_2174	replicative DNA helicase;chromosome replication chain elongation	2.9

A1S_2175	replicative DNA helicase;chromosome replication chain elongation	3.9
A1S_2260	ATP-dependent RNA helicase (DEAD box)	3.2
A1S_2437	putative Nudix hydrolase	4.7
A1S_2504	excinuclease ABC subunit B	4.3
A1S_2551	Tn7-like transposition protein B	2.6
A1S_2587	holliday junction helicase subunit A	2.7
A1S_2603	putative chromosomal replication initiator DnaA-type	3.1
A1S_2626	DNA gyrase	5.1
A1S_2629	site-specific tyrosine recombinase	2.2
A1S_2830	DNA-3-methyladenine glycosylase	2.1
A1S_2831	formamidopyrimidine-DNA glycosylase	3.0
A1S_2908	putative integrase	2.4
A1S_2927	Phage integrase	2.5
A1S_3095	ATP-dependent DNA helicase	2.2
A1S_3287	RecBCD nuclease ssDNA-binding protein	5.0
A1S_3435	3-methyl-adenine DNA glycosylase I	2.9
	putative ATPase	2.1

Energy production and conversion

A1S_0005	putative Cytochrome b precursor	4.0
A1S_0140	NAD-linked malate dehydrogenase	5.1
A1S_0147	ATP synthase protein I	5.7
A1S_0148	membrane-bound ATP synthase F0 sector, subunit a	8.5
A1S_0150	membrane-bound ATP synthase F0 sector, subunit c	9.6
A1S_0151	membrane-bound ATP synthase F0 sector, subunit b	9.4
A1S_0152	membrane-bound ATP synthase F1 sector, delta-subunit	8.9
A1S_0156	membrane-bound ATP synthase F1 sector, epsilon-subunit	7.5
A1S_0200	inorganic pyrophosphatase	7.8
A1S_0257	hypothetical protein A1S_0257	2.3
A1S_0378	EsvG	4.2
A1S_0420	3-isopropylmalate dehydrogenase	4.3
A1S_0429	glutamate:aspartate symport protein (DAACS family)	2.3
A1S_0436	putative Zn-dependent oxidoreductase	3.0
A1S_0480	fumarate hydratase	7.5
A1S_0481	phosphate acetyltransferase	4.9
A1S_0482	acetate kinase (propionate kinase)	4.8
A1S_0558	aconitate hydratase 1	4.6
A1S_0752	NADH dehydrogenase I chain A	8.7
A1S_0753	NADH dehydrogenase I chain B	8.9
A1S_0755	NADH dehydrogenase I chain E	8.7
A1S_0756	NADH dehydrogenase I chain F	9.1
A1S_0757	NADH dehydrogenase I chain G	8.0
A1S_0758	NADH dehydrogenase I chain H	6.6
A1S_0759	NADH dehydrogenase I chain I 2Fe-2S ferredoxin-related	8.4
A1S_0760	NADH dehydrogenase I chain J	7.6
A1S_0761	NADH dehydrogenase I chain K	7.6
A1S_0762	NADH dehydrogenase I chain L	7.6
A1S_0763	NADH dehydrogenase I chain M membrane subunit	8.2
A1S_0764	NADH dehydrogenase I chain N	7.2

A1S_0995	rubredoxin	3.8
A1S_1008	isocitrate lyase	6.2
A1S_1181	putative oxidoreductase aldo/keto reductase family	3.9
A1S_1249	7-Fe ferredoxin	4.3
A1S_1335	phenylacetic acid degradation protein paaN	7.1
A1S_1340	phenylacetate-CoA oxygenase/reductase PaaK subunit	6.0
A1S_1368	pyruvate ferredoxin/flavodoxin oxidoreductase	3.0
A1S_1369	putative oxidoreductase protein	3.0
A1S_1370	oxidoreductase	3.0
A1S_1433	ubiquinol oxidase subunit II	2.1
A1S_1434	ubiquinol oxidase subunit I	2.3
A1S_1601	malate synthase G	6.5
A1S_1631	iron-binding protein	5.4
A1S_1924	cytochrome d terminal oxidase polypeptide subunit I	11.3
A1S_1925	cytochrome d terminal oxidase polypeptide subunit II	10.8
A1S_1986	fumarase C	3.9
A1S_2053	putative iron-containing alcohol dehydrogenase	2.6
A1S_2111	oxygen-insensitive NADPH nitroreductase	5.6
A1S_2126	aconitate hydratase 2	8.9
A1S_2127	aconitate hydratase 2	9.0
A1S_2128	aconitate hydratase 2	8.9
A1S_2166	cytochrome o ubiquinol oxidase subunit II	8.2
A1S_2167	cytochrome o ubiquinol oxidase subunit I	7.5
A1S_2168	cytochrome o ubiquinol oxidase subunit III	6.8
A1S_2169	cytochrome o ubiquinol oxidase subunit IV	8.2
A1S_2248	2-keto-D-gluconate reductase	4.4
A1S_2257	glycerol-3-phosphate dehydrogenase	2.3
A1S_2258	putative nitroreductase	2.7
A1S_2297	putative 4Fe-4S ferredoxin	3.7
A1S_2328	soluble pyridine nucleotide transhydrogenase	3.1
A1S_2338	hypothetical protein (MaeB)	6.7
A1S_2452	NAD-dependent aldehyde dehydrogenases	4.1
A1S_2459	putative oxidoreductase	8.8
A1S_2475	isocitrate dehydrogenase	5.8
A1S_2477	isocitrate dehydrogenase	7.9
A1S_2627	electron transfer flavoprotein alpha-subunit	5.0
A1S_2628	electron transfer flavoprotein beta-subunit	6.8
A1S_2640	putative oxidoreductase molybdopterin	4.4
A1S_2644	nitroreductase	7.1
A1S_2668	phosphoenolpyruvate carboxykinase	3.7
A1S_2702	putative alcohol dehydrogenase	3.2
A1S_2710	hypothetical protein A1S_2710	7.7
A1S_2711	succinate dehydrogenase cytochrome b556 subunit	9.5
A1S_2712	succinate dehydrogenase hydrophobic subunit	9.0
A1S_2713	succinate dehydrogenase flavoprotein subunit	9.4
A1S_2714	succinate dehydrogenase iron-sulfur subunit	7.9
A1S_2715	2-oxoglutarate decarboxylase component of the 2-oxoglutarate dehydrogenase complex (E1)	6.7
A1S_2716	dihydrolipoamide succinyltransferase component of 2-oxoglutarate dehydrogenase complex (E2)	7.2

A1S_2717	dihydrolipoamide dehydrogenase	6.8
A1S_2718	succinyl-CoA synthetase beta chain	7.8
A1S_2719	succinyl-CoA synthetase alpha chain	7.5
A1S_2766	Putative oxydoreductase protein zinc-containing	3.5
A1S_2828	putative FMN oxidoreductase	4.5
A1S_2952	putative pyridine nucleotide-disulfide oxidoreductase class I	2.7
A1S_3025	malate dehydrogenase	6.5
A1S_3085	putative flavohemoprotein	3.8
A1S_3130	succinylglutamic semialdehyde dehydrogenase	3.3
A1S_3151	putative FAD/FMN-containing dehydrogenase	4.8
A1S_3231	putative acetyl-CoA hydrolase/transferase	9.7
A1S_3280	NADP+-dependent succinate semialdehyde dehydrogenase	2.5
A1S_3293	Putative NADPH:quinone reductase and related Zn-dependent oxidoreductase	2.9
A1S_3327	dihydrolipoamide S-acetyltransferase E2 component of the pyruvate dehydrogenase complex	4.6
A1S_3328	pyruvate decarboxylase E1 component of the pyruvate dehydrogenase complex	5.0
A1S_3449	phosphoenolpyruvate carboxylase	4.1
	membrane-bound ATP synthase F1 sector, beta-subunit	9.9
	membrane-bound ATP synthase F1 sector, alpha-subunit	9.6
	membrane-bound ATP synthase F1 sector, gamma-subunit	8.8
	NADH dehydrogenase I chain CD	8.7
	aconitate hydratase 1	5.8
	FAD dependent oxidoreductase	2.5

Inorganic ion transport and metabolism

A1S_0141	putative dyp-type peroxidase	3.9
A1S_0145	transcriptional repressor of Zn transport system (Fur family)	5.6
A1S_0170	putative outer membrane copper receptor (OprC)	5.1
A1S_0412	catalase	9.8
A1S_0530	hypothetical protein A1S_0530	5.7
A1S_0800	bacterioferritin	2.5
A1S_0891	hemerythrin-like metal-binding protein	4.6
A1S_0984	putative carbonic anhydrase	3.8
A1S_0990	polyphosphate kinase	3.0
A1S_1001	ATP-sulfurylase subunit 1	6.8
A1S_1386	catalase	3.0
A1S_1615	PAPS (adenosine 3'-phosphate 5'-phosphosulfate)	3.0
A1S_1860	ring hydroxylating dioxygenase Rieske (2Fe-2S) protein	5.5
A1S_1988	putative intracellular sulfur oxidation protein (DsrE-like)	3.1
A1S_2343	superoxide dismutase	8.3
A1S_2829	putative tonB-dependent receptor protein	2.4
A1S_2924	putative Rhodanese-related sulfurtransferase	5.9
A1S_2935	copper resistance protein B precursor	2.6
A1S_3175	bacterioferritin	3.5
A1S_3379	thiosulfate sulfurtransferase	3.2

Intracellular trafficking, secretion, and vesicular transport

A1S_0528	protein exporting molecular chaperone	4.1

A1S_1565	general secretion pathway protein K	2.5
A1S_1930	cell division protein	2.8
A1S_2521	leader peptidase	3.5
A1S_2591	tolerance to group A colicins single-stranded DNA filamentous phage	2.2
A1S_2594	tolerance to colicins E2 E, A, and K	4.2
A1S_2913	putative preprotein translocase IISP family membrane subunit	4.7
A1S_2915	preprotein translocase IISP family, membrane subunit	3.2
A1S_2916	preprotein translocase IISP family, membrane subunit	3.1
A1S_2980	hypothetical protein A1S_2980	3.6
A1S_2981	Inner membrane protein (IMP) integration factor	4.3
	secretion protein	8.4
	preprotein translocase IISP family membrane subunit	5.6
	preprotein translocase IISP family auxillary membrane component	4.1
	preprotein translocase secretion protein of IISP family	3.8
	preprotein translocase IISP family, part of the channel	3.2

Lipid transport and metabolism

A1S_0034	putative oxoacyl-(acyl carrier protein) reductase	2.2
A1S_0087	Short-chain dehydrogenase/reductase SDR	3.6
A1S_0305	3-ketoacyl-CoA thiolase	4.7
A1S_0312	CDP-diacylglycerol--glycerol-3-phosphate 3-phosphatidyltransferase	3.2
A1S_0496	putative phosphatidylglycerophosphatase B	4.4
A1S_0502	1-hydroxy-2-methyl-2-(E)-butenyl 4-diphosphate synthase	5.5
A1S_0508	putative acyltransferase	3.0
A1S_0509	putative acyl carrier protein	4.1
A1S_0534	NADH-dependent enoyl-ACP reductase	2.7
A1S_0608	acetyl-coenzyme A carboxylase carboxyl transferase (alpha subunit)	5.2
A1S_0817	hypothetical protein A1S_0817	3.0
A1S_0818	hypothetical protein A1S_0818	4.4
A1S_0819	acyl carrier protein (ACP)	4.6
A1S_0863	beta-ketoacyl-ACP synthase I	4.6
A1S_0864	beta-ketoacyl-ACP synthase I	5.2
A1S_0883	putative phospholipid/glycerol acyltransferase	3.2
A1S_0933	putative acyl-CoA thioester hydrolase	2.4
A1S_1208	hypothetical protein A1S_1208	3.4
A1S_1261	putative 3-hydroxyacyl-CoA dehydrogenase	2.1
A1S_1341	enoyl-CoA hydratase/carnithine racemase	4.9
A1S_1342	putative enoyl-CoA hydratase II	5.3
A1S_1343	PaaC	5.7
A1S_1344	thiolase	4.2
A1S_1534	putative dehydratase	2.4
A1S_1568	putative enoyl-CoA hydratase/isomerase	4.2
A1S_1704	acetoin dehydrogenase	2.1
A1S_1729	putative acetyl-CoA acetyltransferase	3.4
A1S_1737	3-hydroxybutyrate dehydrogenase	5.0
A1S_1847	3-oxoadipate CoA-transferase subunit B	9.6
A1S_1848	beta-ketoadipyl CoA thiolase	10.9

A1S_1870	putative oxidoreductase (short chain dehydrogenase)	2.2
A1S_1891	beta-ketoadipyl CoA thiolase	9.5
A1S_1966	hypothetical protein A1S_1966	5.3
A1S_1972	phosphatidate cytidylyltransferase	3.8
A1S_1973	undecaprenyl pyrophosphate synthetase	4.0
A1S_1982	2C-methyl-D-erythritol 24-cyclodiphosphate synthase	2.6
A1S_2010	biotin carboxyl carrier protein of acetyl-CoA carboxylase (BCCP)	5.4
A1S_2011	biotin carboxylase (A subunit of acetyl-CoA carboxylase)	5.6
A1S_2047	putative lysophospholipase	2.7
A1S_2060	putative dehydratase	5.8
A1S_2061	putative short-chain dehydrogenase	5.6
A1S_2062	putative acyl-CoA thiolase	4.3
A1S_2099	hypothetical protein A1S_2099	3.1
A1S_2458	putative fatty acid desaturase	9.3
A1S_2548	putative enoyl-CoA hydratase/isomerase	2.7
A1S_2667	hypothetical protein A1S_2667	2.4
A1S_2734	putative phosphatidylglycerophosphatase B	3.5
A1S_2740	putative oxidoreductase/dehydrogenase	3.3
A1S_2842	putative acetyl-CoA acetyltransferase	2.3
A1S_2869	acetylCoA carboxylase beta subunit	6.3
A1S_2881	putative fatty acid desaturase	5.7
A1S_2886	acyl-CoA dehydrogenase	4.3
A1S_2887	acyl-CoA dehydrogenase A	3.1
A1S_2947	hypothetical protein A1S_2947	4.2
A1S_2990	putative acyltransferase	2.2
A1S_3017	phosphatidylserine synthase	2.2
A1S_3090	acyl-CoA thioesterase II	4.2
A1S_3091	glycerol-3-phosphate acyltransferase	4.1
A1S_3111	putative acyl-CoA dehydrogenase	3.1
A1S_3169	4-hydroxy-3-methylbut-2-enyl diphosphate reductase	4.3
A1S_3224	acyl coenzyme A reductase	3.0
A1S_3309	acetyl-CoA synthetase	3.1
A1S_3344	esterase	2.6
A1S_3378	phosphatidylserine decarboxylase	2.3
A1S_3392	phosphatidylglycerophosphatase A	2.4
	1-deoxy-d-xylulose 5-phosphate reductoisomerase	4.2

Nucleotide transport and metabolism

A1S_0130	GMP synthetase	3.9
A1S_0458	thymidylate synthase	4.0
A1S_0468	hypothetical protein A1S_0468	2.4
A1S_0498	nucleoside diphosphate kinase	5.7
A1S_0607	exopolyphosphatase	3.5
A1S_0696	putative MutT/nudix family protein	2.8
A1S_0746	ribonucleoside-diphosphate reductase beta subunit	7.8
A1S_0747	ribonucleoside diphosphate reductase alpha subunit	6.2
A1S_0765	uracil phosphoribosyltransferase	3.2
A1S_0784	deoxycytidine triphosphate deaminase	2.6
A1S_0829	ribose-phosphate pyrophosphokinase	5.0

A1S_1023	adenylate kinase	4.4
A1S_1066	dihydroorotase	4.9
A1S_1179	adenylosuccinate synthetase	4.5
A1S_1191	aspartate carbamoyltransferase non-catalytic chain	2.9
A1S_1475	phosphoribosylglycinamide formyltransferase 2	4.2
A1S_1571	cytidylate kinase	3.7
A1S_1575	orotidine-5'-phosphate decarboxylase	2.1
A1S_1624	hypothetical protein A1S_1624	6.0
A1S_1678	putative histidine triad family protein	4.1
A1S_1890	3-carboxy-ciscis-muconate cycloisomerase	5.5
A1S_1900	CTP synthase	6.6
A1S_1975	uridylate kinase	6.2
A1S_2187	hypothetical protein A1S_2187	4.9
A1S_2188	hypothetical protein A1S_2188	4.2
A1S_2189	phosphoribosylamine--glycine ligase	2.9
A1S_2211	ADP-ribose pyrophosphatase	2.1
A1S_2251	amidophosphoribosyltransferase	3.5
A1S_2253	dihydroorotate oxydase	5.2
A1S_2441	adenylosuccinate lyase	2.8
A1S_2585	phosphoribosylformylglycinamidine synthase	5.5
A1S_2605	phosphoribosylaminoimidazole synthetase	3.9
A1S_2963	phosphoribosylaminoimidazole carboxylase ATPase subunit	4.5
A1S_2964	phosphoribosylaminoimidazole carboxylase mutase subunit	5.8
A1S_2973	guanine deaminase	2.1
A1S_3035	xanthine phosphoribosyltransferase	2.8
A1S_3170	guanylate kinase	3.4
A1S_3321	IMP dehydrogenase	7.2
A1S_3425	phosphoribosylaminoimidazole-succinocarboxamide synthase	4.7
A1S_3431	putative histidine triad family protein	3.0
	aspartate carbamoyltransferase catalytic subunit	3.2

Posttranslational modification, protein turnover, chaperones

A1S_0013	hypothetical protein A1S_0013	2.6
A1S_0018	FKBP-type peptidyl-prolyl cis-trans isomerase	3.6
A1S_0037	alkali-inducible disulfide interchange protein	3.5
A1S_0047	FKBP-type 22KD peptidyl-prolyl cis-trans isomerase (rotamase)	3.9
A1S_0048	FKBP-type peptidyl-prolyl cis-trans isomerase (rotamase)	3.8
A1S_0135	hypothetical protein A1S_0135	2.7
A1S_0136	glutathione S-transferase	2.2
A1S_0159	glutathione peroxidase	5.9
A1S_0308	beta-hydroxylase	3.5
A1S_0364	curved DNA-binding protein	3.4
A1S_0366	heat shock protein Hsp33	3.8
A1S_0408	putative glutathione S-transferase	2.1
A1S_0455	peptide methionine sulfoxide reductase	4.7
A1S_0475	trigger factor septum formation molecular chaperone	3.6
A1S_0476	ATP-dependent Clp protease proteolytic subunit	4.0
A1S_0477	ATP-dependent Clp protease ATP-binding subunit	3.4
A1S_0529	glutaredoxin	5.4

A1S_0594	putative glutathione S-transferase	2.5
A1S_0606	hypothetical protein A1S_0606	7.1
A1S_0844	ssrA-binding protein (Small protein B)	2.7
A1S_0873	putative arginine-tRNA-protein transferase	2.5
A1S_0875	thioredoxin reductase	3.5
A1S_0937	peptidyl-prolyl cis-trans isomerase	2.1
A1S_1016	urease accessory protein	3.3
A1S_1017	urease accessory protein	4.1
A1S_1018	urease accessory protein	2.5
A1S_1030	DNA-binding ATP-dependent protease La	2.9
A1S_1031	DNA-binding ATP-dependent protease La	2.7
A1S_1180	putative Zn-dependent protease with chaperone function	4.6
A1S_1183	hypothetical protein A1S_1183	3.4
A1S_1186	ATP-dependent protease Hsp 100	5.0
A1S_1195	putative glutathione S-transferase	2.7
A1S_1199	putative glutathionine S-transferase	2.7
A1S_1205	alkyl hydroperoxide reductase C22 subunit	8.7
A1S_1411	putative glutathione S-transferase protein	4.9
A1S_1412	glutathione S-transferase-like protein	3.6
A1S_1469	peptide methionine sulfoxide reductase	5.7
A1S_1470	glutathione peroxidase	6.9
A1S_1474	uridylyltransferase	4.4
A1S_1489	putative glutathione S-transferase	3.1
A1S_1522	predicted redox disulfide bond formation protein OsmC-like protein	2.4
A1S_1545	peptidyl-prolyl cis-trans isomerase	3.0
A1S_1620	hypothetical protein A1S_1620	2.4
A1S_1628	heat shock protein	4.1
A1S_1629	co-chaperone protein (Hsc20)	6.5
A1S_1638	peptidyl-prolyl cis-trans isomerase precursor	4.2
A1S_1639	peptidyl-prolyl cis-trans isomerase precursor	3.2
A1S_1910	ATP-binding protease component	3.4
A1S_1937	putative glutaredoxin-related protein	4.6
A1S_2109	peptidyl-prolyl cis-trans isomerase precursor	2.2
A1S_2170	protoheme IX farnesyltransferase	7.1
A1S_2177	putative proteasome protease	2.5
A1S_2244	putative O-sialoglycoprotein endopeptidase gcp	2.9
A1S_2250	hypothetical protein A1S_2250	3.3
A1S_2296	putative protease	6.0
A1S_2340	HtrA-like serine protease	4.6
A1S_2429	putative ATP-dependent protease	2.9
A1S_2430	putative ATP-dependent protease	2.6
A1S_2444	putative protease (SohB)	2.2
A1S_2481	FKBP-type peptidyl-prolyl cis-trans isomerase	3.4
A1S_2510	chaperone protein	4.6
A1S_2525	putative serine protease	2.8
A1S_2540	putative organic radical activating enzyme	3.7
A1S_2545	bacterioferritin comigratory protein	4.0
A1S_2608	putative protease; putative signal peptide peptidase sppA	2.4
A1S_2634	DNA repair protein	3.5

A1S_2658	heat shock protein	5.1
A1S_2664	chaperone Hsp60	6.5
A1S_2665	chaperone Hsp10	5.6
A1S_2681	cell division protein	5.7
A1S_2758	putative membrane protease subunit	3.5
A1S_2825	putative thiol:disulphide interchange protein (DsbC-like)	2.0
A1S_2880	putative signal peptide	3.4
A1S_2948	thioredoxin C-3	5.4
A1S_2949	hypothetical protein A1S_2949	4.7
A1S_2959	Hsp 24 nucleotide exchange factor	3.7
A1S_2960	chaperone Hsp70	6.2
A1S_3126	peptidase S8 and S53 subtilisin, kexin, sedolisin	3.5
A1S_3347	thiol:disulfide interchange protein precursor	2.6
A1S_3365	disulfide bond formation protein	2.5
A1S_3443	heat shock protein Hsp40	3.3
A1S_3460	putative glutathione S-transferase	2.2
	putative organic radical activating enzyme	4.5
	urease accessory protein	2.9

Regulation		
A1S_0025	putative transcriptional repressor	3.8
A1S_0038	putative transcriptional regulator	2.7
A1S_0072	putative transcriptional regulator (GntR family)	2.0
A1S_0218	nitrogen assimilation regulatory protein P-II 2	6.3
A1S_0220	putative transcriptional regulator	3.9
A1S_0248	DnaK suppressor protein	5.5
A1S_0316	putative transcriptional regulator	2.2
A1S_0320	hypothetical protein A1S_0320	3.4
A1S_0410	hca cluster transcriptional activator (LysR family)	2.4
A1S_0422	putative transcriptional regulator (AraC family)	3.8
A1S_0450	putative transcriptional regulator (TetR-family)	2.5
A1S_0548	putative transcriptional regulator (TetR family)	3.5
A1S_0574	GacS-like sensor kinase protein	2.3
A1S_0618	hypothetical protein A1S_0618	3.0
A1S_0654	regulatory protein ArsR	6.6
A1S_0684	putative toluene tolerance protein Ttg2F	5.1
A1S_0768	putative transcriptional regulator (LysR family)	3.0
A1S_0811	hypothetical protein A1S_0811	4.3
A1S_0944	putative transcriptional regulator (PcaU-like)	2.6
A1S_0992	transcriptional regulator (LysR family)	5.6
A1S_1006	putative transcriptional regulator	3.5
A1S_1007	putative transcriptional regulator	5.7
A1S_1090	putative transcription regulator (AsnC family)	2.8
A1S_1113	putative transcriptional regulator	2.2
A1S_1141	carbon storage regulator	7.1
A1S_1182	cyclic AMP receptor protein	6.2
A1S_1218	heavy metal regulator HmrR	3.1
A1S_1347	PaaX	2.8
A1S_1377	transcriptional regulator acrR family	2.3

A1S_1533	putative transcriptional regulator (AraC family)	3.1
A1S_1540	putative transcriptional regulator (TetR family)	2.2
A1S_1552	chromosome partitioning protein	4.3
A1S_1561	putative transcriptional regulator	3.7
A1S_1578	putative transcriptional regulator	2.8
A1S_1634	iscRSUA operon repressor	5.1
A1S_1713	putative transcriptional regulator (AraC family)	2.8
A1S_1728	putative transcriptional regulator DNA-binding transcriptional regulator (LysR family)	2.1
A1S_1842	Cat operon transcriptional regulator (LysR family)	2.4
A1S_1906	hypothetical protein A1S_1906	3.8
A1S_1939	putative transcriptional regulator	2.4
A1S_1977	two-component regulatory system sensory kinase	2.2
A1S_1978	response regulator protein	3.3
A1S_1979	putative transcriptional regulator	3.4
A1S_1994	hypothetical protein A1S_1994	3.2
A1S_2181	transcriptional factor	3.0
A1S_2223	transcriptional regulator AraC family	23.1
A1S_2320	transcriptional regulator AraC family	8.3
A1S_2431	putative transcriptional regulator	4.0
A1S_2699	putative transcriptional regulator	2.1
A1S_2814	twitching motility protein	3.0
A1S_2815	twitching motility protein	2.3
A1S_2851	putative transcriptional regulator (AraC family)	5.1
A1S_2884	two component signal transduction system kinase sensor component	2.4
A1S_2906	putative sensory transduction histidine kinase	4.9
A1S_3230	sensory histidine kinase (OmpR)	4.4
A1S_3294	putative transcriptional regulator (TetR/AcrR family)	2.6
A1S_3315	putative transcriptional regulator (ArsR family)	4.3
A1S_3341	catabolite repression control protein	2.4
A1S_3376	two-component sensor	3.3
A1S_3417	regulatory proteins IclR	2.5

Resistance/Defense mechanisms

A1S_0774	putative RND family drug transporter	2.1
A1S_1535	putative transport protein	3.3
A1S_1555	lipid transport protein flippase	3.1
A1S_2059	putative esterase	2.9
	beta-lactamase SHV-1b gene	15.5

Secondary metabolites biosynthesis, transport and catabolism

A1S_0470	methionine biosynthesis protein	6.9
A1S_1073	hemolysin-type calcium-binding region	2.6
A1S_1337	phenylacetic acid degradation B	7.5
A1S_1884	protocatechuate 34-dioxygenase alpha chain (3,4-PCD)	11.8
A1S_1885	protocatechuate 34-dioxygenase beta chain (3,4-PCD)	10.8
A1S_2406	hypothetical protein A1S_2406	3.2
A1S_2936	copper resistance protein A precursor	3.1
A1S_3198	23S ribosomal RNA G745 methyltransferase	2.4

A1S_3278	hydrolase isochorismatase family	2.9
A1S_3430	putative dienelactone hydrolase	3.1

Transcription

A1S_0282	transcription antitermination protein	6.8
A1S_0288	DNA-directed RNA polymerase beta' chain	5.6
A1S_0335	transcription termination/antitermination L factor	3.1
A1S_0766	putative cold shock protein	2.6
A1S_1144	merops peptidase family S24	2.2
A1S_1318	GCN5-related N-acetyltransferase	4.0
A1S_1389	DNA polymerase V component	2.8
A1S_1582	transcriptional regulator Cro/CI family	3.3
A1S_2037	EsvI	2.1
A1S_2119	putative acetyltransferase	2.1
A1S_2186	DNA-binding protein	4.8
A1S_2199	GCN5-related N-acetyltransferase	2.3
A1S_2261	putative cold shock protein	3.3
A1S_2262	EsvH	2.9
A1S_2462	RNA helicase	2.4
A1S_2519	ribonuclease III	2.4
A1S_2598	putative RNA polymerase sigma factor	5.5
A1S_2688	transcription elongation factor	3.2
A1S_2706	sigma D (sigma 70) factor of RNA polymerase major sigma factor during exponential growth	5.5
A1S_3045	exoribonuclease R	3.3
A1S_3056	RNA polymerase alpha subunit	7.3
A1S_3113	hypothetical protein A1S_3113	4.1
A1S_3171	RNA polymerase omega subunit	7.5
A1S_3227	putative RNA binding protein	2.4
A1S_3228	putative RNA binding protein	2.6
A1S_3390	transcription termination L factor	4.7

Signal transduction mechanisms

A1S_0050	putative protein tyrosine phosphatase	2.3
A1S_0122	putative morphogenic pathway activator (BolA)	4.2
A1S_0214	universal stress protein	2.3
A1S_0236	response regulator	5.3
A1S_0272	hypothetical protein A1S_0272	4.1
A1S_0413	phosphoenolpyruvate-protein phosphotransferase	3.9
A1S_0579	GTP pyrophosphokinase	5.7
A1S_0620	putative anti-anti-sigma factor	6.0
A1S_0621	putative two-component response regulator	2.9
A1S_0671	protein tyrosine phosphatase	13.8
A1S_1246	putative universal stress protein	3.3
A1S_1419	anti-sigma factor ChrR	2.1
A1S_1625	putative adenylate or guanylate cyclase	4.6
A1S_1626	putative adenylate or guanylate cyclase	2.9
A1S_1949	putative diguanylate cyclase/phosphodiesterase	2.6
A1S_1950	putative universal stress protein	4.6
A1S_2051	putative phosphotyrosine protein phosphatase	3.0

A1S_2072	putative universal stress protein family	8.2
A1S_2417	starvation-induced peptide utilization protein	4.0
A1S_2418	starvation-induced peptide utilization protein	4.6
A1S_2692	putative universal stress protein A (UspA)	4.6
A1S_2751	transcriptional regulator	3.2
A1S_2835	GTP-binding elongation factor family protein	4.2
A1S_2883	transcriptional regulator protein (OmpR family)	3.0
A1S_2997	bis(5'-nucleosyl)-tetraphosphatase symmetrical	3.7
A1S_3030	phosphate starvation-inducible protein (PhoH-like)	3.9
A1S_3172	hypothetical protein (SpoT)	2.8
A1S_3229	two-component response regulator	5.6
A1S_3304	putative two-component response regulator	2.8
A1S_3374	positive pho regulon response regulator	6.7
A1S_3375	positive pho regulon response regulator	5.1

Translation, ribosomal structure and biogenesis

A1S_0014	tyrosyl-tRNA synthetase	2.4
A1S_0020	isoleucyl-tRNA synthetase	4.4
A1S_0042	ribonuclease PH	2.3
A1S_0097	hypothetical protein A1S_0097	4.9
A1S_0165	putative Sua5/YciO/YrdC/YwlC family protein	2.5
A1S_0168	Zinc(II) binding peptide deformylase 1	8.2
A1S_0185	hypothetical protein A1S_0185	3.1
A1S_0247	putative glutamyl t-RNA synthetase	2.5
A1S_0283	50S ribosomal protein	10.2
A1S_0284	50S ribosomal protein	9.3
A1S_0285	50S ribosomal protein	10.2
A1S_0286	50S ribosomal protein	9.8
A1S_0338	ribosome-binding factor A	3.7
A1S_0360	30S ribosomal protein S15	7.6
A1S_0361	polyribonucleotide nucleotidyltransferase	5.4
A1S_0403	ribonuclease E	5.1
A1S_0421	protein chain initiation factor IF-1	7.1
A1S_0447	50S ribosomal protein L33	7.0
A1S_0448	50S ribosomal protein L28	8.9
A1S_0503	histidyl-tRNA synthetase	5.7
A1S_0541	leucyl-tRNA synthetase	4.3
A1S_0542	leucyl-tRNA synthetase	3.0
A1S_0554	peptide chain release factor 3	2.8
A1S_0583	poly(A) polymerase I (PAP)	4.0
A1S_0592	threonyl-tRNA synthetase	5.1
A1S_0593	protein chain initiation factor IF-3	6.3
A1S_0597	50S ribosomal protein L20	9.6
A1S_0601	phenylalanyl-tRNA synthetase alpha-subunit	3.6
A1S_0602	phenylalanyl-tRNA synthetase beta subunit	4.1
A1S_0810	putative ribosomal large subunit pseudouridine synthase B	5.9
A1S_0813	hypothetical protein A1S_0813	2.9
A1S_0816	50S ribosomal protein L32	6.8
A1S_0826	peptidyl-tRNA hydrolase	3.0

A1S_0827	peptidyl-tRNA hydrolase	4.1
A1S_0828	50S ribosomal protein L25	4.7
A1S_0841	ribosomal large subunit pseudouridine synthase D	4.1
A1S_0868	protein chain elongation factor EF-G GTP-binding	8.8
A1S_0998	lysyl-tRNA-synthase	4.3
A1S_1176	alanyl-tRNA synthetase	2.6
A1S_1235	cysteinyl-tRNA synthetase	2.4
A1S_1464	putative tRNA/rRNA methyltransferase	2.9
A1S_1481	putative GTP-binding protein	2.5
A1S_1572	30S ribosomal protein S1	6.3
A1S_1617	30S ribosomal protein S20	4.5
A1S_1693	putative adenine-specific methylase	2.4
A1S_1940	methionine aminopeptidase	5.7
A1S_1961	heat shock protein 15	3.9
A1S_1974	ribosome releasing factor	5.8
A1S_1976	hypothetical protein A1S_1976	4.2
A1S_2108	glutaminyl-tRNA synthetase	5.0
A1S_2113	delta(2)-isopentenylpyrophosphate tRNA-adenosine transferase	3.8
A1S_2171	30S ribosomal protein S6	9.0
A1S_2172	30S ribosomal protein S18	9.8
A1S_2173	50S ribosomal protein L9	9.2
A1S_2245	30S ribosomal protein S21	7.4
A1S_2322	protein chain elongation factor	7.1
A1S_2323	30S ribosomal protein S2	9.1
A1S_2324	methionine aminopeptidase	4.3
A1S_2419	elongation factor P	5.3
A1S_2423	50S ribosomal protein L31	7.1
A1S_2439	tRNA (5-methylaminomethyl-2-thiouridylate)-methyltransferase	3.4
A1S_2476	putative pseudouridine synthase	3.8
A1S_2570	putative siderophore biosynthesis protein; putative acetyltransferase	2.4
A1S_2597	putative tRNA/rRNA methyltransferase	2.0
A1S_2636	putative lysyl-tRNA synthetase	3.5
A1S_2682	cell division protein	6.4
A1S_2683	hypothetical protein A1S_2683	3.5
A1S_2698	putative tRNA/rRNA methyltransferase	2.2
A1S_2720	tryptophanyl-tRNA synthetase	3.6
A1S_2726	seryl-tRNA synthetase	4.8
A1S_2727	seryl-tRNA synthetase	3.9
A1S_2730	50S ribosomal protein L27	3.6
A1S_2731	50S ribosomal protein L21	7.7
A1S_2742	valyl-tRNA synthetase	5.1
A1S_2743	valyl-tRNA synthetase	3.0
A1S_2777	ribonuclease G endoribonuclease G	2.9
A1S_2782	aspartyl/glutamyl-tRNA(Asn/Gln) amidotransferase subunit C	4.1
A1S_2783	aspartyl/glutamyl-tRNA(Asn/Gln) amidotransferase subunit A	6.2
A1S_2784	aspartyl/glutamyl-tRNA(Asn/Gln) amidotransferase subunit B	4.8
A1S_2819	prolyl-tRNA synthetase	3.2
A1S_2894	aspartyl-tRNA synthetase	4.3
A1S_2983	RNase P	3.1

A1S_2984	50S ribosomal protein L34	5.0
A1S_2998	S-adenosylmethionine-6-N'N'-adenosyl	4.2
A1S_3000	50S ribosomal protein L13	9.1
A1S_3001	30S ribosomal protein S9	6.6
A1S_3028	putative tRNA-i(6)A37 modification enzyme	4.0
A1S_3029	putative tRNA-i(6)A37 modification enzyme	3.4
A1S_3055	50S ribosomal protein L17	6.6
A1S_3057	30S ribosomal protein S4	7.4
A1S_3058	30S ribosomal protein S11	7.8
A1S_3059	30S ribosomal protein S13	7.6
A1S_3060	50S ribosomal protein L36	9.0
A1S_3062	50S ribosomal protein L15	7.7
A1S_3063	50S ribosomal protein L30	8.1
A1S_3064	30S ribosomal protein S5	7.9
A1S_3065	50S ribosomal protein L18	7.5
A1S_3066	50S ribosomal protein L6	7.7
A1S_3067	30S ribosomal protein S8	8.9
A1S_3068	30S ribosomal protein S14	8.4
A1S_3069	50S ribosomal protein L5	8.1
A1S_3070	50S ribosomal protein L24	8.2
A1S_3071	50S ribosomal protein L14	7.3
A1S_3072	30S ribosomal protein S17	9.0
A1S_3073	50S ribosomal protein L29	10.2
A1S_3074	50S ribosomal protein L16	8.9
A1S_3075	30S ribosomal protein S3	8.5
A1S_3076	50S ribosomal protein L22	8.7
A1S_3077	50S ribosomal protein L2	9.0
A1S_3078	50S ribosomal protein L23	8.5
A1S_3079	50S ribosomal protein L4	8.2
A1S_3080	50S ribosomal protein L3	8.8
A1S_3081	30S ribosomal protein S10	9.7
A1S_3118	glycyl-tRNA synthetase alpha chain	3.0
A1S_3119	glycyl-tRNA synthetase beta chain	2.6
A1S_3161	50S ribosomal protein L19	6.0
A1S_3162	tRNA (guanine-1-)-methyltransferase	3.9
A1S_3163	16S rRNA processing protein	6.2
A1S_3164	30S ribosomal protein S16	7.4
A1S_3173	hypothetical protein A1S_3173	4.9
A1S_3209	glutamyl-tRNA synthetase	3.2
A1S_3210	glutamyl-tRNA synthetase	3.6
	30S ribosomal protein S12	8.9
	30S ribosomal protein S7	8.9
	protein chain elongation factor	8.8
	tRNA nucleotidyl transferase	3.0

Transporters

A1S_0144	high affinity Zn transport protein	4.6
A1S_0228	hypothetical protein A1S_0228	3.5
A1S_0229	hypothetical protein A1S_0229	2.6

A1S_0243	putative ferrous iron transport protein B	2.2
A1S_0339	pH adaptation potassium efflux system protein G	3.6
A1S_0340	pH adaptation potassium efflux system E transmembrane protein	4.9
A1S_0341	pH adaptation potassium efflux system D transmembrane protein	5.6
A1S_0342	pH adaptation potassium efflux system C transmembrane protein	6.6
A1S_0343	pH adaptation potassium efflux system transmembrane protein	5.3
A1S_0367	glutathione-regulated potassium-efflux system protein (K(+)/H(+) antiporter)	2.0
A1S_0375	magnesium and cobalt efflux protein	3.2
A1S_0446	putative transport protein (CPA2 family)	2.5
A1S_0453	putative biopolymer transport protein (ExbB)	4.5
A1S_0454	putative biopolymer transport protein (ExbD)	5.7
A1S_0485	high-affinity gluconate permease (GntP family)	2.8
A1S_0669	bile acid:sodium symporter	8.3
A1S_0709	putative cation efflux system protein	3.4
A1S_0777	putative threonine efflux protein (RhtC)	2.7
A1S_0783	hypothetical protein A1S_0783	2.8
A1S_0790	hypothetical protein A1S_0790	3.2
A1S_0877	threonine efflux protein	2.4
A1S_0930	high-affinity choline transporter (BCCT family)	2.6
A1S_0931	high-affinity choline transporter (BCCT family)	2.3
A1S_0972	phosphate transporter	3.0
A1S_0979	putative membrane-bound protein in GNT I transport system (GntY)	2.5
A1S_1004	citrate transporter	3.5
A1S_1080	putative lipoprotein	4.1
A1S_1135	putative transporter	3.3
A1S_1136	putative transporter	3.7
A1S_1239	putative transport protein	4.2
A1S_1240	putative transport protein	4.3
A1S_1271	putative chloride transport protein	2.2
A1S_1490	glutamate/aspartate transport protein	2.8
A1S_1505	yyaM	15.8
A1S_1554	putative biopolymer transport protein ExbD/TolR	2.4
A1S_1716	chromate transporter	2.2
A1S_1736	hypothetical protein A1S_1736	3.2
A1S_1917	putative potassium uptake protein	2.2
A1S_2133	hypothetical protein A1S_2133	2.1
A1S_2190	putative lipoprotein	4.8
A1S_2191	putative lipoprotein	3.5
A1S_2192	D-and L-methionine transport protein	3.5
A1S_2193	putative permease protein	3.0
A1S_2196	membrane-associated dicarboxylate transport protein	3.4
A1S_2221	sodium/glutamate symport carrier protein	2.5
A1S_2224	threonine efflux protein	12.8
A1S_2280	aerobic C4-dicarboxylate transport protein	3.2
A1S_2427	putative transporter	2.1
A1S_2445	high-affinity phosphate transport protein	3.4
A1S_2584	MFS family drug transporter	2.3
A1S_2612	transport protein of outer membrane lipoproteins	2.1

A1S_2613	transport protein of outer membrane lipoproteins	2.3
A1S_2633	D-alanine/D-serine/glycine transport protein (APC family)	4.0
A1S_2671	MFS permease	3.1
A1S_2723	putative Na+/H+ antiporter	2.3
A1S_2762	aromatic amino acid transporter (APC family)	4.0
A1S_2763	aromatic amino acid transporter (APC family)	3.4
A1S_2773	putative long-chain fatty acid transport protein	4.0
A1S_2860	putative transport protein (MFS superfamily)	2.2
A1S_2939	ATPase E1-E2 type: Heavy metal translocating P-type ATPase	2.9
A1S_3100	putative toluene tolerance protein (Ttg2D)	5.1
A1S_3101	toluene tolerance efflux transporter	5.3
A1S_3102	toluene tolerance efflux transporter	4.3
A1S_3103	toluene tolerance efflux transporter	3.4
A1S_3214	cation efflux system protein	2.9
A1S_3221	putative transport protein	5.8
A1S_3288	putative transport protein (MFS superfamily)	4.1
A1S_3298	putative high affinity choline transport protein (Bet-like)	4.5
A1S_3300	putative sodium:solute symporter	4.4
A1S_3404	proline transport protein (APC family)	2.9
A1S_3450	putative uracil transport protein (NCS2 family)	2.1

General function prediction only

A1S_0017	putative flavoprotein	3.1
A1S_0035	putative phosphoglycolate phosphatase 2 (PGP 2)	2.7
A1S_0053	MviM protein	3.5
A1S_0054	WbbJ protein	2.8
A1S_0057	capsular polysaccharide synthesis enzyme	3.3
A1S_0134	pirin-related protein	4.7
A1S_0190	hypothetical protein A1S_0190	4.7
A1S_0268	putative DNA binding protein	4.0
A1S_0273	phosphoglycolate phosphatase	2.7
A1S_0290	hypothetical protein A1S_0290	2.3
A1S_0344	putative ATP binding site	3.5
A1S_0348	2-octaprenylphenol hydroxylase of ubiquinone biosynthetic pathway	4.3
A1S_0406	putative phosphoglycolate phosphatase protein	2.3
A1S_0469	hypothetical protein A1S_0469	7.7
A1S_0490	putative hydrolase	2.8
A1S_0499	putative Fe-S-cluster redox enzyme	4.3
A1S_0506	putative GTP-binding protein EngA	4.1
A1S_0516	hypothetical protein A1S_0516	2.0
A1S_0619	putative carbon-nitrogen hydrolase	5.4
A1S_0698	putative anhydratase	3.2
A1S_0703	putative esterase	2.3
A1S_0731	amidohydrolase	3.5
A1S_0738	putative flavoprotein oxidoreductase	7.6
A1S_0815	hypothetical protein A1S_0815	6.4
A1S_0822	putative hydrolase	3.4
A1S_0836	putative signal peptide	2.4
A1S_0840	putative competence protein (ComL)	3.7

A1S_0843	putative flavodoxin or tryptophan repressor binding protein	3.2
A1S_0859	putative glutamine-dependent NAD(+) synthetase (NAD(+) synthase	4.4
A1S_0890	putative glutamine amidotransferase	4.1
A1S_0993	estB	4.6
A1S_0994	rubredoxin reductase	3.9
A1S_1005	putative hemolysin-related protein	2.7
A1S_1050	putative signal peptide	3.3
A1S_1187	CinA-like protein	2.6
A1S_1188	putative N-6 Adenine-specific DNA methylase	2.9
A1S_1237	3-Deoxy-D-manno-octulosonate 8-phosphate (KDO 8-P) phosphatase	2.3
A1S_1245	putative acyltransferase	2.2
A1S_1321	putative hemolysin	2.8
A1S_1339	phenylacetate-CoA oxygenase PaaJ subunit	6.5
A1S_1348	carbonic anhydrases/acetyltransferases isoleucine patch superfamily	3.8
A1S_1395	hypothetical protein A1S_1395	4.6
A1S_1518	putative suppressor of F exclusion of phage T7	3.0
A1S_1579	putative ATPase	4.0
A1S_1644	hypothetical protein A1S_1644	2.9
A1S_1658	putative hydrolase haloacid dehalogenase-like family	2.3
A1S_1690	putative ATPase	3.4
A1S_1833	hypothetical protein A1S_1833	3.4
A1S_1872	putative phosphotransferase	3.0
A1S_1876	putative metallo-beta lactamase	2.2
A1S_1902	hypothetical protein A1S_1902	3.2
A1S_1907	putative peroxidase	4.9
A1S_1920	putative metalloprotease	3.2
A1S_1929	putative oxidoreductase	4.6
A1S_1935	hypothetical protein A1S_1935	3.6
A1S_1942	hypothetical protein A1S_1942	3.1
A1S_2116	hypothetical protein A1S_2116	3.0
A1S_2145	putative kinase	3.4
A1S_2194	putative hydroxyacylglutathione hydrolase	3.1
A1S_2204	paraquat-inducible protein	3.6
A1S_2241	hypothetical protein A1S_2241	3.1
A1S_2242	putative AAA ATPase superfamily	2.3
A1S_2252	putative colicin V producing membrane protein	2.9
A1S_2436	putative transferase	2.4
A1S_2440	putative purine metabolism protein	2.3
A1S_2478	putative trypsin-like serine protease	3.3
A1S_2493	putative 2-nitropropane dioxygenase	3.2
A1S_2498	putative GTP-binding protein (Obg)	3.8
A1S_2514	Short-chain alcohol dehydrogenase of unknown specificity	3.7
A1S_2518	GTP-binding protein16S rRNA-binding,ribosome-associated GTPase	4.0
A1S_2529	hypothetical protein A1S_2529	2.5
A1S_2542	hypothetical protein A1S_2542	4.0
A1S_2590	putative thioesterase	2.7
A1S_2604	putative permease (PerM family)	5.1

A1S_2607	putative hydrolase	2.6
A1S_2662	putative hydrolase	7.0
A1S_2700	putative flavodoxin or tryptophan repressor binding protein	2.3
A1S_2707	hypothetical protein A1S_2707	3.0
A1S_2708	hypothetical protein A1S_2708	6.1
A1S_2722	hypothetical protein A1S_2722	3.0
A1S_2765	putative intracellular protease/amidase	4.0
A1S_2785	putative protease	7.3
A1S_2792	putative esterase of the alpha-beta hydrolase superfamily	2.3
A1S_2824	hypothetical protein A1S_2824	4.0
A1S_2859	putative hemolysin III (HLY-III)	3.2
A1S_2940	copper resistance protein CopC	2.7
A1S_2950	hypothetical protein A1S_2950	2.4
A1S_3003	stringent starvation protein B	2.9
A1S_3021	hypothetical protein A1S_3021	4.9
A1S_3031	hypothetical protein A1S_3031	2.5
A1S_3048	hypothetical protein A1S_3048	3.6
A1S_3084	hypothetical protein A1S_3084	3.2
A1S_3087	putative cell cycle coordination GTPase (EngB)	2.7
A1S_3088	hypothetical protein A1S_3088	2.2
A1S_3097	putative signal peptide	4.5
A1S_3179	hypothetical protein A1S_3179	5.8
A1S_3232	putative acyltransferase	3.2
A1S_3241	putative polyketide synthesis monooxygenase	3.3
A1S_3244	putative homoserine kinase (ThrB)	2.5
A1S_3276	hypothetical protein A1S_3276	2.7
A1S_3349	hypothetical protein A1S_3349	5.1
A1S_3360	putative esterase	2.6
A1S_3436	putative alcohol dehydrogenase	4.4
	malate dehydrogenase FAD/NAD(P)-binding domain	4.6
A1S_0588	hypothetical protein A1S_0588	3.5

Function unknown

A1S_0011	hypothetical protein A1S_0011	3.3
A1S_0015	hypothetical protein A1S_0015	7.2
A1S_0090	hypothetical protein A1S_0090	5.5
A1S_0091	hypothetical protein A1S_0091	3.8
A1S_0128	hypothetical protein A1S_0128	4.2
A1S_0217	hypothetical protein A1S_0217	2.9
A1S_0293	putative signal peptide	2.8
A1S_0323	hypothetical protein A1S_0323	2.8
A1S_0334	hypothetical protein A1S_0334	2.4
A1S_0349	hypothetical protein A1S_0349	4.7
A1S_0352	polyphosphate-AMP phosphotransferase	3.8
A1S_0379	hypothetical protein A1S_0379	4.6
A1S_0385	putative Zinc-binding protein	2.5
A1S_0388	hypothetical protein A1S_0388	3.8
A1S_0428	hypothetical protein A1S_0428	4.2
A1S_0441	hypothetical protein A1S_0441	3.5

A1S_0473	iron-uptake factor	2.1
A1S_0497	hypothetical protein A1S_0497	3.6
A1S_0501	hypothetical protein A1S_0501	4.5
A1S_0504	hypothetical protein A1S_0504	4.6
A1S_0505	hypothetical protein A1S_0505	4.2
A1S_0533	hypothetical protein A1S_0533	5.7
A1S_0550	putative VGR-related protein	3.0
A1S_0552	hypothetical protein A1S_0552	4.7
A1S_0570	hypothetical protein A1S_0570	7.4
A1S_0590	hypothetical protein A1S_0590	3.3
A1S_0704	hypothetical protein A1S_0704	6.1
A1S_0812	hypothetical protein A1S_0812	5.1
A1S_0820	putative peptidoglycan-binding LysM	7.6
A1S_0824	hypothetical protein A1S_0824	2.1
A1S_0842	hypothetical protein A1S_0842	2.8
A1S_0862	hypothetical protein A1S_0862	2.9
A1S_0893	hypothetical protein A1S_0893	3.3
A1S_1038	hypothetical protein A1S_1038	4.0
A1S_1219	glutathione-dependent formaldehyde-activating GFA	2.2
A1S_1244	hypothetical protein A1S_1244	2.1
A1S_1258	hypothetical protein A1S_1258	3.0
A1S_1288	putative VGR-related protein	4.2
A1S_1291	hypothetical protein A1S_1291	4.2
A1S_1293	hypothetical protein A1S_1293	2.6
A1S_1294	hypothetical protein A1S_1294	4.0
A1S_1295	hypothetical protein A1S_1295	3.6
A1S_1296	hypothetical protein A1S_1296	20.1
A1S_1319	hypothetical protein A1S_1319	7.4
A1S_1336	hypothetical protein A1S_1336	8.1
A1S_1338	hypothetical protein A1S_1338	7.7
A1S_1496	hypothetical protein A1S_1496	3.8
A1S_1523	putative signal peptide	6.8
A1S_1630	hypothetical protein A1S_1630	5.4
A1S_1646	hypothetical protein A1S_1646	2.5
A1S_1676	hypothetical protein A1S_1676	2.9
A1S_1684	hypothetical protein A1S_1684	3.9
A1S_1688	hypothetical protein A1S_1688	3.7
A1S_1691	hypothetical protein A1S_1691	2.5
A1S_1886	gamma-carboxymuconolactone decarboxylase (CMD)	9.8
A1S_1911	putative protease	4.5
A1S_1926	hypothetical protein A1S_1926	11.9
A1S_1964	putative signal peptide	2.6
A1S_2048	hypothetical protein A1S_2048	2.9
A1S_2130	hypothetical protein A1S_2130	3.9
A1S_2203	hypothetical protein A1S_2203	3.2
A1S_2205	paraquat-inducible protein A	2.5
A1S_2246	hypothetical protein A1S_2246	6.5
A1S_2263	hypothetical protein A1S_2263	2.6
A1S_2282	hypothetical protein A1S_2282	3.9

A1S_2318	hypothetical protein A1S_2318	2.3
A1S_2342	hypothetical protein A1S_2342	2.5
A1S_2416	hypothetical protein A1S_2416	3.8
A1S_2455	putative signal peptide	2.5
A1S_2466	hypothetical protein A1S_2466	3.8
A1S_2467	hypothetical protein A1S_2467	3.5
A1S_2549	hypothetical protein A1S_2549	2.7
A1S_2615	hypothetical protein A1S_2615	2.2
A1S_2635	hypothetical protein A1S_2635	5.5
A1S_2705	hypothetical protein A1S_2705	3.5
A1S_2721	hypothetical protein A1S_2721	3.7
A1S_2761	hypothetical protein A1S_2761	3.9
A1S_2796	hypothetical protein A1S_2796	2.6
A1S_2806	hypothetical protein A1S_2806	2.8
A1S_2807	hypothetical protein A1S_2807	2.2
A1S_2809	bacteriolytic lipoprotein entericidin B	8.2
A1S_2820	hypothetical protein A1S_2820	9.8
A1S_2823	hypothetical protein A1S_2823	2.7
A1S_2843	hypothetical protein A1S_2843	3.0
A1S_2922	hypothetical protein A1S_2922	5.0
A1S_2925	hypothetical protein A1S_2925	4.4
A1S_2926	hypothetical protein A1S_2926	3.4
A1S_2931	hypothetical protein A1S_2931	8.2
A1S_2951	putative sulfide dehydrogenase	4.1
A1S_2967	hypothetical protein A1S_2967	2.1
A1S_2975	hypothetical protein A1S_2975	2.3
A1S_2978	hypothetical protein A1S_2978	4.6
A1S_2982	hypothetical protein A1S_2982	2.2
A1S_3037	putative ribonuclease (Rbn)	2.8
A1S_3052	hypothetical protein A1S_3052	3.8
A1S_3149	hypothetical protein A1S_3149	4.3
A1S_3178	hypothetical protein A1S_3178	3.8
A1S_3180	putative signal peptide	5.8
A1S_3236	hypothetical protein A1S_3236	4.5
A1S_3242	putative transmembrane protein	3.7
A1S_3301	hypothetical protein A1S_3301	7.4
A1S_3343	hypothetical protein A1S_3343	2.6
A1S_3367	hypothetical protein A1S_3367	4.7
A1S_3369	hypothetical protein A1S_3369	5.1
A1S_2163	hypothetical protein A1S_2163	2.8

Unassigned

A1S_0077	hypothetical protein A1S_0077	3.1
A1S_0123	hypothetical protein A1S_0123	3.3
A1S_0125	hypothetical protein A1S_0125	3.1
A1S_0131	putative adenylyltransferase	3.6
A1S_0133	hypothetical protein A1S_0133	2.1
A1S_0148	F0F1 ATP synthase subunit A	8.4
A1S_0157	hypothetical protein A1S_0157	3.5

A1S_0169	hypothetical protein A1S_0169	11.4
A1S_0201	putative outer membrane protein	3.3
A1S_0207	hypothetical protein A1S_0207	7.4
A1S_0224	hypothetical protein A1S_0224	2.3
A1S_0225	hypothetical protein A1S_0225	3.0
A1S_0244	hypothetical protein A1S_0244	2.2
A1S_0264	hypothetical protein A1S_0264	2.9
A1S_0269	putative general secretion pathway protein	2.1
A1S_0274	anthranilate synthase component I, TrpE	3.3
A1S_0353	hypothetical protein A1S_0353	2.4
A1S_0355	exonuclease V gamma chain	2.7
A1S_0363	hypothetical protein A1S_0363	3.8
A1S_0374	apolipoprotein N-acyltransferase copper homeostasis protein	3.6
A1S_0390	putative type III effector	2.0
A1S_0419	hypothetical protein A1S_0419	5.7
A1S_0434	hypothetical protein A1S_0434	2.4
A1S_0438	hypothetical protein A1S_0438	2.7
A1S_0444	hypothetical protein A1S_0444	6.3
A1S_0445	hypothetical protein A1S_0445	6.6
A1S_0447	RpmG	7.0
A1S_0456	hypothetical protein A1S_0456	2.6
A1S_0509	putative acyl carrier protein	4.0
A1S_0516	hypothetical protein A1S_0516	2.3
A1S_0518	hypothetical protein A1S_0518	2.0
A1S_0526	hypothetical protein A1S_0526	2.7
A1S_0553	hypothetical protein A1S_0553	3.9
A1S_0556	hypothetical protein A1S_0556	2.4
A1S_0561	hypothetical protein A1S_0561	2.9
A1S_0574	GacS-like sensor kinase protein	2.5
A1S_0600	hypothetical protein A1S_0600	3.7
A1S_0615	hypothetical protein A1S_0615	3.5
A1S_0627	hypothetical protein A1S_0627	4.4
A1S_0638	hypothetical protein A1S_0638	2.6
A1S_0640	hypothetical protein A1S_0640	2.1
A1S_0641	hypothetical protein A1S_0641	2.4
A1S_0670	protein tyrosine phosphatase	11.7
A1S_0675	dihydropteroate synthase	7.9
A1S_0683	putative sigma(54) modulation protein RpoX	9.2
A1S_0690	FilA	3.2
A1S_0695	FilF	2.2
A1S_0701	hypothetical protein A1S_0701	3.4
A1S_0702	hypothetical protein A1S_0702	4.6
A1S_0710	putative SMR family drug transporter	4.0
A1S_0736	hypothetical protein A1S_0736	12.7
A1S_0743	hypothetical protein A1S_0743	9.8
A1S_0748	two-component regulatory activator (OmpR family)	4.5
A1S_0749	BfmS	3.3
A1S_0750	hypothetical protein A1S_0750	6.0
A1S_0770	hypothetical protein A1S_0770	2.2

A1S_0771	hypothetical protein A1S_0771	5.8
A1S_0776	putative transcriptional regulator (TetR-family)	2.3
A1S_0779	hypothetical protein A1S_0779	5.8
A1S_0785	hypothetical protein A1S_0785	2.7
A1S_0786	putative signal peptide	2.2
A1S_0787	putative signal peptide	2.4
A1S_0865	hypothetical protein A1S_0865	2.8
A1S_0878	hypothetical protein A1S_0878	3.4
A1S_0892	hypothetical protein A1S_0892	3.6
A1S_0894	outer membrane lipoprotein	3.1
A1S_0895	ferric uptake regulator	2.5
A1S_0903	hypothetical protein A1S_0903	2.2
A1S_0908	RND family multidrug resistance secretion protein	2.4
A1S_0911	hypothetical protein A1S_0911	3.6
A1S_0913	hypothetical protein A1S_0913	2.9
A1S_0914	hypothetical protein A1S_0914	2.9
A1S_0974	hypothetical protein A1S_0974	2.4
A1S_0975	hypothetical protein A1S_0975	2.9
A1S_0997	hypothetical protein A1S_0997	3.1
A1S_0999	putative signal peptide	4.2
A1S_1022	hypothetical protein A1S_1022	2.9
A1S_1027	putative signal peptide	2.6
A1S_1036	hypothetical protein A1S_1036	3.1
A1S_1037	hypothetical protein A1S_1037	3.2
A1S_1042	hypothetical protein A1S_1042	4.7
A1S_1072	hypothetical protein A1S_1072	2.4
A1S_1204	hypothetical protein A1S_1204	2.6
A1S_1238	hypothetical protein A1S_1238	3.2
A1S_1248	hypothetical protein A1S_1248	3.2
A1S_1273	hypothetical protein A1S_1273	3.1
A1S_1290	hypothetical protein A1S_1290	2.3
A1S_1292	putative signal peptide	2.8
A1S_1388	hypothetical protein A1S_1388	6.4
A1S_1462	hypothetical protein A1S_1462	4.1
A1S_1476	hypothetical protein A1S_1476	7.6
A1S_1524	hypothetical protein A1S_1524	3.3
A1S_1526	hypothetical protein A1S_1526	2.2
A1S_1547	organic solvent tolerance protein precursor	2.6
A1S_1574	hypothetical protein A1S_1574	4.6
A1S_1636	putative poly(hydroxyalcanoate) granule associated protein	2.4
A1S_1679	putative signal peptide	4.4
A1S_1689	hypothetical protein A1S_1689	3.5
A1S_1846	3-oxoacid CoA-transferase subunit A	9.7
A1S_1859	aromatic-ring-hydroxylating dioxygenase beta subunit	6.0
A1S_1863	hypothetical protein A1S_1863	5.7
A1S_1879	hypothetical protein A1S_1879	4.8
A1S_1912	hypothetical protein A1S_1912	3.7
A1S_1931	hypothetical protein A1S_1931	3.3
A1S_1932	hypothetical protein A1S_1932	5.3

A1S_1933	hypothetical protein A1S_1933	3.1
A1S_1934	hypothetical protein A1S_1934	3.8
A1S_1951	hypothetical protein A1S_1951	2.9
A1S_1983	putative signal peptide	2.1
A1S_1989	hypothetical protein A1S_1989	2.4
A1S_1998	hypothetical protein A1S_1998	3.5
A1S_2012	putative signal peptide	2.9
A1S_2020	hypothetical protein A1S_2020	2.5
A1S_2041	hypothetical protein A1S_2041	4.1
A1S_2049	hypothetical protein A1S_2049	3.1
A1S_2100	hypothetical protein A1S_2100	2.1
A1S_2131	hypothetical protein A1S_2131	5.1
A1S_2165	hypothetical protein A1S_2165	2.9
A1S_2183	putative signal peptide	7.2
A1S_2185	hypothetical protein A1S_2185	2.0
A1S_2195	hypothetical protein A1S_2195	4.1
A1S_2249	hypothetical protein A1S_2249	2.5
A1S_2256	putative phosphohistidine phosphatase	2.2
A1S_2275	hypothetical protein A1S_2275	3.7
A1S_2285	hypothetical protein A1S_2285	2.5
A1S_2341	HtrA-like serine protease	5.2
A1S_2348	hypothetical protein A1S_2348	2.5
A1S_2371	hypothetical protein A1S_2371	4.9
A1S_2421	hypothetical protein A1S_2421	2.1
A1S_2443	surface adhesion protein putative	2.0
A1S_2469	hypothetical protein A1S_2469	2.8
A1S_2491	putative signal peptide	2.1
A1S_2495	hypothetical protein A1S_2495	2.3
A1S_2505	hypothetical protein A1S_2505	3.3
A1S_2507	hypothetical protein A1S_2507	3.1
A1S_2509	putative chaperone	4.1
A1S_2520	putative signal peptide	3.5
A1S_2538	outer membrane protein CarO precursor	6.4
A1S_2539	putative tetrahydropyridine-2-carboxylate N-succinyltransferase	4.7
A1S_2540	putative organic radical activating enzyme	3.1
A1S_2541	putative organic radical activating enzyme	3.6
A1S_2543	hypothetical protein A1S_2543	3.1
A1S_2552	ATPase	3.3
A1S_2553	transposition site target selection protein D	3.0
A1S_2593	tolerance to group A colicins single-stranded filamentous DNA phage	2.4
A1S_2599	hypothetical protein A1S_2599	5.0
A1S_2600	hypothetical protein A1S_2600	3.8
A1S_2616	hypothetical protein A1S_2616	3.0
A1S_2618	RND efflux transporter	2.1
A1S_2626	DNA gyrase	5.4
A1S_2655	hypothetical protein A1S_2655	3.1
A1S_2659	hypothetical protein A1S_2659	3.2
A1S_2672	putative signal peptide	3.6
A1S_2684	hypothetical protein A1S_2684	2.1

A1S_2696	hypothetical protein A1S_2696	4.8
A1S_2703	hypothetical protein A1S_2703	3.0
A1S_2724	putative hemagglutinin/hemolysin-related protein	5.1
A1S_2728	hypothetical protein A1S_2728	3.5
A1S_2735	AdeI	5.2
A1S_2736	RND family drug transporter	4.4
A1S_2737	AdeK	5.1
A1S_2741	hypothetical protein A1S_2741	3.2
A1S_2753	putative protein (DcaP-like)	4.9
A1S_2757	hypothetical protein A1S_2757	4.8
A1S_2776	hypothetical protein A1S_2776	4.3
A1S_2786	putative signal peptide	2.6
A1S_2787	hypothetical protein A1S_2787	3.3
A1S_2797	hypothetical protein A1S_2797	3.7
A1S_2809	bacteriolytic lipoprotein entericidin B	8.4
A1S_2846	CysI-like sulfite reductase protein	2.4
A1S_2861	putative signal peptide	3.0
A1S_2874	hypothetical protein A1S_2874	2.4
A1S_2895	hypothetical protein A1S_2895	2.8
A1S_2898	hypothetical protein A1S_2898	2.1
A1S_2902	hypothetical protein A1S_2902	2.7
A1S_2926	hypothetical protein A1S_2926	3.5
A1S_2928	hypothetical protein A1S_2928	2.4
A1S_2961	hypothetical protein A1S_2961	3.1
A1S_2985	hypothetical protein A1S_2985	2.0
A1S_2989	putative phospholipase D protein	2.4
A1S_2994	hypothetical protein A1S_2994	3.2
A1S_3004	hypothetical protein A1S_3004	3.3
A1S_3024	hypothetical protein A1S_3024	2.1
A1S_3034	hypothetical protein A1S_3034	2.4
A1S_3043	hypothetical protein A1S_3043	3.5
A1S_3060	50S ribosomal protein L36	8.7
A1S_3099	putative toluene-tolerance protein (Ttg2E)	5.8
A1S_3110	hypothetical protein A1S_3110	2.3
A1S_3112	hypothetical protein A1S_3112	2.1
A1S_3125	putative signal peptide	2.9
A1S_3133	bifunctional N-succinyldiaminopimelate-aminotransferase/acetylornithine transaminase protein	3.7
A1S_3150	putative signal peptide	2.8
A1S_3155	hypothetical protein A1S_3155	3.0
A1S_3186	putative signal peptide	3.7
A1S_3199	hypothetical protein A1S_3199	2.9
A1S_3208	putative peptide signal	10.2
A1S_3213	hypothetical protein A1S_3213	3.0
A1S_3220	cation efflux system protein	2.9
A1S_3233	hypothetical protein A1S_3233	3.8
A1S_3250	hypothetical protein A1S_3250	2.9
A1S_3261	hypothetical protein A1S_3261	3.4
A1S_3297	putative outer membrane protein	2.7

A1S_3297	putative outer membrane protein	2.2
A1S_3303	hypothetical protein A1S_3303	7.1
A1S_3317	putative outer membrane protein	3.5
A1S_3317	putative outer membrane protein	2.5
A1S_3348	putative signal peptide	4.9
A1S_3350	hypothetical protein A1S_3350	5.7
A1S_3368	hypothetical protein A1S_3368	6.0
A1S_3384	hypothetical protein A1S_3384	3.7
A1S_3385	hypothetical protein A1S_3385	7.2
A1S_3387	hypothetical protein A1S_3387	4.4
A1S_3424	putative lipoprotein-34 precursor (NlpB)	5.2
A1S_3454	hypothetical protein A1S_3454	3.3

[a]Fold-repressed in LB + 200 mM NaCl relative to LB without NaCl supplementation.
[b]Transcripts were divided into functional categories based on cluster of orthologous groups (COG) classifications.

Appendix II. Supplementary tables associated with Chapter III

Table 15. Genes that are significantly upregulated in Δ*lpsB* compared to WT.

Fold up-regulation	Locus tag	Description
7.4	A1S_0103	3-hydroxyisobutyrate dehydrogenase
3.1	A1S_0184	hypothetical protein A1S_0184
2.4	A1S_0389	hypothetical protein A1S_0389
2.0	A1S_0452	hypothetical protein A1S_0452
3.0	A1S_0482	acetate kinase (propionate kinase)
2.5	A1S_0548	putative transcriptional regulator (TetR family)
7.9	A1S_0549	hypothetical protein A1S_0549
3.9	A1S_0630	hypothetical protein A1S_0630
4.5	A1S_0631	hypothetical protein A1S_0631
2.7	A1S_0632	DNA primase
2.8	A1S_0633	hypothetical protein A1S_0633
3.8	A1S_0634	hypothetical protein A1S_0634
2.4	A1S_0640	hypothetical protein A1S_0640
2.4	A1S_0641	hypothetical protein A1S_0641
2.3	A1S_0642	hypothetical protein A1S_0642
3.6	A1S_0643	hypothetical protein A1S_0643
5.6	A1S_0644	hypothetical protein A1S_0644
4.4	A1S_0645	hypothetical protein A1S_0645
3.1	A1S_0646	IcmB protein
2.2	A1S_0647	IcmO protein
2.7	A1S_0649	putative phage primase
2.6	A1S_0650	conjugal transfer protein
2.2	A1S_0651	TraB protein
2.5	A1S_0683	putative sigma(54) modulation protein RpoX
2.4	A1S_0801	putative transport protein (permease)
3.4	A1S_0803	trehalose-6-phosphate synthase
2.7	A1S_0823	34 dihydroxy-2-butanone-4-phosphate synthase
2.1	A1S_0836	putative signal peptide
2.1	A1S_0857	hypothetical protein A1S_0857
2.1	A1S_0902	lactoylglutathione lyase-related protein
2.9	A1S_0908	putative MFS family drug transporter
2.4	A1S_0909	putative MFS family drug transporter
3.8	A1S_0909	putative MFS family drug transporter
5.3	A1S_0918	hypothetical protein A1S_0918
2.4	A1S_0918	hypothetical protein A1S_0918
3.2	A1S_0997	hypothetical protein A1S_0997
2.2	A1S_1008	isocitrate lyase
2.3	A1S_1110	hydroxybenzaldehyde dehydrogenase

2.2	A1S_1114	transcriptional regulator for ferulate or vanillate catabolism (GntR family)
2.2	A1S_1141	Carbon storage regulator
2.2	A1S_1219	Glutathione-dependent formaldehyde-activating GFA
3.0	A1S_1220	putative threonine efflux protein
2.8	A1S_1222	possible exonuclease
5.9	A1S_1228	Cold shock protein
3.0	A1S_1249	7-Fe ferredoxin
2.5	A1S_1255	lipid A biosynthesis lauroyl acyltransferase
3.1	A1S_1263	L-2-haloalkanoic acid dehalogenase
3.0	A1S_1266	hypothetical protein A1S_1266
2.9	A1S_1267	putative lactam utilization protein
3.0	A1S_1268	hypothetical protein A1S_1268
3.1	A1S_1269	putative allophanate hydrolase subunit 1 and 2
2.4	A1S_1270	hypothetical protein A1S_1270
3.6	A1S_1319	hypothetical protein A1S_1319
10.2	A1S_1335	Phenylacetic acid degradation protein paaN
10.0	A1S_1336	hypothetical protein A1S_1336
17.9	A1S_1337	Phenylacetic acid degradation B
18.9	A1S_1338	hypothetical protein A1S_1338
17.7	A1S_1339	Phenylacetate-CoA oxygenase PaaJ subunit
10.2	A1S_1340	Phenylacetate-CoA oxygenase/reductase PaaK subunit
32.9	A1S_1341	Enoyl-CoA hydratase/carnithine racemase
16.3	A1S_1342	putative enoyl-CoA hydratase II
18.3	A1S_1343	PaaC
6.0	A1S_1344	Thiolase
6.7	A1S_1345	PaaK
5.2	A1S_1346	phenylacetyl-CoA ligase
2.8	A1S_1347	PaaX
2.4	A1S_1348	Carbonic anhydrases/acetyltransferases isoleucine patch superfamily
2.3	A1S_1354	(Acyl-carrier protein) phosphodiesterase
2.9	A1S_1385	hypothetical protein A1S_1385
4.2	A1S_1386	Catalase
3.8	A1S_1395	hypothetical protein A1S_1395
2.8	A1S_1430	malonate utilization transcriptional regulator (LysR family)
2.6	A1S_1435	hypothetical protein A1S_1435
2.7	A1S_1471	putative transcriptional regulator (AraC family)
3.0	A1S_1476	hypothetical protein A1S_1476
2.7	A1S_1499	hypothetical protein A1S_1499
51.2	A1S_1505	yyaM
3.6	A1S_1512	putative ferredoxin
2.6	A1S_1523	putative signal peptide

4.1	A1S_1526	hypothetical protein A1S_1526
3.0	A1S_1532	glycine cleavage complex protein H
2.3	A1S_1540	putative transcriptional regulator (TetR family)
2.7	A1S_1615	PAPS (adenosine 3'-phosphate 5'-phosphosulfate) x
2.0	A1S_1616	hypothetical protein A1S_1616
2.9	A1S_1620	hypothetical protein A1S_1620
2.5	A1S_1626	putative adenylate or guanylate cyclase
2.6	A1S_1636	putative poly(hydroxyalcanoate) granule associated protein
3.8	A1S_1639	peptidyl-prolyl cis-trans isomerase precursor
5.5	A1S_1658	putative hydrolase haloacid dehalogenase-like family
2.3	A1S_1676	hypothetical protein A1S_1676
2.6	A1S_1680	hypothetical protein A1S_1680
2.5	A1S_1696	hypothetical protein A1S_1696
3.2	A1S_1699	acetoin:26-dichlorophenolindophenol oxidoreductase alpha subunit
4.5	A1S_1700	acetoin:26-dichlorophenolindophenol oxidoreductase beta subunit
2.5	A1S_1701	dihydrolipoamide acetyltransferase
3.8	A1S_1702	dihydrolipoamide dehydrogenase
3.2	A1S_1703	dihydrolipoamide dehydrogenase
2.7	A1S_1704	acetoin dehydrogenase
3.3	A1S_1713	putative transcriptional regulator (AraC family)
2.4	A1S_1734	hypothetical protein A1S_1734
3.7	A1S_1736	hypothetical protein A1S_1736
2.8	A1S_1737	3-hydroxybutyrate dehydrogenase
7.2	A1S_1747	anthranilate dioxygenase reductase
2.2	A1S_1756	transcriptional regulator AraC family
5.6	A1S_1778	putative methylenetetrahydrofolate reductase
2.6	A1S_1786	putative iron transport protein
2.3	A1S_1827	hypothetical protein A1S_1827
3.1	A1S_1833	hypothetical protein A1S_1833
2.5	A1S_1876	putative metallo-beta lactamase
2.4	A1S_1877	hypothetical protein A1S_1877
5.2	A1S_1878	hypothetical protein A1S_1878
4.0	A1S_1896	putative cell division protein (FtsB-like)
2.1	A1S_1906	hypothetical protein A1S_1906
2.3	A1S_1908	3-deoxy-D-arabinoheptulosonate-7-phosphate synthase
2.2	A1S_1924	cytochrome d terminal oxidase polypeptide subunit I
4.3	A1S_1932	hypothetical protein A1S_1932
4.6	A1S_1933	hypothetical protein A1S_1933
3.6	A1S_1934	hypothetical protein A1S_1934
2.5	A1S_1937	putative glutaredoxin-related protein
2.7	A1S_1949	putative diguanylate cyclase/phosphodiesterase
5.7	A1S_1950	putative universal stress protein

7.1	A1S_1954	serine proteinase
2.6	A1S_1986	fumarase C
2.7	A1S_1987	putative UDP-galactose 4-epimerase (GalE-like)
2.4	A1S_1988	putative intracellular sulfur oxidation protein (DsrE-like)
2.6	A1S_1989	hypothetical protein A1S_1989
2.1	A1S_1990	hypothetical protein A1S_1990
2.1	A1S_1995	molybdopterin biosynthesis protein
2.0	A1S_1997	molybdopterin converting factor large subunit
2.4	A1S_1998	hypothetical protein A1S_1998
2.0	A1S_1999	molybdopterin biosynthesis protein A
6.8	A1S_2041	hypothetical protein A1S_2041
5.1	A1S_2042	putative transcriptional regulator (TetR family)
2.9	A1S_2067	transcriptional regulatory protein
2.1	A1S_2072	putative universal stress protein family
2.7	A1S_2080	putative siderophore receptor
2.2	A1S_2081	TonB-dependent siderophore receptor
3.6	A1S_2093	hypothetical protein A1S_2093
4.2	A1S_2101	putative transcriptional regulator
2.3	A1S_2110	UDP-23-diacylglucosamine hydrolase
3.2	A1S_2119	putative acetyltransferase
2.6	A1S_2121	hypothetical protein A1S_2121
2.5	A1S_2146	molybdopterin biosynthesis protein
2.8	A1S_2177	putative proteasome protease
2.9	A1S_2178	putative transglutaminase
3.9	A1S_2180	hypothetical protein A1S_2180
3.5	A1S_2183	putative signal peptide
3.8	A1S_2202	Aspartate racemase
2.4	A1S_2205	paraquat-inducible protein A
2.1	A1S_2206	paraquat-inducible protein A
3.0	A1S_2223	transcriptional regulator AraC family
8.8	A1S_2230	hypothetical protein A1S_2230
8.8	A1S_2230	hypothetical protein A1S_2230
2.3	A1S_2242	putative AAA ATPase superfamily
3.6	A1S_2261	putative cold shock protein
2.1	A1S_2262	EsvH
3.6	A1S_2275	hypothetical protein A1S_2275
2.1	A1S_2291	hypothetical protein A1S_2291
3.3	A1S_2317	putative lipoprotein precursor (RlpA-like)
2.3	A1S_2360	indole-3-glycerol phosphate synthase (IGPS)
2.9	A1S_2406	hypothetical protein A1S_2406
2.6	A1S_2447	EsvD
19.3	A1S_2449	aromatic amino acid transporter (APC family)
85.2	A1S_2450	putative pyruvate decarboxylase

3.1	A1S_2451	Transcriptional regulator AsnC family
23.0	A1S_2452	NAD-dependent aldehyde dehydrogenases
2.4	A1S_2466	hypothetical protein A1S_2466
2.4	A1S_2469	hypothetical protein A1S_2469
3.5	A1S_2475	isocitrate dehydrogenase
2.8	A1S_2485	putative glycosyltransferase
3.0	A1S_2496	putative phosphoserine phosphatase
3.6	A1S_2503	putative outer membrane lipoprotein
6.5	A1S_2567	putative thioesterase
4.3	A1S_2598	putative RNA polymerase sigma factor
3.5	A1S_2599	hypothetical protein A1S_2599
4.2	A1S_2600	hypothetical protein A1S_2600
2.1	A1S_2615	hypothetical protein A1S_2615
3.7	A1S_2638	hypothetical protein A1S_2638
2.3	A1S_2653	transcription elongation factor GreB
2.3	A1S_2654	putative periplasmic binding protein of transport/transglycosylase
2.5	A1S_2666	putative 3'5'-cyclic-nucleotide phosphodiesterase
3.0	A1S_2667	hypothetical protein A1S_2667
3.3	A1S_2696	hypothetical protein A1S_2696
2.4	A1S_2724	putative hemagglutinin/hemolysin-related protein
3.3	A1S_2785	putative protease
2.5	A1S_2792	putative esterase of the alpha-beta hydrolase superfamily
11.1	A1S_2820	hypothetical protein A1S_2820
3.8	A1S_2823	hypothetical protein A1S_2823
2.3	A1S_2843	hypothetical protein A1S_2843
2.2	A1S_2873	hypothetical protein A1S_2873
2.4	A1S_2908	putative integrase
2.5	A1S_2947	hypothetical protein A1S_2947
2.0	A1S_2950	hypothetical protein A1S_2950
2.7	A1S_2975	hypothetical protein A1S_2975
2.1	A1S_2985	hypothetical protein A1S_2985
2.5	A1S_2987	putative lipoprotein precursor
2.8	A1S_3148	NADPH specific quinone oxidoreductase
2.8	A1S_3149	hypothetical protein A1S_3149
4.4	A1S_3155	hypothetical protein A1S_3155
2.8	A1S_3171	RNA polymerase omega subunit
43.3	A1S_3174	putative regulatory or redox component complexing with Bfr in iron storage and mobility (Bfd)
2.8	A1S_3206	S-adenosylmethionine methyltransferase
5.1	A1S_3266	aldo/keto reductase family oxidoreductase
2.3	A1S_3267	hypothetical protein A1S_3267
3.2	A1S_3272	putative transporter (MFS superfamily)

2.3	A1S_3301	hypothetical protein A1S_3301
3.0	A1S_3303	hypothetical protein A1S_3303
2.2	A1S_3374	positive pho regulon response regulator

Table 16. Genes that are significantly downregulated in Δ*lpsB* compared to WT

Fold down-regulation	Locustag	Description
2.7	A1S_0058	Glycosyltransferase
2.0	A1S_0064	putative phosphoglucose isomerase
2.0	A1S_0066	hypothetical protein A1S_0066
10.4	A1S_0067	L-lactate permease
2.3	A1S_0068	L-lactate utilization transcriptional repressor (GntR family)
4.4	A1S_0069	L-lactate dehydrogenase FMN linked
3.4	A1S_0070	D-lactate dehydrogenase NADH independent, FAD-binding domain
4.8	A1S_0095	D-amino acid dehydrogenase
3.7	A1S_0096	alanine racemase 2 PLP-binding, catabolic
3.4	A1S_0097	hypothetical protein A1S_0097
6.1	A1S_0098	D-serine/D-alanine/glycine transport protein
3.3	A1S_0099	D-serine/D-alanine/glycine transport protein
3.6	A1S_0099	D-serine/D-alanine/glycine transport protein
3.1	A1S_0157	hypothetical protein A1S_0157
3.2	A1S_0170	putative outer membrane copper receptor (OprC)
2.0	A1S_0201	putative outer membrane protein
2.1	A1S_0284	50S ribosomal protein
2.1	A1S_0286	50S ribosomal protein
2.9	A1S_0291	hypothetical protein A1S_0291
2.0	A1S_0297	hypothetical protein A1S_0297
2.2	A1S_0340	pH adaptation potassium efflux system E transmembrane protein
2.3	A1S_0341	pH adaptation potassium efflux system D transmembrane protein
2.2	A1S_0342	pH adaptation potassium efflux system C transmembrane protein
2.6	A1S_0343	pH adaptation potassium efflux system transmembrane protein
2.4	A1S_0365	putative amino-acid efflux transmembrane protein
2.2	A1S_0424	putative L-asparaginase I (AnsA)
4.2	A1S_0429	glutamate:aspartate symport protein (DAACS family)
2.3	A1S_0446	putative transport protein (CPA2 family)
2.8	A1S_0485	high-affinity gluconate permease (GntP family)
2.1	A1S_0486	thermoresistant gluconokinase
2.1	A1S_0524	hypothetical protein A1S_0524
2.6	A1S_0525	hypothetical protein A1S_0525
2.2	A1S_0526	hypothetical protein A1S_0526
10.2	A1S_0566	pyridine nucleotide transhydrogenase (proton pump) alpha subunit (part1)

9.4	A1S_0567	pyridine nucleotide transhydrogenase (proton pump) alpha subunit (part2)
10.1	A1S_0568	pyridine nucleotide transhydrogenase beta subunit
2.0	A1S_0608	acetyl-coenzyme A carboxylase carboxyl transferase (alpha subunit)
2.8	A1S_0742	iron-regulated protein
3.0	A1S_0743	hypothetical protein A1S_0743
3.6	A1S_0747	ribonucleoside diphosphate reductase alpha subunit
4.6	A1S_0781	putative MTA/SAH nucleosidase
2.1	A1S_0797	putative chromosome segregation ATPases
2.8	A1S_0806	adenosylmethionine-8-amino-7-oxononanoate aminotransferase
3.0	A1S_0807	8-amino-7-oxononanoate synthase
2.0	A1S_0817	hypothetical protein A1S_0817
2.5	A1S_0852	dioxygenase alpha subunit
2.5	A1S_0854	NAD-dependent succinate aldehyde dehydrogenases
2.7	A1S_0862	hypothetical protein A1S_0862
2.9	A1S_0863	beta-ketoacyl-ACP synthase I
2.2	A1S_0864	beta-ketoacyl-ACP synthase I
2.1	A1S_0868	protein chain elongation factor EF-G GTP-binding
2.0	A1S_0877	threonine efflux protein
2.4	A1S_0891	hemerythrin-like metal-binding protein
2.9	A1S_0921	arginine/ornithine antiporter
3.0	A1S_0922	putative homocysteine S-methyltransferase family protein
2.2	A1S_0930	high-affinity choline transporter (BCCT family)
2.4	A1S_0931	high-affinity choline transporter (BCCT family)
8.8	A1S_0971	methionine synthase
2.1	A1S_1032	hypothetical protein A1S_1032
2.3	A1S_1072	hypothetical protein A1S_1072
2.6	A1S_1088	hypothetical protein A1S_1088
4.6	A1S_1089	hypothetical protein A1S_1089
2.1	A1S_1091	succinylornithine transaminase (carbon starvation protein C)
2.3	A1S_1092	succinylornithine transaminase (carbon starvation protein C)
2.6	A1S_1094	D-serine/D-alanine/glycine transporter
5.4	A1S_1368	Pyruvate ferredoxin/flavodoxin oxidoreductase
5.7	A1S_1369	putative oxidoreductase protein
4.8	A1S_1370	Oxidoreductase
2.4	A1S_1372	hypothetical protein A1S_1372
3.1	A1S_1373	putative acyl-CoA carboxylase alpha chain protein
2.6	A1S_1374	3-methylglutaconyl-CoA hydratase

3.3	A1S_1375	putative propionyl-CoA carboxylase (Beta subunit)
3.8	A1S_1376	Acyl-CoA dehydrogenase
2.5	A1S_1378	putative long chain fatty-acid CoA ligase
2.4	A1S_1441	putative signal peptide
2.8	A1S_1442	taurine ABC transporter periplasmic taurine-binding protein
2.7	A1S_1466	glutaminase-asparaginase
3.0	A1S_1491	glutamate/aspartate transport protein
2.7	A1S_1492	glutamate/aspartate transport protein
2.4	A1S_1503	transmembrane pair
2.7	A1S_1504	Purine-cytosine permease
2.4	A1S_1528	hypothetical protein A1S_1528
2.9	A1S_1530	SSS family major sodium/proline symporter
3.0	A1S_1595	hypothetical protein A1S_1595
2.4	A1S_1810	putative tartrate transporter
2.4	A1S_2016	Phage-related lysozyme
2.2	A1S_2017	hypothetical protein A1S_2017
4.6	A1S_2021	hypothetical protein A1S_2021
5.5	A1S_2022	putative tail fiber
2.0	A1S_2024	Glutamate 5-kinase
3.8	A1S_2025	hypothetical protein A1S_2025
5.0	A1S_2026	hypothetical protein A1S_2026
5.5	A1S_2027	hypothetical protein A1S_2027
2.1	A1S_2035	hypothetical protein A1S_2035
2.2	A1S_2057	methyl viologen resistance protein (MFS superfamily)
2.5	A1S_2068	putative benzoate membrane transport protein
2.1	A1S_2149	putative acyl CoA dehydrogenase oxidoreductase protein
2.0	A1S_2323	30S ribosomal protein S2
2.0	A1S_2427	putative transporter
2.0	A1S_2429	putative ATP-dependent protease
2.1	A1S_2458	putative fatty acid desaturase
2.0	A1S_2470	putative protease
2.1	A1S_2501	glyceraldehyde-3-phosphate dehydrogenase
3.2	A1S_2531	sulfate transport protein
2.0	A1S_2532	sulfate transport protein
2.0	A1S_2532	sulfate transport protein
2.6	A1S_2559	hypothetical protein A1S_2559
2.2	A1S_2626	DNA gyrase
2.6	A1S_2664	chaperone Hsp60
2.5	A1S_2665	chaperone Hsp10
2.3	A1S_2668	phosphoenolpyruvate carboxykinase
2.2	A1S_2687	carbamoyl-phosphate synthase large subunit

2.1	A1S_2701	putative amino acid transport protein (APC family)
2.1	A1S_2715	2-oxoglutarate decarboxylase component of the 2-oxoglutarate dehydrogenase complex (E1)
2.4	A1S_2719	succinyl-CoA synthetase alpha chain
2.1	A1S_2723	putative Na+/H+ antiporter
2.7	A1S_2753	putative protein (DcaP-like)
2.1	A1S_2790	microcin B17 transport protein
3.8	A1S_2793	putative amino-acid transport protein
2.0	A1S_2819	prolyl-tRNA synthetase
2.0	A1S_2838	lysine-specific permease
2.2	A1S_2869	acetylCoA carboxylase beta subunit
2.1	A1S_2897	UDP-N-acetylglucosamine 2-epimerase
3.0	A1S_2919	hypothetical protein A1S_2919
2.3	A1S_2959	Hsp 24 nucleotide exchange factor
2.8	A1S_2960	chaperone Hsp70
2.4	A1S_2968	hypothetical protein A1S_2968
2.1	A1S_2982	hypothetical protein A1S_2982
2.8	A1S_3047	oligopeptidase A
2.2	A1S_3055	50S ribosomal protein L17
2.0	A1S_3060	50S ribosomal protein L36
2.2	A1S_3063	50S ribosomal protein L30
2.1	A1S_3064	30S ribosomal protein S5
2.4	A1S_3065	50S ribosomal protein L18
2.0	A1S_3067	30S ribosomal protein S8
2.5	A1S_3076	50S ribosomal protein L22
2.1	A1S_3079	50S ribosomal protein L4
9.2	A1S_3128	succinylglutamate desuccinylase
7.6	A1S_3130	succinylglutamic semialdehyde dehydrogenase
7.9	A1S_3131	arginine succinyltransferase
9.2	A1S_3132	succinylornithine transaminase
5.5	A1S_3133	bifunctional N-succinyldiaminopimelate-aminotransferase/acetylornithine transaminase protein
5.2	A1S_3133	bifunctional N-succinyldiaminopimelate-aminotransferase/acetylornithine transaminase protein
5.1	A1S_3134	glutamate dehydrogenase (NAD(P)+) oxidoreductase protein
4.3	A1S_3135	putative APC family S-methylmethionine transporter (MmuP)
2.0	A1S_3176	hypothetical protein A1S_3176
2.4	A1S_3211	putative APC family S-methylmethionine transporter (MmuP)
3.5	A1S_3217	RND divalent metal cation efflux transporter
3.8	A1S_3218	EsvF1
3.4	A1S_3218	EsvF1
3.6	A1S_3219	Putative RND family drug transporter

2.8	A1S_3252	putative DNA/RNA non-specific endonuclease G protein
3.0	A1S_3273	putative peptide signal
2.1	A1S_3276	hypothetical protein A1S_3276
2.9	A1S_3283	gamma-aminobutyrate permease
2.1	A1S_3297	putative outer membrane protein
2.0	A1S_3297	putative outer membrane protein
3.4	A1S_3355	hypothetical protein A1S_3355
2.6	A1S_3364	putative VGR-related protein
2.2	A1S_3386	phosphoserine phosphatase
2.0	A1S_3395	glucosamine--fructose-6-phosphate aminotransferase
3.4	A1S_3402	Arginase/agmatinase/formimionoglutamate hydrolase
3.6	A1S_3403	imidazolonepropionase
3.1	A1S_3404	proline transport protein (APC family)
2.9	A1S_3405	histidine ammonia-lyase
2.6	A1S_3406	urocanate hydratase
2.3	A1S_3407	Urocanase
2.6	A1S_3410	putative acyltransferase
4.0	A1S_3413	APC family aromatic amino acid transporter
12.2	A1S_3414	Fumarylacetoacetase
15.4	A1S_3415	Maleylacetoacetate isomerase
10.8	A1S_3416	Glyoxalase/bleomycin resistance protein/dioxygenase
9.1	A1S_3418	4-hydroxyphenylpyruvate dioxygenase
2.4	A1S_3449	phosphoenolpyruvate carboxylase

Appendix III. Supplementary tables associated with Chapter IV

Table 17. Genes that are significantly upregulated in Tn5A7 and Tn20A11 compared to WT and Δ*lpsB*.

Fold upregulation			
Tn5A7	**Tn20A11**	**Locustag**	**Description**
12.6	7.9	A1S_0040	putative oxidoreductase
2.1	2.3	A1S_0211	Transposition Helper
3.6	5.8	A1S_0372	protein secretion chaperone
3.8	5.5	A1S_0648	hypothetical protein A1S_0648
14.9	15.5	A1S_0663	putative DNA helicase
15.6	15.3	A1S_0664	replication C family protein
14.6	14.2	A1S_0665	putative mating pair formation protein
14.7	14.7	A1S_0666	TrbL/VirB6 plasmid conjugal transfer protein
5.1	6.0	A1S_0667	hypothetical protein A1S_0667
3.7	4.7	A1S_0673	putative transposase
3.5	4.3	A1S_0674	putative transposase
2.8	2.3	A1S_0677	transposase
2.1	2.3	A1S_0837	glutamyl tRNA reductase
3.7	2.7	A1S_0945	putative ferredoxin
2.6	3.6	A1S_1046	Lysine exporter protein (LYSE/YGGA)
9.5	7.8	A1S_1172	putative transposase
4.0	2.8	A1S_1241	putative RND family drug transporter
4.9	3.1	A1S_1771	hypothetical protein A1S_1771
11.9	8.0	A1S_1772	Putative MFS family drug transporter
5.9	5.4	A1S_1773	RND family drug transporter
11.9	7.7	A1S_1773	
5.5	5.8	A1S_1823	Transcriptional Regulator TetR family
2.9	2.4	A1S_1846	
2.6	2.4	A1S_1890	3-carboxy-ciscis-muconate cycloisomerase
4.2	3.4	A1S_1952	hypothetical protein A1S_1952
2.6	4.7	A1S_2019	hypothetical protein A1S_2019
3.7	6.1	A1S_2020	
3.8	5.7	A1S_2020	hypothetical protein A1S_2020
8.2	6.2	A1S_2034	hypothetical protein A1S_2034
3.3	3.0	A1S_2086	putative short chain dehydrogenase
3.4	2.0	A1S_2300	Amino acid ABC transporter permease protein
3.9	3.4	A1S_2302	ABC Lysine-arginine-ornithine transporter periplasmic ligand binding protein
4.0	4.6	A1S_2303	transcriptional regulator LysR family
3.4	3.5	A1S_2473	transcriptional regulator LysR family
2.3	2.1	A1S_2504	excinuclease ABC subunit B

6.2	10.8	A1S_2650	GCN5-related N-acetyltransferase
4.3	4.6	A1S_2699	putative transcriptional regulator
3.5	3.5	A1S_2839	hypothetical protein A1S_2839
4.1	4.9	A1S_3259	putative transcriptional regulator YdzF
3.6	4.5	A1S_3260	hypothetical protein A1S_3260
5.6	3.8	A1S_3294	putative transcriptional regulator (TetR/AcrR family)

Table 18. Genes that are significantly downregulated in Tn5A7 and Tn20A11 compared to WT and Δ*lpsB*.

Fold downregulation			
Tn5A7	**Tn20A11**	**Locustag**	**Description**
2.2	2.6	A1S_0034	putative oxoacyl-(acyl carrier protein) reductase
2.4	2.3	A1S_0055	WecE protein
3.3	2.3	A1S_0106	putative enoyl-CoA hydratase/isomerase
2.6	2.6	A1S_0107	putative enoyl-CoA hydratase/isomerase family protein
2.5	2.8	A1S_0130	GMP synthetase
3.4	2.5	A1S_0148	
3.2	2.9	A1S_0150	membrane-bound ATP synthase F0 sector, subunit c
3.6	3.0	A1S_0151	membrane-bound ATP synthase F0 sector, subunit b
2.9	2.5	A1S_0156	membrane-bound ATP synthase F1 sector, epsilon-subunit
3.1	2.4	A1S_0283	50S ribosomal protein
2.7	3.2	A1S_0285	50S ribosomal protein
2.6	2.6	A1S_0288	DNA-directed RNA polymerase beta' chain
2.6	2.3	A1S_0290	hypothetical protein A1S_0290
2.5	3.3	A1S_0292	putative outer membrane protein W
2.2	2.3	A1S_0339	pH adaptation potassium efflux system protein G
2.2	2.9	A1S_0367	glutathione-regulated potassium-efflux system protein (K(+)/H(+) antiporter)
2.2	2.2	A1S_0395	Na+-driven multidrug efflux pump
3.3	3.9	A1S_0402	putative very-long-chain acyl-CoA synthetase
3.1	2.3	A1S_0460	prolipoprotein diacylglyceryl transferase
3.1	2.9	A1S_0483	phosphogluconate dehydratase
3.0	3.3	A1S_0484	hypothetical protein A1S_0484
2.2	2.4	A1S_0492	beta-N-acetyl-D-glucosaminidase
3.0	2.4	A1S_0498	nucleoside diphosphate kinase
2.1	2.6	A1S_0571	hydroxypyruvate isomerase
2.3	3.5	A1S_0600	hypothetical protein A1S_0600
2.7	2.6	A1S_0602	phenylalanyl-tRNA synthetase beta subunit
2.6	2.6	A1S_0614	putative small conductance mechanosensitive ion channel
2.6	2.7	A1S_0615	hypothetical protein A1S_0615
2.8	2.3	A1S_0695	FilF
2.7	2.6	A1S_0746	ribonucleoside-diphosphate reductase beta subunit
2.6	2.3	A1S_0753	NADH dehydrogenase I chain B
2.9	2.1	A1S_0755	NADH dehydrogenase I chain E
2.7	2.3	A1S_0759	NADH dehydrogenase I chain I 2Fe-2S ferredoxin-related
2.6	2.4	A1S_0763	NADH dehydrogenase I chain M membrane subunit
2.3	2.4	A1S_0983	lipase
2.2	2.2	A1S_0994	rubredoxin reductase
2.2	2.1	A1S_1045	Co/Zn/Cd efflux system

2.6	2.3	A1S_1199	putative glutathionine S-transferase
2.3	2.1	A1S_1205	alkyl hydroperoxide reductase C22 subunit
2.0	2.4	A1S_1352	cytochrome B561
3.0	2.3	A1S_1493	glutamate/aspartate transport protein
2.1	2.1	A1S_1521	transketolase
2.9	3.4	A1S_1572	30S ribosomal protein S1
2.4	2.0	A1S_1841	hypothetical protein A1S_1841
3.3	2.9	A1S_1946	1-phosphofructokinase
2.9	2.1	A1S_2124	putative permease (MFS superfamily)
2.8	2.8	A1S_2166	cytochrome o ubiquinol oxidase subunit II
2.6	2.6	A1S_2172	30S ribosomal protein S18
2.4	2.3	A1S_2188	hypothetical protein A1S_2188
2.7	2.7	A1S_2189	phosphoribosylamine--glycine ligase
2.3	2.9	A1S_2296	Putative protease
3.8	2.2	A1S_2418	starvation-induced peptide utilization protein
2.7	3.1	A1S_2428	putative ATP-dependent protease
2.1	2.3	A1S_2526	L-aspartate oxidase
2.5	2.7	A1S_2671	MFS permease
2.3	2.8	A1S_2716	dihydrolipoamide succinyltransferase component of 2-oxoglutarate dehydrogenase complex (E2)
2.6	2.8	A1S_2730	50S ribosomal protein L27
2.5	2.3	A1S_2731	50S ribosomal protein L21
2.5	2.6	A1S_2847	glucose dehydrogenase
3.1	3.6	A1S_2894	aspartyl-tRNA synthetase
2.6	2.3	A1S_2967	hypothetical protein A1S_2967
2.6	2.7	A1S_3000	50S ribosomal protein L13
3.0	2.3	A1S_3037	putative ribonuclease (Rbn)
3.0	3.2	A1S_3056	RNA polymerase alpha subunit
3.0	3.0	A1S_3057	30S ribosomal protein S4
2.9	3.0	A1S_3059	30S ribosomal protein S13
3.0	3.2	A1S_3066	50S ribosomal protein L6
3.0	2.8	A1S_3068	30S ribosomal protein S14
2.9	3.2	A1S_3069	50S ribosomal protein L5
3.0	3.0	A1S_3070	50S ribosomal protein L24
2.9	3.1	A1S_3071	50S ribosomal protein L14
2.9	3.6	A1S_3072	30S ribosomal protein S17
2.9	2.8	A1S_3073	50S ribosomal protein L29
3.0	2.9	A1S_3075	30S ribosomal protein S3
3.1	3.1	A1S_3077	50S ribosomal protein L2
3.1	3.1	A1S_3078	50S ribosomal protein L23
3.0	2.7	A1S_3080	50S ribosomal protein L3
2.6	3.6	A1S_3108	coproporphyrinogen III oxidase
3.0	2.4	A1S_3119	glycyl-tRNA synthetase beta chain

2.6	2.4	A1S_3163	16S rRNA processing protein
4.3	2.6	A1S_3200	phospho-N-acetylmuramoyl-pentapeptide transferase
2.8	2.7	A1S_3201	phospho-N-acetylmuramoyl-pentapeptide transferase
2.6	3.9	A1S_3214	cation efflux system protein
2.5	2.9	A1S_3221	putative transport protein
2.2	2.3	A1S_3328	pyruvate decarboxylase E1 component of the pyruvate dehydrogenase complex
2.0	3.0	A1S_3350	hypothetical protein A1S_3350
2.6	2.4	A1S_3394	hypothetical protein A1S_3394